IODP
INTEGRATED OCEAN DRILLING PROGRAM

ICDP Deutschland

IODP/ICDP

Kolloquium 2015

Steinmann-Institut, Universität Bonn

2. - 4. März 2015

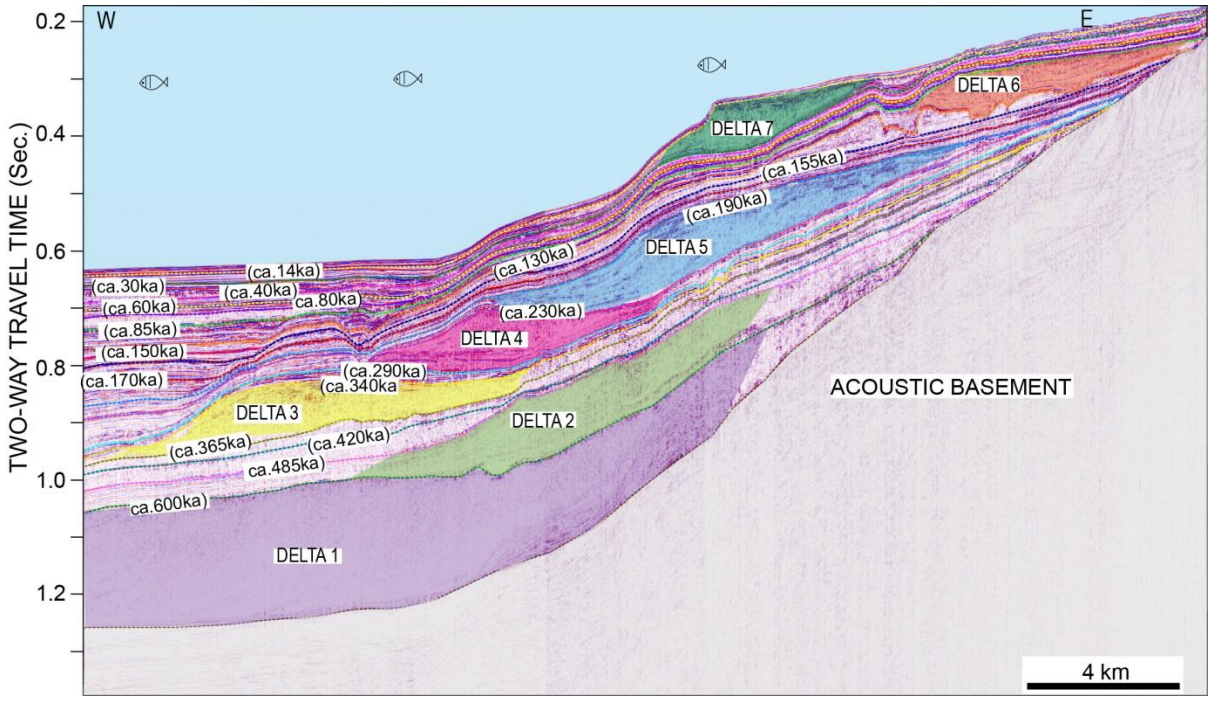

DFG Deutsche Forschungsgemeinschaft

steinmanninstitut

universitätbonn

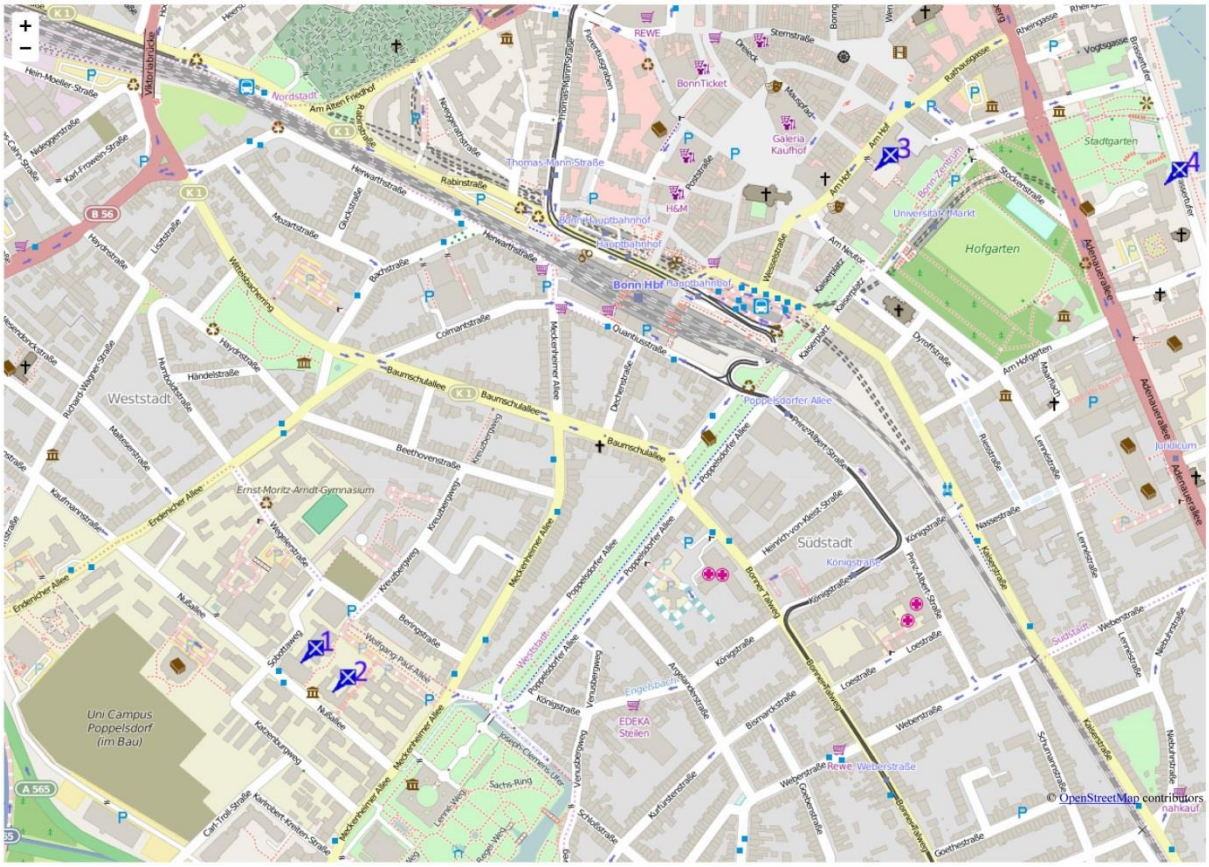

Veranstaltungsort: Neue Anatomie, Hörsaal A, Nussallee 10, Bonn

1. Hörsaal Anatomie, Nussallee 10
2. Steinmann-Institut, Nussallee 8
3. Aula, Uni-Hauptgebäude, Am Hof 1
4. Hotel Königshof, Adenauerallee 9

Cover picture: several lowstand deltas at different stratigraphic depths suggest significant water level fluctuations since the formation of Lake Van, eastern Turkey. The correlation of the ages with the Marine Isotope Stages strongly suggest climatic control on the formation of these deltas (Cukur et al. 2014, J. Paleolimnology 52, 201-214).

Montag, 2. März 2015		
10:00	13:00	**Registrierung** (Hörsaal Anatomie, Nussallee 10)
13:00	13:30	**Eröffnung**
Neues aus den Programmen		
13:30	14:00	Brian Horsfield - **Overview ICDP International** Roland Oberhänsli - **ICDP Rückblick auf 2014 - Wie geht es weiter?**
14:00	14:20	Jochen Erbacher - **IODP Rückblick auf 2014 - Wie geht es weiter?**
Stoffkreisläufe / Tiefe Biosphäre		
14:20	14:40	Philipp Rammensee **A multiple isotope and trace element approach to constrain the oxygenation and metal cycling of 3.5 to 3.2 Ga paleo-oceans**
14:40	15:00	Kai-Uwe Hinrichs **IODP Expedition 337: Exploring the deep biosphere nearly 2.5 km below the seafloor**
15:00	15:20	Tim Engelhardt. **Viral activity and life-cycles in deep subseafloor sediments**
15:20	16:50	**Posterpräsentation** **Kaffeepause**
Neue Projekte, Projektvorschläge 1		
16:50	17:10	Steffen Kutterolf **Paleoclimate, Paleoenvironment, and Paleoecology of Neogene Central America: Bridging Continents and Oceans (NICA-BRIDGE)**
17:10	17:30	Alexander Prokopenko **Hydrologic cycles in Pliocene North America and their climate teleconnections - Initial study of newly recovered drill core from paleo-lake Idaho**
17:30	17:50	Pascal Methe **INFLUINS Deep Drilling Campaign: Data of borehole geophysical and multi sensor core logger measurements**
17:50	18:10	Christian Betzler **Sea level, Currents, and Monsoon Evolution in the Indian Ocean (IODP Exp. 359)**
ab 19:00		**Icebreaker / gemeinsames Abendessen im Hotel Königshof (Adenauer Allee 9)**

Dienstag, 3. März 2015		
Neue Projekte, Projektvorschläge 2		
09:00	09:20	Achim Kopf **Amphibious drilling projects maximise benefits from ICDP and IODP initiatives: The example of the Ligurian slope near Nice**
09:20	09:40	Frank Wiese **From bycatch to main dish - spines of irregular echinoids as monitors for macrofaunal dynamics in the deep sea during Cenozoic critical intervals? A pilot study**
Seismogene Zonen		
09:40	10:00	Robert Kurzawski **Earthquake nucleation in calcareous sediments from offshore Costa Rica triggered by a combined temperature and pore fluid pressure increase, Costa Rica Seismogenesis Project (CRISP)**
10:00	13:00	**Posterpräsentation / Kaffeepause**
*Parallel stattfindend***:**		
11:00	12:30	**Geo-Show „Unterirdisch“**
Fahrtberichte		
13:00	13:15	Ann-Sophie Jonas, Schindlbeck, J.C., IODP Expedition 350 Science Party **Expedition report for IODP Expedition 350: Izu-Bonin-Mariana: The missing half of the subduction factory**
13:15	13:30	P.A. Brandl, Martin Neuhaus, IODP Expedition 351 Scientists **IODP Expedition 351 Izu-Bonin-Mariana Arc Origins - Subduction initiation and evolution of a young island arc**
13:30	13:45	Maria Kirchenbaur, M., Almeev, R., Kutterolf, S., Expedition 352 Scientists **IODP Expedition 352 cruise report: “Testing subduction initiation and ophiolite models by drilling the outer Izu-Bonin-Mariana fore-arc”**
13:45	14:00	Wolfgang Kuhnt **IODP Expedition 353 "Indian Monsoon rainfall"**
Paläozeanographie / Paläoklima / Paläoumwelt 1		
14:00	14:20	Henrike Baumgarten **Age depth-model based on cyclostratigraphic analysis of gamma ray data for the past 630 ka in Lake Ohrid (Macedonia/Albania)**
14:20	14:40	Alexander Francke **Environmental variability in the Balkan Region between the MPT and present day, derived from lacustrine sediments of the 1.2 Ma old Lake Ohrid: The ICDP SCOPSCO project**
14:40	15:00	Frank Schäbitz **Preliminary results from the deep drilling at Chew Bahir, south Ethiopia**
15:00	16:30	**Posterpräsentation / Kaffeepause**
16:30	16:50	Marcus Schwab **Interglacial climate variability recorded in the Dead Sea sediments**
16:50	17:10	Sietske Batenburg **Atlantic Ocean circulation during the latest Cretaceous and early Paleogene: progressive deep water exchange**
17:10	17:30	Anne Holbourn **Early to middle Miocene climate evolution: New insights from IODP Sites U1337 and U1338 (eastern equatorial Pacific Ocean)**
17:30	17:50	Benny Antz **Atlantic Meridional Overturning Circulation during Heinrich-Stadial 1 & 2 as seen by ^{231}Pa/^{230}Th**
17:50	18:10	Frank Lamy **Plio-Pleistocene paleoceanography of the Subantarctic Southeast Pacific linked to Drake Passage throughflow (SUBANTPAC)**

Mittwoch, 4. März 2015		
Paläozeanographie / Paläoklima / Paläoumwelt 2		
08:30	08:50	~~Juliane Müller~~ **~~The Mid Pleistocene Transition in the Gulf of Alaska (NE Pacific): A multi-proxy record of palaeoenvironmental and climatic changes~~**
08:50	09:10	Thomas Felis **Intensification of the meridional temperature gradient in the Great Barrier Reef following the Last Glacial Maximum - Results from IODP Expedition 325**
Magmatische Petrologie & Gase / Fluide		
09:10	09:30	Jonathan Engelhardt **$^{40}Ar/^{39}Ar$ geochronology on ICDP cores from Lake Van, Turkey**
09:30	09:50	Tim Müller **Petrological and geochemical investigation related to the "Wadi Gideah" cross-section in the southern Oman ophiolite: constraints on fast-spreading crust accretion processes in the frame of the ICDP project "The Oman drilling project"**
09:50	10:10	Sören Wilke **Cotectic compositions of rhyolite as a geobarometer for highly evolved melts of the Yellowstone Snake River Plain**
10:10	11:30	**Posterpräsentation** **Kaffeepause**
11:30	11:50	Martin Oeser **Revealing crystal growth and diffusion processes with Fe-Mg chemical and isotopic zoning in MORB olivine**
11:50	12:10	Katja Pesch **B-isotope study of hydrothermal tourmaline in silicified Palaeoarchaean komatiites from the Barberton Greenstone Belt, South Africa**
12:10	13:00	**Posterprämierung und Schlussworte**
13:00		**Tagungsende**

Mittwoch, 4. März 2015	
Im **Anschluss** an das IODP/ICDP Kolloquium	
13:00	**GESEP School 2015: „ Site Survey and Preparatory Work"**
Der modulare Kurs des Deutschen Forschungsbohrkonsortiums GESEP wird von Ingenieuren und Wissenschaftlern mit Erfahrungen in nationalen und internationalen Bohrprogrammen gehalten und soll jungen Wissenschaftlern praktisches Wissen zu Forschungsbohrungen vermitteln. Im Fokus steht dieses Jahr das Thema Bohrtechnik inklusive Ablauf einer Bohrung sowie Bohrlochmessungen und Probenbehandlung vor Ort als wichtige Bestandteile einer Forschungsbohrung. An angewandten Beispielen wird die Herausforderung, Bohrungen – für marine Expeditionen oder kontinentale Projekte - zu planen, vorgestellt.	
ENDE**: Donnerstag, 5. März 2015 ca. 14:00 Uhr**	

Teilnehmerliste

Name	Vorname	Institution und Ort
Abratis	Michael	Institut für Geowissenschaften, Universität Jena
Allabar	Anja	Fachbereich Geowissenschaften, Universität Tübingen
Almeev	Renat	Institut für Mineralogie, Universität Hannover
Antz	Benny	Institut für Umweltphysik, Universität Heidelberg
Bach	Wolfgang	Fachbereich Geowissenschaften, Universität Bremen
Bahlburg	Heinrich	Institut für Geologie und Paläontologie, Universität Münster
Bahr	André	Institut für Geowissenschaften, Universität Heidelberg
Batenburg	Sietske	Institut für Geowissenschaften, Universität Frankfurt
Baumgarten	Henrike	LIAG, Leibnitz-Institut für Angewandte Geophysik, Hannover
Behrmann	Jan	GEOMAR, Helmholtz-Zentrum für Ozeanforschung, Kiel
Beier	Christoph	GeoZentrum Nordbayern, Universität Erlangen-Nürnberg
Betzler	Christian	Institut für Geologie, Universität Hamburg
Beuscher	Sarah	Institut für Geophysik und Geologie, Universität Leipzig
Bieseler	Bastian	Fachbereich Geowissenschaften, Universität Bremen
Blaser	Patrick	Institut für Umweltphysik, Universität Heidelberg
Bornemann	André	IODP, BGR, Bundesanstalt für Geowissenschaften und Rohstoffe, Hannover
Bragagni	Alessandro	Institut für Geologie, Mineralogie und Paläontologie, Universität Bonn
Brauer	Achim	GFZ, Helmholtz-Zentrum Potsdam, Deutsches GeoForschungsZentrum, Potsdam
Bräuer	Karin	Helmholtz-Zentrum für Umweltforschung UFZ, Halle
Buske	Stefan	Institut für Geophysik und Geoinformatik, TU Bergakademie Freiberg
Chen	Chunzhu	Institut für Geologie, Mineralogie und Paläontologie, Universität Bonn
Chiang	Oscar	Institut für Chemie und Biologie des Meeres, Universität Oldenburg
Cohuo	Sergio	Institut für Geosysteme und Bioindikation, TU Braunschweig
Daut	Gerhard	Institut für Geographie, Universität Jena
Deutsch	Alex	Institut für Planetologie, Universität Münster
De Vleeschouwer	David	MARUM - Zentrum für Marine Umweltwissenschaften, Universität Bremen
Pierdominici	Simona	Scientific Drilling ICDP, GFZ, Helmholtz-Zentrum Potsdam, Deutsches GeoForschungsZentrum, Potsdam
Drath	Gabriela	IODP, BGR, Bundesanstalt für Geowissenschaften und Rohstoffe, Hannover
Drewer	Christian	Institut für Geologie und Paläontologie, Universität Münster
Drury	Anna Joy	MARUM, Zentrum für Marine Umweltwissenschaften, Universität Bremen
Dultz	Stefan	Institut für Mineralogie, Universität Hannover
Dupont	Lydie	MARUM - Zentrum für Marine Umweltwissenschaften, Universität Bremen
Egger	Lisa	Institut für Geowissenschaften, Universität Heidelberg
Engelhardt	Jonathan	Institut für Erd- und Umweltwissenschaften, Universität Potsdam
Engelhardt	Tim	Department of Bioscience, Aarhus University, Denmark
Erbacher	Jochen	IODP, BGR, Bundesanstalt für Geowissenschaften und Rohstoffe, Hannover
Erzinger	Jörg	GFZ, Helmholtz-Zentrum Potsdam, Deutsches GeoForschungsZentrum, Potsdam
Escoube	Raphaelle	Institut für Geologie und Mineralogie, Universität Köln
Fabbri	Stefano	Geologisches Institut, Universität Bern, Schweiz
Fehr	Annick	Institute for Applied Geophysics and Geothermal Energy, RWTH Aachen
Feldtmann	Mathias	MARUM - Zentrum für Marine Umweltwissenschaften, Universität Bremen
Felis	Thomas	MARUM - Zentrum für Marine Umweltwissenschaften, Universität Bremen
Fonseca	Raúl	Institut für Geologie, Mineralogie und Paläontologie, Universität Bonn
Förster	Verena	Institut für Erd- und Umweltwissenschaften, Universität Potsdam
Francke	Alexander	Institut für Geologie und Mineralogie, Universität Köln
Frank	Martin	GEOMAR, Helmholtz-Zentrum für Ozeanforschung, Kiel
Frank	Norbert	Institut für Umweltphysik, Universität Heidelberg
Franz	Sven Oliver	Steinmann-Institut, Bereich Geologie, Universität Bonn
Friedrich	Oliver	Institut für Geowissenschaften, Universität Heidelberg
Friese	André	GFZ, Helmholtz-Zentrum Potsdam, Deutsches GeoForschungsZentrum, Potsdam
García-Gallardo	Ángela	Institut für Erdwissenschaften, Universität Graz, Österreich
Gebregiorgis	Daniel	GEOMAR, Helmholtz-Zentrum für Ozeanforschung, Kiel
Geldmacher	Jörg	GEOMAR, Helmholtz-Zentrum für Ozeanforschung, Kiel
Giese	Rüdiger	GFZ, Helmholtz-Zentrum Potsdam, Deutsches GeoForschungsZentrum, Potsdam
Gohl	Karsten	AWI, Helmholtz-Zentrum für Polar- und Meeresforschung, Alfred-Wegener-Institut, Bremerhaven
Grützner	Jens	AWI, Helmholtz-Zentrum für Polar- und Meeresforschung, Alfred-Wegener-Institut, Bremerhaven
Gussone	Nikolaus	Institut für Mineralogie, Universität Münster
Haberzettl	Torsten	Institut für Geographie, Universität Jena
Harms	Ulrich	Scientific Drilling ICDP, GFZ, Helmholtz-Zentrum Potsdam, Deutsches GeoForschungsZentrum, Potsdam
Hasberg	Ascelina	Institut für Geologie und Mineralogie, Universität Köln
Hathorne	Ed	GEOMAR, Helmholtz-Zentrum für Ozeanforschung, Kiel
Hauffe	Torsten	Department of Animal Ecology & Systematics, Universität Giessen
Herder	Fabian	Zoologisches Forschungsmuseum Alexander Koenig, Leibniz Institut für Biodiversität der Tiere (ZFMK)

Herrle	Jens	Institut für Geowissenschaften, Universität Frankfurt
Heuer	Verena	MARUM - Zentrum für Marine Umweltwissenschaften, Universität Bremen
Hinrichs	Kai-Uwe	MARUM - Zentrum für Marine Umweltwissenschaften, Universität Bremen
Hofmann	Peter	Institut für Geologie und Mineralogie, Universität Köln
Holbourn	Ann	Institut für Geowissenschaften, Universität Kiel
Holtz	Francois	Institut für Mineralogie, Universität Hannover
Horsfield	Brian	ICDP International, GFZ, Helmholtz-Zentrum Potsdam, Deutsches GeoForschungsZentrum, Potsdam
Huber	Barbara	Institut für Geologie und Paläontologie, Universität Münster
Huepers	Andre	MARUM - Zentrum für Marine Umweltwissenschaften, Universität Bremen
Iovine	Raffaella	Geowissenschaftliches Zentrum, Universität Göttingen
Jakob	Kim	Institut für Geowissenschaften, Universität Heidelberg
Jehle	Sofie	Institut für Geophysik und Geologie, Universität Leipzig
Jiménez	Núria	BGR, Bundesanstalt für Geowissenschaften und Rohstoffe, Hannover
Jonas	Ann-Sophie	Institut für Geowissenschaften, Universität Kiel
Jovanovska	Elena	Systematics & Biodiversity Lab, Universtät Giessen
Junginger	Annett	Fachbereich Geowissenschaften, Universität Tübingen
Kallmeyer	Jens	GFZ, Helmholtz-Zentrum Potsdam, Deutsches GeoForschungsZentrum, Potsdam
Kämpf	Horst	GFZ, Helmholtz-Zentrum Potsdam, Deutsches GeoForschungsZentrum, Potsdam
Kasper	Thomas	Institut für Geographie, Universität Jena
Kemner	Fabian	GeoZentrum Nordbayern, Universität Erlangen-Nürnberg
Kirchenbaur	Maria	Institut für Geologie und Mineralogie, Universität Köln
Kopf	Achim	MARUM - Zentrum für Marine Umweltwissenschaften, Universität Bremen
Koepke	Jürgen	Institut für Mineralogie, Universität Hannover
Kotthoff	Ulrich	Institut für Geologie, Universität Hamburg
Krastel	Sebastian	ICDP-Deutschland, Institut für Geowissenschaften, Universität Kiel
Krauß	Felix	GFZ, Helmholtz-Zentrum Potsdam, Deutsches GeoForschungsZentrum, Potsdam
Krieger	Katharina	Institut für Geologie und Paläontologie, Universität Münster
Kriegerowski	Marius	GFZ, Helmholtz-Zentrum Potsdam, Deutsches GeoForschungsZentrum, Potsdam
Kroker	Holger	freier Wissenschaftsjournalist, Köln
Koutsodendris	Andreas	Institut für Geowissenschaften, Universität Heidelberg
Kudraß	Hermann-Rudolph	MARUM - Zentrum für Marine Umweltwissenschaften, Universität Bremen
Kühl	Norbert	Institut für Geologie, Mineralogie und Paläontologie, Universität Bonn
Kuhnt	Wolfgang	Institut für Geowissenschaften, Universität Kiel
Kukowski	Nina	Institut für Geowissenschaften, Universität Jena
Kunkel	Cindy	Institut für Geowissenschaften, Universität Jena
Kurzawski	Robert	GEOMAR, Helmholtz-Zentrum für Ozeanforschung, Kiel
Kutterolf	Steffen	GEOMAR, Helmholtz-Zentrum für Ozeanforschung, Kiel
Lamy	Frank	AWI, Helmholtz-Zentrum für Polar- und Meeresforschung, Alfred-Wegener-Institut, Bremerhaven
Lay	Vera	Institut für Geophysik und Geoinformatik, TU Bergakademie Freiberg
Lazarus	David	Museum für Naturkunde, Leibniz-Institut für Evolutions- und Biodiversitätsforschung, Berlin
Lehnert	Oliver	Geozentrum Nordbayern, Universität Erlangen-Nürnberg
Leicher	Niklas	Institut für Geologie und Mineralogie, Universität Köln
Leitzke	Felipe	Institut für Geologie, Mineralogie und Paläontologie, Universität Bonn
Lindhorst	Katja	Institut für Geowissenschaften, Universität Kiel
Lippold	Jörg	Institut für Geologie, Universität Bern, Schweiz
Litt	Thomas	Institut für Geologie, Mineralogie und Paläontologie, Universität Bonn
Lübke	Nathalie	Institut für Geologie, Mineralogie und Geophysik, Universität Bochum
Macario	Laura	Institut für Geosysteme und Bioindikation, TU Braunschweig
Maronde	Dietrich	Institut für Geologie,Mineralogie und Paläontologie, Universität Bonn
Martinez	Mathieu	MARUM - Zentrum für Marine Umweltwissenschaften, Universität Bremen
Methe	Pascal	Institut für Geowissenschaften, Universität Jena
Meyers	Philip A.	Department of Earth and Environmental Sciences, University of Michigan, Ann Arbor, USA
Miebach	Andrea	Institut für Geologie, Mineralogie und Paläontologie, Universität Bonn
Miladinova	Irena	Institut für Geologie,Mineralogie und Paläontologie, Universität Bonn
Morlock	Marina	Geologisches Institut, Universität Bern, Schweiz
Müller	Tim	Institut für Mineralogie, Universität Hannover
Münker	Carsten	Institut für Geologie und Mineralogie, Universität Köln
Munz	Philipp	Fachbereich Geowissenschaften, Universität Tübingen
Mutterlose	Jörg	Institut für Geologie, Mineralogie und Geophysik, Universität Bochum
Neuhaus	Martin	Institut für Geophysik und extraterrestrische Physik, TU Braunschweig
Nowak	Marcus	Fachbereich Geowissenschaften, Universität Tübingen
Oberhänsli	Hedwig	Museum für Naturkunde, Leibniz-Institut für Evolutions- und Biodiversitätsforschung, Berlin
Oberhänsli	Roland	ICDP-Deutschland, Institut für Erd- und Umweltwissenschaften, Universität Potsdam
Oeser-Rabe	Martin	Institut für Mineralogie, Universität Hannover
Osborne	Anne	GEOMAR, Helmholtz-Zentrum für Ozeanforschung, Kiel
Pabich	Stephanie	Institut für Mineralogie, Universität Münster
Pälike	Heiko	MARUM - Zentrum für Marine Umweltwissenschaften, Universität Bremen

Panagiotopoulos	Konstantinos	Integrated Research Training Group, Universität Köln
Pesch	Katja	Institut für Mineralogie und Lagerstättenlehre, RWTH Aachen
Pfaender	Jobst	Museum für Naturkunde, Berlin
Pickarski	Nadine	Institut für Geologie, Mineralogie und Paläontologie, Universität Bonn
Pierdominici	Simona	Scientific Drilling ICDP, GFZ, Helmholtz-Zentrum Potsdam, Deutsches GeoForschungsZentrum, Potsdam
Pletsch	Thomas	BGR, Bundesanstalt für Geowissenschaften und Rohstoffe, Hannover
Prader	Sabine	Centre of Natural History, Institut für Geologie, Universität Hamburg
Preuß	Oliver	Fachbereich Geowissenschaften, Universität Tübingen
Prokopenko	Alexander	Department of Earth and Ocean Sciences, University of South Carolina, Columbia, USA
Pross	Jörg	Institut für Geowissenschaften, Universität Heidelberg
Raddatz	Jacek	GEOMAR, Helmholtz-Zentrum für Ozeanforschung, Kiel
Rammensee	Philipp	Institut für Geowissenschaften, Universität Frankfurt
Reiche	Sönke	Institute for Applied Geophysics and Geothermal Energy, RWTH Aachen
Renaudie	Johan	Museum für Naturkunde, Leibniz-Institut für Evolutions- und Biodiversitätsforschung, Berlin
Roehrlich	Dagmar	freie Wissenschaftsjournalistin, Köln
Roeser	Patricia	Institut für Geologie, Mineralogie und Paläontologie, Universität Bonn
Röhl	Ulla	MARUM - Zentrum für Marine Umweltwissenschaften, Universität Bremen
Romero	Oscar	MARUM - Zentrum für Marine Umweltwissenschaften, Universität Bremen
Sarnthein	Michael	Institut für Geowissenschaften, Universität Kiel
Schäbitz	Frank	Seminar für Geographie und ihre Didaktik, Universität Köln
Schäfer	Andreas	Institut für Geologie, Mineralogie und Paläontologie, Universität Bonn
Scheibner	Birgit	Institut für Geologie und Mineralogie, Universität Köln
Schier	Katharina	Institut für Geologie und Paläontologie, Universität Münster
Schindlbeck	Julie C.	GEOMAR, Helmholtz-Zentrum für Ozeanforschung, Kiel
Schlüter	Nils	Geowissenschaftliches Zentrum, Abteilung Geobiologie, Universität Göttingen
Schmincke	Hans-Ulrich	GEOMAR, Helmholtz-Zentrum für Ozeanforschung, Kiel
Schmitt	Ralf-Thomas	Museum für Naturkunde, Leibniz-Institut für Evolutions- und Biodiversitätsforschung, Berlin
Schneider	Kathrin	Institut für Geologie und Mineralogie, Universität Köln
Schneider	Ralf	Institut für Geowissenschaften, Universität Kiel
Schulz	Hartmut	Fachbereich Geowissenschaften, Universität Tübingen
Schwab	Markus	GFZ, Helmholtz-Zentrum Potsdam, Deutsches GeoForschungsZentrum, Potsdam
Schwalb	Antje	Institut für Geosysteme und Bioindikation, TU Braunschweig
Schwenk	Tilmann	Fachbereich Geowissenschaften, Universität Bremen
Simon	Helge	Institut für Geophysik und Geoinformatik, TU Bergakademie Freiberg
Stein	Rüdiger	AWI, Helmholtz-Zentrum für Polar- und Meeresforschung, Alfred-Wegener-Institut, Bremerhaven
Steinke	Stephan	MARUM - Zentrum für Marine Umweltwissenschaften, Universität Bremen
Steinmann	Lena	Fachbereich Geowissenschaften, Universität Bremen
Stelbrink	Björn	Systematics & Biodiversity Lab, Universtät Giessen
Stipp	Michael	GEOMAR, Helmholtz-Zentrum für Ozeanforschung, Kiel
Strack	Dieter	International Oil & Gas Consultant, Ratingen
Strauß	Harald	Institut für Geologie und Paläontologie, Universität Münster
Stuch	Beatrix	DFG, Deutsche Forschungsgemeinschaft, Bonn
Sumita	Mari	GEOMAR, Helmholtz-Zentrum für Ozeanforschung, Kiel
Teichert	Barbara	Institut für Geologie und Paläontologie, Universität Münster
Thiede	Jörn	GEOMAR, Helmholtz-Zentrum für Ozeanforschung, Kiel
Timmerman	Martin	ICDP-Deutschland, Institut für Erd- Und Umweltwissenschaften, Universität Potsdam
Trütner	Sebastian	MARUM - Zentrum für Marine Umweltwissenschaften, Universität Bremen
Türke	Andreas	Fachbereich Geowissenschaften, Universität Bremen
Uenzelmann-Neben	Gabriele	AWI, Helmholtz-Zentrum für Polar- und Meeresforschung, Alfred-Wegener-Institut, Bremerhaven
Umlauft	Josephine	Institut für Geophysik und Geologie, Univerität Leipzig
Urlaub	Morelia	GEOMAR, Helmholtz-Zentrum für Ozeanforschung, Kiel
Vahlenkamp	Maximilan	MARUM - Zentrum für Marine Umweltwissenschaften, Universität Bremen
van der Löcht	Julia	Institut für Geologie und Mineralogie, Universität Köln
Vandieken	Verona	Institut für Chemie und Biologie des Meeres, Universität Oldenburg
Virgil	Christopher	Institut für Geophysik und extraterrestrische Physik, TU Braunschweig
Voelker	Antje	Divisão de Geologia e Georecursos Marinhos, Instituto Português do Mar e da Atmosfera (IPMA), Lissabon, Portugal
Voigt	Silke	Institut für Geowissenschaften, Universität Frankfurt
Vossel	Hannah	Institut für Geologie, Mineralogie und Paläontologie, Universität Bonn
Wagner	Bernd	Institut für Geologie und Mineralogie, Universität Köln
Wagner	Luise	Universität Bonn
Wainwright	Ashlea	Institut für Geologie, Mineralogie und Paläontologie, Universität Bonn
Wang	Meng	Institut für Mineralogie, Universität Hannover
Wefer	Gerold	MARUM - Zentrum für Marine Umweltwissenschaften, Universität Bremen
Westerhold	Thomas	MARUM - Zentrum für Marine Umweltwissenschaften, Universität Bremen
Weyer	Stefan	Institut für Mineralogie, Universität Hannover
Wiersberg	Thomas	Scientific Drilling ICDP, GFZ, Helmholtz-Zentrum Potsdam, Deutsches GeoForschungsZentrum, Potsdam

Wiese	Frank	Geowissenschaftliches Zentrum Göttingen, Universität Göttingen
Winkler	Amelia	DFG, Deutsche Forschungsgemeinschaft, Bonn
Wörner	Gerhard	Geowissenschaftliches Zentrum Göttingen, Universität Göttingen
Wilke	Sören	Institut für Mineralogie, Universität Hannover
Wilke	Tom	Institut für Tierökologie & Spezielle Zoologie, Universität Gießen
Wonik	Thomas	LIAG, Leibnitz-Institut für Angewandte Geophysik, Hannover
Yosef Nejad	Davood	Institut für Geologie, Mineralogie und Paläontologie, Universität Bonn
Zhang	Chao	Institut für Mineralogie, Universität Hannover
Zirner	Aurelia	Institut für Geologie, Mineralogie und Paläontologie, Universität Bonn
Zolitschka	Bernd	Institut für Geographie, Universität Bremen

Felis, T., McGregor, H.V., Linsley, B.K., Tudhope, A.W., Gagan, M.K., Suzuki, A., Inoue, M., Thomas, A.L., Esat, T.M., Thompson, W.G., Tiwari, M., Potts, D.C., Mudelsee, M., Yokoyama, Y., Webster, J.M.	Intensification of the meridional temperature gradient in the Great Barrier Reef following the Last Glacial Maximum - Results from IODP Expedition 325	IODP	40
Flores-Estrella, H., Umlauft, J., Schmidt, A., Korn, M.	Localization of CO_2 degassing zones, mofettes, using dense small array data and Matched Field Processing analysis in the NW Bohemia/Vogtland region, Czech Republic	ICDP	41
Foerster, V., Asrat, A., Cohen, A., Junginger, A., Lamb, H.F, Schäbitz, F., Trauth, M.H., HSPDP Science Team	Three promising tonnes of sediment cores from Chew Bahir, south Ethiopia, to reconstruct 0.5 Ma of climatic history	ICDP	41
Francke, A., Wagner, B., Zanchetta, G., Sulpizio, R., Leicher, N., Gromig, R., Just, J., Baumgarten, H., Lindhorst, K., Wonik, T., Krastel, S., Lacey, J., Leng, M., Vogel, H., SCOPSCO Science Team	Environmental variability in the Balkan Region between the MPT and present day, derived from lacustrine sediments of the 1.2 Ma old Lake Ohrid: The ICDP SCOPSCO project	ICDP	42
Friese,A., Vuillemin, A., Alawi, M., Wagner, D., Kallmeyer, J.	Microbial populations in iron-rich sediments of Lake Towuti at varying bottom water oxygenation levels – Results of a pilot study for the 2015 ICDP drilling campaign	ICDP	45
García Gallardo, A., Grunert, P., Piller, W.E., Jiménez Espejo, F.J., Van der Schee, M., Sierro Sanchez, F.	The influence of the Mediterranean Outflow Water on the Late Miocene Gulf of Cádiz.	IODP	46
Gebregiorgis, D., Hathorne, E.C., Giosan, L., Collett, T.S., Nürnberg, D., Frank, M.	Pleistocene Indian Monsoon rainfall variability	IODP	46
Gussone, N., Teichert, B.M.A., Friedrich, O.	Evaluation of calcareous dinoflagellate cysts as recorders for temperature changes and fluctuations in ocean chemistry	IODP	48
Haberzettl, T., Frenzel, P., Kasper, T., Mäusacher, R., Reicherter, K., Schwalb, A., Spiess, V., Wang, J., Wilke, T., Zhu, L., Daut, G.	Lake Nam Co (central Tibetan Plateau) - a high-potential ICDP drilling site	ÎCDP	49
Hasberg, A., Melles, M., Vogel, H., Russel, J.	ICDP drilling at Lake Towuti, Indonesia, in 2015: settings, site survey, and objectives for paleoclimatological research	ICDP	50
Hathorne, E.C., Frank, M., Kirkpatrick, J., Peketi, A., Sagar, N., Expedition 353 Scientists	Rare Earth Element (REE) concentrations of IODP Expedition 353 pore waters from the Bay of Bengal: Implications for the REE budget of seawater and palaeo-circulation studies using Nd isotopes	IODP	51
Hauffe, T., Jovanovska, E., Stelbrink, B., Wagner, B., Levkov, Z., Francke, A., Albrecht, C., Wilke, T.	The SCOPSCO deep drilling program in ancient Lake Ohrid: Unravelling the geological and environmental drivers leading to the extraordinary biodiversity in Europe's oldest lake	ICDP	51
Hinrichs, K.-U. & 43 co-authors	IODP Expedition 337: Exploring the deep biosphere nearly 2.5 km below the seafloor	IODP	53
Hockun, K., Mollenhauer, G., Schefuß, E., PASADO Science Team	PASADO Lipids'- paleoenvironmental reconstruction in Southern Patagonia	ICDP	54
Holbourn, A. Kuhnt, W., Lyle, M., Schneider, L., Romero, O., Kochhann, K.G.D., Andersen, N.	Early to middle Miocene climate evolution: New insights from IODP Sites U1337 and U1338 (eastern equatorial Pacific Ocean)	IODP	57
Holbourn, A., Kuhnt, W., Clemens, S.C., Prell, W., Andersen, N.	Cryosphere expansion and East Asian monsoon variability during the Miocene (16.5-5 Ma): Insights from ODP Site 1146 (South China Sea)	IODP	60
Huber, B., Bahlburg, H., Drewer, C.	Denudation history of the St. Elias orogen: working programme of a provenance study of sediments from the Surveyor Fan, Gulf of Alaska	IODP	60
Hüpers, A., Trütner, S., Ikari, M.J., Kopf, A.J.	Friction properties of rocks sampled from a fossil accretionary prism	IODP	61
Inoue, M., Gussone, N., Koga, Y., Iwase, A., Suzuki, A., Sakai, K., Kawahata, H.	Controlling factors of Ca isotope fractionation in Porites corals evaluated by culture experiments and downcore records	IODP	62

Iovine, R.S., Wörner, G., Pabst, S., Arienzo, I., Civetta, L., D'antonio, M., Orsi, G.	The history of the Campi Flegrei (Napoli, Italy) magma system through time: the key to understand present and future volcanic processes.	ICDP	63
Jakob, K., Friedrich,O., Pross, J.	Deciphering early Pleistocene sea level variability and millennial-scale climate fluctuations in the eastern equatorial Pacific	IODP	63
Jehle, S., Bornemann, A., Deprez, A., Speijer, R.P.	The paleoenvironmental impact of the Latest Danian Event and response of planktic foraminifera at ODP Site 1210 (Shatsky Rise, Pacific Ocean)	IODP	66
Jiménez, N., Krüger, M.	Degradation of complex organic matter by methanogenic microbial communities in deep subsurface systems	IODP	68
Kallmeyer, J., Grewe, S., Glombitza, C., Kitte, J.A.	Microbial abundance in lacustrine sediments, a case study from Lake Van, Turkey	ICDP	69
Kemner, F., Beier, C., Haase, K.	The magmatic and geochemical evolution of oceanic intraplate volcanoes: constraints from the Louisville Seamounts and other Pacific hotspots	IODP	69
Kopf, A.J.	Amphibious drilling projects maximise benefits from ICDP and IODP initiatives: The example of the Ligurian slope near Nice	IODP & ICDP	70
Kotthoff, U., Andrén, T., Bauersachs, T., Fanget, A.-S., Granoszewski, W., Groeneveld, J., Quintana Krupinski, N., Peyron, O., Stepanova, A., Cotterill, C., Expedition 347 Science Party	Reconstructing palaeo-environmental and climatic conditions in the Baltic region: A multi-proxy comparison from IODP Site M0059 (Little Belt)	IODP	71
Krastel, S., Mountjoy, J., Crutchley, G., Koch, S., Dannowski, A., Pecher, I., Bialas, J.	Understanding slow-slipping submarine landslides: 3D seismic investigations of the Tuaheni landslide complex as support for IODP Ancillary Project Letter 841APL	IODP	72
Krauß, F., Simon, H., Giese, R., Buske, S., Hedin, P., Juhlin, C., Lorenz, H.	Zero-Offset VSP in the COSC-1 borehole	ICDP	73
Kriegerowski, M., Cesca, S.	Approaching Q factor tomography of Western Bohemia using a master and slave event method	ICDP	74
Kunkel, C., Aehnelt, M., Gaupp, R., Abratis, M., Kukowski, N., Totsche, K. U., INFLUINS Scientific Drilling Team	Sedimentology of the Middle Buntsandstein in the INFLUINS Scientific Deep Drilling in the Thuringian Syncline: Implications for Aquifer Characteristics	ICDP	75
Kurzawski, R.M., Stipp, M., Niemeijer, A., Spiers, C.J., Behrmann, J. H.	Earthquake nucleation in calcareous sediments from offshore Costa Rica triggered by a combined temperature and pore fluid pressure increase, Costa Rica Seismogenesis Project (CRISP)	IODP	75
Kutterolf, S., Brenner, M., Freundt, A., Krastel, S., Meyer, A., Muñoz, A., Pérez, L., Schwalb, A.	Paleoclimate, Paleoenvironment, and Paleoecology of Neogene Central America: Bridging Continents and Oceans (NICA-BRIDGE)	ICDP	76
Lamy, F., Abelmann, A., Anderson, R., Arz, H., Cortese, G., Esper, O., Frank, M., Gohl, K., Hall, I., Harada, N., Hebbeln, D., Kilian, R., Kuhn, G., Lange, C., Lembke-Jene, L., Mackensen, A., Martinez-Garcia, A., Ninnemann, U., Nürnberg, D., Pahnke, K., Polonia, A., Stoner,J., Tiedemann, R., Uenzelmann-Neben, G., Winckler, G.	Plio-Pleistocene paleoceanography of the Subantarctic Southeast Pacific linked to Drake Passage throughflow (SUBANTPAC)	IODP	77
Lay, V., Buske, S., Kovacs, A., Gorman, A.	Seismic site characterization for the Deep-Fault-Drilling-Project Alpine Fault	ICDP	78
Lazarus, D.	Cenozoic plankton evolution: a tale of young and old oceans, old and young clades?	IODP	80
Lehnert, O., Meinhold, G., Wu, R., Calner, M., Joachimski, M.M.	A Lower–Middle Ordovician composite $\delta^{13}C$ record for central Sweden based on drillcores from the Siljan impact structure	ICDP	81
Leicher, N., Zanchetta, G., Sulpizio, R., Giaccio, B., Nomade, S., Wagner, B., Francke, A.	First tephrostratigraphic results of the DEEP site record in Lake Ohrid, Macedonia	ICDP	84

Schäbitz, F., Wagner, B., Viehberg, F.A., Wennrich, V., Rethemeyer, J., Just, J., Klasen, N., Asrat, A., Lamb, H., Foerster, V., Trauth, M.H., Junginger, A., Cohen, A., HSPDP Science Team	Preliminary results from the deep drilling at Chew Bahir, south Ethiopia	ICDP	114
Schindlbeck, J.C., Kutterolf, S., IODP Expedition 350 and 352 Science Parties	Izu-Bonin-Arc tephrostratigraphy- evolution, provenance, cyclicities (IODP Exp. 350 & 352)	IODP	115
Schindlbeck, J.C., Kutterolf, S., Freundt, A.	Galápagos Plinian volcanism- evidence in ODP/IODP Legs offshore Central America	IODP	116
Schlüter, N., Wiese, F., Reich, M.	Persistence of atelostomate sea urchins (Spatangoida and Holasteroida; irregular echinoids) in the deep sea, or repeated migration events into the deep-sea?	IODP	116
Schwenk, T., Spieß, V., France-Lanord, C., IOPD Exp. 354 Scientific Party	The Bengal Fan stratigraphy as a function of tectonic and climate – Analysis of seismic data from the Bay of Bengal and a first comparison to IODP Expedition 354 results	IODP	118
Schwenk, T., Mohtadi, M., Gernhardt,F., Bergmann, F., Wenau, S.	Pre-site survey for IODP Expedition 363 (West Pacific Warm Pool) – Results from Cruise SO-228 (May 2013)	IODP	119
Simon, H., Krauss, F., Hedin, P., Buske, S., Giese, R., Juhlin, C.	A combined surface and borehole seismic survey at the COSC-1 borehole	ICDP	120
Stein, R., Blackman, D., Inagaki, F., Larsen, H.-C.	Earth and Life Processes Discovered from Subseafloor Environment – A Decade of Science Achieved by the Integrated Ocean Drilling Program (IODP)	IODP	121
Steinmann, L., Spiess, V., Sacchi, M.	Resurgence and collapse processes at the Campi Flegrei caldera (Italy): Results from a seismic reflection Pre-Site Survey for combined IODP/ICDP drilling campaigns	ICDP	122
Strauss, H., Montinaro, A., Fugmann, A., Krieger, K., Schier, K., Mason, P., Galic, A.	Peering into the Cradle of Life: stable isotopic investigation of Paleoarchean sediments from the 3.23 – 3.55 billion years old Barberton Greenstone Belt, South Africa	ICDP	125
Sumita, M., Schmincke, H.-U.	Chronological, petrological, volcanological, hydrological and paleoclimatological evolution of a 219 m core drilled at Site 2 into Lake Van during the Paleovan ICDP Drilling project, a preliminary synthesis	ICDP	126
Teichert, B.M.A., Schacht, V., Gussone, N., März, C., Strauss, H.	Constraining the dynamics of fluid flow at the northeastern Pacific continental margin	IODP	127
Türke, A., Bach, W.	Palagonitization of basalt glass in the flanks of mid-ocean ridges: implications for the bioenergetics of oceanic intracrustal ecosystems	IODP	127
Uenzelmann-Neben, G., Gruetzner, J.	A seismic approach to the paleoceanography of the eastern South Atlantic	IODP	130
Vossel, H., Litt, T., Reed, J.M.	The diatom flora of Lake Kinneret (Israel) – Palaeolimnological evidence for Holocene climate change and human impact in the southeastern Mediterranean	ICDP	131
Westerhold, T., Röhl, U., Frederichs, T., Bohaty, S.M., Zachos, J.C.	Towards a complete and accurate Eocene chronostratigraphic framework	IODP	132
Westerhold, T., Bohaty, S.M., Uenzelmann-Neben, G., 862-Pre Proponents	Maurice Ewing Bank–Georgia Basin Depth Transect: A Southern Ocean Perspective on Paleogene Climate Evolution (IODP 862-Pre)	IODP	133
Wiese, F., Schlüter, N., Reich, Zirkel, J., M., Herrle, J.	From bycatch to main dish – spines of irregular echinoids as monitors for macrofaunal dynamics in the deep sea during Cenozoic critical intervals? A pilot study.	IODP	134
Wilke, S., Almeev, R., Christiansen, E. H., Holtz, F.	Cotectic compositions of rhyolite as a geobarometer for highly evolved melts of the Yellowstone Snake River Plain	ICDP	136
Zhang, C., Koepke, J., Godard, M., France, L.	Mid-Ocean Ridge Gabbro-Diorite-Tonalite Plutonic System Recovered from IODP Hole 1256D, Eastern Pacific: Implications for the Nature of Axial Melt Lens beneath Fast-spreading Ridges	IODP	138

Fahrtberichte

IODP Expedition 351 Izu-Bonin-Mariana Arc Origins – Subduction initiation and evolution of a young island arc

P.A. BRANDL[1,2], M. NEUHAUS[3] AND IODP EXPEDITION 351 SCIENTISTS

1 GeoZentrum Nordbayern, Friedrich-Alexander-Universität Erlangen-Nürnberg, Schloßgarten 5, 91054 Erlangen, Germany
2 Research School of Earth Sciences, The Australian National University, 142 Mills Road, Acton ACT 2601, Australia
3 Institut für Geophysik und extraterrestrische Physik. Technische Universität Braunschweig, Mendelsohnstr. 3, 38106 Braunschweig, Germany

Subduction initiation plays a key role in global plate tectonics and is considered a major driver of mantle processes. Despite this fact, the detailed processes of subduction initiation are poorly constrained. There exist numerous competing models describing it in various tectonic settings; two of the most prevalent are induced or spontaneous (e.g., Stern, 2004). Due to this uncertainty, further understanding of subduction initiation and subsequent island arc inception has been identified as one of the main scientific objectives of the 2013-2023 science plan of the International Ocean Discovery Program (IODP; http://www.iodp.org). In this respect, the Izu-Bonin-Mariana (IBM) intra-oceanic island arc system is a prime location for further investigation and has been intensively studied over the past few decades (e.g., Reagan et al., 2010; Ishizuka et al., 2011). In the past, dredge, submersible and ocean drilling expeditions collected samples and information on subduction processes along the margin of the Philippine Sea Plate (PSP). However, previous studies were focused on areas that were not the most appropriate for investigating subduction initiation of the IBM subduction zone and island arc.

The primary scientific objectives of IODP Expedition 351 Izu-Bonin-Mariana Arc Origins were thus (1) to determine the origin and composition of the basement prior to arc inception, (2) to identify and model the process of subduction initiation, (3) to determine the compositional evolution of the early IBM island arc and (4) to establish the geophysical properties of the Amami Sankaku Basin (Arculus et al., 2013). In order to achieve these goals, the Amami Sankaku Basin (Fig. 1) to the west of the Kyushu-Palau Ridge (KPR), the nascent IBM arc, was identified as the ideal drilling location. Subduction in this region is believed to have started about 52 Ma ago (Ishizuka et al., 2014) with active island arc volcanism along the KPR. Intra-arc rifting separated the KPR from the currently active IBM system about 22-25 Ma ago, preserving a snapshot of the depositional and tectonic conditions at that time. Despite challenging drilling conditions due to deep water (4700 m) and thick sediment cover (>1400 m), Site U1438 (IBM-1) was successfully drilled.

IODP Expedition 351 cored the entire sedimentary section and into the oceanic igneous crust, which likely underlies the KPR itself, by establishing four successively deeper holes. An additional hole was drilled as a dedicated downhole logging hole. From Site U1438, sediments were recovered and identified as belonging to four different

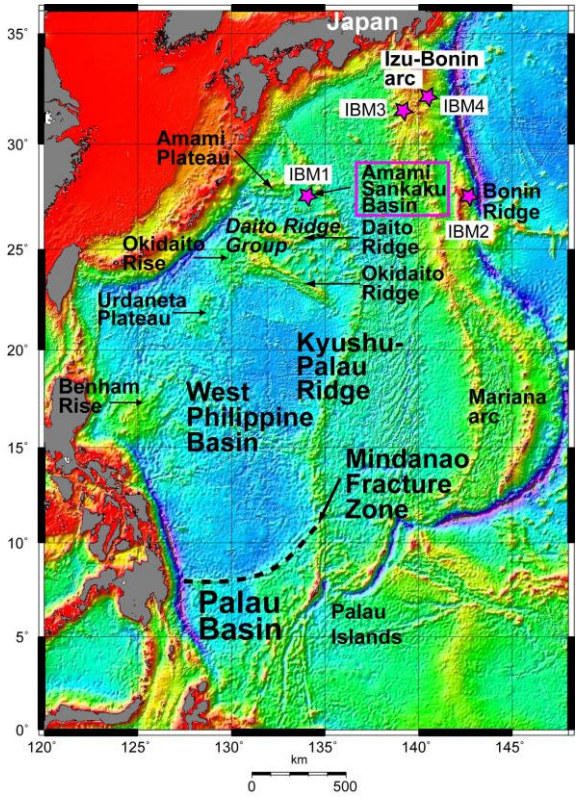

Fig. 1. Bathymetric map of the Western Pacific with locations of the proposed drilling locations for IODP Expeditions 350, 351 and 352. Site U1438 (IBM-1) is located in the Amami Sankaku Basin, west of Kyushu-Palau Ridge.

lithostratigraphic units (I-IV) adding up to a total penetration of more than 1460 m (Fig. 2). At the sediment-basement contact, a further 150 m thick section of the oceanic igneous crust was cored, and contains fresh basaltic lava flows. The sediments consisted of a sequence of unconsolidated pelagic and hemipelagic sediments post-dating the time of active arc volcanism in this region (Lithostratigraphic Unit I). Clays and episodic foraminifer ooze are accompanied by cm- to dm-thick layers of volcanic ash, likely originating from volcanic eruptions in the western Pacific. Unit II becomes progressively consolidated and sediments eventually lithify. These sedimentary rocks consist of numerous cycles of gravity flow deposits shed from the KPR during its latest activity stage. The Unit II-III boundary exhibits the first occurrence of coarse-grained volcaniclastic sediments, reflecting a more active phase of the KPR and/or a more proximal location of Site U1438 relative to the arc. Unit III contains material up to pebble- or even cobble-size, and is pumice-dominated in the upper stratigraphic part and more scoria-rich in the lower. Fresh magmatic minerals typical of island arcs, such as clinopyroxenes and amphiboles, are present throughout Unit III. As a result of the presence of coarse sediments, sedimentation rates during the deposition of Unit III were relatively high and the sequence itself is more than 1000 m thick. Below that, Unit IV is made up of finer-grained sediments and likely reflects deposition during island arc inception and subduction initiation about 50 Ma ago. Nonmagnetic core barrels were used for drilling the Site, resulting in a high-quality magnetostratigraphy that is consistent with biostratigraphic datums. However, the quality of the magnetostratigraphic record is reduced throughout Unit II and became completely uncertain in the

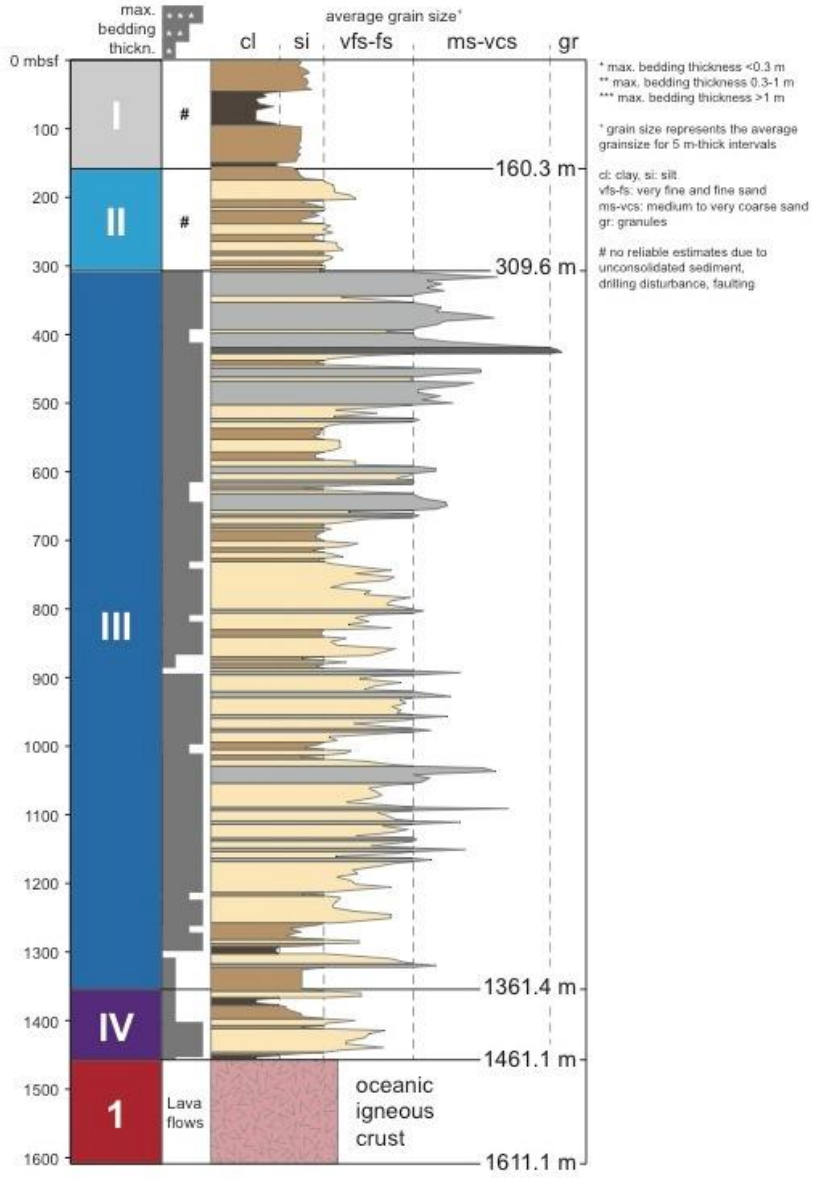

Fig. 2. Lithostratigraphic summary of Site U1438 (IBM-1)

middle of Unit III. Despite this, sparse but continuous biostratigraphic constraints were established essentially to the oceanic basement (including Unit IV).

IODP Expedition 351 added another of only a few drill sites that successfully penetrated more than 100 m into the oceanic igneous crust. The local igneous basement is composed of several distinct basaltic lava flows. However, since distinct cooling or mineralogical units were impossible to identify with shipboard techniques, igneous Unit 1 was described as a single Unit with minor variations in mineralogy and grain size. The age and composition of the underlying basement are crucial for identifying and modelling the process of subduction initiation.

Planned downhole logging operations included using the so-called triple combination tool string,, measuring density, porosity and resistivity, the formation microscanner and sonic tool string (FMS-Sonic), the versatile seismic imager (VSI) and the Göttingen Borehole Magnetometer (GBM). However, borehole stability and/or diameter issues led to the decision to drill an additional and dedicated logging hole after coring was completed. All logging data (triple combination, FMS-Sonic, VSI and GBM) are of high quality and consistent with the core data, supplementing information collected from lithostratigraphy. In the future, shipboard analyses together with post-cruise research should uncover interesting aspects and further insights into the process of subduction initiation and island arc inception. Overall, IODP Expedition 351 Izu-Bonin-Mariana Arc Origins was outstanding in terms of drilling operations and the achievement of all primary goals set out in the Scientific Prospectus (Arculus et al., 2013). However, many aspects of the shipboard results are currently under embargo and thus we ask for some patience for published results.

References:

Arculus, R.A., Ishizuka, O.I. & Bogus, K.A. (2013), IODP Expedition 351 Scientific Prospectus, doi:10.2204/iodp.sp.351.2013.

Ishizuka, O., Tani, K., Reagan, M. K., Kanayama, K., Umino, S., Harigane, Y., Sakamato, I., Miyajima, Y. & Dunkley, D. J. (2011). The timescales of subduction initiation and susebquent evolution of an oceanic island arc. Earth and Planetary Science Letters 306, 229–240.

Ishizuka, O., Tani, K. & Reagan, M. K. (2014). Izu-Bonin-Mariana forearc crust as an modern ophiolite analogue. Elements 10, 115–120.

Reagan, M. K. et al. (2010). Fore-arc basalts and subduction initiation in the Izu-Bonin-Mariana system. Geochemistry Geophysics Geosystems 11, Q03X12.

Stern, R. J. (2004). Subduction initiation: spontaneous and induced. Earth and Planetary Science Letters 226, 275–292.

Expedition report for IODP Expedition 350: Izu-Bonin-Mariana: The missing half of the subduction factory

A.-S. JONAS[1], J. C. SCHINDLBECK[2], IODP EXPEDITION 350 SCIENCE PARTY[3]

1 Institute of Geosciences, Christian-Albrechts-University, D-24118 Kiel, Germany
2 GEOMAR, Helmholtz Center for Ocean Research Kiel, D-24148 Kiel, Germany
3 IODP Exp. 350 science party: Andrews, G., Barker, A., Berger, J., Blum, P., Bongiolo, E., Bordiga, M., Busby, C., DeBari, S., Gill, J., Hamelin, C., Jia, J., John, E., Jutzeler, M., Kars, M., Kita, Z., Konrad, K., Mahony, S., Martini, M., Miyazaki, T., Musgrave, R., Nascimento, D., Nichols, A., Ribeiro, J., Sato, T., Schmitt, A., Straub, S., Tamura, Y., Vautravers, M., Yang, Y.

Previous drilling efforts to the Izu-Bonin-Mariana (IBM) arc system have focused mainly on the IBM fore arc and the magmatic evolution of the volcanic front through 50 Ma. Rear-arc IBM magmatic history has not been similarly well studied in spite of its importance in mass balance and flux calculations for crustal evolution, in establishing whether and why arc-related crust has inherent chemical asymmetry, in testing models of mantle flow and the history of mantle depletions and enrichments during arc evolution, and in testing models of intracrustal differentiation. IODP Expedition 350 (30 March–30 May 2014) from Keelung, Taiwan to Yokohama, Japan was the first of three closely related IODP expeditions drilling the Izu-Bonin-Mariana arc system in 2014 (Fig. 1). To understand the evolution of the whole IBM crust, IODP Exp. 350 drilled the Izu rear-arc region at Site U1437 located ~ 330 km west of the Izu-Bonin trench and ~ 90 km west of the arc-front volcanoes Myojinsho and Myojin Knoll, at 2117 mbsl.

We set sail from Keelung, Taiwan to our first drill site, IODP Site U1436 (proposed Site IBM-4) in the western part of the Izu-Bonin fore-arc basin ~60 km east of the arc-front volcano Aogashima and ~170 km west of the axis of the Izu-Bonin Trench, 1.5 km west of ODP Site 792 (Fig. 1, Fig. 2), at 1776 mbsl. The objective at Site U1436 was to obtain cores to 150 m depth for geotechnical testing in preparation of a potential future deep (5500 mbsf) drilling program with the D/V Chikyu. Drilling at Site U1436 yielded a rich, relatively complete 131.72 m thick succession of Late Pleistocene fore-arc sedimentation that is strongly influenced by frontal arc explosive volcanism as indicated by distinctive mafic and felsic ash layers that may record large-volume eruptions on the Izu arc front. In an attempt to get better recovery at a specific depth interval, Site U1436 was drilled in three additional holes (U1436B, C, and D) at the end of the cruise, after further drilling at Site U1437 became impossible due to the failure of the subsea camera cable, to better constrain the undisturbed thickness of specific mafic ash layers.

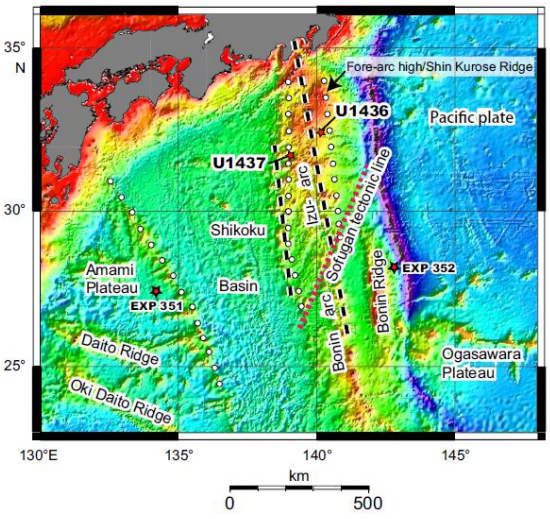

Fig. 1. Bathymetric map of the NE Philippine Sea, IBM arc system, and Exp. 350, 351 and 352 sites positions. Dashed lines = wide-angle seismic profiles; lines of circles = conspicuous N-S rows of long-wave-length magnetic anomalies (Expedition 350 Scientists, 2014, Preliminary Report).

After completion of operations at Hole U1436A, we moved to the primary Site U1437 (proposed Site IBM-3), which is located in a volcano-bounded basin between two major construc¬tional volcanic ridges (Fig. 2): the Manji and Enpo rear-arc seamount chains in the Izu rear arc, ~330 km west of the axis of the Izu-Bonin Trench and ~90 km west of the arc-front volcanoes Myojinsho and Myojin Knoll, at 2117 mbsl. The primary scientific objective for Site U1437 was to characterize “the missing half of the subduction factory”; this was because numerous ODP/Integrated Ocean Drilling Program sites had been drilled in the arc to fore-arc region (i.e., ODP Site 782A Leg 126), but this was the first site to be drilled in the rear part of the Izu arc. A complete view of the arc system is needed to understand the formation of oceanic arc crust and its evolution into continental crust. Site U1437 had excellent core recovery in Holes U1437B and U1437D, and we succeeded in hanging the longest casing ever in the history of R/V JOIDES Resolution scientific drilling (1085.6 m) in Hole U1437E and drilled a total depth of 1806.5 m. Shipboard biostratigraphy and magneto-stratigraphy set the age covered by the upper 1303 m of the Site U1437 sediment succession from Pleistocene to upper Miocene. The age model has not been extended deeper since no magnetostratigraphic or biostratigraphic datums were detectable from 1303 to 1806 mbsf. The sedimentary succession recovered from the three holes of Site U1437 was divided into seven lithostratigraphic units. Lithostratigraphic Unit I from 0-682.12 mbsf is 0-4.3 Ma in age and is composed mainly of mud or mudstone with > 25% dispersed ash, referred to as tuffaceous mud/ tuffaceous mudstone. Subsequent lithostratigraphic Unit II (682.12 - 728.1 mbsf) has much more abundant tephra layers and much less tuffaceous mudstone, and the tephra layers are coarser (lapilli-size) than in units I and III. Unit III from 728.1 to 1017.88 mbsf consists of tuffaceous mudstone and less abundant tuff layers. Lithostratigraphic Unit IV from 1017.88 to 1120.11 mbsf is composed of coarse-grained tuff and polymictic lapilli tuff and lapillistone layers with minor tuffaceous mudstone intervals. Underlying Unit V (1120.11-1312.21 mbsf) is distinguished largely based on its intervals of monomictic, reversely graded lapilli tuff, which contrast with the polymictic, dominantly lithic lapilli tuff layers of the overlying and underlying lithostratigraphic units. Unit VI from 1320.00 to 1459.80 mbsf is dominated by thick beds of lapilli tuff and lapillistone with lesser tuff and minor tuffaceous mudstone intervals and is further characterized by abundant polymictic lithic and pumice lapilli tuffs. The only igneous unit observed at Site U1437 consists of a

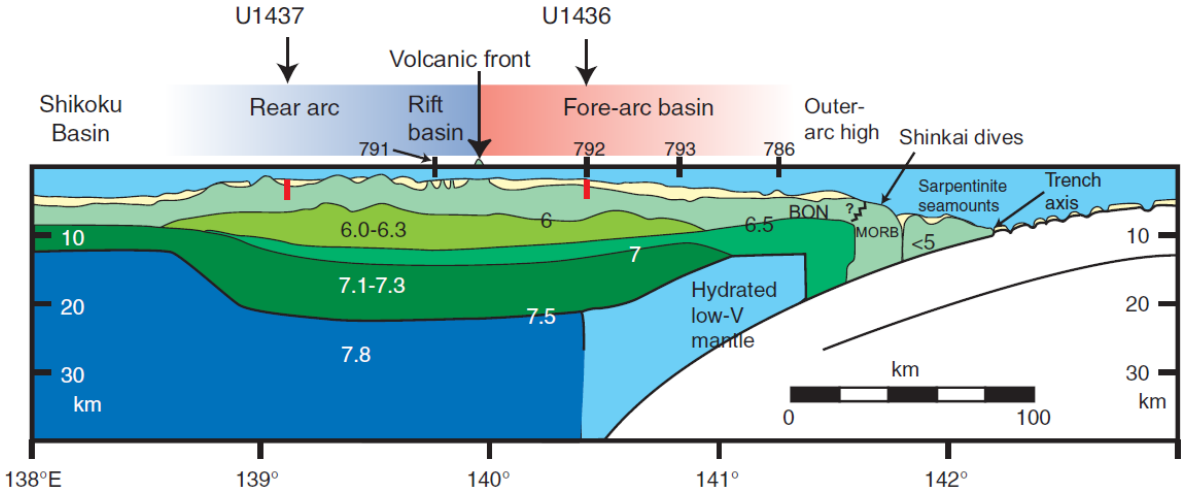

Fig. 2. Wide-angle seismic profile across Izu arc with P-wave velocities for upper, middle, and lower crust (greens) and for mantle (blues) (From Expedition 350 Scientists, 2014; modified after DeBari et al, 1999; based on data from Suyehiro et al., 1996.). ODP and IODP sites are projected onto this line of section.

single rhyolite intrusion at 1389 mbsf, which lies within lithostratigraphic Unit VI. The top of the lowermost lithostratigraphic Unit VII is at 1459.8 mbsf, and Hole U1437E ended in Unit VII. Unit VII is dominated by thick bedded, nongraded, nonstratified, poorly sorted, coarse-grained angular andesitic lapilli tuff. Some clasts have quenched margins, jigsaw-fit textures, and intricate fluidal or peperitic margins and the unit is thus interpreted to be a vent-proximal deposit.

After completion of drilling operations at Site U1437 and a short return to Site U1436, Expedition 350 ended in Yokohama, Japan on May 30, 2014.

References:

DeBari, S. M., Taylor, B., Spencer, K., and Fujioka, K., 1999. A trapped Philippine Sea plate origin for MORB from the inner slope of the Izu-Bonin trench. Earth and Planetary Science Letters, 174, 183-197

Expedition 350 Scientists, 2014. Izu-Bonin-Mariana rear arc: the missing half of the subduction factory. International Ocean Discovery Program Preliminary Report, 350. http://dx.doi.org/10.14379/ iodp.pr.350.2014 .

Suyehiro, K., Takahashi, N., Ariie, Y., Yokoi, Y., Hino, R., Shinohara, M., Kanazawa, T., Hirata, N., Tokuyama, H., and Taira, A., 1996. Continental crust, crustal underplating, and low-Q upper mantle beneath an oceanic island arc. Science, 272(5260): 390–392. http://dx.doi.org/10.1126/science.272.5260.390.

IODP Expedition 352 cruise report:

"Testing subduction initiation and ophiolite models by drilling the outer Izu-Bonin-Mariana fore-arc"

M. KIRCHENBAUR[1], R. ALMEEV[2], S. KUTTEROLF[3] AND EXPEDITION 352 SCIENTISTS

1 Institut für Geologie und Mineralogie, Universität zu Köln, Zülpicher Strasse 49b, 50674 Köln
2 Institut für Mineralogie, Leibniz Universität Hannover, Callinstrasse 3, 30167 Hannover
3 GEOMAR Helmholtz Zentrum für marine Forschung Kiel, Wischhofstrasse 1-3, 24148 Kiel

The process of subduction is considered as one of the major manifestations of a dynamic Earth, with subduction zones stretching for over 55 000 km across our planet. Yet, surprisingly little is known about how subduction initiates in the first place. The Izu-Bonin-Mariana (IBM) system presents one of the key localities to study subduction initiation, arc evolution, and continental crust formation. Additionally, many ophiolites are now associated with subduction initiation and the IBM fore-arc provides a similar lava stratigraphy as found in many ophiolites. The main objectives of IODP Expedition 352 were therefore to: (1) obtain a high-fidelity record of magmatic evolution during subduction initiation and early arc development; (2) test the hypothesis that fore-arc basalts (FAB) lie beneath boninites and understand chemical gradients within these units and across the transition; (3) use drilling results to understand how mantle melting processes evolve during and after subduction initiation; and (4) test the hypothesis that the fore-arc lithosphere created during subduction initiation is the birthplace of supra-subduction zone (SSZ) ophiolites.

Expedition 352 IBM fore-arc started on July 30th 2014 in Yokohama (Japan) and ended on September 29th 2014 in Keelung (Taiwan). During this time four sites were drilled (U1439, U1440, U1441, U1442) and a total of 1.22 km of igneous basement and 0.46 km of sediments were successfully cored. The two deep-water Holes U1440B and U1441A (4775 and 4447 m below sea level [mbsl], respectively) were drilled to 383.6 and 205.7 m below seafloor (mbsf), respectively and recovered mostly Fore-arc Basalts (FABs). A sediment cover of 101 m was recovered in Hole U1440A and 83 m in Hole U1441A consisting of pumice-rich volcaniclastic deep water sediments that were affected to different extents by tectonically triggered local gravity redeposition and current reworking. From the two shallower sites to the west (3128 and 3162 mbsl, respectively), Holes U1439C (to 544.3 mbsf) and U1442A (to 529.8 mbsf), mainly boninites were cored with a 200 m sediment cover in Hole U1439A and a 83 m sediment cover in Hole U1442A. Overall, the drilled sediments at all four sites range in age from Eocene to recent and the major lithologies include nannofossil ooze, mud and coarse sand, and volcaniclastic material including a total of 132 air fall tephra layers that record at least three major episodes of highly explosive volcanism (latest Pliocene to Pleistocene, late Miocene to earliest Pliocene, and Oligocene).

Overall, and within the scope of post-cruise research, Expedition 352 successfully recovered four lava sequences that are rooted in their own feeder dike system, providing evidence for the temporal evolution of volcanic activity during the initiation of subduction in the IBM fore-arc. The recovered sequences include: (1) a lava stratigraphy that largely reflects a change from decompressional melting to flux melting; (2) a sediment cover that provides the opportunity to study paleogeographic implications of the region and the geochemical character of and controls on the pelagic and hemipelagic sediments; as well as (3) a continuous record of mainly air-fall tephras that will contribute information to the temporal evolution of the volcanic activity of the IBM and also to a more dedicated study regarding cyclicities and potential provenances of explosive volcanism.

Abstracts

ICDP

Chemical and isotope composition of drilling mud gas sampled at the INFLUINS borehole EF-FB 1/12 (Thuringian Basin, Germany)

M. ABRATIS[1], T. WIERSBERG[2], M. GÖRLITZ[1], W. A. BRAND[3], L. VIERECK[1], N. KUKOWSKI[1], K. U. TOTSCHE[1]

1 Friedrich Schiller Universität Jena, Institut für Geowissenschaften, Burgweg 11, 07749 Jena
2 Helmholtz-Zentrum Potsdam, Deutsches GeoForschungsZentrum GFZ, Wissenschaftliches Bohren, Telegrafenberg A69, 14473 Potsdam
3 Max-Planck-Institut für Biogeochemie, Hans-Knöll-Str. 10, 07745 Jena

Drilling mud gas was monitored and sampled during standard rotary and core drilling of the 1179 m deep INFLUINS borehole EF-FB 1/12 to gain information on the composition of gases and their distribution at depth of the Thuringian Syncline (Germany).

The total abundance of formation gases in drilling mud was low. Methane, helium, hydrogen and carbon dioxide were detected in drilling mud when the drill hole encountered gas-rich strata, reaching maximum concentration of 55 ppmv He, 1400 ppmv of CH_4, 400 ppmv of hydrogen and 1.1 vol-% of CO_2. We therefore consider the INFLUINS borehole to be relatively dry.

The drilling mud gas composition is linked with the drilled strata: Buntsandstein and Muschelkalk show different formation gas composition and are therefore hydraulically separated. The correlation between hydrogen and helium and the high relative helium abundance rules out any artificial origin of hydrogen and suggest a radiolytic origin. Ratios $CH_4/(C_2H_6/C_3H_8)$ <50 imply that hydrocarbons derive from thermal degradation of organic matter. Stable isotope studies of carbon and hydrogen yield $\delta^{13}C_{CH4}$ ranging from -26.3‰ to -40.5‰ and δD_{CH4} ranging from -109‰ to -268‰. This points out to a thermogenic instead of a biogenic source for the methane. Abundances of all noble gases and isotope ratios of He, Ne and Ar were determined on five samples. While Ne and Ar isotope ratios for all samples are indistinguishable from air, $^3He/^4He$ ratios are always lower than air, revealing the presence of a deep helium source in all samples. Two samples from shallower depth yield air-corrected $^3He/^4He$ ratios ≤0.03 Ra typical for radiogenic helium production in the crust. For two samples from greater depth, slightly higher air-corrected $^3He/^4He$ ratios of 0.188 ± 0.076 Ra and 0.220 ± 0.058 Ra, respectively, were observed, indicating small contributions of non-radiogenic helium.

ICDP

Experimental study on the production of rhyolites from basaltic sources in the bimodal Snake River Plain-Yellowstone province

R. ALMEEV[1], B. CHARLIER[1], O. NAMUR[1], F. HOLTZ[1], M. WANG[1], J. SHERVAIS[2]

1 Institute of Mineralogy, Leibniz University of Hannover, Germany
2 Utah State University, USA

Tholeiitic basalts from many tectonic environments are commonly associated with silica-rich eruptive products. This association is commonly bimodal, with a noticeable dearth of intermediate compositions. Silica-rich rocks are generally enriched in iron, alkalis and incompatible elements and are referred to as A-type magmas. Two processes are usually invoked to explain their origin: (1) protracted fractional crystallization of parental basalts or (2) partial melting of a mafic source in the middle or upper crust. Silicate liquid immiscibility could also explain the bimodal character of tholeiitic provinces. However, even if immiscible textures occur in the mesostasis of tholeiitic basalts worldwide, evidence for large-scale separation of immiscible melts in volcanic setting has yet to be shown.

The Snake River Plain-Yellowstone (SRPY) province preserves a unique record of bimodal magmatism (tholeiitic basalts-rhyolites). Moreover, the ICDP HOTSPOT drilling project (2010-2012) has retrieved two deep cores, the Kimama core dominated by basaltic rocks and the Kimberley core dominated by rhyolites. These samples allow investigating the origin of A-type magmas, and their potential link with basalts in unprecedented detail. The Kimama core was drilled to a depth of 1912 meters (Shervais et al., 2013). The Kimama section consists almost entirely of basalt, with thin intercalations of sediment in the upper 200 m and lower 300 m of the hole. Detailed lithologic and geophysical logging has documented ~557 basalt flows, comprising at least 30 flow groups (13 m to 170 m thick) representing distinct time periods, and magma batches, with the oldest lavas being ~6 Ma in age (Bradshaw et al., 2012; Champion and Duncan, 2012; Potter et al., 2012). At least 3 horizons with evolved ferrobasaltic compositions similar to those found at Craters of the Moon National Monument (Leeman et al., 1976) have also been documented. Fractionation is evident in many flow groups, and there is a progression from more primitive basalts at depth to evolved basalts upsection. The Kimberly drill core is dominated by massive rhyolite and welded ashflow tuffs, with basalt/sediment intercalations and thin altered ash inter-beds (Shervais et al., 2013). Two basalt flow groups, 30 and 70 meters thick, pre-date the Shoshone rhyolite (6.25 Ma) and may be older than the oldest flows in the Kimama core.

In our new research project (started in February 2015), we are going to conduct complementary investigations of natural core samples and an extensive experimental work to determine whether the origin of A-type rhyolites in SRPY is best explained by fractional crystallization, silicate liquid immiscibility or partial melting in the crust. In 2014, we collected a set of natural samples from the Kimama core (~180) for the proposed study. First, we will perform a detailed mineralogical and petrographical investigation of the lavas to determine their pre-eruptive

conditions (thermobarometry) and further choose adequate basalts best representatives of liquid compositions for experimental study. Second, we will carry out three different sets of experiments simulating the formation of rhyolitic liquids from basaltic source by different mechanisms: (1) equilibrium and fractional crystallization experiments to identify the liquid line of descent of these basalts; (2) immiscibility experiments to determine whether these basalts might have encountered a two-liquid immiscibility field and (3) partial melting experiments of gabbro and basalt. Experimental results will then be compared with published, unpublished (cooperation with colleagues from USA) and our own natural data, to determine which of these three processes best explains the major and trace element composition of SRPY rhyolites. This project will also add to the current understanding of phase equilibria in tholeiitic ferrobasalts, especially related to immiscibility for which phase diagrams are poorly known. It will also put new constraints on the liquids produced by partial melting of dry mafic rocks, a topic which is currently underrepresented in the experimental literature.

References:

Bradshaw, R.W., Christiansen, E.H., Dorais, M.J., Shervais, J.W., Potter, K.E., 2012. Source and crystallization characteristics of basalts in the Kimama core: Project Hotspot Snake River Scientific Drilling Project, Idaho. Eos Trans. AGU: V13B-2840

Champion, D., Duncan, R.A., 2012. Paleomagnetic and $^{40}Ar/^{39}Ar$ studies on tholeiite basalt samples from "HOTSPOT" corehole taken at Kimama, Idaho, central Snake River Plain. Eos Trans. AGU: V13B-2842.

Potter, K.E., Shervais, J.W., Champion, D., Duncan, R.A., Christiansen, E.H., 2012. Project Hotspot: temporal compositional variation in basalts of the Kimama core and implications for magma source evolution, Snake River scientific drilling project, Idaho. Eos Trans. AGU: V13B-2839.

Leeman, W. P., C. J. Vitaliano, et al. (1976). "Evolved Lavas from Snake-River Plain - Craters of Moon-National-Monument, Idaho." Contributions to Mineralogy and Petrology **56**(1): 35-60.

Shervais, J.W., Schmitt, D.R., Nielson, D., Evans, J.P., Christiansen, E.H., Morgan, L.A., Pat Shanks, W.C., Prokopenko, A.A., Lachmar, T., Liberty, L.M., Blackwell, D.D., Glen, J.M., Champion, D., Potter, K.E., Kessler, J.A., 2013. First results from HOTSPOT: The Snake River Plain Scientific Drilling Project, Idaho, U.S.A. Scientific Drilling, 15: 36-45.

IODP

Atlantic Meridional Overturning Circulation during Heinrich-Stadial 1 & 2 as seen by $^{231}Pa/^{230}Th$

B. ANTZ[1], J. LIPPOLD[2], H. SCHULZ[3], N. FRANK[1],

A. MANGINI[1]

1 Institut für Umweltphysik, Universität Heidelberg, Deutschland
2 Institut für Geologie, Universität Bern, Schweiz
3 Fachbereich Geowissenschaften, Universität Tübingen

Assessing the sensitivity of the Atlantic Meridional Overturning Circulation (AMOC) is a major challenge for paleoclimatology, because its strength and structure is a crucial element of the global heat- and carbon distribution. Here the focus is set on how excessive freshwater input through abrupt melting of continental ice sheets can affect its overturning vigour. Such forcing can be tested by investigating its behaviour during extreme iceberg discharge events into the open North Atlantic during the last glacial period, so called Heinrich-Events [Heinrich 1988; Hemming 2004].

The sedimentary activity ratio $^{231}Pa/^{230}Th$ has been increasingly used as a kinematic circulation proxy in the Atlantic Ocean over the past decade [Gherardi et al. 2009; McManus et al. 2004; Lippold et al. 2012]. In general, a Pa/Th signal close to the production ratio of 0.093 points to a weakened AMOC, while ratios below indicate export of ^{231}Pa out of the Atlantic and hence an active AMOC.

Here, we present a compilation of $^{231}Pa/^{230}Th$ ratios from several Atlantic sediment cores across Heinrich Stadial 1 (~17 ka BP) and 2 (~24 ka BP). The comparison of the profiles demonstrates the potential pitfalls when interpreating a single $^{231}Pa/^{230}Th$ profile in terms of reflecting AMOC. E. g. core IODP 1313 (Mid Atlantic Ridge, 3412 m water depth) shows $^{231}Pa/^{230}Th$ between

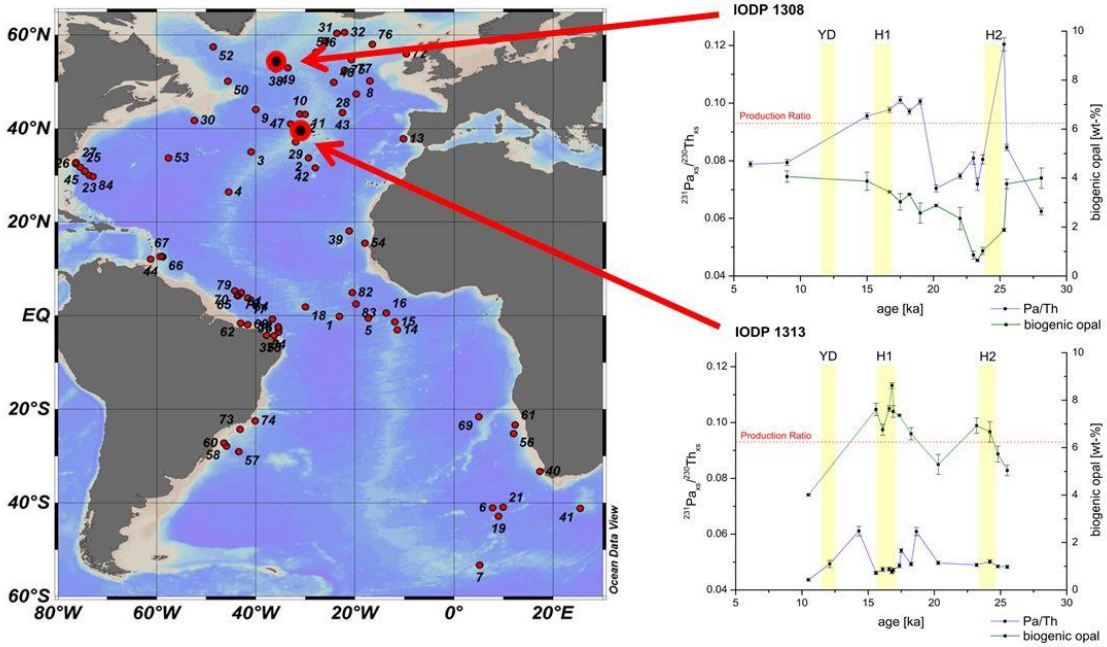

Fig. 1. Left: Map of available $^{231}Pa/^{230}Th$ data locations. Right: Two examples of $^{231}Pa/^{230}Th$ and biogenic opal measurements (IODP 1308, IODP 1313)

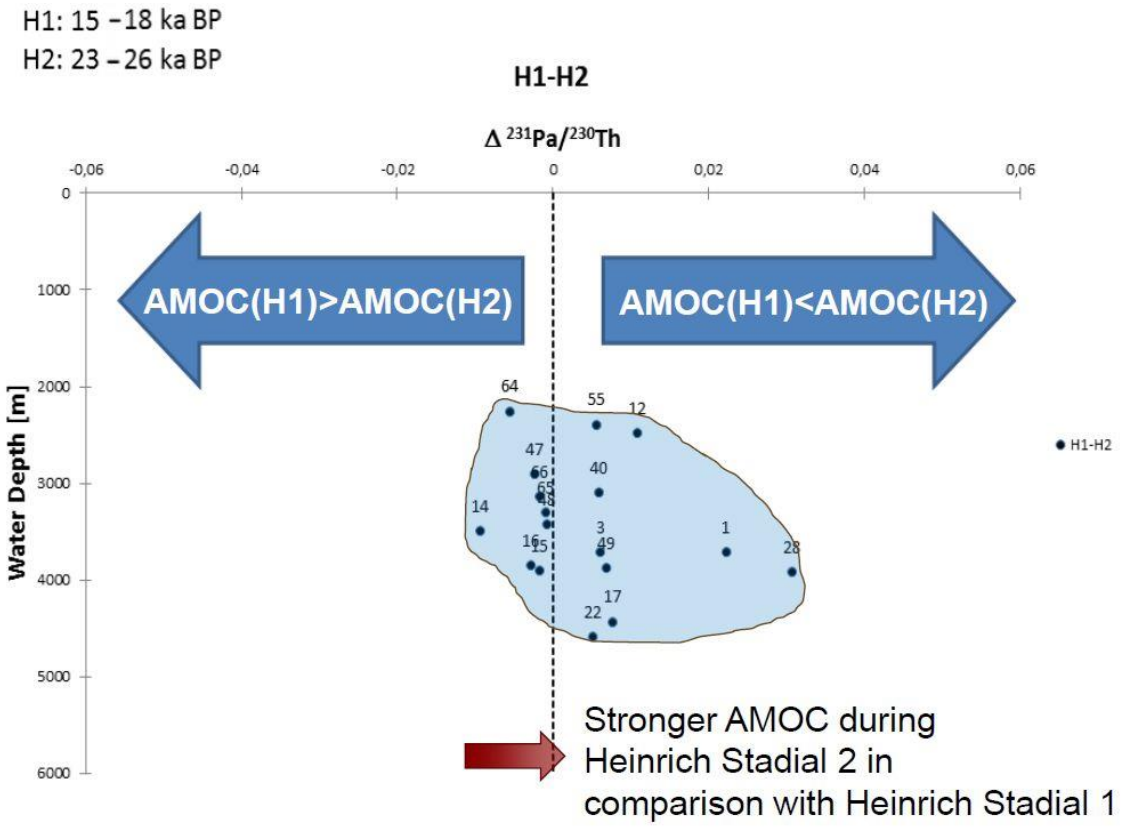

Fig. 2. Illustration of $\Delta^{231}Pa/^{230}Th$ values of selected $^{231}Pa/^{230}Th$ records of our data compilation.

0.04 and 0.06, which would indicate a vigorous circulation over the entire time period of observation.

On the other hand core IODP 1308 (northern North-Atlantic, 3871 m water depth) shows values close to the production ratio and above during Heinrich Stadials, lower values at Holocene and LGM.

Such divergency can be explained by $^{231}Pa/^{230}Th$ dependence on water depth, latitude, water mass and water mass age [Luo et al. 2010; Lippold et al. 2011], but also on changes in bioproductivity, in particular the flux of biogenic opal [Anderson et al. 1983A; Bradtmiller et al. 2007; Chase et al. 2002]. Since ^{231}Pa has a pronounced affinity to biogenic opal, $^{231}Pa/^{230}Th$ ratios above the production ratio may indicate the influence of particle flux composition.

To avoid misleading interpretations, our data set is accompanied by measurements of biogenic opal concentrations. We have found large variations of opal contents, but no significant correlation to $^{231}Pa/^{230}Th$ can be observed.

With an inverse model approach [Luo et al. 2010] strengths of the AMOC before, during and after the Heinrich-Stadials 1 & 2 will be derived from this database.

Preliminary qualitative results from the new data point to a different AMOC strength during Heinrich Stadial 1 and Heinrich Stadial 2. $^{231}Pa/^{230}Th$ values between 15-18 ka (HS1) and 23-26 ka (HS2) from the same sediment cores in general show a stronger overturning behavior during HS2 than while HS1. The impact of iceberg discharges on the North Atlantic deep-water formation was appearantly stronger during Heinrich-Stadial 1 than compared to Heinrich-Stadial 2. Although this interpretation is already a legitimate result, the need for more high resolved data during Heinrich-Stadials 1 & 2 is obvious.

References:

Anderson, B., M. Bacon and P. Brewer, 1983A. Removal of ^{230}Th and ^{231}Pa at ocean margins. Earth and Planetary Science Letters, 66, 73-90.

Böhm, E., J. Lippold, M. Gutjahr, M. Frank, P. Blaser, B. Antz, J. Fohlmeister, N. Frank, M. B. Andersen & M. Deininger, 2014. Strong and deep Atlantic meridional overturning circulation during the last glacial cycle. Nature 517, 73–76.

Bradtmiller, L., R. Anderson, M. Fleisher and L. Burckle, 2007. Opal burial in the equatorial Atlantic Ocean over the last 30 kyr: implications for glacial-interglacial changes in the ocean silicon cycle. Paleoceanography, 22, PA4216.

Chase, Z., R. Anderson, M. Fleisher and P. Kubik, 2002. The influence of particle composition and particle flux on scavenging of Th, Pa and Be in the ocean. Earth and Planetary Science Letters, 204, 215-229.

Delworth, T., P. Clark, M. Holland, W. Johns, T. Kuhlbrodt, J. Lynch-Stieglitz, C. Morrill, R. Seager, A. Weaver and R. Zhang, 2008. Chapter 4. The Potential for Abrupt Change in the Atlantic Meridional Overturning Circulation. Synthesis and Assessment Product 3.4 Report by the U.S. Climate Change Science Program, U.S. Geological Survey (USGS).

Francois, R., 2007. Paleoflux and paleocirculation from sediment ^{230}Th and $^{231}Pa/^{230}Th$. Proxies in Late Cenozoic Paleoceanography. C. H.-M. a. A. d. Vernal, Elsevier**,** 681-716.

Gherardi, J.-M., L. Labeyrie, S. Nave, R. Francois, J. F. McManus, *and* E. Cortijo, 2009. Glacial-interglacial circulation changes inferred from 231Pa/230Th sedimentary record in the North Atlantic region, Paleoceanography, 24, PA2204.

Gherardi, J., Y. Luo, R. Francois, J. McManus, S. Allen and L. Labeyrie, 2010. Reply to comment by S. Peacock on "Glacial-interglacial circulation changes inferred from $^{231}Pa/^{230}Th$ sedimentary record in the North Atlantic region". Paleoceanography. 25, PA2207.

Heinrich, H., 1988. Origin and Consequences of Cyclic Ice Rafting in the Northeast Atlantic Ocean during the Past 130,000 Years. Quaternary Research, 29, 142-152.

Hemming, S. R., 2004. Heinrich events: Massive late Pleistocene detritus layers of the North Atlantic and their global climate imprint, Rev. Geophys., 42, RG1005.
Hodell, D., J. Channell, J. Curtis, O. Romero and U. Röhl, 2008. Onset of "Hudson Strait" Heinrich events in the eastern North Atlantic at the end of the middle Pleistocene transition (~ 640 ka)? . Paleoceanography. 23, PA4218.
Keigwin, D. and E. Boyle, 2008. Did North Atlantic overturning halt 17,000 years ago? Paleoceanography. 23, PA1101.
Lippold, J., J. Grützner, D. Winter, Y. Lahaye, A. Mangini and M. Christl, 2009. Does sedimentary $^{231}Pa/^{230}Th$ from the Bermuda Rise monitor past Atlantic Meridional Overturning Circulation?, Geophyscial Research Letters 36: L12601
Lippold, J., Y. Luo, R. Francois, S. Allen, J. Gherardi, S. Pichat, B. Hickey and H. Schulz, 2012. Strength and Geometry of the glacial Atlantic Meridional Overturning Circulation. Nature Geoscience, 10.1038/NGEO1608.
Luo, Y., R. Francois and S. Allen, 2010. Sediment $^{231}Pa/^{230}Th$ as a recorder of the rate of the Atlantic meridional overturning circulation: insights from a 2-D model. Ocean Science, 6, 381–400.
Lynch-Stieglitz, J., J. Adkins, W. Curry, T. Dokken, I. Hall, J. Herguera, J. Hirschi, E. Ivanova, C. Kissel, O. Marchal, T. Marchitto, I. McCave, et al., 2007. Atlantic Meridional Overturning Circulation During the Last Glacial Maximum. Science. Vol. 316, no. 5821, 66 - 69.
McManus et al., 2004. Collapse and rapid resumption of Atlantic meridional circulation linked to deglacial climate change, Nature, 428, 834-837.
Rahmstorf, S., 2002. Ocean circulation and climate during the past 120,000 years. Nature 419, 207-214.
Rahmstorf, S., 2005. Thermohaline circulation hysteresis: A model intercomparison. Geophys. Res. Lett. 32.
Yu, E., R. Francois and M. Bacon, 1996. Similar rates of modern and last-glacial ocean thermohaline circulation inferred from radiochemical data, Nature 379: 689-694.

IODP

The evolution of the subsurface properties at the Iberian Margin during the Mid-Pleistocene (700 – 1400 ka, Site U1385)

ANDRÉ BAHR[1], DAVID HODELL[2], LUKE SKINNER[2], AND THE SHACKLETON SITE PROJECT MEMBERS[3]

1 Institute of Earth Sciences, Im Neuenheimer Feld 234, 69120 Heidelberg, Germany
2 Department of Earth Sciences, University of Cambridge, Downing Street, Cambridge, Cambridgeshire, CB2 3EQ, UK
3 F. Abrantes, G. D. Acton, B. Balestra, E. Llave Barranco, G. Carrara, S. Crowhurst, E. Ducassou, R. D. Flood, J.-A. Flores, S. Furota, J. Grimalt, P. Grunert, F. J. Jimenez-Espejo, J. Kyoung Kim, T. Konijnendijk, L. A. Krissek, J. Kuroda, B. Li, J. Lofi, V. Margari, B. Martrat, M. D. Miller, F. Nanayama, N. Nishida, C. Richter,T. Rodrigues, F. J. Rodríguez-Tovar, A. C. Freixo Roque, M. F. Sanchez Goni, F. J. Sierro Sánchez, A. D. Singh, L. Skinner, C. R. Sloss, Y. Takashimizu, R. Tjallingii, A. Tzanova, C. Tzedakis, A. Voelker, C. Xuan, and T. Williams

During the mid-Pleistocene Transition (MPT), at around ~900 ka, a fundamental shift in the glacial/interglacial cyclicity from a "41 kyr world" into the present-day "100 kyr world" took place accompanied by a distinct growth of glacial ice shields1. The growth of ice volume goes along with more pronounced winter cooling in high altitudes, necessary to sustain large ice sheets2. In this project we investigate the influence of low and mid-latitude circulation changes on the observed high-latitude cooling. For this purpose, we study surface and subsurface properties (temperature, salinity) on Site 1385 ("Shackleton Site"), drilled during IODP Exp. 339 at the Iberian Margin. Focus is the time interval of ca. 700 – 1400 kyr (MIS 18 – 44), which captures the major changes during the MPT. Site 1385 is located at the eastern margin of the North Atlantic Subtropical Gyre, an area characterized by the accumulation of warm and saline subsurface waters. These gyre waters are a major source for the salt and heat transported northward by the Gulf Stream and North Atlantic Current and therefore represent a pivotal component of the thermohaline circulation. The extend of the North Atlantic Subtropical Gyre, on the other hand, is directly affected by variations in ice shield expansion: enhanced glacial ice volume should lead to a southward shifts of wind fields accompanied by a strengthening of the surface wind stress due to an increased latitudinal temperature gradient. The direct coupling of ocean-atmosphere processes makes the North Atlantic Subtropical Gyre therefore very sensitive to climate changes. The present study aims to shed light on the behavior of the North Atlantic Subtropical Gyre during the MPT, in particular regarding its response to ice volume change. For this purpose, combined $\delta^{13}C$, $\delta^{18}O$ and Mg/Ca records on the shallow dwelling foraminifer Globigerinoides bulloides and the deep dweller (i.e. ~200-300 m water depth) Globorotalia inflata were obtained. The combination of $\delta^{18}O$ and Mg/Ca-derived surface and subsurface temperatures (SST, and Tsub, respectively) allows for the calculation of the ice-volume corrected $\delta^{18}O_{seawater}$ ($\delta^{18}O_{ivc-sw}$) as an approximation of salinity.

SST and subT generally follows the glacial-interglacial pattern (Fig. 1). However, we observe that the long-term trend of subT as well as of $\delta^{18}O_{ivc-sw}$ are opposed to that of successively more intensified glacials imprinted into the SST record. Notably, relatively weak glacials such as MIS 38 and 40 are accompanied by persistent and strong subsurface cooling, interpreted as a much reduced or absent influence of gyre waters. Subsequent glacials do not show this degree of subsurface cooling, with the exception of the prominent MIS 22. This unexpected and complex behaviour of the subtropical gyre circulation might be explained by a southward shift and strengthening of the Westerlies during glacials over the course of the MPT. Intensified surface winds cause a deepening of the thermocline at the Iberian Margin, which could on subsurface level at least partly compensate for the stronger surface cooling. An enhanced meridional SST contrast (Fig. 1) during the MPT also argues in favor of stronger zonal wind fields, in support of our interpretation. A strengthening and southward displacement of the mid-latitude wind fields would have far reaching consequences not only for the oceanic circulation but alter the moisture distribution over the continent.

References:

1 Clark, P. U. et al. The middle Pleistocene transition: characteristics, mechanisms, and implications for long-term changes in atmospheric pCO2. Quaternary Science Reviews 25, 3150-3184 (2006).
2 McClymont, E. L., Sosdian, S. M., Rosell-Melé, A. & Rosenthal, Y. Pleistocene sea-surface temperature evolution: Early cooling, delayed glacial intensification, and implications for the mid-Pleistocene climate transition. Earth-Science Reviews 123, 173-193 (2013).
3 Ruddiman, W. F., Raymo, M. E., Martinson, D. G., Clement, B. M. & Backman, J. Pleistocene evolution: Northern hemisphere ice sheets and North Atlantic Ocean. Paleoceanography 4, 353-412, doi:10.1029/PA004i004p00353 (1989).
4 Schefuß, E., Sinninghe Damsté, J. S. & Jansen, J. H. F. Forcing of tropical Atlantic sea surface temperatures during the mid-Pleistocene transition. Paleoceanography 19, PA4029 (2004).
5 Lisiecki, L. E. & Raymo, M. E. A Pliocene-Pleistocene stack of 57 globally distributed benthic delta O-18 records. Paleoceanography 20, PA1003 (2005).
6 Laskar, J. et al. A long-term numerical solution for the insolation quantities of the Earth. A&A 428, 261-285 (2004).

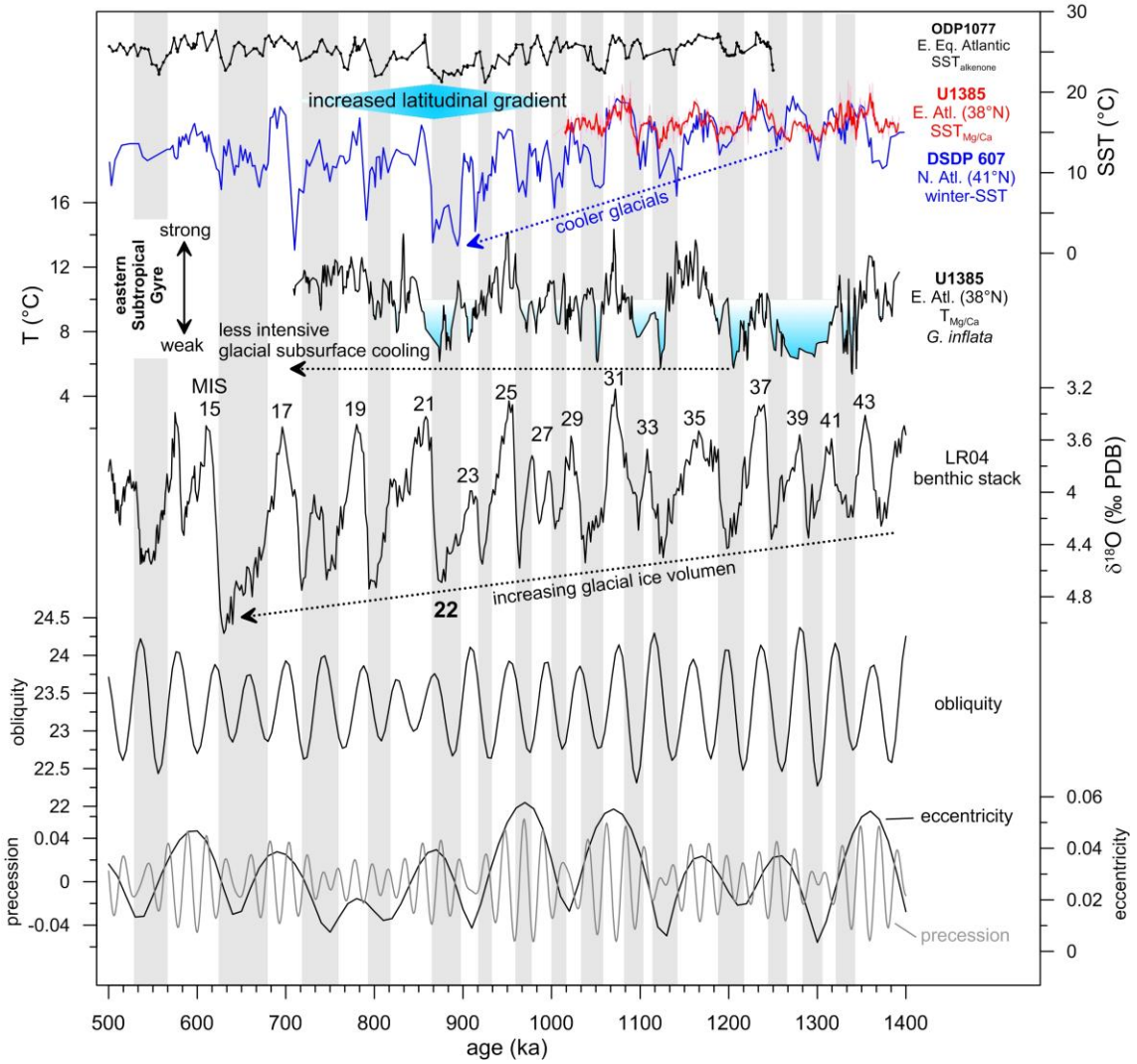

Fig. 1. Mid-Pleistocene climatic evolution: SST records indicate a successive high latitude cooling during glacials until MIS 22 (DSDP Site 607, winter-SST based on faunal transfer functions[3], blue line). Compared to SST records from the mid-latitude Atlantic (Iberian Margin Site U1385, SSTMg/Ca obtained on G. bulloides, 3pt smooth, red) and the tropical Atlantic (ODP Site 1077, SSTalkenone[4], black) this translates into an increase of the latitudinal SST gradient. Subsurface temperatures at the Iberian Margin (Site U1385, Mg/Ca-based temperatures on G. inflata, 3 pt. smooth) record a long-term trend to a strengthened eastern branch of the Atlantic Subtropical Gyre (i.e. subsurface warming) during glacials. This is opposed to the general trend to more pronounced cooling and continental ice volume growth during glacials (c.f. LR04 benthic stack[5] with annotated Marine Isotope Stages, MIS). For comparison, orbital parameters are given[6]. Glacials are marked by grey bars.

IODP

Atlantic Ocean circulation during the latest Cretaceous and early Paleogene: progressive deep water exchange

S.J. BATENBURG[1*], S. VOIGT[1], O. FRIEDRICH[2], T. KLEIN[1], C. NEU[1], A. OSBORNE[3], M. FRANK[3]

1 Institut für Geowissenschaften, Goethe-Universität Frankfurt, Altenhöferallee 1, 60438, Frankfurt am Main, Germany
2 Institut für Geowissenschaften, Universität Heidelberg, Im Neuenheimer Feld 234-236, 69120 Heidelberg, Germany
3 GEOMAR Helmholtz-Zentrum für Ozeanforschung Kiel, Wischhofstr. 1-3, 24148 Kiel, Germany
* corresponding author: batenburg@em.uni-frankfurt.de

Although ocean circulation plays a major role in the distribution of heat across the planet, the mode of deep water formation and exchange in the greenhouse world of the Late Cretaceous is poorly understood. The Atlantic Ocean was narrower than the present day, and submarine highs of volcanic origin restricted the flow of waters at depth. The deeper domains of the Atlantic Ocean functioned as sub-basins, in which different mechanisms of deep-water formation may have operated at the same time. To disentangle tectonic constraints on circulation from climate-driven patterns, this study aims to assess the role of submarine barriers and to determine the timing of the establishment of a true deep-water connection between the North and South Atlantic. Here we present new neodymium isotope data (ε_{Nd}) of ferromanganese sediment coatings from a wide geographical and bathymetric range of ocean drill sites across the Atlantic Ocean for the latest Cretaceous and early Paleogene. Comparison with existing data enables us to identify distinct deep and intermediate water masses and to follow their development through time. In particular, the new data from Site U1403, Newfoundland, Sites 525 and 1267, Walvis Ridge, Site 369, Canary Islands and Site 516, Rio Grande Rise, resolve the interval spanning and following the K/Pg boundary in detail. To assess whether the Nd isotope signature of bulk sediment coatings represents a genuine sea water signal, accompanying measurements of Nd isotopes are performed on different archives. Overall, the ε_{Nd} data from the North and South Atlantic display a similar decrease throughout the Maastrichtian and early Paleocene, although marked leads and lags are observed. From 60 Myr onwards, a deep water mass with a common Nd isotope signature prevailed over a broad range of water depths, indicating the onset of a global mode of thermohaline circulation.

Geological Setting

Nd isotope data have been generated for three sites in the South Atlantic; DSDP Site 516F on top of the Rio Grande Rise, DSDP Site 525A, on top of the Walvis Ridge, and ODP Site 1267, at the base of the northern flank of the Walvis Ridge, as well as for two sites in the North Atlantic; DSDP Site 369A near the Canary Islands and IODP Site U1403 at the base of the J-Anomaly Ridge near Newfoundland.

Rationale

Because the oceanic residence time of Nd and the global mixing time of the ocean are similar, the isotopic composition of Nd in deep waters, expressed as εNd(t), behaves quasi-conservatively and can serve as a tracer for water-mass mixing in the past. Nd isotope signatures of ferromanganese-oxide coatings allow the reconstruction of past deep water masses at a significantly higher spatial and temporal resolution than commonly achieved by fossil fish debris. Concomitant measurements of $\varepsilon_{Nd(t)}$ values in three different archives; fish teeth, ferromanganese coatings of bulk sediments and of foraminifera, will provide a test for the potential influence of partial dissolution of detrital particles on the isotopic composition of the coatings.

Age control

For the Maastrichtian-Paleocene intervals of the studied sites, detailed bulk stable carbon isotope stratigraphies ($\delta^{13}C$) are being generated at high resolution. Recently, Maastrichtian carbon isotope stratigraphy has proven to be a powerful tool for global correlation (Voigt et al. 2012). The observed $\delta^{13}C$ pattern at Site U1403 (Friedrich et al., in prep.) can be correlated in detail to the orbitally tuned $\delta^{13}C$ record of Zumaia-Sopelana, northern Spain (Batenburg et al. 2012). Cyclostratigraphic analyses of XRF data of U1403 provide additional age constraints to test potential nannofossil datum diachroneity.

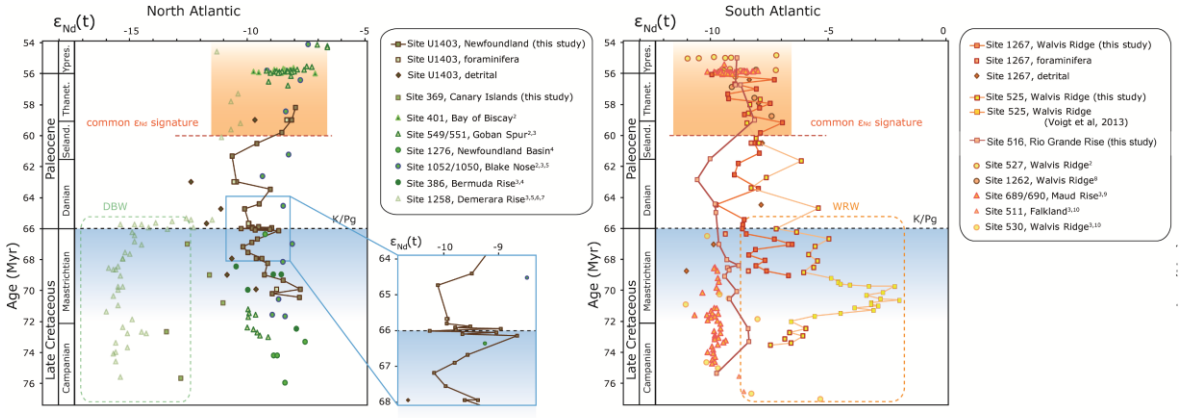

Fig. 1. Preliminary Nd isotope data of ferromanganese coatings, foraminifera and detritus for Sites U1403, 369, 516, 1267 and 525 in comparison to published data (1Voigt et al., 2013; 2Thomas et al., 2003; 3Martin et al., 2012; 4Robinson and Vance, 2012; 5MacLeod et al., 2008; 6Jiménez-Berrocoso et al., 2010; 7MacLeod et al., 2011; 8Via and Thomas, 2006; 9Scher &Martin, 2004; 10Robinson et al., 2010). DBW: Demerara Bottom Water, WRW: Walvis Ridge Water.

Circulation

The $\varepsilon_{Nd(t)}$ records at Sites 1267 and 525 at Walvis Ridge show that an early Maastrichtian excursion to highly radiogenic values reflects a brief interval at 72-70 Ma, related to a period of increased hotspot volcanism. From 69 Myr onwards, $\varepsilon_{Nd(t)}$ values at the crest of Walvis Ridge (Site 525) continuously decreased until 60 Myr ago, when they reached values of approximately -8. This long-term trend likely reflects cessation of magmatic activity with subsequent cooling of oceanic crust and deepening of the Walvis Ridge from shallow to deep bathyal depths.

Site 516 on the Rio Grande Rise displays a parallel trend to less radiogenic values until 62 Myr ago, when $\varepsilon_{Nd(t)}$ signatures rose again and eventually converged to similar values as those measured at Walvis Ridge.

At Site U1403 near Newfoundland, relatively negative seawater $\varepsilon_{Nd(t)}$ signatures in the 67-62 Ma interval of ~-10 are distinct from those recorded further south in the North Atlantic. Possible explanations include elevated unradiogenic weathering inputs from the North American craton, or the influence of regionally formed deep water masses with a less radiogenic signatures, such as those recorded at Demerara Rise (Martin et al., 2012; MacLeod et al., 2008; Jiménez-Berrocoso et al., 2010; MacLeod et al., 2011) and at Site 369 (this study). In the latest Maastrichtian, the Site U1403 $\varepsilon_{Nd(t)}$ record displays a short-term positive excursion prior to the K/Pg boundary (67-66 Ma) followed by a sudden drop to unradiogenic values at the boundary. This may reflect the oceanographic response to climatic changes in the pre-extinction interval and to climatic upheaval following the impact. This supports the hypothesis of Galeotti et al. (2004) that cooling caused by the impact winter may have driven millenial-scale changes in deep ocean circulation.

Conclusion

The Nd isotope data of Sites U1403, 516, 1267 and 525 indicate the occurrence of a common deep-water neodymium isotope signature ($\varepsilon_{Nd(t)}$ -8) in the North and South Atlantic since 60 Ma. At this time, the sub-basins of the deep Atlantic became fully connected. A deepwater mass with a common $\varepsilon_{Nd(t)}$ signature, likely originating in the high southern latitudes, prevailed over a broad range of water depths, indicating vigorous deep ocean circulation. Between 62 and 60 Ma, the vertical stratification of the Atlantic Ocean decreased and a global mode of thermohaline circulation commenced.

Outlook

New data will be generated for selected North and South Atlantic sites, focusing on the role of barriers and gateways through the latest Cretaceous and early Paleogene. Additional Pb isotope analyses will assist the evaluation of weathering inputs and thus help to identify potential source regions of deep water formation. Measurements of different Nd isotope archives will allow to assess whether the $\varepsilon_{Nd(t)}$ signatures of bulk sediment coatings represent a true sea water signature. $\delta^{13}C$ stratigraphies will provide a high resolution correlation tool to tie the oceanographic records to the astronomically tuned time scale.

References:

Batenburg, S. J., Sprovieri, M., Gale, A. S., Hilgen, F. J., Hüsing, S., Laskar, J., Liebrand, D., Lirer, F., Orue-Etxebarria, X., Pelosi, N. & Smit, J. (2012). Cyclostratigraphy and astronomical tuning of the Late Maastrichtian at Zumaia (Basque country, Northern Spain). Earth and Planetary Science Letters, 359, 264-278.

Galeotti, S., Brinkhuis, H., & Huber, M. (2004). Records of post–Cretaceous-Tertiary boundary millennial-scale cooling from the western Tethys: A smoking gun for the impact-winter hypothesis?. Geology, 32(6), 529-532.

Expedition 342 Scientists, 2012. Paleogene newfoundland sediment drifts. Integrated Ocean Drilling Program: Preliminary Reports, (342), 1-263.

Friedrich et al., in prep.

Jiménez-Berrocoso, Á., MacLeod, K. G., Martin, E. E., Bourbon, E., Londoño, C. I., & Basak, C. (2010). Nutrient trap for Late Cretaceous organic-rich black shales in the tropical North Atlantic. Geology, 38(12), 1111-1114.

MacLeod, K. G., Londoño, C. I., Martin, E. E., Berrocoso, Á. J., & Basak, C. (2011). Changes in North Atlantic circulation at the end of the Cretaceous greenhouse interval. Nature Geoscience, 4(11), 779-782.

MacLeod, K. G., Martin, E. E., & Blair, S. W. (2008). Nd isotopic excursion across Cretaceous ocean anoxic event 2 (Cenomanian-Turonian) in the tropical North Atlantic. Geology, 36(10), 811-814.

Martin, E. E., MacLeod, K. G., Jiménez Berrocoso, A., & Bourbon, E. (2012). Water mass circulation on Demerara Rise during the Late Cretaceous based on Nd isotopes. Earth and Planetary Science Letters, 327, 111-120.

Robinson, S. A., & Vance, D. (2012). Widespread and synchronous change in deep- ocean circulation in the North and South Atlantic during the Late Cretaceous. Paleoceanography, 27(1).

Robinson, S. A., Murphy, D. P., Vance, D., & Thomas, D. J. (2010). Formation of "Southern Component Water" in the Late Cretaceous: Evidence from Nd-isotopes. Geology, 38(10), 871-874.

Scher, H. D., & Martin, E. E. (2004). Circulation in the Southern Ocean during the Paleogene inferred from neodymium isotopes. Earth and Planetary Science Letters, 228(3), 391-405.

Shipboard Scientific Party, 2004. Site 1267. In Zachos, J.C., Kroon, D., Blum, P., et al., Proc. ODP, Init. Repts., 208: College Station, TX (Ocean Drilling Program), 1–77.

Thomas, D. J., Bralower, T. J., & Jones, C. E. (2003). Neodymium isotopic reconstruction of late Paleocene–early Eocene thermohaline circulation. Earth and Planetary Science Letters, 209(3), 309-322.

Via, R. K., & Thomas, D. J. (2006). Evolution of Atlantic thermohaline circulation: Early Oligocene onset of deep-water production in the North Atlantic. Geology, 34(6), 441-444.

Voigt, S., Gale, A.S., Jung, C., and Jenkyns, H.C., 2012. Global correlation of Upper Campanian - Maastrichtian successions using carbon-isotope stratigraphy: development of a new Maastrichtian timescale. Newsletters on Stratigraphy 45, 25-53.

Voigt, S., Jung, C., Friedrich, O., Frank, M., Teschner, C., & Hoffmann, J. (2013). Tectonically restricted deep-ocean circulation at the end of the Cretaceous greenhouse. Earth and Planetary Science Letters, 369, 169-177.

ICDP

Age depth-model based on cyclostratigraphic analysis of gamma ray data for the past 630 ka in Lake Ohrid (Macedonia/Albania)

H. BAUMGARTEN[1], T. WONIK[1], A. FRANCKE[2], B. WAGNER[2],

G. ZANCHETTA[3] AND THE SCOPSCO SCIENCE TEAM

1 Leibniz Institute for Applied Geophysics, Hannover, Germany
2 University of Cologne, Institute for Geology and Mineralogy, Cologne, Germany
3 University of Pisa, Dipartimento di Scienze della Terra, Pisa, Italy

Lake Ohrid is located at the border between Macedonia and Albania (40°70′ N, 20°42 E) and is assumed as the oldest lake in Europe. The lake with a surface area of 360 km² has trapped sediments and volcanic ashes over more than 1.5 Ma and hence, contains essential information of major climatic and environmental change of the central northern Mediterranean region. Seismic investigations indicate a sediment fill of the lake basin up to a thickness of 700 m. Several pre-site studies (e.g. multichannel seismic and shallow coring) have demonstrated the potential of Lake Ohrid to yield a complete climate record with continuous sedimentation and several tephra layers are promising to provide age control (Lindhorst et al., 2014;

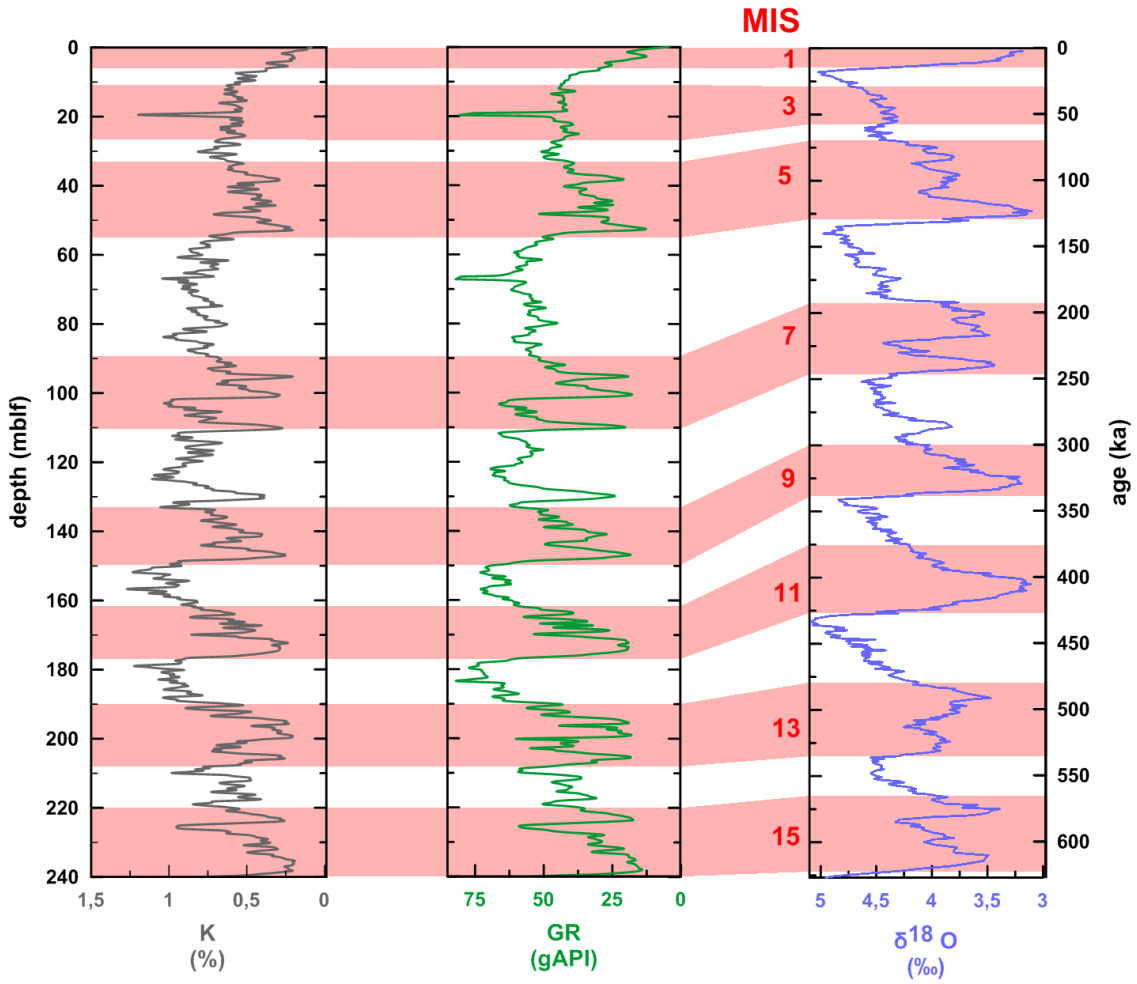

Fig. 1. Correlation of GR and K data from 0 to 240 mblf with LRO4 (Lisiecki and Raymo, 2005, 2007) from 0 to 630 ka. Several MIS (interglacials) correlate with periods of low GR. GR and K data is displayed on inverse scale for easier visual correlation. K – potassium content, GR – total gamma radiation, MIS – Marine Isotope Stages, mblf – meter below lake floor.

Vogel et al., 2010a; Wagner et al., 2014). In the frame of the ICDP project SCOPSCO (Scientific Collaboration on Past Speciation Conditions in Lake Ohrid), several scientific questions are addressed: age and origin of the lake, paleoclimatic change during the Quaternary, tephrostratigraphy, and driving forces for the outstanding biodiversity.

A deep drilling campaign was performed and four sites were multiple cored in spring 2013. The "Deep site" is located in the central deep basin of Lake Ohrid and was targeted for drilling operation to a depth of 569 m below lake floor (mblf) and an overall core recovery of 95 % was achieved. Within two logging campaigns high-quality continuous downhole logging data were acquired by the use of the following tools: spectral gamma ray (SGR), magnetic susceptibility (MS), resistivity, dipmeter, borehole televiewer and sonic (vp). To depth match logging and core data, two parameters were used: K-contents from SGR with K-intensities from XRF-scanning, and MS measured downhole with MS from Multi Sensor Core Logging (MSCL). Depth shifts of up to 4 m were observed between the composite profil and the downhole logging data. These shifts are generated because the downhole data originates from one hole (C; down to 470 mblf) and the core composite record is composed of four different holes which are tens of meters apart from each other. The depth of a distinct sediment layer differs between these holes.

First results revealed that the bottom part (below 430 mblf) is characterized by coarser grained deposits while the upper part yields fine grained pelagic sediments. The borehole logging data shows strong contrasts in all physical properties, in particular in SGR, MS, resistivity and seismic velocity (vp). The transition from the shallow water facies to the lacustrine facies at 430 mblf is is clearly visible in the data, e.g. by higher gamma ray values of 70 gAPI at the bottom compared to the pelagic sediments showing mean values of 45 gAPI.

Strong cyclicity is evident in Lake Ohrid's pelagic sediment facies, whereas the signal is most pronounced in the total gamma ray and in the contents of potassium (and thorium). The data was compared with the widely used global climate reference record (LRO4-stack from benthic $\delta^{18}O$) (Lisiecki and Raymo, 2005, 2007). The time span which was tested for correlation, was framed based on current age estimates from dating of tephra deposits in the cores ($^{40}Ar/^{39}Ar$). These eight layers could be identified clearly in the downhole logging data either by high values in potassium or magnetic susceptibility. After the anchor points from these tephra were set, the curves were correlated and a very similar cyclicity is evident. The data

shows high correlation (R^2 = 0.75), whereas low gamma ray, potassium (K) and thorium (Th) correlate with interglacial periods and therefore glacial-interglacial dynamics can be read from these data easily (Fig. 1). The fluctuation in the data is likely controlled by the input and deposition of clastics (K and Th-source) which are suggested as increased during glacial conditions. In particular due to reduced (to none) calcium carbonate deposition and reduced input of organic matter (TOC source) during cold (glacial) periods, the influence of content of clastic material seems amplified. During warm (interglacial) periods, carbonate production and preservation is increased (Vogel et al., 2010a). In conjunction with higher TOC flux, the clastic content of the sediments is reduced and the gamma ray, K and Th data respond to this development by lower values. If either the total content of clastics is lower during warm periods or the relative amount is decreased over carbonate (and TOC), cannot be distinguished at this point. However, less vegetation cover during cold periods is likely and suggests also increased erosion in the catchment and subsequent higher input of clastic material.

To further investigate the cyclic characteristics of the data, spectral analysis was applied (sliding window method) and several emphasized wavelengths were observed. The distribution of the cycles is non-uniform over the dataset and a break in the spectral characteristics occurs at about 110 mblf (Fig. 2). The high amplitudes were linked with orbital cycles and thereafter, a strong 100 ka cycle was observed which is in agreement with cyclostratigraphic studies of several sedimentary records for the past c. 900 ka (Berger and Loutre, 2010). Based on the distribution of the signals, sedimentation rates which range from 30 to 45 cm/ka were calculated. According to our calculations these rates show a jump at 110 mblf and are apart from this constant over large parts of the sedimentary succession.

The effect of compaction on the spectral characteristics and associated calculations of sedimentation rates was estimated by modelling of the original thickness of the sediment layers (decompacted). To estimate the degree of compaction, the initial porosity is required. In-situ porosity can be gained by neutron porosity logging or deviated, e.g. from bulk density. These tools operate with nuclear methods and the import procedure in foreign countries is usually extremely complicated and seldom successful. Therefore, the radioactive tools from LIAG could not be used at Lake Ohrid. However, porosity could be derived from sonic (vp) (Erickson and Jarrard, 1998), that was recorded continuously from below 30 mblf. The initial porosity was determined thereafter at 80 % and the compaction coefficient was estimated at 0.39 km^{-1}. To decompact the sediments, these parameters were used as input data for modeling and the 2D model was calculated for layers of 50 m thickness. The modeling process starts with the removal of the top layer and subtraction of its overburden pressure. The thickness of the lowermost layer is calculated after pressure is released and these steps are repeated downwards. The resulting thicknesses of the sediment layers after decompaction show a quasi-linear increase with greater depth. This trend is in accordance with the average linear increase of vp towards greater depth. The decompaction of the sediment layers ranges from 10 to 30 % and the cumulative thickness of the sediment sequence (present thickness of 240 m) is increased by 36 m (original thickness of 276 m). To determine the effect of decompaction on the spectral analysis, the GR data was stretched and subsequently

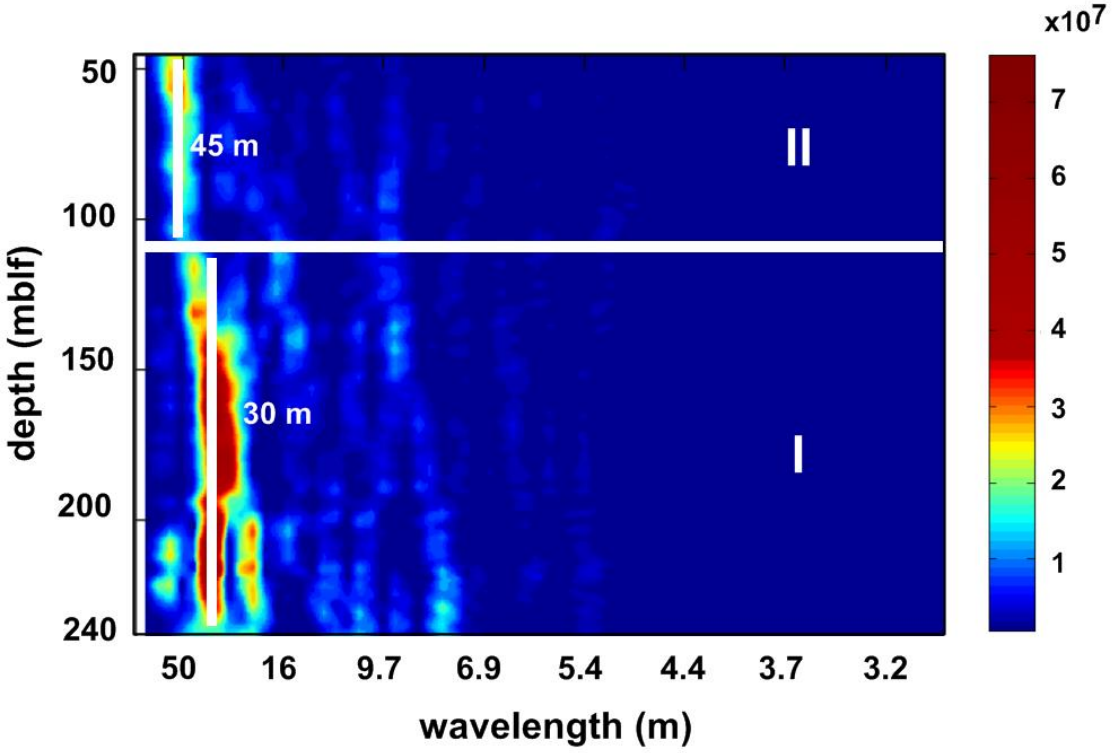

Fig. 2. Three-dimensional spectral plot from sliding window analysis of GR data from 0 to 240 mblf. Two high amplitudes with wavelengths of 30 m and 45 m are indicated by color (amplitude). Based on the break in the spectral characteristics at about 110 mblf, the three-dimensional spectral plot was subdivided into a lower interval I (240 to 110 mblf) and an upper interval II (110 to 0 mblf).

spectral analyzed by sliding window. An average increase of the sedimentation rates of 14 % was determined and these rates were corrected thereafter.

The results from sliding window analysis were compared with the sedimentation rates from tie points (correlation of LRO4 with GR and K). The latter show more variable results (22 to 55 cm/ka) but the overall trend of lower sedimentation rates in the bottom part (below 110 mblf) to increased values towards the top is comparable.

The strong response to the global climate signal (LRO4) suggests that the GR, K and Th data reflects a cyclic change of undisturbed, continuous sedimentation and the conditions were constant over a long period of time and prevailing in balance with the global climate. A robust depth age relationship was created by these climate proxies derived from spectral gamma ray logging in conjunction with age control from tephra layers, and thereafter the sediments from 0 mblf to 240 mblf span 630 ka.

References:

Berger, A., Loutre, M.F., 2010. Modeling the 100-kyr glacial-interglacial cycles. Global and Planetary Change 72, 275-281.

Lindhorst, K., Krastel, S., Reicherter, K., Stipp, B., Wagner, B., Schwenk, T., 2014. Sedimentary and tectonic evolution of Lake Ohrid (Macedonia/Albania). Basin Research. 0, 1-18.

Lisiecki, L.E., Raymo, M.E., 2005. A Pliocene-Pleistocene stack of 57 globally disturbed benthic delta (super 18) O records. Paleoceanography 20, PA 1003.

Lisiecki, L.E., Raymo, M.E., 2007. Plio-Pleistocene climate evolution; trends and transitions in glacial cycle dynamics. Quaternary Science Reviews 26, 56-69.

Vogel, H., Wagner, B., Zanchetta, G., Sulpizio, R., Rosen, P., 2010a. A paleoclimate record with tephrochronological age control for the last glacial-interglacial cycle from Lake Ohrid, Albania and Macedonia. Journal of Paleolimnology 44, 295-310.

Wagner, B., Wilke, T., Krastel, S., Zanchetta, G., Sulpizio, R., Reicherter, K., Leng, M.J., Grazhdani, A., Trajanovski, S., Francke, A., Lindhorst, K., Levkov, Z., Cvetkoska, A., Reed, J.M., Zhang, X., Lacey, J.H., Wonik, T., Baumgarten, H., Vogel, H., 2014. The SCOPSCO drilling project recovers more than 1.2 million years of history from Lake Ohrid. Sci. Dril. 17, 19-29.

IODP

Sea level, Currents, and Monsoon Evolution in the Indian Ocean (IODP Exp. 359)

C. BETZLER[1], T. LÜDMANN[1], J. REIJMER[2], G. EBERLI[3], P. SWART[3], A. DROXLER[4], M. TIWARI[5], E. GISCHLER[6], C. HÜBSCHER[7], L. GIOSAN[8]

1 Institut für Geologie, Universität Hamburg, Bundesstr. 55, 20146 Hamburg, Germany
2 Dept. of Sedimentology and Marine Geology, VU Amsterdam, De Boelelaan 1085, 1081 HV Amsterdam, The Netherlands
3 Comparative Sedimentology Laboratory, University of Miami, 4600 Rickenbacker Causeway, Miami, FL 33149, USA
4 Dept. of Earth Science, Rice University, P.O. Box 1892, Houston, TX 77251-1892, USA
5 National Centre For Antarctic & Ocean Research, Headland Sada, Vasco-da-Gama – 403804, Goa, India
6 Institut für Geowissenschaften, Goethe-Universität, Altenhoeferallee 1, 60438 Frankfurt am Main, Germany
7 Institut für Geophysik, Universität Hamburg, Bundesstr. 55, 20146 Hamburg, Germany
8 Woods Hole Oceanographic Institution, 266 Woods Hole Rd., MS# 22, Woods Hole, MA 02543-1050, USA

IODP Expedition 359 scheduled in October an November 2015 is designed to address the sea level, current and monsoon evolution in the Indian Ocean. Six proposed sites are located in the Maldives and one site in Kerala Konkan Basin on the western Indian continental margin. The Maldives carbonate edifice bears a unique and mostly unread Indian Ocean archive of the evolving Cenozoic icehouse world. It has great potential to serve as a key area for a better understanding of the effects of this global evolution in the Indopacific realm. Based mainly on seismic stratigraphic data, a model for the evolution of this carbonate bank has been developed, showing how changing sea level and ocean current patterns shaped the bank geometries. A dramatic shift in development of the carbonate edifice from a sea-level to a predominately current-controlled system is thought to be directly linked to the evolving Indian monsoon. Fluctuations of relative sea level control the stacking pattern of depositional sequences during the lower to middle Miocene. This phase was followed by a two-fold configuration of bank development: bank growth continued in some parts of the edifice, whilst in other places banks drowned. Drowning steps seem to coincide with onset and intensification of the monsoon related current system and the deposition of giant sediment-drifts. The shapes of drowned banks attest to the occurrence of these strong currents. The drift sediments, characterized by off-lapping geometries, formed large-scale prograding complexes, filling the Maldives Inner Sea basin. Because the strong current swept most of the sediment around the atolls away, relict banks did not prograde, and steady subsidence was balanced by aggradation of the atolls, which are still active today.

One important outcome of IODP Expedition 359 is the ground-truthing of the hypothesis that the dramatic, pronounced change in the style of the sedimentary carbonate sequence stacking was caused by a combination of relative sea-level fluctuations and ocean current system changes. Answering this question will directly improve our knowledge on processes shaping carbonate platforms and their stratigraphic records. Our findings would be clearly applicable to other Tertiary carbonate platforms in the Indo-Pacific region, and to numerous others throughout the geological record. In addition, the targeted successions will allow calibrating of the Neogene oceanic $\delta^{13}C$ record with data from a carbonate platform to platform-margin series. This is becoming important, as such records are the only type that exist in deep time. Drilling will provide the cores required for reconstructing changing current systems through time that are directly to the evolution of the Indian monsoon. As such the drift deposits will provide a continuous record of Indian Monsoon development in the region of the Maldives. This data will be valuable for a comparison with proposed site KK-03B in the Kerala-Konkan Baisn Basin (see below) and other monsoon-dedicated IODP expeditions.

The proposed site in the Kerala-Konkan Basin provides the opportunity to recover co-located oceanic and terrestrial records for monsoon and pre-monsoon climate in the eastern Arabian Sea and India, respectively. The site is located on a bathymetric high immediately northward of the Chagos-Laccadive Ridge and is, thus, not affected by strong tectonic, glacial and non-monsoon climatic processes that affect fan sites fed by Himalayan rivers. The cores are expected to consist of a continuous sequence of foraminifera-rich pelagic sediments with subordinate cyclical siliciclastic inputs of fluvial origin from the Indian

Peninsula for the Neogene and a continuous paleoclimate record at orbital time scales into the Eocene and possibly the Paleocene.

ICDP

Constraints on cooling of the lower ocean crust from epidote veins in the Wadi Gideah section, Oman Ophiolite

B. BIESELER[1], A. DIEHL[1], N. JÖNS[1,2], W. BACH[1]

1 Fachbereich Geowissenschaften, Universität Bremen, Klagenfurter Str. GEO, 28359 Bremen
2 present address: Institut für Geologie, Mineralogie und Geophysik, Ruhr-Universität Bochum, 44800 Bochum

Background

We report results from SPP1006-funded research, aimed at unraveling the history of fluid-rock interaction during crustal accretion and obduction of the Oman ophiolite, using metasomatic rocks and hydrothermal veins. The project is relevant to future ICDP-funded drilling in Oman, which will provide essentially full crustal penetration of the ophiolite. Understanding the conditions and processes of fluid-rock interactions in the evolution of the ophiolite from sea to summit were identified as main scientific goal of the drilling program. Determining the depth, extent, and timing of high temperature hydrothermal alteration in the ocean crust has been identified as key research question that can be tackled by drilling in Oman.

We are funded to investigate metasomatic reactions of rocks from well-characterized sections in the Sumail and Wadi Tayin blocks that will be critical to placing the results to be obtained from drilling into a proper geological context. We have sampled diopsidites and nephrites, rodingites, and epidosite veins and are in the process of detailed petrological and geochemical investigations of these rocks. We here report results from studies of epidote veins from the Wadi Gideah section in the Wadi Tayin block, which is target reference section for lower crust of the drilling program, and a classic profile of ocean crust alteration by circulating seawater (Gregory and Taylor Jr., 1981).

Geological setting

The Oman Ophiolite is a 500 km long, 50-100 km wide and 10-15 km thick thrust sheet of oceanic lithosphere, located in the southeast of the Arabian Peninsula along the coastline of the Gulf of Oman. Formed at an oceanic spreading center in the Tethyan Sea, this fragment of oceanic lithosphere was obducted on the Arabian continental margin during the late Cretaceous (Lippard et al., 1986). Intra-oceanic thrusting initiated only 1-2 Ma after crustal accretion (around 95 Ma) and the ophiolite was emplaced onto the Permian-Mesozoic passive continental margin of the Arabian plate by around 78 Ma (e.g., Hacker et al., 1996; Rioux et al., 2013). Although much of the subduction-obduction history of the Oman Mountains remains unresolved, the ophiolite is widely accepted to represent the best exposure of fast-spread oceanic lithosphere worldwide (e.g., Boudier and Coleman, 1981; France et al., 2009; Nicolas et al., 2000).

Rationale

Many details of the accretion of oceanic crust along mid-ocean ridge spreading centers remain poorly understood. For instance, seismic investigations indicate that the lower crust accreted along fast-spreading ridges is cooled efficiently shortly after accretion (Dunn et al., 2000). The proposed amount of cooling requires efficient removal of the latent heat of crystallization by deep circulation of seawater within 5-6 km of the ridge axis. Recent numerical modeling results support the notion that such deep near-axial hydrothermal circulation may be possible (Hasenclever et al., 2014). Geochemical studies of hydrothermal rocks and veins provided some indications for circulation of seawater deep into the hot gabbroic lower crust (e.g., Nehlig and Juteau, 1988; Gregory and Taylor Jr., 1981; Bosch et al., 2004). But the timing and overall fluxes of this deep circulation and its role in removing

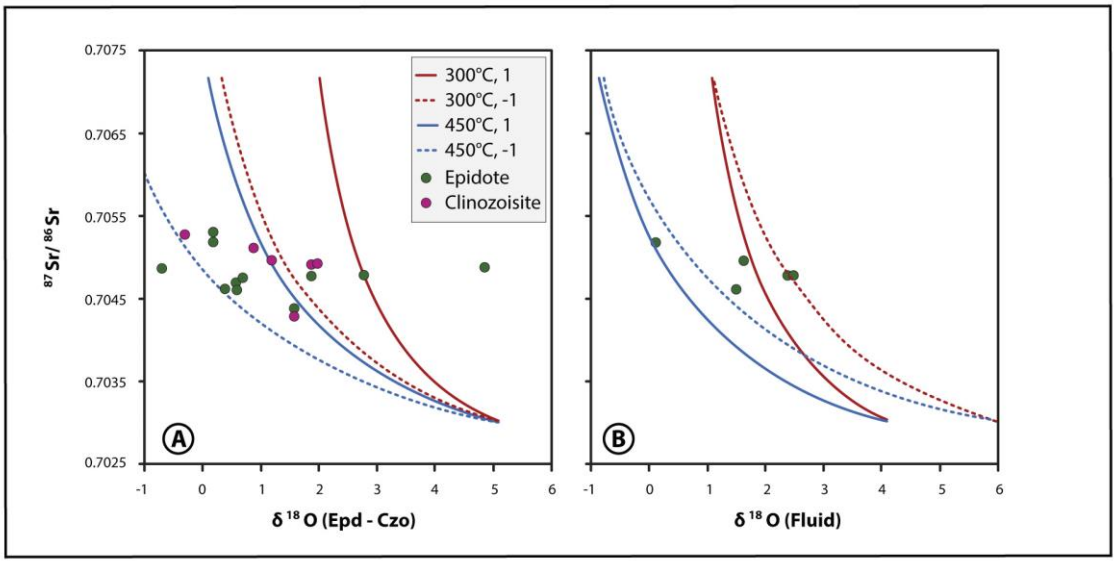

Fig. 1. Plot of Sr vs. O isotopic compositions predicted for water-to-rock ratios increasing from 0.01 to 20 and intial $^{87}Sr/^{86}Sr$ ratios of 0.7033 (basement) and 0.7074 (Cretaceous seawater). $\delta^{18}O$ of the intial fluids was set to -1 permil (Cretaceous seawater) and +1 permil (seawater affected by water-rock reactions in the overlying dikes and lavas). Panel A shows measured data and model trends for epidote veins; panel B shows calculated $\delta^{18}O$ compositions for the microthermometrically determined formation temperatures in comparison with model trends for fluid compositions.

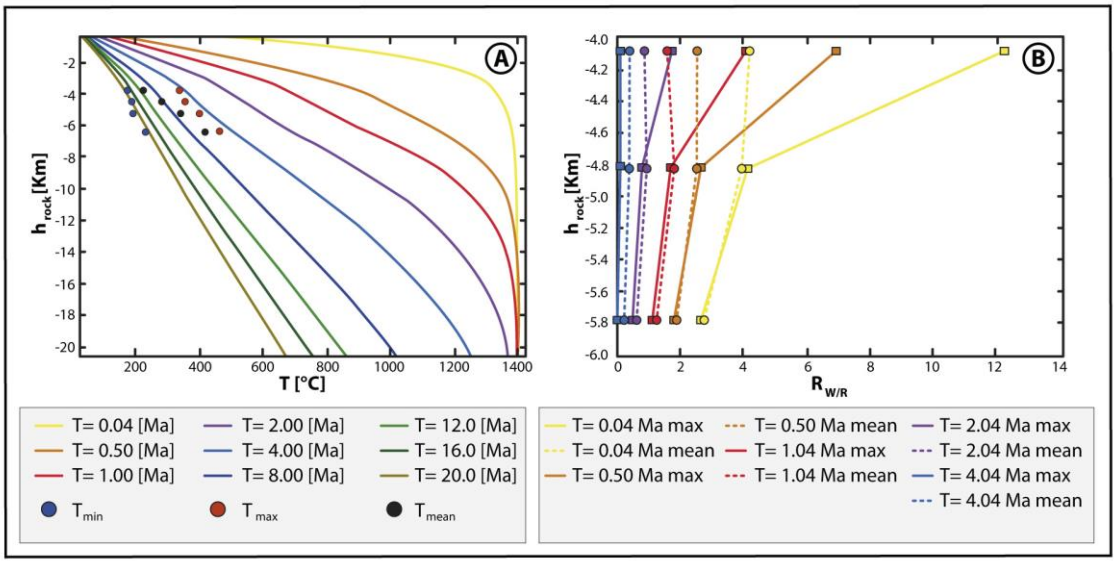

Fig. 2. Conductive cooling model predicting the thermal evolution in the absence of hydrothermal cooling (panel A). Panel B shows numerical modeling results of the water-to-rock ratios (i.e. time-integrated fluid flux) required to cause the observed thermal gradients as a function of time. Note that uniform water-to-rock ratios of around one are predicted to prevail between 1 and 2 Ma of crustal evolution.

latent heat of crystallization remains unresolved.

We investigated epidote veins from the Wadi Gideah section in terms of fluid inclusion microthermometry as well as Sr and O isotope composition to determine temperatures and water fluxes during vein formation and used computational modeling to develop plausible scenarios for the development of the observed temperature – fluid flux relations.

Results

Nineteen samples of monomineralic epidote/clinozoisite veins were collected from twelve locations in the Wadi Tayin block; of which 18 vein samples are lower crustal Wadi Gideah section and one is from the root zone of sheeted dykes in Wadi Amadhi. $^{87}Sr/^{86}Sr$ ratios feature a narrow range from 0.70429 to 0.70512, while O isotope compositions vary between -0.7 and +4.9 (7.4) permil in $\delta^{18}O_{SMOW}$. These compositions indicate uniform water-rock ratios between 1 and 2 and formation temperatures in the range of 300 to 450°C (Figure 2A). There is no systematic trend in Sr and O isotope compositions down section. Fluid inclusion homogenization temperatures for a subset of five samples range from 225°C to 418°C in the Wadi Gideah section and record 340°C for the Wadi Amahdi basal sheeted dike sample. Salinities are uniform throughout and scatter closely around seawater values. The considerable range of temperatures likely reflects entrapment temperatures (Tmax) and last resetting upon cooling (Tmin). A conductive cooling model allows us to associate ages with gradients the different temperatures estimates display. These ages range between 4 Ma (for Tmax) to 20 Ma (for Tmin) (Figure 2A). They represent maximum ages because any convective cooling by circulating seawater would lead to the development of lower temperatures earlier in crustal evolution.

Discussion

Given the geological history – with oceanic thrusting starting only 1-2 Ma after the crust had been accreted – the ages are consistent with the observed temperature gradient only if the recorded cooling episodes took place long after thrusting initiated. But evidence for the involvement of thrust-derived fluids and even late intrusives is lacking in the Wadi Gideah. Based on the Sr isotope compositions it appears more plausible that the epidote veins record seawater circulation prior to imbrication. However, if the epidotes recorded cooling within the first 0.1 Ma (i.e. within 5-7 km off axis) and hence were witnesses of vigorous near-axial hydrothermal circulation that efficiently cooled the crystallizing lower crust, the Sr (and O) isotopic compositions (set by water-rock ratios, i.e., time-integrated water flux) should vary drastically down-section (Figure 2B). This is clearly not the case, as the water-rock ratios are uniform throughout a 3 km section of lower crust. Also, axial high-temperature water-rock interactions commonly result in supercritical phase separation, which causes large variations in fluid salinities. Again, this is not the case for the epidote veins from Wadi Gideah, which exclusively host fluid inclusions with seawater salinities. The most plausible explanation for the origin of the epidote veins is that they formed in 1-2 Ma old off-axis crust. This is 2 to 4 times early than the minimum ages predicted from the pure conductive cooling model. Our results therefore suggest that off-axis hydrothermal cooling reaches the base of the crust within 50-100 km off the axis. This deep circulation provides an efficient mechanism for mining heat that escapes the crust in the flanks of mid-ocean ridges where >75% of the global oceanic hydrothermal heat flux is expected to take place.

Acknowledgements:

We thank the DFG (SPP1006) for funding (grant BA1605-13). We furthermore thank Friedrich Lucassen and Simone Kasemann for help with measuring the Sr isotope compositions. Andreas Pack (U Göttingen) is thanked for measuring the O isotope compositions of the epidotes.

References:

Bosch, D., Jamais, M., Boudier, F., Nicolas, A., Dautria, J.-M., Agrinier, P. (2004): Deep and High-temperature Hydrothermal Circulation in the Oman Ophiolite – Petrological and Isotopic Evidence. Oxford Journals - Journal of Petrology, 45, 1181-1208.

Boudier, F. & Coleman, R. G. (1981): Cross Section Through the Peridotite in the Samail Ophiolite, Southeastern Oman Mountains. Journal of Geophysical Research, 86, 2573-2592.

Dunn, R. A., Toomey, D. R., Solomon, S. C. (2000): Three-dimensional seismic structure and physical properties of the crust and shallow mantle beneath the East Pacific Rise at 9°30'N. Journal of Geophysical Research, 105, 23537-23555.

France, L., Ildefonse, B., Koepke, J. (2009): Interactions between magma and hydrothermal systerm in Oman ophiolite and in IODP Hole 1256D: Fossilization of a dynamic melt lens at fast spreading ridges. G3 - Geochemistry Geophysics Geosystems, 10 (10).

Gregory, R.T., Taylor Jr., H.P. (1981): An Oxygen Isotope Profile in a Section of Cretaceous Oceanic Crust, Samail Ophiolite, Oman: Evidence for δ18O Buffering of the Oceans by Deep (>5 km) Seawater-Hydrothermal Circulation at Mid-Ocean Ridges. Journal of Geophysical Research, 86, 2737-2755.

Hacker B. R. & Mosenfelder, J.L. (1996): Metamorphism and deformation along the emplacement thrust of the Samail ophiolite, Oman. Earth and Planetary Science Letters, 144, 435-451.

Hasenclever J., Theissen-Krah S., Rüpke L. H., Morgan J. P., Iyer K., Petersen S.,Devey C. W. (2014): Hybrid shallow on-axis and deep off-axis hydrothermal circulation at fast-spreading ridges. Nature, 508, doi:10.1038/nature13174.

Nehlig, P. & Juteau, T. (1988): Deep crustal seawater penetration and circulation at ocean ridges: Evidence from the Oman ophiolite. Marine Geology, 84, 209-228.

Nicolas, A., Boudier, E., Ildefonse, B., Ball, E. (2000): Accretion of Oman and United Arab Emirates ophiolite - Discussion of a new structural map. Marine Geophysical Researches, 21, 147-179.

Rioux, M., Bowring, S., Kelemen, P., Gordon, S., Miller, R., Dudás, F. (2013): Tectonic development of the Samail ophiolite: High-precision U-Pb zircon geochronology and Sm-Nd isotopic costraints on crustal growth and emplacement. Journal of Geophysical Research, 118, 2085-2101.

IODP

Extraction of neodymium from different phases of deep sea sediments by weak selective leaching

P. BLASER[1], J. LIPPOLD[2], N. FRANK[1], M. GUTJAHR[3], E. BÖHM[1]

1 Ruprecht-Karls-Universität Heidelberg, Germany
2 Universität Bern, Switzerland
3 GEOMAR, Helmholtz Centre for Ocean Research, Kiel, Germany

The ocean circulation is one of the key players in the climate system and the strength of the Atlantic Meridional Overturning Circulation (AMOC) closely correlates to major climatic shift in Earth's younger past. Reconstructing the AMOC of the past in detail is thus crucial in order to get insight into its interaction with the whole climate system. Depending on the surrounding continents, oceanic water masses adopt a certain neodymium isotope composition ($^{143}Nd/^{144}Nd$, expressed as ε_{Nd}), which can be used as a quasi conservative tracer. Nd is adsorbed to deep sea sediments directly from bottom waters and archived in the authigenic sediment fraction [1]. This renders Nd isotopes a well suited proxy for past deep-water provenance. There are several different archives available for the extraction of seawater derived Nd from pelagic sediments. The most important ones are fish debris, corals, foraminifera tests and authigenic ferromanganese accretions, both in the form of nodules and crusts, as well as dispersed in the sediment as cements. However, the extraction of a purely bottom-water derived Nd isotope signature is not trivial, since other fractions containing Nd, like volcanogenic or terrigenic minerals, can contaminate the sample.

This is especially problematic when using dispersed authigenic metal coatings, since they cannot be mechanically separated from the remaining sediment. On the other hand, these coatings would present the ideal archive for authigenic Nd, for they are present in practically all sedimentary environments, take up trace elements in high concentrations, can be used in high temporal resolution and leached off the bulk sediment very efficiently. Several attempts have been made to use weak acids, in part with the help of reducing chemicals, in order to selectively leach these authigenic ferromanganese coatings off the bulk sediment, without attacking sources of non-authigenic Nd. While some of these studies were successful, most could not provide a procedure applicable to all sedimentary environments. Especially sediments containing volcanogenic material (e.g. from Iceland or the Azores [2]) have been shown to be challenging, because these volcanogenic particles are easily leached with commonly used acids, and thus contaminate the extracted solution [3]. The most common alternative, namely obtaining seawater εNd from authigenic accretions bound to foraminiferal tests has lately become the preferred since most reliable method [4]. However, due to the advantages mentioned above, the method of leaching bulk sediment was further investigated with a variety of different samples.

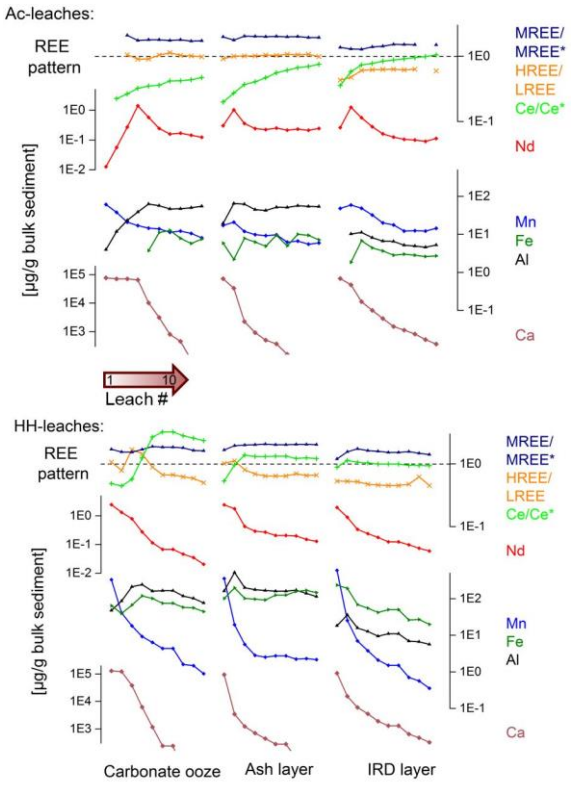

Fig. 1. Typical evolution of the elemental composition in the extracted leachate for three samples from site Me-68-91. The lines show the leached masses of Ca, Al, Fe, Mn and Nd and REE ratios from leach number 1 (left) to 10 (right). The upper panel displays data from the ten successive Ac-leaches, the lower panel for HH-leaches. Note the logarithmic Y-axes.

In this project several core-top and older sediments across the Atlantic were leached in ten consecutive steps with either dilute buffered acetic acid or an acid-reductive solution (commonly called Ac- and HH-leach). The leachates were analysed on their elemental and Nd isotope compositions, as well as rare earth element (REE) distributions. By graduating the total leaching procedure into smaller stages the results display which processes take place in the course of sediment leaching in the laboratory. While carbonate in the sediment dominates the course of the chemical reactions due to its high reactivity, the

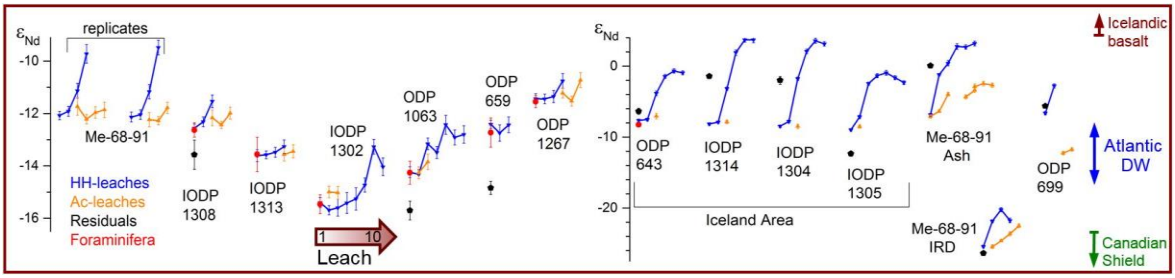

Fig. 2. The evolution of the extracted Nd isotope signal during ten successive Ac-or HH-leaches for fifteen diferent sediment samples. The data point to the left of each sample corresponds to leach number 1. Also shown are the values for picked foraminifera and the dissolved residual sediment after ten HH-leaches, where available. Note the two different Y-axis scales in the left and right panels. The arrows to the right indicate typical εNd for three important endmembers.

presence of volcanogenic detritus clearly governs the development of the extracted Nd isotopy. This is demonstrated through a strong positive excursion in εNd in all samples in the vicinity of Iceland and in an Icelandic ash layer. However, the excursion occures only after the carbonate has been dissolved and extracted. In all seven cases where sufficient foraminifera tests could be retrieved for comparison, the first applied HH-leach yielded an Nd isotopy equal to that of the foraminifera. Since this is also the case in one of the samples containing volcanogenic material, this finding suggests that one simple weak HH-leach without prior carbonate removal could reliably extract the same Nd isotope signal from bulk sediment as is obtained by picking and dissolving foraminifera. Furthermore, the data suggest that Al/Nd ratios are a good proxy for the seawater origin of the extracted solution, as proposed earlier [5]. In contrast, other quality proxies, like REE patterns correlate less with the contamination from non-authigenic sedimentary fractions. One of the samples contained large amounts of reformed authigenic dolomite and ice rafted debris (IRD), resulting in the extraction of a clearly terrigenic Nd isotopy. This example shows that authigenic carbonates probably pose a problematic sedimentary environment that cannot be reliably leached by this method, but needs to be identified from the solution and then omitted.

These results lead the way to a simple and efficient sediment leaching technique for future bottom water Nd isotope analyses in palaeoceanography, that is widely applicable and reliable if some simple extra parameters are supplementarily measured.

References:

[1] Crocket, K., Vance, D., & Gutjahr, M. (2011). Persistent Nordic deep-water overflow to the glacial North Atlantic. Gelology, 39(6), 515–518.
[2] Elmore, A., & Piotrowski, A. (2011). Testing the extraction of past seawater Nd isotopic composition from North Atlantic deep sea sediments and foraminifera. Geochemistry, Geophysics, Geosystems, 12(9), 12.
[3] Wilson, D., Piotrowski, A., Galy, A., & Clegg, J. (2013). Reactivity of neodymium carriers in deep sea sediments: implications for boundary exchange and paleoceanography. Geochimica et Cosmochimica Acta, 109, 197–221.
[4] Tachikawa, K., Piotrowski, A. M., & Bayon, G. (2014). Neodymium associated with foraminiferal carbonate as a recorder of seawater isotopic signatures. Quaternary Science Reviews, 88, 1–13.
[5] Gutjahr, M., Frank, M., & Stirling, C. (2007). Reliable extraction of a deepwater trace metal isotope signal from Fe–Mn oxyhydroxide coatings of marine sediments. Chemical Geology, 242(3-4), 351–370.

IODP

Potential impact of salinity changes on viruses in subsurface sediments from the Baltic Sea

O.E. CHIANG, B. ENGELEN, V. VANDIEKEN

Institut für Chemie und Biologie des Meeres, Carl von Ossietzky Universität Oldenburg,Carl-von-Ossietzky Straße 9-11, D-26129 Oldenburg, Germany, www.pmbio.icbm.de

The marine subsurface sediment (>1 meter below seafloor) is an environment with extremely low metabolic activity that still harbors a high abundance of viruses (Middelboe et al., 2011, Engelhardt et al., 2014). Viruses have been detected in sediments as deep as 320 m and as old as 14 Ma (Middelboe et al., 2011, Engelhardt et al., 2014). Both, the high densities of viruses and high virus-to-prokaryotes ratios, suggest that viruses may have a significant effect on the bioavailable carbon within the deep biosphere. Nonetheless, their ecological importance is still unclear. In surface sediments, viruses impact microbial communities by regulating their composition and diversity. They also influence cycling of organic matter and nutrients, accelerating transformations from living biomass to dissolved states (dissolve organic matter; Danovaro et al., 2008).

Several studies have shown evidence that both, environmental (e.g., salinity and oxygen) and biological factors (e.g., host abundance, predators) influence viral distribution and activity in marine sediments (e.g., Glud & Middelboe, 2004, Carreira et al., 2013). Viral and prokaryotic activities are in general well correlated along vertical and horizontal gradients (Glud & Middelboe, 2004). Additionally, increasing evidence suggests that physical and chemical variability (e.g., gradients in salinity, oxygen) can have a strong influence on viral dynamics because such factors have a significant effect on host activity. We have previously shown that 6 out of 13 bacterial isolates of the deep biosphere contained mitomycin-inducible prophages and genes of lysogenetic phages are present down to 100 m depth in various sediments (Engelhardt et al., 2011, Engelhardt et al., 2013). However, the induction of virus proliferation by environmental stress (e.g., salinity change) has not been shown for bacteria of the deep biosphere. In general, prophages can be induced to become free phage-particles when host cells are exposed to stress (Fuhrman, 1999). Thus, changes in salinity can constitute a stimulus for induction of prophages.

Sediments from the Baltic Sea have undergone alterations between limnic, brackish and marine conditions during their geological history due to repeated glaciations. Sediments from the Baltic Sea (up to 100 m depth) were sampled during IODP Exp. 347 from 4 sites (M0059, M0060, M0063, M0065) with the aim to investigate the potential impact of salinity changes on prokaryotic and viral communities as well as viral activity within the deep subsurface. In an initial stage, cultivation of fresh sediment was carried out in liquid enrichments with three media of different salinities (i.e., freshwater, brackish, marine) under anoxic conditions. By repeated transfer in anoxic deep-agar dilution series, new bacterial strains have been isolated into pure cultures. The new strains belong to, e.g., gammaproteobacterial *Vibrio* and *Shewanella*, deltaproteobacterial *Desulfovibrio* and Gram-positive *Firmicutes* including genera of *Tepidibacter*, *Aeromonas* and *Desulfosporosinus*. Many strains are facultative anaerobes, i.e., growth occurs in the presence and absence of oxygen, similar to other cultivated bacteria from subsurface sediments (Köpke et al., 2005). Some strains have been identified to possess temperate phages. In a next stage, bacteria will be investigated towards their salinity tolerance and their prophages will be characterized by electron microscopy and pulsed-field gel electrophoresis (PFGE). Furthermore, induction of prophages under different salinities conditions will be analyzed.

The overall goal of the project is contribute to understanding the dynamics of viruses in relation to salinity-change events during the paleoenvironmental history of the Baltic Sea. We hypothesize that changes of salinity may stimulate viral production, and therefore, virus-host interactions. Furthermore, we will investigate if viruses are produced in deep sediments and if the induction of temperate phages is a potential source of these viruses. In the past, events of high virus production due to salinity changes might have had major impacts for the prokaryotic community and the biogeochemical cycles in Baltic Sea sediments.

References:

Carreira C, Larsen M, Glud RN, Brussaard CPD, Middelboe M (2013) Heterogeneneouos distribution of prokaryotes and viruses at the microscale in a tidal sediment. Aquat Microb Ecol 69: 183-192

Danovaro R, Corinaldesi C, Filippini M, Fischer UR, Gessner MO, Jacquet S, Magagnini M, Velimirov B (2008). Viriobenthos in freshwater and marine sediments: a review. Freshwater Biol 53: 1186–1213

Engelhardt T, Sahlberg M, Cypionka H, Engelen B (2011) Induction of prophages from deep-subseafloor bacteria. Environ Microbiol Reports 3: 459-465

Engelhardt T, Sahlberg M, Cypionka H & Engelen B (2013) Biogeography of Rhizobium radiobacter and distribution of associated temperate phages in deep subseafloor sediments. ISME Journal 7: 199-209

Engelhardt T, Kallmeyer J, Cypionka H, Engelen B (2014) High viruses-to-cell ratios indicate ongoing production of viruses in deep subsurface sediments. ISME J 8: 1503-1509

Glud RN, Middelboe M (2004) Virus and bacteria dynamics of a coastal sediment: Implication for benthic carbon cycling. Limnol Oceanogr 49: 2073–2081

Köpke B, Wilms R, Engelen B, Cypionka H, Sass H (2005) Microbial diversity in coastal subsurface sediments: a cultivation approach using various electron acceptors and substrate gradients. Appl Environ Microbiol 71: 7819-7830

Middelboe M, Glud RN, Filippini M (2011) Viral abundance and activity in the deep sub-seafloor biosphere. Aquat Microb Ecol 63: 1-8

IODP

Late Tortonian to Messinian (6 – 8 Ma) magnetostratigraphy from IODP Site U1337 (equatorial Pacific): towards an accurate orbital calibration of the late Miocene

A.J. DRURY[1], T. WESTERHOLD[1], T. FREDERICHS[2],

R. WILKENS[3]

1 MARUM - Center for Marine Environmental Sciences, University of Bremen, Leobener Strasse, 28359 Bremen, Germany

2 Department of Geosciences, University of Bremen, P.O. Box 330440, D-28334 Bremen, Germany

3 School of Ocean and Earth Science and Technology (SOEST), University of Hawai`i at Manoa, Honolulu, Hawai'i, United States of America

The late Tortonian to Messinian (6 – 8 Ma) portion of the Neogene Geological Time Scale is based on astronomical tuning of sedimentary cycles in road-cut outcrops in the Mediterranean basin [*Hilgen et al.*, 1995; *Krijgsman et al.*, 1999]. Crucially, these sections are also used to calibrate the $^{40}Ar/^{39}Ar$ 'rock-clock' synchronisation, which adjusted the age of the Fish Canyon sanadine (FC) $^{40}Ar/^{39}Ar$ standard to 28.201 ± 0.046 Ma [*Kuiper et al.*, 2008]. However, other studies utilising astronomically tuned deep-sea sedimentary successions have calculated a younger age for the FC standard (~ 27.9 Ma) [*Channell et al.*, 2010, *Westerhold et al.*, 2012]. One possible explanation for this discrepancy in FC standard age could be a issue in the astronomical tuning of the Mediterranean sections. Road-cut sections are often more difficult to integrate and interpret than deep-see sedimentary successions from ODP and IODP expeditions, which are based on multiple hole sedimentary splices and the integration of multiple sites.

Most of the Mediterranean ash layers used for the 'rock-clock' synchronisation are located in magnetic polarity chrons C3An.2n, C3.Ar and C3Bn. To test the 'rock-clock' synchronisation very accurate absolute ages for these magnetic polarity chrons using astronomically calibrated records outside of the Mediterranean between 6 and 8 Ma are needed. High-quality and high-resolution chemo-, magneto-, and cyclostratigraphy at a single DSDP, ODP or IODP site covering these magnetic polarity chrons currently does not exist in any published record. Also, there has been no attempt so far to combine a high-resolution oxygen isotope stratigraphy with an appropriate magnetic polarity record for the late Tortonian to Messinian outside the Mediterranean for records older than 6.5 Ma. Due to possible diachrony of bio-events between different ocean basins only the combination of high-quality isotope and magnetic polarity records will provide the precision and accuracy necessary to test the 'rock-clock' synchronisation.

The lack of appropriate records changed with the core retrieval at IODP Site U1337 (4463 meters below sea level) located on ~24 Ma crust between the Galapagos and Clipperton Fracture Zones in the Pacific Ocean [*Pälike et al.*, 2010]. Shipboard investigations showed that Site U1337 is characterized by meter-scale cyclic alternations in color and lithology (Milankovitch related cycles), a basic magnetostratigraphy, enough carbonate and a sedimentation rate of ~2 cm/kyr in the interval from 6 to 8 Ma. Stratigraphic correlation provided a complete spliced

record to ~220 m composite depth [*Pälike et al.*, 2010]. Post-cruise work refined the shipboard splice at U1337 ensuring a complete sedimentary succession retrieved [*Wilkens et al.*, 2013].

Here we report on the preliminary results of our project to generate a high-quality benthic stable isotope and magnetic polarity record at the same location. From Site U1337, almost 400 discrete palaeomagnetic cube samples were taken and analysed between 110 and 167 m CCSF-A (core composite depth below seafloor from the *Wilkens et al.*, 2013 splice). The natural remanent magnetization (NRM) of these samples is low (1.37E-01 mA/m). However, the discrete inclination and declination corroborates the existing shipboard whole-core measurements. In addition, the discrete measurements improve the interpretation of the magnetic stratigraphy at Site U1337 in areas where the shipboard data are ambiguous. Where initial discrete measurements were unclear, additional discrete sampling in parallel holes has greatly enhanced the validity of the record.

Using the combined discrete and shipboard data, a preliminary palaeomagnetic stratigraphy for Site U1337 was constructed, in which 14 reversals were successfully identified from the top of Chron C3An.1n (6.033 Ma, *Lourens et al.*, 2004) to the bottom of Chron C4n.2n (8.108 Ma). The new palaeomagnetic record allows to clearly identify eight reversals including Chrons C3r/C3An.1n (6.033 Ma), C3An.1n/C3An.1r (6.252 Ma), C3An.1r/C3An.2n (6.436 Ma), C3An.2n/C3Ar (6.733 Ma), C3Br.1r/C3Br.1n (7.251 Ma), C3Br.1n/C3Br.2r (7.285 Ma), C4n.1n/C4n.1r (7.642 Ma), C4n.1r/C4n.2n (7.695 Ma). The remaining six reversals (C3Ar/C3Bn, C3Bn/C3Br.1r, C3Br.2r/C3Br.2n, C3Br.2n/C3Br.3r, C3Br.3r/C4n.1n and C4n.2n/C4r.1r) between 6 and 8.1 Ma in the Geomagnetic Polarity Time Scale are more difficult to identify and locate precisely, partially due to noisy data and occasional low sampling resolution. To identify the remaining six reversals, additional sampling in parallel holes and at increased resolution will be used to sufficiently constrain the exact reversal positions.

Initial investigations of the samples for benthic foraminiferal isotopic analysis show that the coarse fraction (>63 μm) ranges between 2 and 6 weight%, which reflects the dominance of siliceous and calcareous nannofossils in the sediments due to the location of Site U1337 in the equatorial high-productivity zone. The epifaunal benthic foraminifera *Cibicidoides mundulus* is sufficiently present and well preserved for stable $\delta^{18}O$ and $\delta^{13}C$ analyses.

In addition to the preliminary work on the integrated Site U1337 chemo- and magnetostratigraphy, late Miocene sediments from ODP Site 982 were XRF core scanned to verify the shipboard splice between 182 and 271 mcd (metres composite depth). Offsets were found, and the splice was revised accordingly. The splice was also extended by ~32 m to 280 rmcd (revised metres composite depth). Using the revised splice, ~ 11 m of gaps, and a number of smaller overlaps appear in the published benthic isotope data from Site 982 [*Hodell et al.*, 2001]. Some gaps and/or overlaps are ~2-3 meters long, which is equivalent to ~ 40 – 50 kyr (Hodell et al., 2001 age model) and could be the source of reported inconsistencies between Site 982, Ain el Beida and ODP Site 999 isotope records [*Bickert et al.*, 2004; *van der Laan et al.*, 2012].

References:

Bickert, T., G. H. Haug, and R. Tiedemann (2004), Late Neogene benthic stable isotope record of Ocean Drilling Program Site 999: Implications for Caribbean paleoceanography, organic carbon burial, and the Messinian Salinity Crisis, *Paleoceanography*, *19*(1), n/a–n/a, doi:10.1029/2002PA000799.

Channell, J. E. T., D. A. Hodell, B. S. Singer, and C. Xuan (2010), Reconciling astrochronological and 40Ar/39Ar ages for the Matuyama-Brunhes boundary and late Matuyama Chron, *Geochemistry, Geophys. Geosystems*, *11*, doi:10.1029/2010GC003203.

Hilgen, F. J., W. Krijgsman, C. G. Langereis, L. J. Lourens, A. Santarelli, and W. J. Zachariasse (1995), Extending the astronomical (polarity) time scale into the Miocene, *Earth Planet. Sci. Lett.*, *136*, 495–510, doi:10.1016/0012-821X(95)00207-S.

Hodell, D. A., J. H. Curtis, F. J. Sierro, and M. E. Raymo (2001), Correlation of late Miocene to early Pliocene sequences between the Mediterranean and North Atlantic, *Paleoceanography*, *16*(2), 164–178, doi:10.1029/1999pa000487.

Krijgsman, W., F. J. Hilgen, I. Raffi, F. J. Sierro, and D. S. Wilson (1999), Chronology, causes and progression of the Messinian salinity crisis, *Nature*, *400* (August), 652–655, doi:10.1038/23231.

Kuiper, K. F., A. Deino, F. J. Hilgen, W. Krijgsman, P. R. Renne, and J. R. Wijbrans (2008), Synchronizing rock clocks of Earth history., *Science*, *320*, 500–504, doi:10.1126/science.1154339.

Lourens, L., F. J. Hilgen, N. J. Shackleton, J. Laskar, and D. Wilson (2004), The Neogene Period, in *A Geologic Time Scale 2004*, edited by F. M. Gradstein, J. G. Ogg, and A. G. Smith, pp. 409–440, Cambridge University Press.

Pälike, H., M. Lyle, H. Nishi, I. Raffi, K. Gamage, A. Klaus, E. 320/321 Scientists, and Expedition 320/321 Scientists (2010), Expedition 320/321 summary, in *Proceedings of the Integrated Ocean Drilling Program*, vol. 320, edited by H. Pälike, M. Lyle, H. Nishi, I. Raffi, K. Gamage, A. Klaus, and E. 320/321 Scientists, pp. 2–141.

Van der Laan, E., F. J. Hilgen, L. J. Lourens, E. de Kaenel, S. Gaboardi, and S. Iaccarino (2012), Astronomical forcing of Northwest African climate and glacial history during the late Messinian (6.5-5.5Ma), *Palaeogeogr. Palaeoclimatol. Palaeoecol.*, *313-314*, 107–126, doi:10.1016/j.palaeo.2011.10.013.

Westerhold, T., U. Röhl, and J. Laskar (2012), Time scale controversy: Accurate orbital calibration of the early Paleogene, *Geochemistry, Geophys. …*, *13*, doi:Q06015 10.1029/2012gc004096.

Wilkens, R. H., G. R. Dickens, J. Tian, J. Backman, and E. 320/321 Scientists (2013), Data report: revised composite depth scales for Sites U1336, U1337, and U1338, in *Proceedings of the Integrated Ocean Drilling Program, Scientific Results*, edited by H. Pälike, M. Lyle, H. Nishi, I. Raffi, K. Gamage, A. Klaus, and E. 320/321 Scientists.

ICDP

Mechanisms of alteration of basaltic and rhyolitic glasses considering solution chemistry and passivating properties of palagonite – a case study on ICDP drilling sites Hawaii and Snake River

S. DULTZ[1], H. BEHRENS[1], F. TRAMM[1], M. PLÖTZE[2]

1 Institute of Mineralogy, Leibniz Universität Hannover, Callinstr. 3, D-30167 Hannover

2 Institute for Geotechnical Engineering, ETH Zürich, CH-8093 Zürich

Volcanic glasses are thermodynamically instable and easily react with hydrous fluids resulting in large elemental release to the environment. The exchange rate between glasses and environment is strongly affected by temperature, solution chemistry (pH, kind of electrolytes), microbial colonization of glass/palagonite and the mode of the glass alteration mechanism. Alteration layers on basaltic and rhyolitic glasses are common in volcanic rocks and may act as a diffusion barrier that slows down glass alteration. Our investigations on ICDP drilling cores from Hawaii (HSDP) and Snake River Plain (SRP) revealed pronounced glass alteration for both sites. At SRP high

shares of glass compounds released are removed by solution hindering the formation of palagonite. Indication for a microbially mediated congruent dissolution of the glass and precipitation at an inward moving reaction front of palagonite was obtained on Hawaii drilling cores. Open spaces were observed in zones with microtunnels between the primary glass and the palagonite easing conditions for fluid exchange and hence glass alteration. Fundamental differences in the modeled course of glass corrosion can be expected for a diffusion-controlled and an interface-controlled glass alteration process.

Our major objective is the clarification of the relevant mechanism(s) of glass alteration at both drilling sites by using on the one hand ICDP samples for determination of micromorphological patterns and on the other hand synthetic rhyolithic to basaltic glasses in dissolution experiments. Visualization and quantitative description of the size of open spaces between the glass and the palagonite layer was determined by tomography and high pressure intrusion of a molten alloy with subsequent microscopic investigations of sections of these samples. Microbial growth patterns on glass surfaces were determined using different microscopic methods. Here much expertise was gained by determinations of reference glass samples from sites with conducive environmental conditions for microbial growth (Dultz et al., 2014). For identification of the driving force of glass alteration and separation of biotic effects from abiotic ones, geochemical investigations along transects were performed with a microprobe. In a simulation of glass alteration in the laboratory a systematic study of the generation of positive charge on surfaces of synthetic glasses relevant for the two drilling sites under investigation was included. Here the zeta potential was determined as the characteristic parameter of the solid-liquid interface.

The pore volume of palagonite samples studied by Hg-porosimetry strongly depends on the amount of glass preserved and the presence of phenocrysts and quench crystals. For samples from HSDP pore volume vary from 0.6 vol.% for a weakly altered glass with quench textures and 19.6 vol.% for almost completely altered glass particles. High shares of pores are between pore radii in the range from 2 to 10 nm which is due to the presence of smectites, which has particle sizes less than 200 nm. Some of the samples show a tendency to bimodal distribution of pore sizes with a second maximum in the range of 900 to 8000 nm, which probably can be attributed to fractures in the samples. In sections intruded with the molten alloy open spaces at the glass palagonite interface were observed which may act as conduits for fluid exchange with circulating waters.

A marked redistribution of elements during glass dissolution and formation of secondary phases in the fracture filling palagonite sheet can be deduced from microprobe analysis. In the HSDP sample from 7524 ftbsl, FeO and TiO_2 are strongly enriched in palagonite as compared to the basaltic glass, 20 vs. 11.5 wt.% for FeO, 5.4 vs. 2.8 wt.% for TiO_2, whereas P_2O_5 is slightly enriched. In contrast Si, Al, Mn, Mg, Ca, K and Na are depleted during alteration and lost to the surrounding solution. The marked removal of glass compounds during alteration was indicated by the formation of open spaces at the interface between glass and palagonite and shrinkage fractures. By microprobe analysis of palagonite, typically low totals (70-85 wt.%) were obtained since the material is composed by hydrated phases (H_2O is not measured by

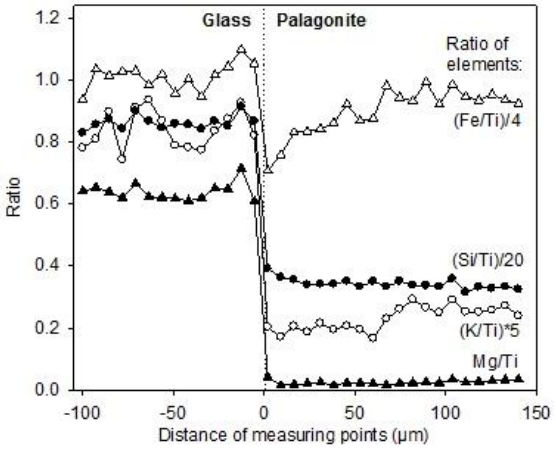

Fig. 1. Tracing fine-scaled changes in chemical composition during formation of palagonite by the ratio of elements along a transect from the glass into the palagonite. The transect has a length of 240 µm. The distance between the measuring points is 7.3 µm.

EMPA) and particles are quite small, i.e. sizes in the submicrometer-range. For the glass and phenocrysts, totals were always close to 100. Hence, comparison of data can provide qualitative trends on element turnover only. To overcome this problem to a part, ratios of elements were calculated for data collected along a transect from the glass to the palagonite (Fig. 1).

From the ratio of elements for the less mobile Fe and Ti it could be derived, that some Fe is lost during formation of palagonite. This is most pronounced for palagonite in direct contact with the glass. Hence ratios of elements were calculated in relation to Ti. The reason why the amount of Fe in relation to Ti is decreasing in the zone where microorganisms show the strongest activity might be assigned to the fact that microorganisms take influence on mobilization of weakly soluble elements e.g. through the release of specific enzymes and organic acids. From the K/Ti ratio it can be derived that with increasing distance from the glass there is some increase in K during palogonitization. K can derive also from circulating seawater and can be related with the presence of smectites in palagonite (Alt and Mata, 2000). Remarkably the ratio of Mn has a similar course as K.

A key parameter for the dissolution of glasses is the composition of the leaching fluid, i.e. the fluid may control the presence and absence of palagonite formation. In batch experiments the effect of common cations and anions in leaching waters on the solubility of a synthetic basaltic glass was studied. It was found that solutions with the monovalent cations Na^+ and K^+ tend to decrease Si-release from the basaltic glass in comparison to deionized water, whereas the divalent cations Mg^{2+} and Ca^{2+} increase Si-release from the glass at concentrations of 2.5 and 5 mmol/L. It is assumed that efficient neutralization of deprotonated $Si\text{-}O^-$ sites by monovalent cations can accelerate polymerization, leading to smaller Si release in comparison with absence of electrolytes. For the anions under investigation some increase was obtained for Cl^- and

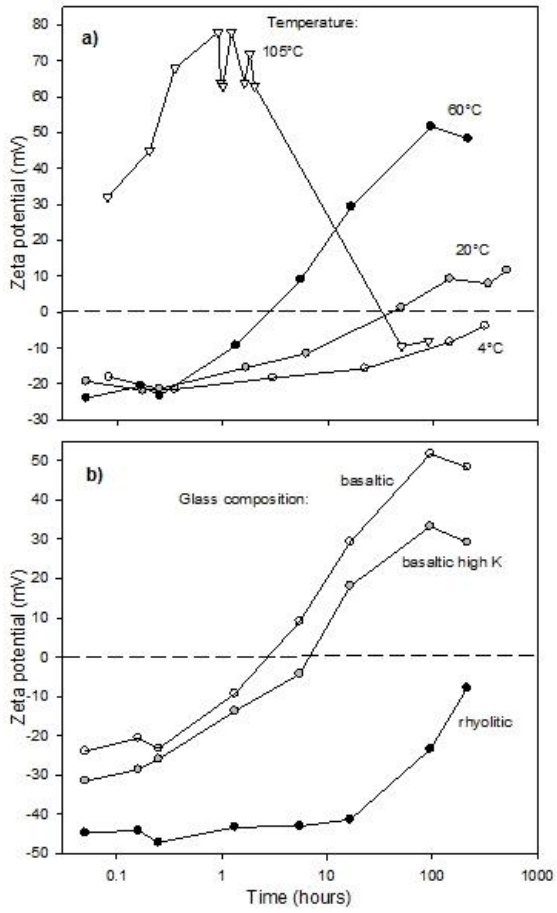

Fig. 2a, b. Effect of 5 mmol/L $Ca(NO_3)_2$ solution on the evolution of zeta potential of powdered basaltic glass in time sequences up to 650 h representing initial stages of dissolution (a). Experiments at 4, 20, 60, and 105°C. The pH of the suspensions was between 6.0 and 6.5. b: Effect of glass composition (rhyolithic, basaltic high K and basaltic) on the zeta potential in time sequences up to 200 h. Experiments at 60°C in 5 mmol/L $Ca(NO_3)_2$ solution with the powdered synthetic glasses.

SO_4^{2-}, whereas oxalate ($C_2O_4^{2-}$), which is known to form stable complexes with Fe has the strongest effect on Si-release, highly dependent on concentration. During the runtime of the experiments the pH of the suspensions was controlled and found to be stable between pH 6.0-6.5, which is due to the wide solution/solid ratio chosen.

The zeta potential (ζ) was determined for the three glasses in suspension to characterize properties of the solid-liquid interface as a function of pH, cation and anion concentration and time. Using the same solid/solution ratio as in the suspension for determining the effect of different electrolytes on Si release, the course of zeta potential was determined in time sequence at four different temperatures (4-105°C) and for three different synthetic glasses. By the addition of divalent cations charge reversal of the zeta potential from negative to positive values was observed (Fig. 2). Indication was obtained that increasing molecular level surface roughness in more advanced stages of the dissolution experiment hinders exact zeta potential determination. The generation of positive charge on glass in dependence of temperature is shown in Fig. 2a for Ca^{2+}, which is the most common cation in the pore solutions of many rocks.

Temperature had strong effects on the absolute value as well as the time needed for reaching point of zero charge and generation of positive charge. Highest values for the zeta potential were obtained for basaltic glass exposed to 105°C indicating that the process inducing positive surface charge is most extensive at the highest temperature of the experiment. It is thought the observed charge reversal is due to the formation of Fe-oxides/hydroxides on the outer surface of the glass, as the content of FeO in the basaltic glass is relatively high (12.19 wt.%) and the point of zero charge of goethite and hematite, two common Fe-oxides is between pH 6-8. Chemically reactive electrons in the suspensions due to dissolved O_2 in the solutions can transform metal ions present in the reduced state Fe^{2+} and Mn^{2+} on or in vicinity to the glass surface to their higher oxidation state stable in oxic water. Oxidation of Fe^{2+} in the glass (volume oxidation) which might be facilitated by formation of a porous leached layer will increase positive charge and need of electrostatic charge balancing. In oxidation experiments with Fe^{2+}-bearing glasses, Cook and Cooper (2000) observed diffusion of Fe ions to the glass surface. Here, absorption of released Fe-ions on the glass surface and subsequent formation of Fe-oxides is likely. Positively charged surface sites may be formed by the oxidation of Fe-hydoxo complexes. For clarification X-ray photoelectron spectroscopy (XPS) is planned.

The generation of positively charged surface sites is an interesting issue as bacterial cells and also dissolved organic matter in pore water have a negative surface charge and will be attracted by positively charged surface sites. The electrostatic stabilization of microorganisms on glass surfaces might be an important factor for the frequently observed bioalteration of basaltic glasses and is likely to explain the generation of dissolution cavities on glass surfaces by bacteria to some part. Besides micotunneling issues in the basaltic glass surface of HSDP samples, in the palagonite layer from the glassy rim of a pillow (8808 ftbsl) longish branching structures were observed. It appears that the longish structures are located in a certain layer in the palagonite parallel to the rim of basaltic glass. The cross-sectional dimensions and the observed branching is typical for fungal hyphae, but observations on hypal structures in this environment are scarce (Ivarsson et al., 2013).

References:

Alt, J.C., Mata, P., 2000. On the role of microbes in the alteration of submarine basaltic glass: a TEM study. Earth and Planetary Science Letters 181, 301-313.

Cook, G.B., Cooper, R.F., 2000. Iron concentration and the physical processes of dynamic oxidation in an alkaline earth aluminiosilicate glass. American Mineralogist 85, 397-406.

Dultz, S., Boy, J., Dupont, C., Halisch, M., Behrens, H., Welsch, A.-M., Erdmann, M., Cramm, S., Helsch, G., Deubener, J., 2014. Alteration of a submarine basaltic glass under environmental conditions conducive for microorganisms: growth patterns of the microbial community and mechanism of palagonite formation. Geomicrobiology Journal 31, 813–834.

Ivarsson, M., Bengston, S., Skogby, H., Belivanoa, V., Marone, F., 2013. Fungal colonies in open fractures of subseafloor basalt. Geo-Marine Letters, doi: 10.1007/s00367-013-0321-7

IODP

Forcing of West African climate during the Pliocene

L.M. DUPONT, R.R. KÜCHLER, F. VALLÉ, E. SCHEFUß

MARUM – Center for Marine Environmental Sciences, University of Bremen, DE28359 Bremen, Germany

The Pliocene epoch is a period of profound reorganizations in the Earth's climate system and the time interval between 3.3 and 3.0 Ma – called the Mid-Pliocene Warm Period (MPWP, Dowsett 2007) – is often referred to as analogue scenario for a future warm climate. However, relatively little is known about low-latitude hydrology and the associated development of tropical vegetation during this time period. Therefore, our project strived for understanding of the variability of climate and vegetation in West Africa and its driving forces during the Pliocene.

To provide deeper insights into the development of climate and vegetation in West Africa during the Pliocene and the possible effects of ocean circulation, we conducted a combined pollen-biomarker study on well-dated continuous marine archives from the tropical northeast Atlantic. It turned out that West Africa was generally wetter during the Pliocene than during the last glacial cycle and that aridity changes were driven by an interplay of local insolation and the latitudinal temperature gradient and that effects of Atlantic deep water circulation on vegetation and climate were still small during the Pliocene. This changed with the growth of the ice-sheets on the Northern Hemisphere since 2.7 Ma; NE trade winds became stronger and the influence of North Atlantic sea surface temperatures on West African climate increased. During the early Pliocene (~5-4.5 Ma) arid spells occurred less frequently in West Africa. Savannahs already existed, but changed in composition around 3.0 Ma and contained more woody elements in the Pliocene than in the late Pleistocene (past 0.15 Ma). Due to an exceptional orbital configuration, a prolonged humid period occurred between 3.24 and 3.20 Ma.

Development of the Hadley Cell has been associated with sea surface temperature (SST) gradients; the Hadley Cell would have been weak during the Pliocene because the meridional SST gradient in the Pacific was weak (Brierley et al. 2009). To test if there is a dependence of the Hadley Cell to SST during the Pliocene we compared proxy records of precipitation, trade winds strength, dust and humidity in Africa with Atlantic SST records and the Atlantic SST gradient. A tentative correlation between dust and SST is found only for the latest Pliocene during the intensification of the Northern Hemisphere glaciations, when pollen records indicate intermittent increase of NE trade wind vigor. It seems that the NE trade winds strengthen in association with increased ice on the Northern Hemisphere and increased atmospheric gradients rather than with strong oceanic gradients. Changes in West African humidity seem to be linked to the latitudinal insolation gradient (Davis & Brewer 2009) associated with the orbital configuration.

References:

Brierley CM, Fedorov AV, Liu Z, Herbert TH, Lawrence KT, Lariviere JP (2009) Greatly Expanded Tropical Warm Pool and Weakened Hadley Circulation in the Early Pliocene. Science 323, 1714-1718.

Davis BS, Brewer S (2009) Orbital forcing and role of the latitudinal insolation/temperature gradient. Climate Dynamics 32, 143-165.

Dowsett HJ (2007) The PRISM palaeoclimate reconstruction and Pliocene sea-surface temperature. Williams M, et al. (eds). Deep-Time perspectives on Climate Change: Marrying the Signal from Computer Models and Biological Proxies. The Micropalaeontological Society, Special Publication. The Geological Society, London: 459-480.

IODP

From greenhouse to icehouse: Reconstructing surface-water characteristics of the western North Atlantic during the Oligocene based on dinoflagellate cysts (IODP Expedition 342, Newfoundland Drift)

L.M. EGGER[1], J. PROSS[1], O. FRIEDRICH[1], R.D. NORRIS[2],

P.A. WILSON[3], EXPEDITION 342 SCIENTISTS

1 Institute of Earth Sciences, University of Heidelberg, Im Neuenheimer Feld 234, 69120 Heidelberg, Germany
2 Scripps Institution of Oceanography, University of California, San Diego, 9500 Gilman Drive, La Jolla, CA 92093-0244, USA
3 School of Ocean and Earth Science, National Oceanography Centre, University of Southampton, Southampton SO14 3ZH, UK

Although being characterized by highly dynamic paleoclimate and paleoceanographic conditions, the Oligocene epoch (33.9–23.03 Ma) represents in many ways a somewhat neglected chapter in Cenozoic climate history. This situation is at least partially due to the stratigraphic incompleteness of many Oligocene successions. The relative paucity of Oligocene strata as often encountered in deep-marine sedimentary archives likely results from the onset of strong bottom-water circulation near the Eocene/Oligocene boundary, while coeval shallow-water sequences often exhibit unconformities caused by glacially induced eustatic sea-level fluctuations. With regard to the notorious incompleteness of Oligocene sedimentary archives, the sedimentary sequences recovered during IODP Expedition 342 (Sites U1405, U1406, and U1411) off Newfoundland represent a rare exception to the rule. Being apparently complete, they provide a unique window into the Oligocene world.

As a first deliverable, this project aims at generating a chronostratigraphically calibrated dinocyst biostratigraphy for the higher-latitude North Atlantic, using the precise magnetostratigraphical framework available for the Oligocene portion of the Newfoundland Drift sequence. In a second step, critical intervals of the Oligocene (i.e., Eocene/Oligocene transition, Oi-2b glaciation, Oligocene/Miocene transition) are to be studied in relatively high resolution (~15 ka) for their dinoflagellate cysts, which will be used to decipher surface-water characteristics. This will lead to a better understanding of ocean circulation patterns during the Oligocene and the Oligocene climate system as a whole.

Our first results from the Eocene/Oligocene transition interval and the lower Oligocene from Site U1406 show that the Newfoundland Drift material yields excellently preserved, remarkably diverse dinoflagellate cyst assemblages; to date, >110 cyst taxa have been identified. Of particular significance is the repeated occurrence of the

high-latitude taxon *Svalbardella cooksoniae*, which testifies to transient surface-water cooling pulses off Newfoundland during the early Oligocene.

ICDP

$^{40}Ar/^{39}Ar$ geochronology on ICDP cores from Lake Van, Turkey

J. ENGELHARDT, M. SUDO, R. OBERHÄNSLI

Institut für Erd- und Umweltwissenschaften, Universität Potsdam

Multi- and single-grain total fusion on alkali feldspars from six volcaniclastic deposits resulted in Pleistocene isochron ages that are in good agreement with a climate-stratigraphic age-model (Stockhecke et al., 2014) for the Ahlat Ridge composite core. Feldspar phenocrysts from the three stratigraphically highest samples yielded consistent isochron ages that are significantly older than the model's prediction. Distinct stratigraphic and paleomagnetic time markers of similar stratigraphic positions contradict to these radiometric dates (Stockhecke et al., 2014). Partial resorption features of inherited feldspar domains and the involvement of excess ^{40}Ar indicate incomplete degassing of the resorbed domains as an explanation. To evaluate the magmatic history of the different feldspars EMPA mappings of trace elements that could be interpreted as Ar diffusion couples between the domains are currently conducted. The volcaniclastic samples bear unaltered K-rich ternary feldspar and fresh to altered glass shards of predominantly rhyolitic composition. Pore water samples from ICDP Paleovan cores indicate a limited pore water exchange within the Quaternary lake sediments. Whereas applying the $^{40}Ar/^{39}Ar$ method on feldspars resulted in ages timing a late-stage crystallization, glass shards have the potential to date the eruption. Nevertheless, volcanic glass is prone to modifications such as hydrous alteration (palagonitization) and devitrification (Cerling et al., 1985). These modifications affect the glass' chemistry and challenge the application of the $^{40}Ar/^{39}Ar$ method. Inclusion-free and low-vesicular glass shards from deposits with neutral to alkaline pore water environments are currently analysed by single-shard total fusion and stepwise-heating analytics. Gaining precise radiometric ages from two phases has the potential to quantify the effect of aqueous alteration of rhyolitic low-vesicular glass shards and to increase the temporal resolution in the climate-stratigraphic age-model (Stockhecke et al., 2014) on the deposition of the lake sediments. Vice versa the core's previous age model has the ability to mark feldspar $^{40}Ar/^{39}Ar$ ages as misleading eruption ages. $^{40}Ar/^{39}Ar$ geochronology on Paleovan cores offers unique opportunities to monitor the effect of alteration on the Ar-systematics of volcanic glass shards and identifies a period of incorporation and incomplete degassing of inherited feldspar domains.

References:

Cerling, T.E., Brown, F.H., Bowman, J.R., 1985. Low-Temperature Alteration of Volcanic Glass - Hydration, Na, K, O-18 and Ar Mobility. Chemical Geology, 52 (3-4), 281-293.

Stockhecke, M., Kwiecien, O., Vigliotti, L., Anselmetti, F., Beer, J., Çağatay, N. M., Channell, J. E. T., Kipfel, R., Lachner, J., Litt, T., Pickarski, N., Sturm, M., 2014. Chronostratigraphy of the 600,000 year old continental record of Lake Van (Turkey). Quarternary Science Reviews 104, 8-17

IODP

Viral activity and life-cycles in deep subseafloor sediments

T. ENGELHARDT[1], W.D. ORSI[2], B.B. JØRGENSEN[1]

1 Center for Geomicrobiology, Department of Bioscience, Aarhus University, Ny Munkegade 116, 8000 Aarhus C, Denmark

2 Department of Marine Chemistry and Geochemistry, Woods Hole Oceanographic Institution, 266 Woods Hole Road, Woods Hole, MA

With an estimated number exceeding 10^{29} cells of bacteria and archaea, the deep biosphere of marine sediments comprises a total microbial abundance similar to that of the global ocean[1]. Viruses are highly abundant in marine subsurface sediments and can even exceed the number of prokaryotes[2]. Viruses in the oceans have long been recognized to be a major factor in element cycling (viral shunt) and a driving force for the diversification and evolution of microbial communities. For the deep subseafloor, however, their activity and quantitative impact on microbial populations are still poorly understood. Direct estimates of viral activity by slurry incubations in the subsurface are hampered by extremely low rates of prokaryotic metabolism and growth. Modeled estimates suggest that the low energy flux only allows microbial biomass turnover times on the order of tens to thousands of years[3]. Viral turnover may occur on a similar timescale. Here, we use gene expression data from published continental margin subseafloor metatranscriptomes[4] to qualitatively assess viral diversity and activity in sediments up to 159 meters below seafloor. The metatranscriptomic data targeting these new aspects revealed 4,651 representative viral homologs (RVHs), representing 2.2% of all metatranscriptome sequence reads, which have close translated homology (average 77%, range 60-97% amino acid identity) to viral proteins. The diversity and predominance of RVHs change in a depth-dependent manner. Archaea-infecting RVHs (Lipothrixviridae, Bicaudaviridae and Rudiviridae) are exclusively detected in the upper 30 mbsf, whereas RVHs for filamentous viruses (Inoviridae) predominate in the deepest sediment layers.

For the viral life-cycles, we distinguish between lysogeny, which is the integration of the viral genome into the host cell chromosome (prophage), and the lytic cycle that leads to cell lysis and the release of de novo produced viruses. RVHs indicative of lysogenic phage-host-interactions and lytic activity, notably cell lysis, are detected at all analyzed depths and suggest a dynamic virus-host association in the marine deep biosphere. Ongoing lytic viral activity is further indicated by the expression of CRISPR-associated (clustered, regularly interspaced, short palindromic repeat) cascade genes involved in cellular defense against viral attacks. The data indicate the activity of viruses in the marine deep biosphere and suggest that viruses indeed cause cell mortality and may play an important role in the turnover of subseafloor microbial biomass.

References:

[1] Kallmeyer, J., Pockalny, R., Adhikari, R.R., Smith, D.C., and D'Hondt, S. (2012) Global distribution of microbial abundance and biomass in subseafloor sediment. Proceedings of the National Academy of Sciences of the United States of America 109: 16213-16216.

[2] Engelhardt, T., Kallmeyer, J., Cypionka, H., and Engelen, B. (2014) High virus-to-cell ratios indicate ongoing production of viruses in deep subsurface sediments. Isme Journal 8: 1503-1509.
[3] Lomstein, B.A., Langerhuus, A.T., D'Hondt, S., Jørgensen, B.B., and Spivack, A.J. (2012) Endospore abundance, microbial growth and necromass turnover in deep sub-seafloor sediment. Nature 484: 101-104.
[4] Orsi, W.D., Edgcomb, V.P., Christman, G.D., and Biddle, J.F. (2013b) Gene expression in the deep biosphere. Nature 499: 205-211.

ICDP

B-isotope study of hydrothermal tourmaline in silicified Palaeoarchaean komatiites from the Barberton Greenstone Belt, South Africa

K. FARBER[1], A. DZIGGEL[1], F.M. MEYER[1], R.B. TRUMBULL[2], M. WIEDENBECK[2]

1 Institute of Mineralogy and Economic Geology, RWTH Aachen, Wüllnerstraße 2, 52062 Aachen, Germany
2 GFZ German Research Centre for Geosciences, Telegrafenberg, Potsdam, Germany

Many Archaean greenstone belts contain pervasively silicified volcano-sedimentary sequences, yet the reason for the silicification is not well understood. The hydrothermal systems are often regarded as a result of circulation of Archaean seawater in shallow sub-seafloor convection cells (Hofmann and Harris, 2008), but other fluid sources, such as hydrothermal fluid derived from submarine vent systems, are also discussed. In the 3.5-3.3 Ga Onverwacht Group of the Barberton greenstone belt in South Africa, strongly silicified volcano-sedimentary rocks are present throughout the stratigraphic sequence. The silicification is predominantly observed at the top of mafic to ultramafic lava flows at the contact with sedimentary chert horizons (Hofmann and Harris, 2008). A unique feature of the hydrothermal systems is the presence of locally abundant tourmaline, reflecting high contents of dissolved boron. As tourmaline is stable in a large range of P-T-conditions and generally resistent to intracrystalline diffusion (Dutrow and Henry, 2011; Van Hinsberg et al., 2011), the boron isotope record can be used to provide direct information on the source of boron. In this study, we analysed boron isotopes in tourmaline from the 3.3 Ga Mendon Formation, the uppermost unit of the Onverwacht Group. By using secondary ion mass spectronometry (SIMS), tourmaline grains can be measured in-situ and thus small-scaled isotopic differences can be resolved.

Tourmalines from outcrop samples were investigated. These samples comprise a silicified, finely laminated sedimentary chert that has previously been interpreted as stromatolite, and five highly altered and silicified komatiites. Based on textural characteristics, the komatiites are subdivided into (1) spinifex-textured silicified komatiite, (2) foliated and deformed fuchsite chert, and (3) brecciated fuchsite chert. The samples mainly consist of quartz, fuchsite, and Cr-spinel, and locally contain tourmaline, chlorite and/or carbonate. Tourmaline is mainly associated with fuchsite,with grain sizes varying between 30 and 200 µm. Many crystals show patchy colour zoning from greenish to brown.

In the two spinifex-textured komatiites, tourmaline forms faint-coloured, euhedral crystal aggregates, or occurs as subhedral grains that contain abundant inclusions of Cr-spinel, rutile, and quartz. Similar inclusion-rich tourmalines have also been found in the brecciated samples. One brecciated samples additionally contains ~20-100 µm large, columnar-euhedral tourmaline grains rimming earlier formed tourmaline or forming clusters in the matrix. The foliated and deformed sample contains euhedral tourmaline that locally shows hourglass zoning. In the silicified sediment, aggregates made up of euhedral tourmaline form monomineralic layers and veins crosscutting the layering.

Electron microprobe analysis (EMPA) indicates that tourmaline from the Mendon Formation is generally poor in Ca and Mn and has X_{Mg} values (X_{Mg} = Mg / (Mg + Fe)) varying between 0.57 and 0.85. The grains are mainly dravites of the alkali group; one sample varies in composition between dravite and Mg-Foitite (Fig. 1). Compositional maps show a slight patchy zoning in Al and in Fe-Mg. The most pronounced zoning is observed for Cr, which concentration strongly varies from trace amounts to up to 4 wt.% (0.5 Cr a.p.f.u.). One brecciated sample locally shows Cr-enrichment in contact with mica, whereas tourmaline in the other brecciated sample and in the foliated chert shows Cr-enrichment in the core of tourmaline. Tourmaline in the stromatolitic sample is characterised by Cr-rich zones around Cr-spinel inclusions. In all samples, the late overgrowths have the lowest Cr-concentrations of < 0.05 a.p.f.u..

In-situ boron isotope analysis was conducted using the Cameca 1280-HR instrument at the SIMS laboratory of the GFZ Potsdam. The measured $\delta^{11}B$ values are calculated relative to the NBS SRM-951 standard, with an overall error of ~1 ‰. The total range of $\delta^{11}B$ values varies from -21 to +8 ‰ (Fig. 2). Based on the variation in $\delta^{11}B$ ratios, the samples can be divided into two groups: a first group of

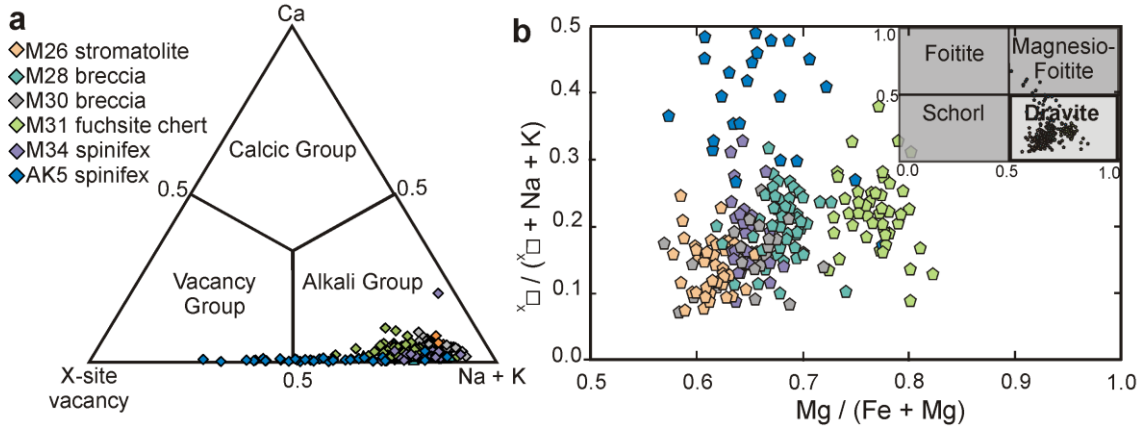

Fig. 1. Tourmaline classification diagrams of EMPA analyses (after Henry et al., 2011).

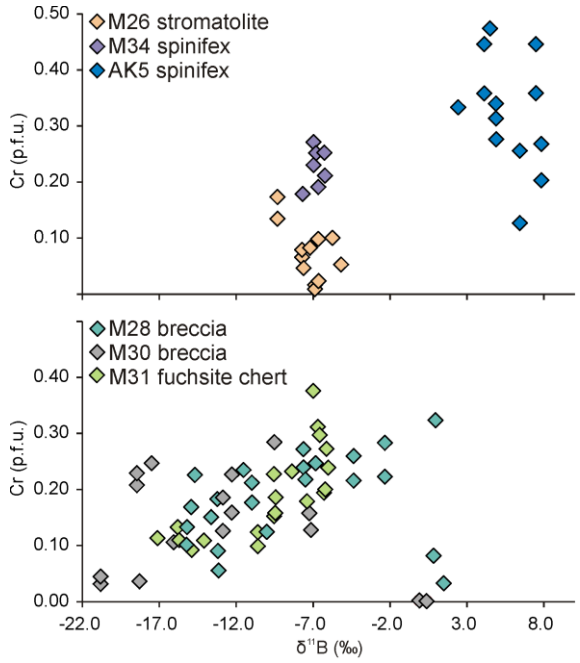

Fig. 2. δ^{11}B vs. Cr-content subdivided by their variation within one sample.

samples with only a small (<4 ‰) range in tourmaline δ^{11}B values (the spinifex-textured komatiites and silicified sediment, Fig. 2a), and a second group of tourmaline with a large range in δ^{11}B values of up to 18 ‰ (brecciated and foliated samples; Fig. 2b). With the exception of one spinifex-texured komatiite yielding positive δ^{11}B values ,all other samples record values of -5 to -8 ‰. Samples with the high variations showed unusually low δ^{11}B of up to -21 ‰. The δ^{11}B composition in these samples is positively correlated with the Cr-content (Fig. 2b).

The characteristic differences in B-isotope composition of different geologic reservoirs allows us to attribute, the isotope composition of the Barberton samples to different boron sources (Marschall and Jiang, 2011; Van Hinsberg et al., 2011). Thus, the positive boron isotope values of the exceptional spinifex-textured sample are clear evidence for the influence of seawater. The δ^{11}B values are similar to modern seafloor serpentinites and are thus interpreted to reflect interaction of seawater with Archaean crust.

The intermediate B-isotope compositions (-5 to -8 ‰) as present in all other samples may represent a fluid whose B-source lies in the greenstone magmas (mantle-derived) and/or in the granitoids surrounding the greenstone belt. Similar δ^{11}B values of -6 to -4 ‰, interpreted to reflect hydrothermal remobilisation of evaporitic boron, have also been reported from tourmaline preserved in late quartz veins from the Barberton greenstone belt (Byerly and Palmer, 1991).

The exceptionally negative boron isotopes to -21 ‰ require a very light fluid source. Typically, such light boron isotope ratios are attributed to non-marine evaporites or mature continental crust (Marschall and Jiang, 2011; Van Hinsberg et al., 2011). There is no evidence for non-marine evaporites in the Onverwacht Group, and although granitoids surround the greenstone belt, they are generally much younger than the zones of silicification, and many of them are primitive (trondhjemitic to tonalitic) in composition. The only evidence for a Palaeoarchaean mature continental crust is given by rare S-type granite clasts in the basal conglomerate of the Moodiees Group (Sanchez-Garrido et al., 2011). Whatever the source of the isotopically light boron, our data show that it only occurs only in the deformed and brecciated samples, i.e. in rocks that record evidence for fluid infiltration after silicification. These samples also show the largest isotopic diversity in the study, and the negative δ^{11}B values are mainly found in the rims of tourmaline A full explanation for the large range of δ^{11}B remains open but we suggest that it is related to the poly-phase fluid-rock interaction in these samples .

References:

Byerly, G.R., Palmer, M.R., 1991. Tourmaline Mineralization In The Barberton Greenstone-Belt, South-Africa - Early Archean Metasomatism By Evaporite-Derived Boron. Contributions To Mineralogy And Petrology 107, 387-402.

Dutrow, B.L., Henry, D.J., 2011. Tourmaline: A Geologic DVD. Elements 7, 301-306.

Henry, D.J., Novak, M., Hawthorne, F.C., Ertl, A., Dutrow, B.L., Uher, P., Pezzotta, F., 2011. Nomenclature of the tourmaline-supergroup minerals. American Mineralogist 96, 895-913.

Hofmann, A., Harris, C., 2008. Stratiform alteration zones in the Barberton greenstone belt: a window into subseafloor processes 3.5–3.3 Ga ago. Chemical Geology 257, 224-242.

Marschall, H.R., Jiang, S.Y., 2011. Tourmaline Isotopes: No Element Left Behind. Elements 7, 313-319.

Sanchez-Garrido, C.J.M.G., Stevens, G., Armstrong, R.A., Moyen, J.-F., Martin, H., Doucelance, R., 2011. Diversity in Earth's early felsic crust: Paleoarchean peraluminous granites of the Barberton Greenstone Belt. Geology 39, 963-966.

Van Hinsberg, V.J., Henry, D.J., Marschall, H.R., 2011. Tourmaline: an ideal indicator of its host environment. The Canadian Mineralogist 49, 1-16.

IODP

European Petrophysics Consortium: Activities for ESO in the International Ocean Discovery Program

A. FEHR[1], J. LOFI[2], S. MORGAN[3], A.G. MCGRATH[3], E. HANENKAMP[3], S.J. DAVIES[3], S. REICHE[1], C. CLAUSER[1]

1 Institute for Applied Geophysics and Geothermal Energy (GGE), E.ON Energy Research Center, RWTH Aachen University, Mathieutsr. 10, D-52074 Aachen, Germany
2 Géosciences Montpellier, Université Montpellier, 2, Place E. Bataillon, F-34095 Montpellier cedex 5, France
3 University of Leicester, Department of Geology, University Road, Leicester, LE1 7RH, UK

The International Ocean Discovery Program (IODP) is an international marine research drilling program dedicated to globally explore Earth's geological history and structure of the crust by monitoring and sampling sub seafloor environments. For the worldwide offshore drilling activities of IODP, three drilling systems, two research vessels (D/V CHIKYU and JOIDES Resolution) and Mission-specific platforms are operated depending on location and scientific aim of the expedition.

As part of the European Petrophysics Consortium (EPC), the Institute for Applied Geophysics and Geothermal Energy at RWTH Aachen University contributes to the International Ocean Discovery Program (IODP) by providing staff and technical equipment for marine expeditions and performing petrophysical lab analysis of rock and sediment samples drilled during IODP expeditions. The EPC comprises the Department of Geology University of Leicester (UK) (coordinator), the

Department of Geoscience University of Montpellier (F) and the Institute for Applied Geophysics and Geothermal Energy at RWTH Aachen University (D). EPC carries out geophysical logging and petrophysical activities for the European Science Operator (ESO) and forms part of the wider International Scientific Logging Consortium that includes the Borehole Research Group at the Lamont-Doherty Earth Observatory and the Center for Deep Earth Exploration.

In all IODP boreholes standard geophysical logging is performed. In their position as Petrophysics Staff Scientist, scientists from EPC are responsible for planning and coordination of downhole logging and petrophysical measurements, supervising the work and leading the processing and first interpretation of the acquired data. The Petrophysics Staff Scientist is assisted by a team of petrophysicists from EPC and works in close cooperation with the physical properties specialists from the Science Party of the expedition. For more than 20 years, scientists from GGE have regularly been taking part in IODP Expeditions.

In 2013-2014, Annick Fehr (EPC Aachen) participated as Petrophysics Staff Scientist in IODP Expedition 347 Baltic Sea Paleoenvironment. The aim of Expedition 347 was to explore the environmental changes in the Baltic Sea over the last 130 000 years and to acquire the most complete possible record of the paleoceanographic and microbiological evolution preserved within the sediments in this region. Therefore 30 boreholes on 8 sites offshore Denmark and Sweden were drilled and more than 1620 m of high quality sediment core collected. EPC performed downhole logging and Multi Sensor Core Logger measurements offshore, thermal conductivity and natural gamma ray measurements on whole-round cores before the start of the Onshore Party (OSP) and density, P-Wave, digital imaging and color reflectance measurements during the OSP at MARUM in Bremen.

In 2015, IODP Expedition 357 Atlantis Massif seafloor processes will be the next Mission Specific Platform Expedition.

IODP

Intensification of the meridional temperature gradient in the Great Barrier Reef following the Last Glacial Maximum - Results from IODP Expedition 325

T. Felis[1], H.V. McGregor[2], B.K. Linsley[3], A.W. Tudhope[4], M.K. Gagan[2], A. Suzuki[5], M. Inoue[6], A.L. Thomas[4,7], T.M. Esat[2,8,9], W.G. Thompson[10], M. Tiwari[11], D.C. Potts[12], M. Mudelsee[13,14], Y. Yokoyama[6], J.M. Webster[15]

1 MARUM—Center for Marine Environmental Sciences, University of Bremen, 28359 Bremen, Germany
2 Research School of Earth Sciences, The Australian National University, Canberra, Australian Capital Territory 0200, Australia
3 Lamont-Doherty Earth Observatory, Columbia University, Palisades, New York 10964, USA
4 School of GeoSciences, University of Edinburgh, Edinburgh EH9 3JW, UK
5 Geological Survey of Japan, National Institute of Advanced Industrial Science and Technology, Tsukuba 305-8567, Japan
6 Atmosphere and Ocean Research Institute, The University of Tokyo, Kashiwa 277-8564, Japan
7 Department of Earth Sciences, University of Oxford, Oxford OX1 3AN, UK
8 Australian Nuclear Science and Technology Organisation, Institute for Environmental Research, Kirrawee DC, New South Wales 2232, Australia
9 Department of Nuclear Physics, Research School of Physical Sciences and Engineering, The Australian National University, Canberra, Australian Capital Territory 0200, Australia
10 Department of Geology and Geophysics, Woods Hole Oceanographic Institution, Woods Hole, Massachusetts 02543, USA
11 National Centre for Antarctic & Ocean Research, Vasco-da-Gama, Goa 403804, India
12 Department of Ecology & Evolutionary Biology, University of California, Santa Cruz, California 95064, USA
13 Alfred Wegener Institute, Helmholtz Centre for Polar and Marine Research (AWI), 27570 Bremerhaven, Germany
14 Climate Risk Analysis, Heckenbeck, 37581 Bad Gandersheim, Germany
15 Geocoastal Research Group, School of Geosciences, The University of Sydney, Sydney, New South Wales 2006, Australia

Tropical south-western Pacific temperatures are of vital importance to the Great Barrier Reef (GBR), but the role of sea surface temperatures (SSTs) in the growth of the GBR since the Last Glacial Maximum remains largely unknown. Here we present records of Sr/Ca and $\delta^{18}O$ for Last Glacial Maximum and deglacial corals that were drilled by Integrated Ocean Drilling Program (IODP) Expedition 325 along the shelf edge seaward of the modern GBR. The Sr/Ca and $\delta^{18}O$ records of the precisely U-Th dated fossil shallow-water corals show a considerably steeper meridional SST gradient than the present day in the central GBR. We find a 1–2 °C larger temperature decrease between 17°S and 20°S about 20,000 to 13,000 years ago. The result is best explained by the northward expansion of cooler subtropical waters due to a weakening of the South Pacific gyre and East Australian Current. Our findings indicate that the GBR experienced substantial and regionally differing temperature change during the last deglaciation, much larger temperature changes than previously recognized. Furthermore, our findings suggest a northward contraction of the Western Pacific Warm Pool during the LGM and last deglaciation, and serve to explain

anomalous drying of northeastern Australia at that time. Overall, the GBR developed through significant SST change and, considering temperature alone, may be more resilient than previously thought.

References:
Webster, J. M., Yokoyama, Y. & Cotteril, C. & the Expedition 325 Scientists. *Proceedings of the Integrated Ocean Drilling Program* Vol. 325 (Integrated Ocean Drilling Program Management International Inc., 2011).
Felis, T., McGregor, H. V., Linsley, B. K., Tudhope, A. W., Gagan, M. K., Suzuki, A., Inoue, M., Thomas, A. L., Esat, T. M., Thompson, W. G., Tiwari, M., Potts, D. C., Mudelsee, M., Yokoyama, Y., Webster, J. M. Intensification of the meridional temperature gradient in the Great Barrier Reef following the Last Glacial Maximum. *Nature Communications* 5, 4102, doi:10.1038/ncomms5102 (2014).

ICDP

Localization of CO_2 degassing zones, mofettes, using dense small array data and Matched Field Processing analysis in the NW Bohemia/Vogtland region, Czech Republic

H. FLORES-ESTRELLA, J. UMLAUFT, A. SCHMIDT, M. KORN

Institut für Geophysik und Geologie, Universität Leipzig, Talstraße 35, 04103 Leipzig, Germany

The NW Bohemia/Vogtland region is characterized by currently ongoing geodynamic processes within the intracontinental lithospheric mantle. Among others, this activity results in the occurrence of earthquake swarms as well as CO_2 degassing zones, called mofettes. These two natural phenomena are related to each other since it is considered that fluid flow and fluid-induced effective stress trigger earthquake swarms. Though on the surface they appear spatially separated, their connection could be explained by the existence of pathways within the crust that allow efficient and permanent fluid transport. To investigate the structure and depth position of these pathways it is first needed to locate them.

Considering the CO_2 degassing zones as noise sources we set up different arrays of 30 stations and recorded this high and steady noise. We applied the localization method Matched Field Processing (MFP) to locate the sources. First, we tested the applicability of this method at the Dolní Částkov Borehole, which acts as an artificial mofette; therefore, the noise source position is known. On this site we were able to locate satisfactorily the noise source position using eight hours of continuous records. Due to the assumed interaction between earthquake swarms and the mofettes, we applied the MFP method after two different earthquakes on different time lapses and noticed some changes on the position of the noise sources.

At the area of South Hartoušov we used also 30 stations to measure 16 hours of continuous noise divided in two days. At this area we were able to detect two fundamental noise sources: probably one natural mofette and one fluid pathway within the subsoil. The MFP analysis seems to be promising on locating noise sources due to the CO_2 degassing zones. The next steps will be to research deeper and to try to map the CO_2 pathways.

ICDP

Three promising tonnes of sediment cores from Chew Bahir, south Ethiopia, to reconstruct 0.5 Ma of climatic history

V. FOERSTER[1], A. ASRAT[2], A. COHEN[3] A. JUNGINGER[4], H.F. LAMB[5], F. SCHÄBITZ[6], M.H. TRAUTH[1], THE HSPDP SCIENCE TEAM

1 University of Potsdam, Institute of Earth and Environmental Science; Karl-Liebknecht-Str. 24-25; Germany
2 Addis Ababa University, School of Earth Sciences; P. O. Box 1176, Addis Ababa; Ethiopia
3 University of Arizona, Department of Geosciences, Tucson, AZ 85721; USA
4 Eberhard Karls Universität Tübingen, Department of Earth Sciences, Senckenberg Center for Human Evolution and Palaeoenvironment (HEP-Tübingen); Hölderlinstrasse 12, 72074 Tübingen, Germany
5 Aberystwyth University, Department of Geography and Earth Sciences; Aberystwyth SY23 3DB; U.K.
6 University of Cologne, Seminar for Geography and Education; Gronewaldstrasse 2; 50931 Cologne; Germany

Chew Bahir, as a newly explored and just recently ICDP-cored climatic archive, lies between the Main Ethiopian Rift and the Omo-Turkana basin, site of the oldest known fossils of anatomically modern humans. Today Chew Bahir is a saline mudflat in a deep tectonically-bound basin that contains a several kilometre thick sedimentary infill. This basin was cored during a ICDP-supported deep drilling campaign in Oct–Dec 2014, as the last out of five sites of the *Hominin Sites and Paleolakes Drilling Project*' (HSPDP). As a key part of HSPDP, which aims at understanding the role of environmental changes in human evolution, the Chew Bahir cores will elucidate palaeoenvironments of the last 500 kyrs covering the transition into the Middle Stone Age, and the origin and dispersal of *Homo sapiens*.

We present here the initial outcome of the recent successful drilling campaign, giving a first overview of the recovered material from the Chew Bahir basin, including core site selection, a synthesis of the prior studies, employed drilling techniques and preliminary field data. We also provide a summary of the proxies expected, and the sampling plan. Duplicate sediment cores, HSPDP-CHB14-2A and 2B, were retrieved, to 278.58 m and 266.38 m below surface respectively, consist of more than 115 sections each, which all sum up to nearly 3t of sediment. The recovered material is comprised of mostly fine green-greyish to light coloured and reddish clays intercalated by mica-rich sand layers and several potential tephras. The recovery proportions for both cores exceed 85%. Based on the extrapolation of the sedimentation rates from short cores (Foerster et al., 2012, Foerster et al., 2014, Trauth et al., 2015) taken in a NW-SE transect across the basin, we anticipate a record covering at least the last 500,000 yrs BP. The good recovery and relatively high time resolution of the cores promise a continuous environmental record that will allow tests of climate-evolution hypotheses relevant to human origins.

References:
Foerster, V., Junginger, A., Langkamp, O., Gebru, T., Asrat, A., Umer, M., Lamb, H., Wennrich, V., Rethemeyer, J., Nowaczyk, N., Trauth, M.H., Schäbitz, F., 2012. Climatic change recorded in the sediments of the Chew Bahir basin, southern Ethiopia, during the last 45,000 years. Quater- nary International 274, 25–37.

Foerster, V., Junginger, A., Asrat, A., Umer, M., Lamb, H.F., Weber, M., Rethemeyer, J., Frank, U., Brown, M.C., Trauth, M.H., Schaebitz, F., 2014. 46, 000 years of alternating wet and dry phases on decadal to orbital timescales in the cradle of modern humans: the Chew Bahir project, southern Ethiopia. Climate of the Past Discussions 10, doi:10.5194/cpd-10-1-2014, 1–48.

Trauth, M.H., Bergner, A., Foerster, V., Junginger, A., Maslin, M., Schaebitz, F., (accepted). Episodes of Environmental Stability vs. Instability in Late Cenozoic Lake Records of Eastern Africa. Journal of Human Evolution.

HSPDP: http://hspdp.asu.edu/

ICDP

Environmental variability in the Balkan Region between the MPT and present day, derived from lacustrine sediments of the 1.2 Ma old Lake Ohrid: The ICDP SCOPSCO project

A. FRANCKE[1], B. WAGNER[1], G. ZANCHETTA[2], R. SULPIZIO[2,3], N. LEICHER[1], R. GROMIG[1], J. JUST[1], H. BAUMGARTEN[4], K. LINDHORST[5], T. WONIK[4], S. KRASTEL[5], J. LACEY[6,7], M. LENG[6,7], H. VOGEL[8] AND THE SCOPSCO SCIENCE TEAM

1 University of Cologne, Institute for Geology and Mineralogy, Cologne, Germany
2 University of Pisa, Dipartimento di Scienze della Terra, Pisa, Italy
3 University of Bari, Dipartimento di Scienze della Terra e Geoambientali, Bari, Italy
4 Leibniz Institute for Applied Geosciences, Hannover, Germany
5 Christian-Albrechts-Universität zu Kiel, Institute of Geosciences, Kiel, Germany
6 University of Nottingham, School for Geography, Nottingham, UK
7 NERC Isotope Geosciences Facilities, British Geological Survey, Nottingham, UK
8 University of Bern, Institute of Geological Sciences & Oeschger Centre for Climate Change Research, Bern, Switzerland

Lake Ohrid, considered to be the oldest lake of Europe, is located at the border of Macedonia and Albania (40°70′ N, 20°42 E, 698 m asl) in a tectonic active, N-S trending graben. The lake is about 30 km long, 15 km wide and covers a surface area of about 358 km^2. The tub-shaped bathymetry of the lake basin is relatively simple with a maximum water depth of 293 m and a mean water depth of 150 m. With about 212 described endemic species, Lake Ohrid is the most diverse lake in the world when the surface area is taken into account. The catchment area of Lake Ohrid comprises about 2393 km^2 and also includes Lake Prespa, which drains into Lake Ohrid via the intensively karstified rocks of the Galicica Mountain range. Up to 50% of the inflow to Lake Ohrid originates from Lake Prespa, with the remainder coming from direct precipitation and river and surface runoff from the up to 2200 m high surrounding mountains. The lake level of Lake Ohrid is balanced by evaporation (40%), and by surface outflow via the Crn Drim River to the North (60%).

Chronostratigraphic interpretation of prominent cyclic patterns of hydro-acoustic data (Lindhorst et al., 2014), and molecular clock analyses of DNA data (summarized by Wagner and Wilke, 2011) implied that the lake is around 2 Ma old. Several studies on pilot cores that were recovered from shallow water depths in lateral parts of Lake Ohrid yielded the high potential of Lake Ohrid as a valuable paleoenvironmental and /-climatological archive for the Balkan Area (Wagner et al., 2008; Vogel et al., 2010a), and of the tephrostratigraphic history of the central Mediterranean Region (Sulpizio et al., 2010; Vogel et al., 2010b) during the last glacial – interglacial cycle. Moreover, several mass wasting deposits can be observed at Lake Ohrid, which potentially can be used to reconstruct the seismotectonic history of the area (Reicherter et al., 2011; Wagner et al., 2012). In order to obtain more information about the history of the lake back to its formation, more than 2100 m of sediment were recovered from 5 different drill sites between 2011 and 2013 within the scope of the ICDP SCOPSCO (Scientific Collaboration On Past Speciation Conditions in Lake Ohrid) project. Although the analytical work on most of the sediment cores is in progress, first results already imply that the recovered sediments have the potential to substantially improve the understanding of the geological, biological, and environmental history of Lake Ohrid and the central Mediterranean Region, and to address the main targets of the SCOPSCO project. The main targets are (1) to reveal the precise age and origin of Lake Ohrid, (2) to unravel the seismotectonic history of the lake area including effects of major earthquakes and associated mass wasting events, (3) to obtain a continuous record containing information on volcanic activities and climate changes in the central northern Mediterranean region, and (4) to better understand the impact of major geological/environmental events on general evolutionary patterns and shaping an extraordinary degree of endemic biodiversity as a matter of global significance.

A 10 m long sediment core (Co1262) from the so-called “LINI”-site, recovered in 2011 using a UWITEC piston and gravity corer offshore the Lini Peninsula provides a high-resolution record of environmental change and seismotectonic history since the Late Glacial period on the basis of a robust chronology defined by 3 tephra layer and 6 radiocarbon ages. Wagner et al. (2012) have shown that two Mass Wasting Deposits (MWD) occur in core Co1262. The uppermost, about 2 m thick MWD was probably triggered by seismotectonic activity, as its timing coincides with a strong earthquake in the early 6th century AD. A high-resolution study of isotope and geochemical data of the “LINI” sequence improved the understanding of organic matter and calcite formation and preservation in the sediments of Lake Ohrid (Lacey et al., 2014). This study will help to understand the proxy data obtained on the long sediment sequences of Lake Ohrid, recovered during the deep drilling campaign in 2013.

The deep drilling campaign in 2013 was operated by DOSECC (Drilling, Observation and Sampling of the Earth´s Continental Crust) using the DLDS (Deep Lake Drilling System). Between March and June 2013, four drill sites were cored in Lake Ohrid with and overall recovery of more than 95% at each site. Three of these drill sites are located along the eastern and southeastern shoreline of the lake (CERAVA, GRADISTE, PESTANI). The aims of these three drill sites are to gather more information (1) about the hydrological variability in Lake Ohrid (“CERAVA”-site, deepest hole: 90.48 m), (2) about biodiversity and mass wasting (“GRADISTE”-site, deepest hole: 123.41 m), and (3) about the early development of the lake basin (“PESTANI”-site, deepest hole: 194.50 m). At the main drill site in central parts of the lake, the “DEEP”-site, more than 1500 m of sediments were recovered down to a maximum penetration depth of 568.92 m. Gravel and pebble-sized material hampered a deeper penetration,

although hydro-acoustic data implied an overall sediment thickness at the "DEEP"-site of at least 680 m (Wagner et al., 2014). The coarse-grained basal deposits of the "DEEP"-site sequence indicate that fluvial conditions prevailed when the graben structure of modern Lake Ohrid formed as a pull-apart basin. Fluvial conditions and/or shallow lacustrine water conditions apparently persist until ca. 420 m sediment depth, indicated by very heterogeneous deposits consisting clayey, silt-sized or gravelly deposits with intercalated peat layer. First biogeochemical analyses on core catcher material and magnetic susceptibility measurements (MS) on the whole core yielded negligible Total Inorganic Carbon (TIC) contents and high MS values below 420 m sediment depth. Above 420 m sediment depth, the deposits appear homogenous and consist of silt-sized material with varying TIC contents and MS values. The overall homogenous appearance of the deposits and the fine grain-size imply more pelagic sedimentation in deeper water depths and probably indicates the formation of modern Lake Ohrid. Previous studies on the pilot cores from Lake Ohrid have shown that high TIC contents correlates with interglacial periods. The TIC content predominantly depends on the amount photosynthesis-induced precipitated endogenic calcite in the sediments (Leng et al., 2010; Vogel et al., 2010a). In the "DEEP"-site sequence, the high TIC contents correspond to low MS values, which might imply that interglacial deposits contain low amounts of clastic material. In contrast, glacial sediments are characterized by high amounts of clastic matter (high MS) and by low calcite contents (low TIC), respectively. Oscillations of TIC and MS data, with a high frequency between 420 and 250 m sediment depth and a

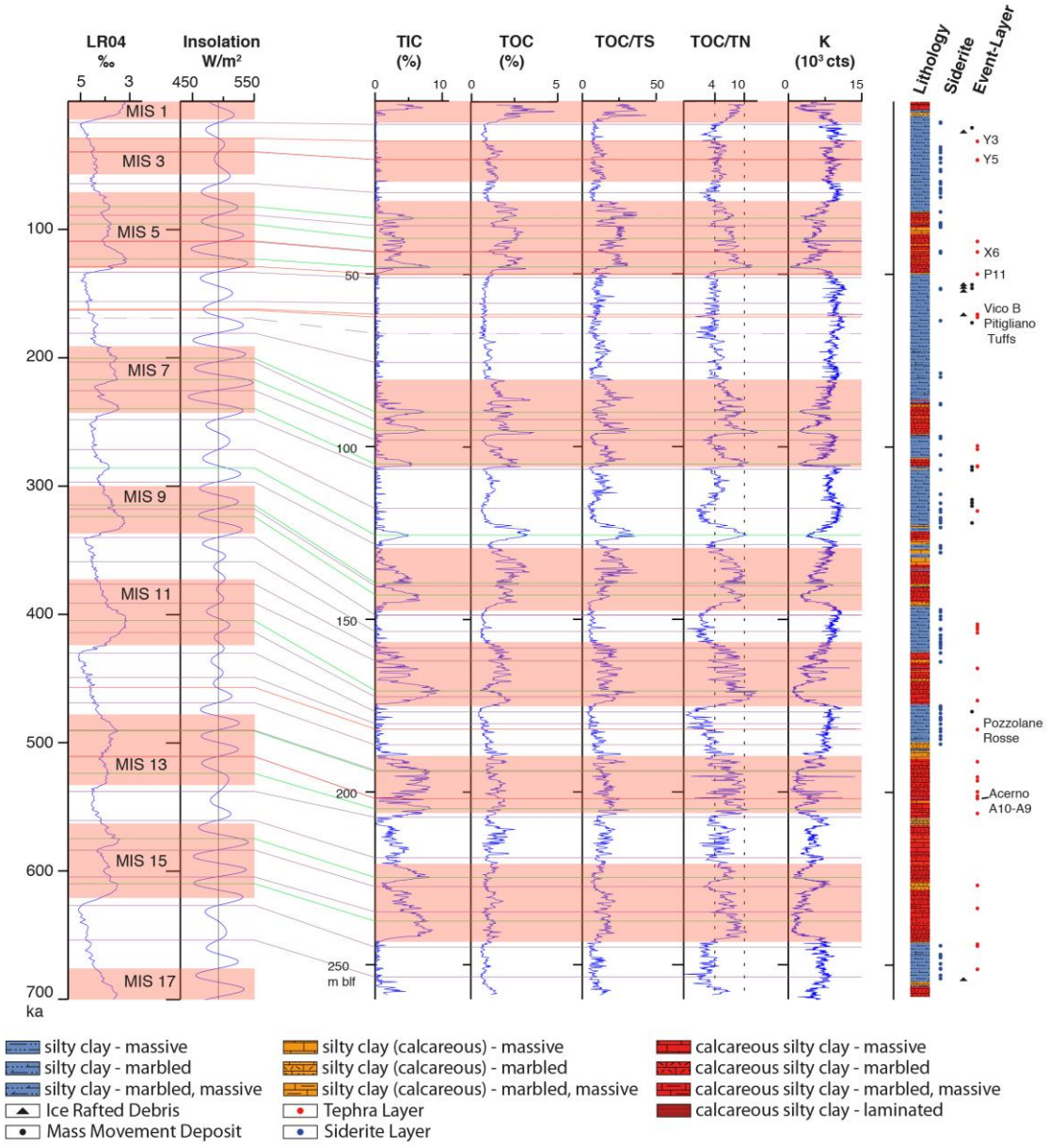

Fig. 1. Biogeochemistry data (TIC, TOC, TOC/TS, TOC/TN) , XRF data (K), and lithological information of the upper 260 m of the "DEEP"-site sequence. The red lines indicated chronological tie points derived from tephrostratigraphic information. Cross correlation points to the global benthic isotope stack LR04 by Lisiecki and Raymo (2005) and summer (21. June) local insolation patterns at 41°N (Laskar et al., 2004) are indicated by green (LR04 isotopic minima versus TIC peaks) and purple (insolation patterns versus TOC, TOC/TN, and TOC/TS minima) lines. For further information about the cross correlation see text. Red shaded areas in LR04 and the local insolation mark global interglacial periods after Lisiecki and Raymo (2005) and were transferred to the "DEEP"-site sequence.

lower frequency afterwards, can be correlated to a succession of glacial/interglacial cycles with a shift from a dominant Milankovitch´s obliquity band (40 ka) to a dominate Milankovitch´s eccentricity band (100 ka). The succession of the cyclic shifts implies that Lake Ohrid is at least 1.2 Ma old (Wagner et al., 2014).

Since October 2013, the sediment cores from the "DEEP"-site have been opened, processed, and sampled at the University of Cologne. The processing of the cores includes high-resolution XRF scanning, MSCL-scanning, line-scan imaging, visual core descriptions, core correlation, and compositing. Sub-sampling is carried out at 8 cm resolution for proxy data analyses, and at 48 cm resolution for paleomagnetic studies. Small aliquots from tephra layers are directly sampled after core opening and analyzed for their geochemical composition at the University of Pisa, Italy. Presently, the sediment cores from the upper 300 m of the "DEEP"-site sequence are opened and subsampled. High-resolution biogeochemistry data (TIC, TOC, TN, TS) and XRF-scanning data are measured to 260 m sediment depth. A chronology for the upper 260 m of the "DEEP"-site sequence was established by using tephrochronological tie points, and by stratigraphic tuning of the biogeochemistry data to the global benthic isotope stack LR04 by Lisiecki and Raymo (2005), and to local daily insolation patterns (21. June) at 41°N (Laskar et al., 2004 Fig. 1). Tephrostratigraphy and tephrochronology were used to obtain first order tie points. Tuning peak TIC values in the "DEEP"-site sequence to isotopic minima of the global benthic isotope LR04 stack was used to generate second order tie points. Minima in TOC content (Total Organic Carbon) and TOC-related ratios were tuned with increasing trends in the local daily insolation patterns. Orbital tuning was cross checked by the occurrence of well-dated tephra layers Y5, X-6, P11, and Acerno A10-A9 (Fig. 1). The established chronology implies that the upper 260 m of the "DEEP"-site sequence correspond to the time period between ca. 660 ka and present day. A more detailed comparison between the allocation of the MIS (defined by Lisiecki and Raymo, 2005) and the lithological information of the "DEEP"-site sequence yield that changes in the lithology only partly correspond with glacial/interglacial boundaries (Fig. 1). The lithology of the "DEEP"-site sequence predominantly depends on the calcite content in the sediments and can be separated into three facies (Fig. 1). Facies 1 (blue) and facies 2 (yellow) appear marbled or massive and have negligible and moderate calcite contents. Sporadically, sand lenses or gravel grains interpreted as ice rafted debris appear in facies 1, whereas siderite layers can be found in both facies 1 and 2, defined by distinct peaks in the TIC data. Facies 3 (red) contains high amounts of calcite and appear massive or marbled. Laminated structures in facies 3 occur only in the uppermost, Holocene parts of the sequence. The discrepancy between warm climate conditions at Lake Ohrid during interglacial periods and low or moderate calcite contents indicated by the lithology can be explained by dilution of calcite and is also evident in the biogeochemistry data. For example, the TOC/TN ratios around 4 (i.e. during glacial periods) might imply oxidation of organic matter (Leng et al., 1999), which may cause CO2 release from the surface sediments and a slight acidification of the bottom waters. Acidification could also trigger the formation of diagenetic siderite in the slightly anoxic porewater close to the redox boundary, such as also described at Lake Prespa (Leng et al., 2013). Diagenetic processes close to the redox boundary and a sulfidic (micro-) environment during the earlier history of Lake Ohrid probably also triggered the formation of greigite (Fe_3S_4), which can frequently be found in the deposits of the "DEEP"-site sequence below 130 m sediment depth.

Summarized, the lithological, (bio-)geochemical, paleomagentic, and tephrostratigraphic data of the "DEEP"-site sequence imply that the sediment record of Lake Ohrid will become a key record for the paleoenvironmental and tephrostratigraphic history for the central Mediterranean Region. First results indicate that the recovered deposits provide a unique potential to address the main questions of the SCOPSCO project, i.e. to define the precise age of the lake, to clarify why Lake Ohrid has such a high number of endemic species, and to establish a detailed history of the seismotectonic, the environmental and the tephrostratigraphic development in the Lake Ohrid area.

References:

Lacey, J., Francke, A., Leng, M., Vane, C., and Wagner, B.: A high-resolution Late Glacial to Holocene record of environmental change in the Mediterranean from Lake Ohrid (Macedonia/Albania), International Journal of Earth Sciences, 1-16, 10.1007/s00531-014-1033-6, 2014.

Laskar, J., Robutel, P., Joutel, F., Gastineau, M., Correia, A. C. M., and Levrard, B.: A long-term numerical solution for the insolation quantities of the Earth, Astronomy & Astrophysics, 428, 261-285, 10.1051/0004-6361:20041335, 2004.

Leng, M. J., Roberts, N., Reed, J. M., and Sloane, H. J.: Late Quaternary palaeohydrology of the Konya Basin, Turkey, based on isotope studies of modern hydrology and lacustrine carbonates, Journal of Paleolimnology, 22, 187-204, 10.1023/a:1008024127346, 1999.

Leng, M. J., Baneschi, I., Zanchetta, G., Jex, C. N., Wagner, B., and Vogel, H.: Late Quaternary palaeoenvironmental reconstruction from Lakes Ohrid and Prespa (Macedonia/Albania border) using stable isotopes, Biogeosciences, 7, 3109-3122, 10.5194/bg-7-3109-2010, 2010.

Leng, M. J., Wagner, B., Boehm, A., Panagiotopoulos, K., Vane, C. H., Snelling, A., Haidon, C., Woodley, E., Vogel, H., Zanchetta, G., and Baneschi, I.: Understanding past climatic and hydrological variability in the Mediterranean from Lake Prespa sediment isotope and geochemical record over the Last Glacial cycle, Quaternary Science Reviews, 66, 123-136, 10.1016/j.quascirev.2012.07.015, 2013.

Lindhorst, K., Krastel, S., Reicherter, K., Stipp, M., Wagner, B., and Schwenk, T.: Sedimentary and tectonic evolution of Lake Ohrid (Macedonia/Albania), Basin Research, 0, 1-18, 10.1111/bre.12063, 2014.

Lisiecki, L. E. and Raymo, M. E.: A Pliocene-Pleistocene stack of 57 globally distributed benthic δ18O records, Paleoceanography, 20, PA1003, 10.1029/2004pa001071, 2005.

Reicherter, K., Hoffmann, N., Lindhorst, K., Krastel, S., Fernandez- Steeger, T., Grützner, C., and Wiatr, T.: Active basins and neotectonics: morphotectonics of the Lake Ohrid Basin (FYROM and Albania), Zeitschrift der Deutschen Gesellschaft für Geowissenschaften, 162, 217-234, 10.1127/1860-1804/2011/0162-0217, 2011.

Sulpizio, R., Zanchetta, G., D'Orazio, M., Vogel, H., and Wagner, B.: Tephrostratigraphy and tephrochronology of lakes Ohrid and Prespa, Balkans, Biogeosciences, 7, 3273-3288, 10.5194/bg-7-3273-2010, 2010.

Vogel, H., Wagner, B., Zanchetta, G., Sulpizio, R., and Rosén, P.: A paleoclimate record with tephrochronological age control for the last glacial-interglacial cycle from Lake Ohrid, Albania and Macedonia, Journal of Paleolimnology, 44, 295-310, 10.1007/s10933-009-9404-x, 2010a.

Vogel, H., Zanchetta, G., Sulpizio, R., Wagner, B., and Nowaczyk, N.: A tephrostratigraphic record for the last glacial-interglacial cycle from Lake Ohrid, Albania and Macedonia, Journal of Quaternary Science, 25, 320-338, 10.1002/jqs.1311, 2010b.

Wagner, B., Reicherter, K., Daut, G., Wessels, M., Matzinger, A., Schwalb, A., Spirkovski, Z., and Sanxhaku, M.: The potential of Lake Ohrid for long-term palaeoenvironmental reconstructions, Palaeogeography, Palaeoclimatology, Palaeoecology, 259, 341-356, 10.1016/j.palaeo.2007.10.015, 2008.

Wagner, B. and Wilke, T.: Preface "Evolutionary and geological history of the Balkan lakes Ohrid and Prespa", Biogeosciences, 8, 995-998, 10.5194/bg-8-995-2011, 2011.

Wagner, B., Francke, A., Sulpizio, R., Zanchetta, G., Lindhorst, K., Krastel, S., Vogel, H., Rethemeyer, J., Daut, G., Grazhdani, A., Lushaj, B., and Trajanovski, S.: Possible earthquake trigger for 6th century mass

wasting deposit at Lake Ohrid (Macedonia/Albania), Clim. Past, 8, 2069-2078, 10.5194/cp-8-2069-2012, 2012.
Wagner, B., Wilke, T., Krastel, S., Zanchetta, G., Sulpizio, R., Reicherter, K., Leng, M. J., Grazhdani, A., Trajanovski, S., Francke, A., Lindhorst, K., Levkov, Z., Cvetkoska, A., Reed, J. M., Zhang, X., Lacey, J. H., Wonik, T., Baumgarten, H., and Vogel, H.: The SCOPSCO drilling project recovers more than 1.2 million years of history from Lake Ohrid, Sci. Dril., 17, 19-29, 10.5194/sd-17-19-2014, 2014.

ICDP

Microbial populations in iron-rich sediments of Lake Towuti at varying bottom water oxygenation levels – Results of a pilot study for the 2015 ICDP drilling campaign

A. FRIESE, A. VUILLEMIN, M. ALAWI, D. WAGNER AND J. KALLMEYER

Helmholtz Centre Potsdam, GFZ German Research Centre for Geosciences, Section 4.5 Geomicrobiology, 14473 Potsdam, Germany

Lake Towuti is a deep tectonic basin, located on the Island of Sulawesi, central Indonesia. Its geographic position allows for recording paleoclimatic changes related to the tropical Western Pacific warm pool in its sedimentary sequence (Fig. 1A). It was therefore chosen as an ICDP drilling location, the campaign is planned for summer 2015.

The catchment is mainly composed of ophiolitic rocks and lateritic soils (Fig. 1B). Due to massive iron (hydr)oxide inflows from the laterites, phosphorus adsorption onto the iron (hydr)oxides and subsequent burial, phosphorus is strongly depleted in the water column, leading to ultra-oligotrophic conditions. Through this process, weathering in the catchment exerts strong control on the trophic state of the lake. As Lake Towuti mixes at least occasionally, its bottom waters face different levels of oxygenation, making the sediment and its metalliferous substrates a peculiar environment for microbial communities. These settings possibly result in enhanced preservation of organic matter (OM) in the lacustrine record.

Two pilot campaigns were conducted in 2013 and 2014 during which up to 80 cm long gravity cores were taken at three different sites (60, 150, 200 m water depth; Fig. 1C), corresponding to oxic, suboxic and anoxic bottom waters. The intermediate site (150 m water depth) will be one of the two sites of the forthcoming ICDP drilling campaign and the main target of the geomicrobiological investigations, as, for the first time in ICDP history, a dedicated core for geomicrobiological analyses will be drilled.

Given the unusual composition of the sediment and the lack of any basic biogeochemical data, this multiproxy pilot study aims to establish the relationship between biogeochemistry and microbial communities in iron-rich anoxic sediments as well as provide a chance to optimize analytical procedures well in advance of the actual drilling campaign. The short gravity cores were sampled on site for pore water, cell counts, sulfate reduction rates and genetic analyses. 16S rRNA fingerprinting of microbial populations was performed on separate intra- and extracellular DNA fractions.

Phosphorus sorption was expected to vary in accordance to bottom water oxygenation and to further influence primary productivity along with the type of sedimented OM. Indeed, total organic carbon and C_{org}/N ratios measured in bulk sediments showed a gradual increase of values from the shallow site toward the deep site. Microbial cell densities were highest at the shallow site in comparison to the intermediate and deep sites (i.e. log10 from 0 to 20 cm depth = 9.6 to 8.2, 8.4 to 7.8, and 8.1 to 7.7) and were related to the availability of labile OM and sulfate in the pore water. At the intermediate site, sporadic mixing of the water column was recorded as variations of the organic carbon content while structurally

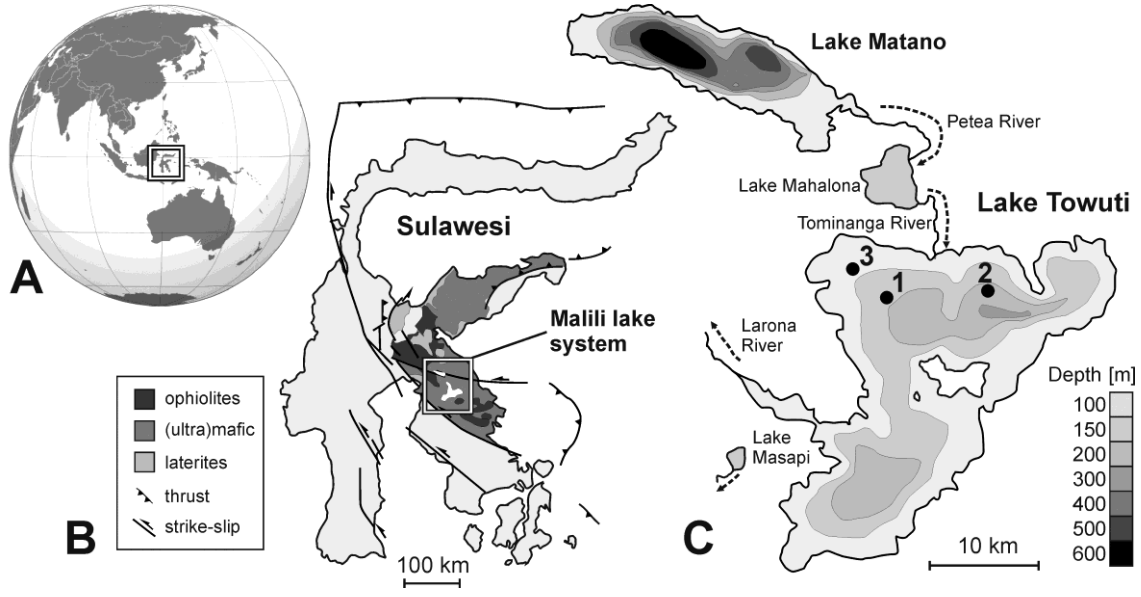

Fig. 1. Lake Towuti location and settings. (A) Map of Asia and Oceania displaying the location of Sulawesi Island. (B) Map of Sulawesi illustrating the geological context of the Malili lake system. (C) Bathymetric map of Lake Matano and Lake Towuti displaying the three sites (150, 200, 60 m depth) at which gravity cores were retrieved.

affecting archaeal populations. At the deep site, the highly refractory OM coupled to the depletion of electron acceptors already in the water column resulted in lowest microbial cell densities. Radiotracer incubation experiments showed that sulfate reducing bacteria were active at the shallow site, whereas they were only detectable at the two other sites, supposedly due to the initially low sulfate concentrations of these sediments. Due to extremely low concentrations of dissolved phosphorus and nitrogen in the pore water, microbes were mainly provided with nutrients through the degradation of labile OM within sediments, which led to the rapid turnover of extracellular DNA in the uppermost sediment layers.

Despite the iron-rich and ultra-oligotrophic conditions of Lake Towuti, the sediments were shown to be substantially colonized by microbes, albeit at different degrees for each of the three sites. Microbial density, diversity and activity decrease with increasing water depth due to decreasing availability of electron acceptors and easily degradable organic matter.

IODP

The influence of the Mediterranean Outflow Water on the Late Miocene Gulf of Cádiz.

ÁNGELA GARCÍA GALLARDO[1], PATRICK GRUNERT[1,2], WERNER E. PILLER[1], FRANCISCO JOSÉ JIMÉNEZ ESPEJO[3], MARLIES VAN DER SCHEE[4], FRANCISCO SIERRO SANCHEZ[4].

1 Institute for Earth Sciences, University of Graz, NAWI-Graz, Austria
2 Department of Earth and Planetary Sciences, Rutgers University, USA
3 Department of Earth and Planetary Sciences, Nagoya University, Japan.
4 Department of Geology, University of Salamanca, Spain.

Tectonic forcing plays an important role on the opening and closure of ocean gateways. The tectonically-induced opening of the Gibraltar Strait 5.23 Ma ago allowed the re-filling of the Mediterranean Sea and subsequently led to the formation of the Mediterranean Outflow Water (MOW). It became an important component of North Atlantic circulation as warmer and more saline water mass after its exit through the strait contributing to the alteration of the deep water circulation and the global heat transport. The early history of MOW is not well known yet, and this project, funded by the Austrian Science Fund (FWF), takes part of the research goals of Expedition 339 of the Integrated Ocean Drilling Program (IODP), focused on a better understanding of the environmental significance of the MOW and its role in global climate since the Pliocene.

Quantitative analyses of benthic foraminifera from IODP Site U1387C have been completed on the Late Miocene in order to reconstruct paleoceanographic changes in the Gulf of Cádiz. The studied interval spans from 625 to 865 mbsf (meters below sea-floor) and is dominated by hemipelagic deposits. The first results from this interval show assemblages with a high species diversity of autochthonous taxa (i.e. *Cibicidoides spp*., *Globobulimina spp*., *Uvigerina spp*.) and the presence of some shelf dwelling taxa (*Ammonia spp*., *Elphidium spp*. and *Asterigerinata spp*.). The latter come from intervals with coarser sediments indicating downslope transport with shallower water sediments, likely related to tectonic activity. The restriction of the Gibraltar Strait and the disruption of exchange between the Mediterranean and the North Atlantic during the Late Messinian are reflected in the rare abundance of epibenthic taxa. Furthermore, benthic foraminifera are generally proved to be excellent indicators of variations in the oxygen content of bottom waters. In our samples, the obtained results will be used in combination with XRF records (S, Ba, Br) to detect changes in bottom water oxygenation and export productivity. An improved age model will provide the accurate timeline to place the Miocene events from IODP Site U1387C.

IODP

Pleistocene Indian Monsoon rainfall variability

D. GEBREGIORGIS[1], E.C. HATHORNE[1], L. GIOSAN[2], T.S. COLLETT[3], D. NÜRNBERG[1], M. FRANK[1]

1 GEOMAR Helmholtz-Zentrum für Ozeanforschung Kiel, Wischhofstr. 1-3, 24148 Kiel, Germany
2 Woods Hole Oceanographic Institution, 360 Woods Hole Rd., Woods Hole, MA 02543, USA
3 U.S. Geological Survey, Box 25046, MS-939 Denver, Colorado 80225, USA

The Indian monsoon is a prominent feature of the large-scale Asian summer monsoon circulation that directly affects the livelihoods of over a billion people. The Indian monsoon circulation is fundamentally driven by asymmetric heating of the Ocean and Indo-Asian landmasses leading to a strong pressure gradient between low pressure cells over the continent and high pressure cells in the southern subtropical Indian Ocean inducing large-scale shifts in the position of the Inter-tropical Convergence Zone (ITCZ). The Indian monsoon exhibits pronounced variability over a wide range of time scales from interannual (e.g. Webster and Yang, 1992) to decadal, centennial (e.g. Fleitmann et al., 2003), millennial and orbital time-scales (e.g. Overpeck et al., 1996). Many records of the East Asian monsoon have been generated from China and the South China Sea while past variability of the Indian Monsoon is mostly known from records of monsoon wind strength over the Arabian Sea. This study uses the unique long sediment core NGHP Site 17 obtained by the IODP vessel *JOIDES Resolution* in the Andaman Sea to examine the past variability of Indian Monsoon precipitation in the Indian sub-continent and Indo-China and directly over the ocean. The age model of Site 17 is based on correlation of benthic *C. wuellerstorfi* $\delta^{18}O$, which shows 1.75 ‰ glacial-interglacial ~100 kyrs cycles, to the LR04 global benthic $\delta^{18}O$ stack (Lisiecki and Raymo, 2005), further controlled by five ^{14}C dates and the youngest Toba ash layer (Ali et al., submitted). On this basis, we examine orbital scale phase relationships between surface and thermocline waters and infer changes in upper

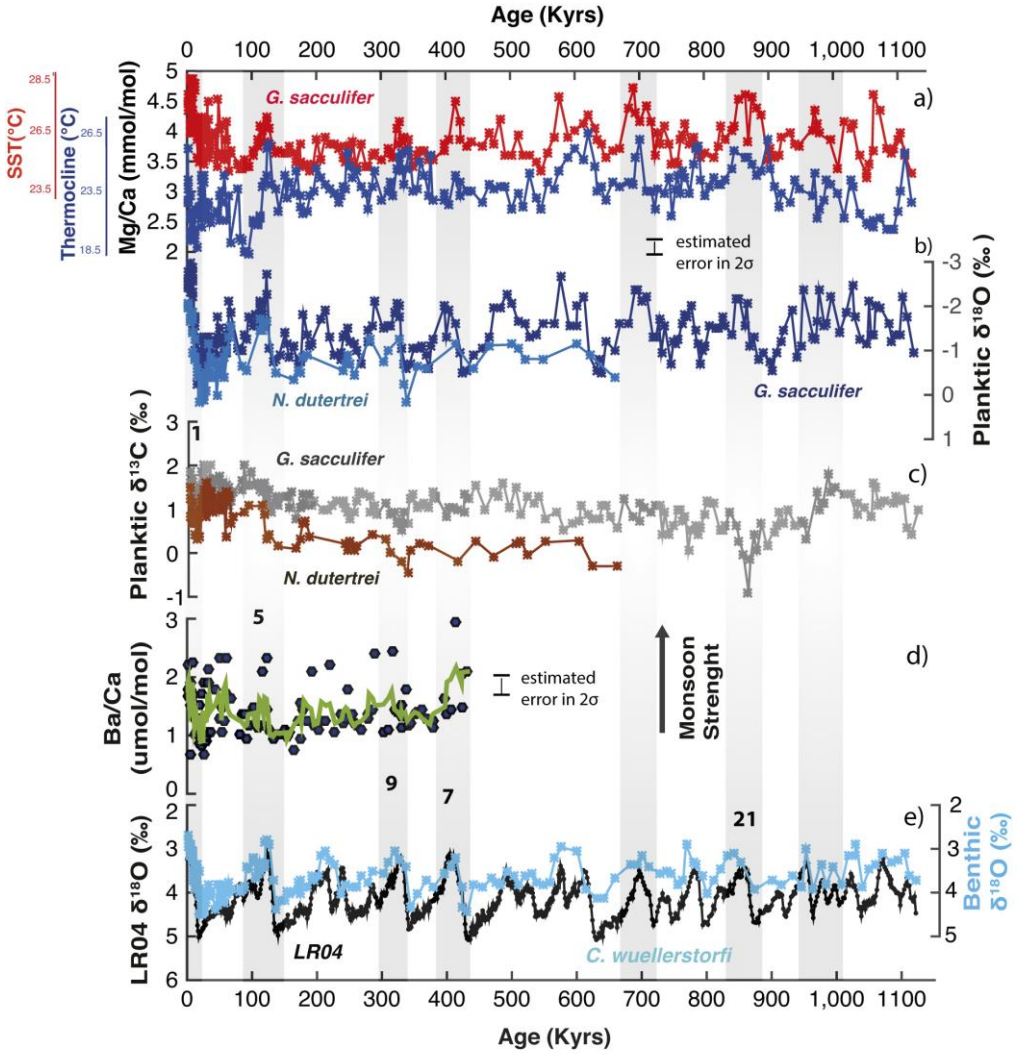

Fig 1. a) Mg/Ca ratios and temperature estimates based on the calibrations of Dekens et al.(2002) for mixed layer inhabiting *G. sacculifer* and thermocline dwelling *N. dutertrei*. Headers show the estimated temperature range for G. sacculifer and N. dutertrei. Error bars for Mg/Ca measurements (2σ is ± 0.05 mmol/mol) based on repeated analysis (n = 10) of ECRM 752-1 (Greaves et al., 2008). b) Oxygen Isotope ratios of planktic foraminifera *G. sacculifer* and *N. dutertrei*. c) $\delta^{13}C$ records of planktic foraminifera *G. sacculifer* and *N. dutertrei*. d) Ba/Ca ratios for mixed layer inhabiting *G. sacculifer*. Solid line denotes 3pts-moving average. Error bars for Ba/Ca measurements (2σ is ± 0.33 umol/mol) based on repeated analysis (n = 10) of ECRM 752-1 (Greaves et al., 2008). e) Oxygen Isotope ratios of benthic foraminifera *C. wuellerstorfi* and the benthic foraminiferal $\delta^{18}O$ stack (black, Lisiecki and Raymo, 2005). Benthic *C. wuellerstorfi* δ18O values adjusted to equilibrium by adding 0.64‰ (Shackleton and Hall, 1984).

column stratification resulting from freshwater input, and monsoon intensity spanning the last ~1100 kyrs, but our study will eventually provide a complete Pleistocene record.

The monsoon related influx of freshwater to the Bay of Bengal and Andaman Sea leads to a low salinity surface layer and a strong stratification of the upper 200 meters. A sediment trap study in the region suggests that the abundances of mixed layer dwelling planktonic foraminifera *G. ruber* and *G. sacculifer* are not biased towards a particular season (Guptha et al., 1997). The thermocline dwelling *N. dutertrei* is also found throughout the year but with a broad peak at the initiation and during the summer monsoon (Guptha et al., 1997). We utilize the ecological habitats of *G. sacculifer* and *N. dutertrei* to investigate the freshwater-induced stratification with paired Mg/Ca and $\delta^{18}O$ analyses to estimate seawater $\delta^{18}O$ ($\delta^{18}O_{sw}$). Forminiferal Ba/Ca, a proxy for river runoff with high Ba concentrations (e.g. Bahr et al., 2013), was also investigated to infer changes in monsoon strength.

The glacial interglacial variability in *G. sacculifer* and *N. dutertrei* $\delta^{18}O$ records exceeds those of the benthic foraminiferal species by ~0.5‰ pointing to a considerable impact of temperature and salinity (Figure 1b). $\delta^{13}C$ records for *G. sacculifer* and *N. dutertrei* show limited glacial-interglacial changes compared to $\delta^{18}O$ records, with thermocline dwelling *N. dutertrei* showing values lower than *G. sacculifer*. Mg/Ca-temperature records for *G. sacculifer* and *N. dutertrei* similarly show pronounced glacial-interglacial changes. Interglacials are marked by decreases in the temperature gradient between *G. sacculifer* and *N. dutertrei* either reflecting significant shoaling of the

thermocline and the vertical migration of *N. dutertrei* or a comparatively warm thermocline. The first results for the difference between *G. sacculifer* and *N. dutertrei* $\delta^{18}O_{sw}$ indicate that upper ocean stratification was strong during the LGM and for some periods during MIS 3. *G. sacculifer* Ba/Ca values point to enhanced river runoff during peak interglacials and significantly less runoff particularly during the LGM, in line with sea surface $\delta^{18}O_{sw}$ trends. The spectral analysis of the Ba/Ca record unfortunately does not reveal significant periodicities. Preliminary spectral analyses of both planktonic and benthic $\delta^{18}O$ records indicate strong spectral power ($p<0.01$) at the two main orbital frequencies corresponding to 41 kyrs and 23 kyrs, but with slightly stronger spectral power at the obliquity band, indicating enhanced monsoon response. Depth domain spectral analysis of planktonic $\delta^{18}O$ records also indicates similar pacing corresponding to the two main orbital periods and confirms that the spectral signal is not an artifact of the age model. Our spectral results are broadly inline with other monsoon studies covering this time period from the southern Bay of Bengal (e.g. Bolton et al., 2013) and the South China Sea (e.g. Wang et al., 2008), although the precession cycle is shown to dominate spectral signal in these records.

In summary, the NGHP Site 17 proxy records suggest that the Indian monsoon is dominated by variance at the obliquity and precession cycles with relatively weaker forcing at the eccentricity band in response to large scale changes in global ice volume. Northern hemisphere summer insolation and Southern Hemisphere latent heat export are in phase during the obliquity band and this is the likely reason for a stronger obliquity related monsoon response than for the precession band (Clemens and Prell, 2003). This indicates monsoon variations are more likely sensitive to the export and cross-equatorial transport of latent heat than to external insolation forcing over the Asian Plateau (Clemens and Prell, 2003).

References

Ali, S., Hathorne, E.C., Frank, M., Gebregiorgis, D., Stattegger, K., Giosan, L., Collett ,T.S., Stumpf, R., 2014. South Asian monsoon history over the past 60 kyr recorded by radiogenic isotopes and clay mineral assemblages in the Andaman Sea. Geochemistry, Geophysics, Geosystems (In review).

Bahr, A., Schönfeld, J., Hoffmann, J., Voigt, S., Aurahs, R., Kucera, M., Flögel, S., Jentzen, A. and Gerdes, A., 2013. Comparison of Ba/Ca and as freshwater proxies: A multi-species core-top study on planktonic foraminifera from the vicinity of the Orinoco River mouth. Earth and Planetary Science Letters, 383(0): 45-57.

Fleitmann, D., Burns, S.J., Mudelsee, M., Neff, U., Kramers, J., Mangini, A. and Matter, A., 2003. Holocene Forcing of the Indian Monsoon Recorded in a Stalagmite from Southern Oman. Science, 300(5626): 1737-1739.

Clemens, S.C. and Prell, W.L., 2003. A 350,000 year summer-monsoon multi-proxy stack from the Owen Ridge, Northern Arabian Sea. Marine Geology, 201(1): 35-51.

Dekens, P.S., Lea, D.W., Pak, D.K., Spero, H.J., 2002. Core top calibration of Mg/Ca intropical foraminifera: refining paleotemperature estimation. Geochem.Geophys.Geosyst. 3 (4).

Greaves, M., Caillon, N., Rebaubier, H., Bartoli, G., Bohaty, S., Cacho, I., Clarke, L., Cooper, M., Daunt, C. and Delaney, M., 2008. Interlaboratory comparison study of calibration standards for foraminiferal Mg/Ca thermometry. Geochemistry, Geophysics, Geosystems, 9(8).

Guptha, M., Curry, W., Ittekkot, V. and Muralinath, A., 1997. Seasonal variation in the flux of planktic Foraminifera; sediment trap results from the Bay of Bengal, northern Indian Ocean. The Journal of Foraminiferal Research, 27(1): 5-19.

Lisiecki, L. E. and M. E. Raymo, 2005. A Pliocene-Pleistocene stack of 57 globally distributed benthic $\delta^{18}O$ records. Paleoceanography, 20, PA1003.

Overpeck, J., Anderson, D., Trumbore, S. and Prell, W., 1996. The southwest Indian Monsoon over the last 18 000 years. Climate Dynamics, 12(3): 213-225.

Shackleton, N.J., Hall, M.A., 1984. Oxygen and Carbon Isotope Stratigraphy of Deep Sea Drilling Project Hole 552A: Plioepleistocene Glacial History. Initial Reports of the Deep Sea Drilling Project, pp. 599-609.

Webster, P.J., Magana, V.O., Palmer, T., Shukla, J., Tomas, R., Yanai, M.u. and Yasunari, T., 1998. Monsoons: Processes, predictability, and the prospects for prediction. Journal of Geophysical Research: Oceans (1978–2012), 103(C7): 14451-14510.

IODP

Evaluation of calcareous dinoflagellate cysts as recorders for temperature changes and fluctuations in ocean chemistry

N. GUSSONE[1], B.M.A. TEICHERT[2], O. FRIEDRICH[3]

1 Institut für Mineralogie - Universität Münster, Corrensstr. 24, 48149 Münster
2 Institut für Geologie und Paläontologie - Universität Münster, Corrensstr. 24, 48149 Münster
3 Institut für Geowissenschaften - Universität Heidelberg, Im Neuenheimer Feld 234-236, 69120 Heidelberg

Dinoflagellates significantly contribute to the oceanic primary production and are used as stratigraphic and paleoenvironmental indicators. They can form cysts, composed of organic-material, silicate or calcium carbonate. The latter group, the so-called calcareous dinoflagellates, provides an archive for long-term changes in the ocean chemistry and past environmental changes (Hildebrand-Habel and Willems, 2000). They are particularly useful as proxy archives recording ocean surface conditions (e.g. temperature, pH), as they form at the deep chlorophyll maximum depth in the water column (Zonneveld, 2004). It has been shown that the $\delta^{18}O$ of the dominant calcareous dinoflagellate species *Thoracosphaera* records reliable sea surface temperatures (SST) in specimens from laboratory cultures, surface waters and sediment samples (Zonneveld, 2004; Zonneveld et al., 2007). Furthermore, the applicability as long-term archive is indicated by the observation that their cysts are comparatively insensitive to dissolution.

Culture experiments demonstrate a significant dependence of Sr/Ca ratios of *T. heimii* cysts on temperature (Gussone et al., 2010). The gradient of 0.016 mmol/mol $°C^{-1}$ is sufficiently large to be applied as additional SST proxy and used to correct for changes in salinity, influencing the $\delta^{18}O$ of carbonate shells.

Furthermore, minor changes of Ca isotope fractionation in *T. heimii* have been shown in relation to the environmental parameters temperature, salinity and pH (Gussone et al., 2010), making it a promising archive for the reconstruction of $\delta^{44/40}Ca_{seawater}$.

The aim of this study is to test the applicability and preservation potential of calcareous dinoflagellate cysts as recorders for Sr/Ca ratios as paleo-SST proxy and $\delta^{44/40}Ca$ as measure for changes in the oceanic Ca budget over geological time scales. We investigated sediments from IODP Hole 690C from the Weddel Sea (Southern Ocean), a site which is located close to the potential source region of Late Cretaceous southern component waters (e.g. Friedrich et al., 2009). The abundant dinoflagellate species

Pirumella krasheninnikovii and *Orthopithonella globosa* were handpicked from the time interval 73-68 Ma (used size fraction 63-125 µm) and cleaned following the procedure for coccolithophores and dinoflagellates (Gussone et al. 2006, 2010).

In the investigated time interval, *Pirumella krasheninnikovii* and *O. globosa* show a significant increase in $\delta^{44/40}$Ca of about 0.3‰ and both calcareous dinoflagellate species exibit within uncertainty identical values. The Ca isotope composition of benthic and planktonic foraminifers are offset, but reveal the same increase. In contrast, bulk $CaCO_3$ shows a deviating record. This demonstrates that $\delta^{44/40}$Ca of the different microfossils has not been equilibrated by recrystallisation, but is likely a pristin proxy signal. However, the absolute $\delta^{44/40}$Ca values for the late Cretaceous seawater are offset by about half a permill, applying the respective present day fractionation factors for dinoflagellates and foraminifers. The origin of this offset is yet unconstrained, but might be related to the impact of changing ocean chemistry on species specific biomineralisation-related fractionation processes.

The trend of Sr/Ca ratios of *P. krasheninnikovii* and *O. globosa* show a decrease during the investigated period, sychronous to the temperature drop revealed by δ^{18}O (Friederich et al., 2009). However, the dinoflagellate Sr/Ca ratios suggest a significantly larger amplitude of temperature change compared to the δ^{18}O-based SST reconstruction, if the Sr/Ca vs. temperature calibration of *Thoracosphaera heimii* is applied. Possible explanations which will be discussed include differences in the seawater chemical composition of the present and Cretaceous oceans and/or interference of several environmental parameters like temperature and carbonate chemistry of the water.

References:

Friedrich, O., Herrle, J.O., Cooper, M.J., Erbacher, J., Wilson, P.A. & Hemleben, C., 2009. The early Maastrichtian carbon cycle perturbation and cooling event: implications from the South Atlantic Ocean. Paleoceanography 24: PA2211, doi:10.1029/2008PA001654.

Gussone, N., Langer, G., Thoms, S., Nehrke, G., Eisenhauer, A., Riebesell, U., Wefer, G., 2006. Cellular calcium pathways and isotope fractionation in Emiliania huxleyi. Geology 34 (8), 625–628.

Gussone, N., Zonnefeld, K. and Kuhnert, H., 2010. Minor element and Ca isotope composition of calcareous dinoflagellate cysts of *Thoracosphaera heimii*. Earth and Planetary Science Letters 289, 180-188.

Hildebrand-Habel, T. and Willems, H., 2000. Distribution of calcareous dinoflagellates from the Maastrichtian to middle Eocene of the western South Atlantic Ocean. Int. J. Earth Sci. (Geol. Rundsch.) 88, 694–707.

Zonneveld, K.A.F., 2004. Potential use of stable oxygen isotope composition of *Thoracosphaera heimii* for upper water column (thermocline) temperature reconstruction. Mar. Micropaleontol. 50, 307–317.

Zonneveld, K.A.F., Mackensen, A., Baumann, K.-H., 2007. Stable oxygen isotopes of *Thoracosphaera heimii* (Dinophyceae) in relationship to temperature; a culture experiment. Mar. Micropaleontol. 64, 80–90.

ICDP

Lake Nam Co (central Tibetan Plateau) - a high-potential ICDP drilling site

T. HABERZETTL[1], P. FRENZEL[2], **T. KASPER[1]**, R. MÄUSACHER[1], K. REICHERTER[3], A. SCHWALB[4], V. SPIESS[5], J. WANG[6], T. WILKE[7], L. ZHU[6], G. DAUT[1]

1 Friedrich-Schiller-University Jena, Institute of Geography, Physical Geography, Loebdergraben 32, 07743, Jena, Germany
2 Friedrich-Schiller-University Jena, Institute of Earth Sciences, General and Historic Geology, Burgweg 11, 07749, Jena, Germany
3 Reinisch-Westfälische Technische Hochschule Aachen, Neotectonics and Natural Hazards, Lochnerstrasse 4-20, 52056 Aachen, Germany
4 Technical University Braunschweig, Institute of Geosystems and Bioindication, Postbox 3329, 38106 Braunschweig, Germany
5 University of Bremen, Department Geosciences, Postbox 330 440, 28334 Bremen, Germany
6 Chinese Academy of Sciences, Institute of Tibetan Plateau Research, Lin Cui Road, Chaoyang District, Beijing 100101 P.R. China
7 Justus Liebig University Giessen, Department of Animal Ecology & Systematics, Heinrich-Buff-Ring 26-32, 35392 Giessen, Germany

Nam Co represents one of the largest and deepest lakes on the Tibetan Plateau (TP). Seismic data show an infill of >800 m of well layered undisturbed sediments in the central part of the lake likely covering several glacial/interglacial cycles. Sediment accumulation rates measured on a 10.4 m long reference core, seismostratigraphic investigations, and molecular clock analyses suggest an age of the seismically imaged sequence between 460 and 1,900 ka. However, no basement reflector has been found yet promoting the existence of even older sequences. Multiproxy studies on the reference core provided an excellent high-resolution paleoenvironmental record covering the past 24 ka cal BP validated by extensive modern process studies and multi-dating approaches.

Situated on the central part of the TP, Nam Co is at an ideal location filling a gap in two ICDP/IODP transects. Due to this location at the modern intersection of Monsoon (increased precipitation) and Westerlies (increased evaporation) paleoclimate proxies clearly reflect the spatial and temporal interplay and thus the dominance of one of the two circulation systems. Considering that almost one third of the population of the world depends on the water supply from the TP the future hydrological development which is dependent on the interplay of the two systems will clearly have a major societal impact. To define parameters for future climate change scenarios (IPCC) and their consequences for ecosystems, it is of paramount importance to improve our knowledge of timing, duration, and intensity of past climatic variability and environmental impact, especially on long time scales.

Furthermore, the TP is characterized by a high degree of endemism of organisms that are dependent on continuously existing water bodies. Nam Co likely served as a dispersal centre for these organisms, as most other lakes desiccated during dry glacial periods of the Cenozoic. Nam Co appears to be a first class example for studying the link between geological and biological evolution in highly isolated TP ecosystems over long time scales. A continuous

high-resolution record for these long time scales from Nam Co will further enable to study denudation rate changes under varying climatic and tectonic settings, and contribute to a better understanding of the Quaternary geomagnetic field.

ICDP

ICDP drilling at Lake Towuti, Indonesia, in 2015: settings, site survey, and objectives for paleoclimatological research

A. HASBERG[1], M. MELLES[1], H. VOGEL[2], J. RUSSEL[3]

1 Institute of Geology and Mineralogy, University of Cologne, Zülpicher Str. 49a, 50974 Cologne, Germany, email: ahasber1@smail.uni-koeln.de
2 Department of Geology, University Bern, Switzerland
3 Department of Geology, Brown University, Providence, USA

This presentation concerns the DFG project "Decadal- to orbital-scale climate variability in the Indo-Pacific Warm Pool during the past ca. 650,000 years" (grant no. ME 1169/26-1) that was approved in February 2014 but, due to the aspired drilling at Lake Towuti in spring 2015, got started as late as 1 January 2015. The project is part of the DFG 'Towuti Bundle', in which two other projects approved focus on evolutionary biology (T. von Rintelen, Museum für Naturkunde Berlin) and geomicrobiology (J. Kallmeyer, GFZ German Research Centre for Geosciences Potsdam).

Lake Towuti has a surface area of 560 km^2 and a maximum water depth of 203 m. It is located at 318 m above sea level close to the equator on the island Sulawesi in Indonesia (2.75°S, 121.5°E), which is in the centre of the Western Pacific Warm Pool, the heart of the El Niño-Southern Oscillation (ENSO). The lake experiences a tropical humid climate. Annual average air temperature is 25.7°C and precipitation averages 2540 mm/yr. The moisture sources for this region are derived primarily from northeasterly and southeasterly flow associated with the boreal and austral summer monsoons. Precipitation variability in the region is strongly controlled by these circulation systems, by local sea surface temperature, and by the variability in the Walker Circulation vis-à-vis the ENSO (Aldrian and Susanto 2003). El Niño events result in severe droughts and lake-level reductions (Tauhid and Arifian 2000).

The pre-site survey for the international Towuti Drilling Project commenced in 2007. It was intensified in 2010, when first funding was provided by the DFG (VO 1591/2-1) and the German Ministry of Education and Research (BMBF) (IDN 10/006). Field work focused on hydrological, bathymetric, and seismic surveys, along with first piston coring down to 20 m below lake floor (blf). The data as yet obtained span the last 60,000 years and have confirmed the great potential of Lake Towuti for paleoclimate research (Russel et al. 2014). Wet conditions and rainforest ecosystems were present during the Holocene and during Marine Isotope Stage 3, interrupted by severe drying between ~33,000 and 16,000 yr BP. This demonstrates that central Indonesian hydrology varies strongly in response to high-latitude climate forcing, suggesting an important role for the western Pacific in amplifying global climate change during glacial-interglacial cycles. According to the seismic data, which comprise high-resolution CHIRP data as well as lower-resolution single-channel and multi-channel airgun data, the sediment infill of Lake Towuti consists of two major sedimentary units. First, a well-stratified sequence of lacustrine sediment up to 150 m thick, which at the site to be investigated within the scope of the DFG project (ICDP Site 2) is strongly influenced by riverine input in the uppermost 65 m. Second, a more poorly stratified section between 150 and 200 m blf that probably reflects fluvial and lacustrine sediments deposited during the formation of the Towuti basin. Extrapolating the sedimentation rates in the piston cores, the stratified lacustrine sediments down to 150 m blf should provide a continuous record penetrating down to about ~650,000 years BP.

The overall aim of the DFG project is to contribute to a better understanding of the climatic and environmental history in the western equatorial Pacific region during the past five to six glacial/interglacial cycles. Major paleoclimatic questions of the Towuti Drilling Project are:

- What is the dominant pacing and rhythm of tropical Pacific hydrology during the past 650,000 years?
- Is the hydrological response during the Last Glacial Maximum in Lake Towuti similar to other glacial maxima during the late Pleistocene?
- What are the effects of Sunda Shelf exposure on the Pacific Walker Circulation?
- Do abrupt events in the North Atlantic consistently affect Indo-Pacific hydrology?

The DFG project will partipate in the preparation and execution of the drilling campaign at Lake Towuti, which is scheduled for May/June 2015, as well as the core opening, description, logging, and subsampling at the US National Lacustrine Core Facility, LacCore (Univ. of Minnesota, USA). Subsequent analytical work at the University of Cologne will focus on ICDP Site 2 in the northern part of Lake Towuti. It will comprise XRF scanning (ITRAX Scanner, Cox), microstructural analyses (microscopy of thin sections), smear-slide analyses (polarization microscopy), radiocarbon dating (inhouse at Cologne AMS), grain-shape analyses (FlowCAM, Fluid Imaging Technol.), grain-size analyses (saturn DigiSizer^{TM} 5200, micromeritics), coarse-fraction analyses (binocular microscopy), and analyses of the TOC, TN, TS, and carbonate contents (Dimatoc 100, Dimatec Co. and vario microcube, Elementar Co.) as well as bulk mineralogy (X'Pert Powder diffractometer, PANalytical Co.).

The results from the analytical work are expected to provide importan information that (i) contributes to the dating of the sediment record, (ii) helps to decipher the long-term development of Lake Towuti, with its formation and the onset of riverine input from other Malili lakes, (iii) contributes to the reconstruction of the precipitation-controlled riverine inflow from the Mahalano River during the past ~80,000 years with up to decadal resolution, (iv) helps to identify the dimension and potential reasons for lake-level fluctuations in Towuti, (v) supports the understanding of the variability in mixing and stratification of Towuti, and (vi) contributes to the reconstruction of weathering conditions and soil erosion in the lake´s catchment. The project thus will generate partly unique

paleoenvironmental and paleoclimatological data that will not only complement respective research by other international projects on Lake Towuti but also provide important background information for the associated biological projects.

References:
Aldrian E. and Susanto R.D. (2003): Identification of three dominant rainfall regions within Indonesia and their relationship to sea surface temperature. - International Journal of Climatology, 23: 1435-1452.
Russell J.M., Vogel H., Konecky B.L., Bijaksana S., Huang Y., Melles M., Wattrus N., Costa K. & King J.W. (2014): Glacial forcing of central Indonesian hydroclimate since 60,000 y B.P. - PNAS, 111 (14): 5100-5105.
Tauhid Y.I. and Arifian J. (2000): Long-term observations on the hydrological condition of Lake Towuti. - Jurnal Sains & Teknologi Modifikasi Cuaca, 1: 93-100.

IODP

Rare Earth Element (REE) concentrations of IODP Expedition 353 pore waters from the Bay of Bengal: Implications for the REE budget of seawater and palaeo-circulation studies using Nd isotopes

E.C. HATHORNE[1], M. FRANK[1], J. KIRKPATRICK[2], A. PEKETI[3] N. SAGAR[4] AND EXPEDITION 353 SCIENTISTS

1 GEOMAR Helmholtz Centre for Ocean Research Kiel
2 Univeristy of Rhode Island, RI, USA
3 National Institute of Oceanography, Goa, India
4 National Geophysical Research Institute (NGRI), Hyderabad, India

The radiogenic isotope composition of the rare earth element Nd in seawater generally reflects the age and type of rocks supplying Nd to the ocean via dust and rivers and the subsequent advection of the signal through ocean circulation. The past seawater Nd isotope composition can be obtained by analysing authigenic phases in marine sediments and has been widely applied to reconstruct ocean circulation (e.g. Piotrowski et al., 2005; Böhm et al., 2015). It is clear that release of Nd from sediments suspended in the water column and on continental margins is important for the marine Nd budget but the underlying processes and the size of the source terms remain poorly constrained. A significant component of the sedimentary flux of REEs has been suggested to come from the pore waters of reducing sediments based on data from regions such as the Chesapeake Bay (Sholkovitz and Elderfield, 1988) and the Californian margin (Haley et al., 2004). The Bay of Bengal (BoB) receives some the highest amounts of suspended sediment globally from the Ganges-Brahmaputra rivers. Recent measurements of seawater in the BoB suggest there is significant release of Nd from the sediments accumulating on the Bengal Fan (Singh et al., 2012). Here we utilise a new online preconcentration ICP-MS technique that requires small sample sizes and minimal preparation (Hathorne et al., 2012) to extend the pore water REE dataset to the BoB and the Andaman Sea.

IODP Expedition 353 "Indian Monsoon Rainfall" obtained sediment cores from diverse sedimentary regimes in the BoB and the Andaman Sea including pelagic sedimentation fed by distal terrigenous inputs (Site U1443), turbidite deposits dominated by quartz sand on the Bengal Fan (Site U1444), and clay rich hemipelagic sediments with some intervals of bioclastic turbidites in the Mahanadi Basin (Sites U1445 & Site U1446) and on the slope of the Andaman Islands (Site U1447). The organic carbon content and hence the reactivity of the sediments varies greatly between these sites. There is no sulphate reduction at Site U1443 while depletion of pore water sulphate starts around 20 m below sea floor (mbsf) at Sites U1444, U1445, U1446, and U1447. The pore water dissolved iron profiles also vary widely between the different sites. Fan site U1444 Fe concentrations are often >100 μM in the upper 100 mbsf while the next highest maximum is 56 μM found at Site 1446. The other sites display comparably high dissolved iron concentrations, in some cases even below 200 mbsf. This variability and the general association of high REE with high iron concentrations in marine sediment pore waters (e.g. Haley et al., 2004) suggests that these samples should show a wide range of REE concentrations and patterns reflecting the different depositional and diagenetic processes. Comparison of the REE concentration data from these diverse sites should allow a better estimation of the the total flux of REEs from BoB sediments to seawater. Knowing which sediments are more likely to impart their Nd isotope signature on bottom seawater will improve the paleoceanographic interpretation of sedimentary Nd isotope records from the region.

References:
Böhm et al., 2015, Nature
Haley et al., 2004, Geochimica et Cosmochimica Acta, 68, 1265–1279
Hathorne et al., 2012, Geochem. Geophys. Geosyst.13, Q01020, doi:10.1029/2011GC003907
Piotrowski et al., 2005, Science, 307, 1933-1938
Sholkovitz and Elderfield, 1988, Global Biogeochemical Cycles, 2, 157-176
Singh et al., 2012, Geochimica et Cosmochimica Acta 94, 38–56

ICDP

The SCOPSCO deep drilling program in ancient Lake Ohrid: Unravelling the geological and environmental drivers leading to the extraordinary biodiversity in Europe's oldest lake

T. HAUFFE[1], E. JOVANOVSKA[1], B. STELBRINK[1], B. WAGNER[2], Z. LEVKOV[3], A. FRANCKE[2], C. ALBRECHT[1], T. WILKE[1]

1 Department of Animal Ecology and Systematics, Justus Liebig University Giessen, Heinrich-Buff-Ring 26-32, 35392 Giessen, Germany
2 Institute of Geology and Mineralogy, University of Cologne, Zülpicher Str. 49a, 50674 Köln, Germany
3 Institute of Biology, Ss. Cyril and Methodius University, Arhimedova 3, 1000 Skopje, Republic of Macedonia

Ancient lakes, i.e., extant lakes that have continuously existed since the Last Glacial Maximum, maintain a substantial proportion of the worldwide freshwater biodiversity. The evolutionary and ecological processes leading to this high degree of biodiversity, however, are still not well comprehended. Two hypotheses have been formulated: (1) ancient lakes function as sinks for extralimital relic species ("reservoir function"), and (2) they serve as sites for intralacustrine speciation ("cradle function"). Moreover, in the case of intralacustrine speciation, it often remains unknown whether their endemic species evolved shortly after the respective lake

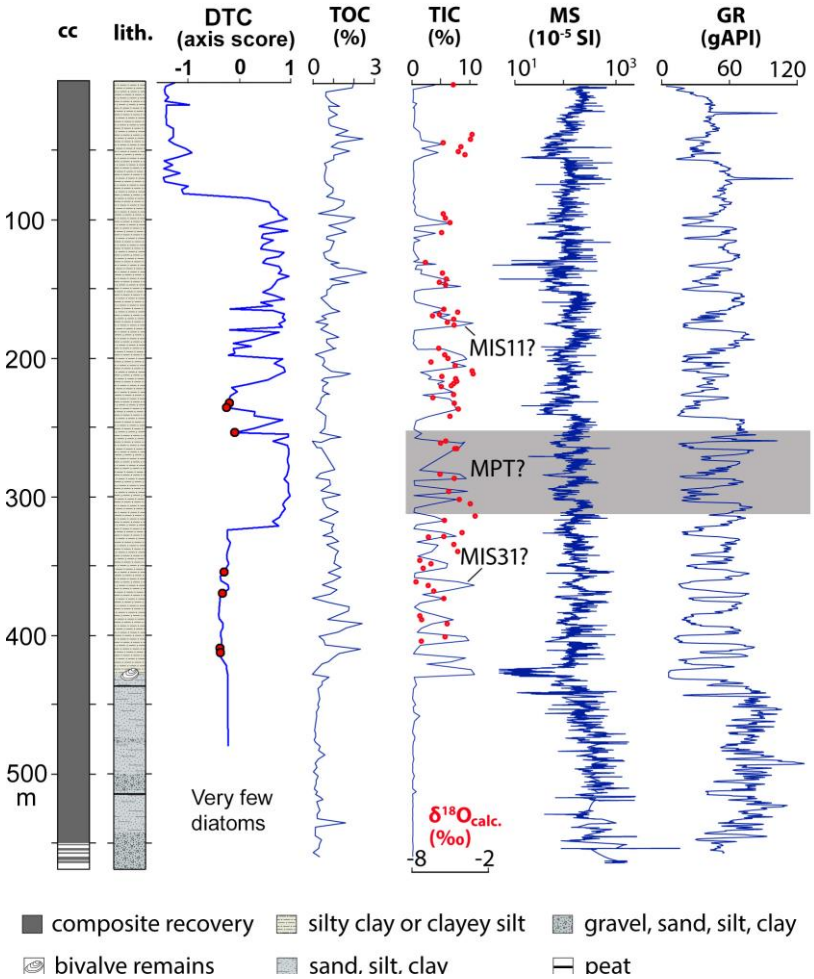

Fig. 1. Diagram linking diatom community turnover (DCT) with the geological evolution of Lake Ohrid. Turnover, independently of abundancies differences, was inferred by constraining a multivariate ordination by series of sine waves similar to a Fourier decomposition. Communities causing turnover higher than by chance alone are highlighted by red dots. Composite core recovery (cc), lithology (lith.), total organic carbon (TOC), total inorganic carbon (TIC), magnetic susceptibility, spectral gamma ray (GR), and the tentative identification of the Middle Pleistocene transition (MPT) and Marine isotope stages (MIS) were presented by Wagner, et al., 2014. (modified figure reproduced under CC-BY-3.0 license).

came into existence or whether they are considerably younger than the lake.

For many biota from ancient lakes in Africa, Asia, and South America, it has been demonstrated that the majority of the taxa evolved through intralacustrine speciation. Furthermore, many groups of species are considerably younger than the actual lake as past catastrophic or near-catastrophic events (e.g., desiccation, full glaciation or salinization) may have caused a 'reset' of some or all biota in these ecosystems. Though ancient lakes are generally characterized by a high buffer capacity for environmental fluctuations, global climate changes such as those during the Eemian interglacial period massively affected tropical ancient lakes.

Over the past decades, several ancient lakes, such as Lake Ohrid on the Balkan Peninsula, were sites of International Continental Scientific Drilling Programs. Ancient Lake Ohrid constitutes the oldest and, with almost 350 endemic species, the most biodiverse lake in Europe. In order to unravel its geological and, for the first time, also its biological history, an international research initiative – the Scientific Collaboration On Past Speciation Condition in Lake Ohrid (SCOPSCO) program – was launched.

The initiative combines sedimentological, tephro-stratigraphical, seismic and paleontological (diatoms, mollusks, ostracods) studies of lake sediment cores with molecular-dating of speciation events and evolutionary modelling approaches applied to extant taxa. A main goal is to study the influence of major geological and environmental events on the evolution of endemic taxa.

In a post-drilling project, which started in August 2014 and is hosted by the University of Giessen, the following questions are addressed aiming at unravelling the geological and environmental drivers leading to the extraordinary biodiversity in Lake Ohrid:

a) Is the lack of catastrophic or near-catastrophic events a major reason for its high endemic biodiversity?
b) Did Lake Ohrid function as sink for extralimital relic species ("reservoir function") or did it mainly serve as site for intralacustrine speciation ("cradle function")?
c) Has the lake's presumed high buffer capacity for environmental change resulted in decreased extinction and/or increased speciation events?

d) Which geological and environmental factors or which combination of factors triggered speciation events and/or turnovers in species compositions over time?

Preliminary analyses of sediment core and borehole logging data from drill sites with a maximum penetration depth of 569 m below lake floor and an overall recovery of > 95 % (Fig. 1) indicate that Lake Ohrid is more than 1.2. Ma old (Wagner, et al., 2014). Intriguingly, these data reinforce the results of our preliminary molecular-dating analyses conducted prior to the drilling operation, suggesting that a rapid sequence of speciation events in Lake Ohrid started approximately 1.4-1.5 My ago. Moreover, preliminary geological and paleontological data from core catcher samples suggest that the extraordinary biodiversity in Lake Ohrid is largely driven by: 1) the long existence of the lake, 2) the lack of catastrophic events during its lifetime, 3) the high buffer capacity of the lake to environmental change and/or the high resilience of its taxa, and 4) distinct turnovers in species composition over time promoting frequency dependent selection (Fig. 1). The cumulative effect of these factors, in turn, resulted in overall low extinction rates and continuous speciation.

In the coming months, we aim at extending our preliminary analyses of core catcher materials to the actual cores currently being processed at the universities of Cologne and Skopje. Moreover, we will continue dating speciation events in order to obtain both a precise species-community and an evolutionary model for explaining changes in species-compositions and speciation rates by environmental factors and geological events.

Our project will not only help unravelling patterns and processes of biological evolution in Europe's oldest lake, it also aims at demonstrating that geological and paleontological data from sediment cores in combination with molecular information from extant taxa can contribute to a better understanding of the driving forces of speciation. Lake Ohrid appears to be a first class example for studying the link between geological and biological evolution in highly isolated ecosystems over comparatively long time scales.

References:

Wagner, B., Wilke, T., Krastel, S., Zanchetta, G., Sulpizio, R., Reicherter, K., Leng, M.J., Grazhdani, A., , Trajanovski, S., Francke, A., Lindhorst, K., Levkov, Z., Cvetkoska, A., Reed, J.M., Zhang, X., Lacey, J.H., Wonik, T., Baumgarten, H. and Vogel, H. (2014). The SCOPSCO drilling project recovers more than 1.2 million years of history from Lake Ohrid. Scientific Drilling, 17, 19-29.

IODP

IODP Expedition 337: Exploring the deep biosphere nearly 2.5 km below the seafloor

KAI-UWE HINRICHS,[1*] FUMIO INAGAKI,[2,3*] YUSUKE KUBO,[4,5] MARSHALL W. BOWLES,[1] VERENA B. HEUER,[1] WEI-LI HONG,[6] TATSUHIKO HOSHINO,[2,3] AKIRA IJIRI,[2,3] HIROYUKI IMACHI,[3,7] MOTOO ITO,[2,3] MASANORI KANEKO,[3,8] MARK A. LEVER,[9,A] YU-SHIH LIN,[1,B] BARBARA A. METHÉ,[10] SUMITO MORITA,[11] YUKI MORONO,[2,3] WATARU TANIKAWA,[2,3] MONIKA BIHAN,[10] STEPHEN BOWDEN,[12] MARCUS ELVERT,[1] CLEMENTS GLOMBITZA,[9] DORIS GROSS,[13] GUY HARRINGTON,[14] TOMOYUKI HORI,[15] KELVIN LI,[10] DAVID LIMMER,[12] CHANGHONG LIU,[16] MASAFUMI MURAYAMA,[17] NAOHIKO OHKOUCHI,[3,8] YOUNG-SOO PARK,[18] STEPHEN PHILLIPS,[19] XAVIER PRIETO-MOLLAR,[1] MARCELLA PURKEY,[20] NATASCHA RIEDINGER,[21,C] YOSHINORI SANADA,[4,5] JUSTINE SAUVAGE,[22] GLEN SNYDER,[23,D] RITA SUSILAWATI,[24] YOSHINORI TAKANO,[3,8] EIJI TASUMI,[7] TAKESHI TERADA,[25] HITOSHI TOMARU,[26] ELIZABETH TREMBATH-REICHERT,[27] YASUHIRO YAMADA[5,28]

[1]MARUM Center for Marine Environmental Sciences, University of Bremen, D-28359 Bremen, Germany. [2]Kochi Institute for Core Sample Research, Japan Agency for Marine-Earth Science and Technology (JAMSTEC), Japan. [3]Research and Development Center for Marine Resources, JAMSTEC, Japan. [3]MARUM Center for Marine Environmental Sciences, University of Bremen, D-28359 Bremen, Germany. [4]Center for Deep-Earth Exploration, JAMSTEC, Japan. [5]Research and Development Center for Ocean Drilling Science, JAMSTEC, Japan. [6]College of Earth, Ocean, and Atmospheric Sciences, Oregon State University, OR, U.S.A. [7]Department of Subsurface Geobiological Analysis and Research, JAMSTEC, Japan. [8]Department of Biogeochemistry, JAMSTEC, Japan. [9]Center for Geomicrobiology, Department of BioScience, Aarhus University, Denmark. [10]Department of Environmental Genomics, J. Craig Venter Institute, MD, U.S.A. [11]Geological Survey of Japan, AIST, Japan. [12]Department of Petroleum Geology, University of Aberdeen, United Kingdom. [13]Department of Applied Geological Sciences and Geophysics, Montanuniversität, Leoben, Austria. [14]Earth Science School of Geography, Earth, and Environmental Sciences, University of Birmingham, United Kingdom. [15]Research Institute for Environmental Management Technology, National Institute of Advanced Industrial Science and Technology (AIST), Japan. [16]The State Key Laboratory of Pollution Control and Resources Reuses, School of Life Science, Nanjing University, China. [17]Center for Advanced Marine Core Research, Kochi University, Japan. [18]Petroleum and Marine Resources Research Division, Korea Institute of Geoscience and Mineral Resources (KIGAM), Korea. [19]Department of Earth Sciences, University of New Hampshire, NH, U.S.A. [20]Department of Earth and Atmospheric Sciences, University of Nebraska-Lincoln, NE, U.S.A. [21]Department of Earth Sciences, University of California Riverside, CA, U.S.A. [22]Graduate School of Oceanography, University of Rhode Island, RI, U.S.A. [23]Department of Earth Science, Rice University, TX, U.S.A. [24]School of Earth Science, University of Queensland, Brisbane, Australia. [25]Marine Works Japan Ltd., Yokohama, Japan. [26]Department of Earth Sciences, Chiba University, Japan. [27]Geological and Planetary Sciences, California Institute of Technology, CA, U.S.A. [28]Department of Urban Management, Graduate School of Engineering, Kyoto University, Japan.

Present affiliation: [a]Department of Environmental Systems Science, ETH Zurich, Switzerland. [b]Department of Oceanography, National Sun Yat-Sen University, Taiwan. [c]Boone Pickens School of Geology, Oklahoma State University, OK, U.S.A. [d]Gas Hydrate Research Laboratory, Meiji University, Japan.

IODP Expedition 337 was the first scientific initiative to drill and study a subseafloor hydrocarbon system using riser-technology. With Site C0020 (41°10.5983′N, 142°12.0328′E, 1,180 m water depth) the expedition

targeted a natural gas field in the tectonically active forearc basin offshore the Shimokita Peninsula of Japan (Inagaki et al., 2010). When the upper 365 m of this site were explored by non-riser drilling in 2006, methane hydrates were found in combination with conspicuously high concentrations of microbial cells (Aoike et al., 2007) and suggested the existence of an active subseafloor biosphere that benefits from organic matter and nutrients expelled from deeper sources such as coalbeds (Inagaki et al., 2010). In 2012, Hole C0020A was deepened and spot-cored down to a total depth of 2466 meters below seafloor (mbsf) by riser-drilling. Thirteen coal layers with thicknesses >30 cm were identified and samples were recovered from seven of them at around 2000 mbsf (Inagaki et al., 2012; 2013). The coal is of low maturity and embedded in an intertidal and wetland sequence that was deposited in a continuously subsiding basin from middle/late Paleogene through early/middle Miocene, before the paleoenvironment gradually changed from a shallow-marine setting to an offshore continental shelf environment in the Pliocene (Inagaki et al., 2012). Due to the relatively low geothermal temperature gradient of 24°C km^{-1} at this site (Inagaki et al., 2013), the coalbeds and deepest horizons are well within the temperature range permissive of microbial life (i.e., <60°C). The ultra-deep drilling and recovery of coalbed samples thus provide unprecedented opportunities to assess the limits of life in the deep subseafloor, to study biological and abiotic processes in hydrocarbon reservoirs, and to elucidate the role of hydrocarbon reservoirs as energy and carbon sources for the deep biosphere.

Our shipboard and post-cruise investigations provide evidence for the existence of microbial communities in sediment associated with lignite coalbeds buried ~2 km below the seafloor off the Shimokita Peninsula, Japan, where ongoing microbial formation of methane is indicated by various lines of isotopic evidence as well as by molecular biomarkers. Rigorous protocols aimed at minimizing and correcting for sample contamination resulted in robust cell concentration estimates that are drastically lower than extrapolations of global cell distributions along continental margins would predict, yet activation of microbial communities in coalbed–bearing horizons is indicated by elevated concentrations. The microbial ecosystem buried more deeply than 1.5 km is taxonomically distinct from shallower ecosystems at this location. This presentation will highlight the major post-cruise results pertaining to the limits of life in the deep biosphere.

References:
Aoike K. (ed.) (2007) CK06-06 D/V Chikyu shakedown cruise offshore Shimokita. Laboratory Operation Report: Yokahama, JAMSTEC-CDEX.
Inagaki F., Hinrichs K.-U., Kubo Y., and the Expedition 337 Project Team (2010) Deep coalbed biosphere off Shimokita: microbial processes and hydrocarbon system associated with deeply buried coalbed in the ocean. IODP Scientific Prospectus, 337.
Inagaki F., Hinrichs K.-U., Kubo Y., and the Expedition 337 Scientists (2012) Deep coalbed biosphere off Shimokita: microbial processes and hydrocarbon system associated with deeply buried coalbed in the ocean. IODP Preliminary Report, 337.
Inagaki F., Hinrichs K.-U., Kubo Y., and the Expedition 337 Scientists (2013) Deep coalbed biosphere off Shimokita: microbial processes and hydrocarbon system associated with deeply buried coalbed in the ocean. IODP Proceedings, 337. doi:10.2204/iodp.proc.337.2013.

ICDP

PASADO Lipids- paleoenvironmental reconstruction in Southern Patagonia

K. HOCKUN[1], G. MOLLENHAUER[1,2], E. SCHEFUß[1] AND THE PASADO SCIENCE TEAM
1 MARUM – Zentrum für Marine Umweltwissenschaften, Universität Bremen, Leobener Straße, 28359 Bremen
2 Alfred Wegener Institut Helmholtz- Zentrum für Polar- und Meeresforschung, Am Handelshafen 12, 27570 Bremerhaven

Southern Patagonia is a key region for paleoclimatic reconstruction in the Southern Hemisphere as it is the only landmass located in the Southern Hemisphere westerly wind (SHW) region. Most paleoclimatic studies focused on the Chilean side of the Andes or the Andean region (Kilian and Lamy, 2012). Only a few promising sedimentary archives exist in the southeastern part of Argentina. Within the framework of the ICDP PASADO ("Potrok Aike Maar Lake Sediment Archive Drilling Project") drilling campaign, a core (51°58´S, 70°23´W) was drilled in 2007 in Laguna Potrok Aike (LPTA), a volcanic maar situated in the Pali Aike volcanic field in Southern Patagonia (Fig. 1). A high resolution sedimentary record was recovered. At present, the climate in our study area is mainly influenced by the SHW and the topography of the landmass (Mayr et al., 2007a,b).

Extensive studies with the focus on multiproxy approaches have been carried out within the framewort of the PASADO project. Regional calibrations for pollen, diatom and chironomid associations have been established in order to reconstruct temperature and precipitation changes in Southern Patagonia. In addition, several approaches have been taken to infer paleo-hydrological changes and associated lake-level variations (Haberzettl et al., 2007a; Haberzettl et al., 2005; Haberzettl et al., 2008), yielding, however, inconclusive results in comparison with the reconstructions based on archives in the Andean region. Furthermore, so far no quantitative paleoclimatic reconstructions exist for temperature and hydrological changes.

Therefore, the PASADO Lipids project started in 2011 aiming to provide new insights into the climate history of southern South America by using organic-geochemical proxies based on lipid biomarkers. We study abundances and compound-specific isotope compositions (δD, $\delta^{13}C$) of biomarkers derived from terrestrial and aquatic plants including *n*-alkanes and n-fatty acids as well as temperature- and pH-sensitive abundance ratios of microbial membrane lipids (glycerol dialkyl glycerol tetraethers, GDGTs). Based on the GDGTs lake temperature changes using TEX_{86} (TetraEther index of GDGTs with 86 carbon atoms) shall be inferred, as well as soil temperature and soil pH changes using the MBT/CBT indices (methylation ratio/cyclization ratio of branched tetraethers). Compound-specific δD values of biomarkers from aquatic and terrestrial sources are expected to reflect the local hydrology and changes in the lake water balance in particular. Combining all datasets will allow to develop an improved mechanistic understanding of terrestrial climatic conditions in the Southern Hemisphere.

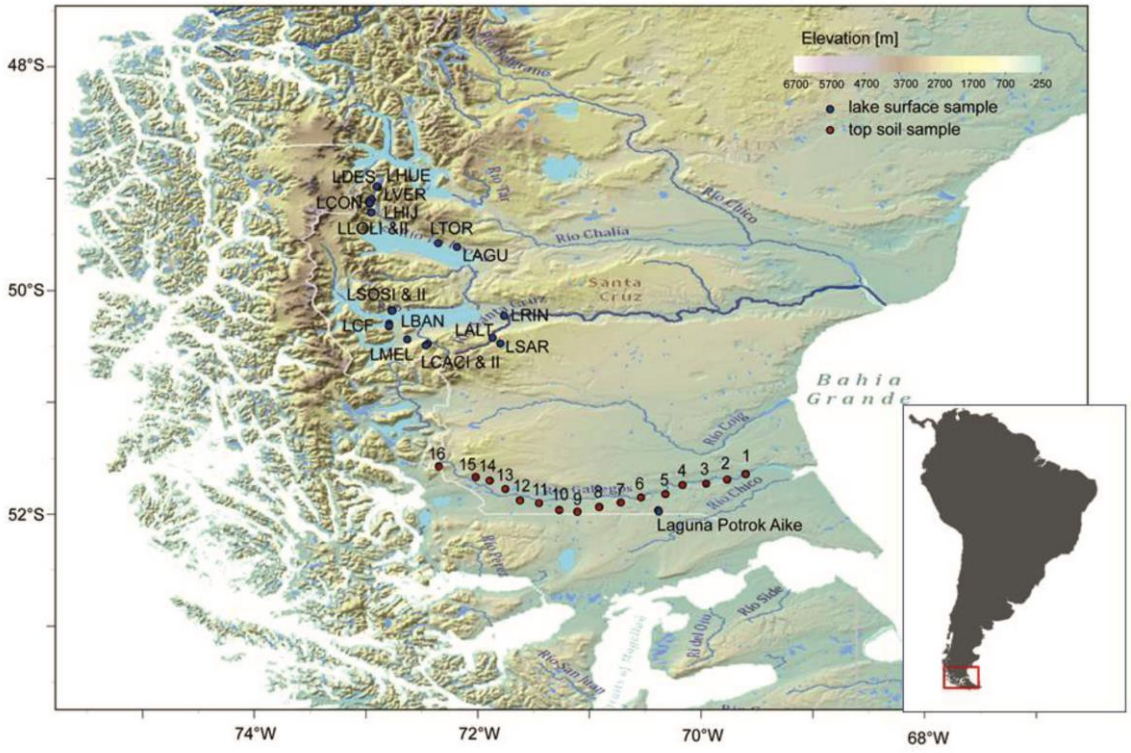

Fig. 1. Map of Southern Patagonia with location of Laguna Potrok Aike, elevation map with core location.

To investigate the isotope signal in wax lipids derived from higher terrestrial plants in relation to moisture sources and fractionation effects during evaporation and transpiration we analysed 16 top-soil samples along a W-E transect along the same latitude as LPTA. Long-chain *n*-alkanes (*n*-C_{29} & *n*-C_{31}) in the top soils show similar ranges of compound-specific δD and $\delta^{13}C$ compositions as in investigated sediment samples of LPTA. The δD values of the *n*-C_{31} alkane vary from -225‰ to -195‰ and show an increase from W to E which might indicate the higher relative influence of the Atlantic (isotopically enriched) moisture over south-east Patagonia. The compound-specific $\delta^{13}C$ values of the *n*-C_{31} alkane (range: -34.9‰ to -32.7‰) also show an increase from W to E which is interpreted as higher water-use-efficiency of the C_3 plants in the east due to higher aridity, i.e., lower mean annual precipitation amounts. The positive correlation of $\delta^{13}C$ and δD signals suggests that fractionation effects due to higher evapo-transpiration in the east partly cause the observed trend in long-chain *n*-alkane δD values.

Furthermore, we characterized the lipid biomarker signatures of terrestrial plants, aquatic macrophytes, soils, dust traps, sediment traps and lake surface sediments from Laguna Potrok Aike to identify suitable tracers for paleo-reconstructions. We distinguished the *n*-alkane distribution of all samples and also the isotopic signature of the most abundant *n*-alkanes. The results show differences in the distribution as well as in the isotopic values of *n*-alkanes. The *n*-alkane distribution of the aquatic marcophyte samples show a predominance of *n*-C_{23} and *n*-C_{25}, while the distribution of *n*-alkanes from the terrestrial plants are predominated by *n*-C_{29} and *n*-C_{31}. The soil samples contain a mixture of these long and short chain compounds with *n*-C_{29} as most abundant contributor. The two sediment traps from 30 and 90 meter water depth contain a mixture of *n*-alkanes from terrigenous and aquatic sources, the same applies for the surface sediment of LPTA. The terrestrial-derived long-chain *n*-C_{29} and *n*-C_{31} alkanes are consistently more depleted in deuterium (around -230 ‰ VSMOW) than the macrophyte-derived *n*-C_{23} and *n*-C_{25} alkanes (around -170 ‰ VSMOW). The same is true for $\delta^{13}C$ values. The macrophyte-derived *n*-C_{23} alkanes are more enriched in carbon (around -18 ‰ VPDB) as the terrestrially-derived *n*-C_{29} and *n*-C_{31} alkanes (around -30 ‰ VPDB). Isotopic signals in dust traps are limited to terrestrially-derived *n*-C_{29} and *n*-C_{31} alkanes and show $\delta^{13}C$ values around -33 ‰ VPDB and δD values ranging from -200 to -210‰ VSMOW for *n*-C_{29} *n*-alkane. These results help us to identify the source of the different components and to understand their isotopic signal.

48 PASADO core samples of the last 20.000 years have been analyzed. The downcore data show high variability in the abundance of the n-alkyl lipids (Fig. 2a) with higher contributions of macrophyte-derived shorter-chain *n*-alkanes in the pre-Holocene section. Possibly, this indicates a more proximal position of shallow lake areas to the core site due to lower lake levels. δD values of the *n*-C_{29} alkane, derived from higher plant leaf waxes and inferred to refelct the precipitation signal, range from -230 to -190 ‰ V-SMOW (Fig. 2d) in Laguna Potrok Aike sediments. The δD values of the *n*-C_{29} alkane are much depleted (around –

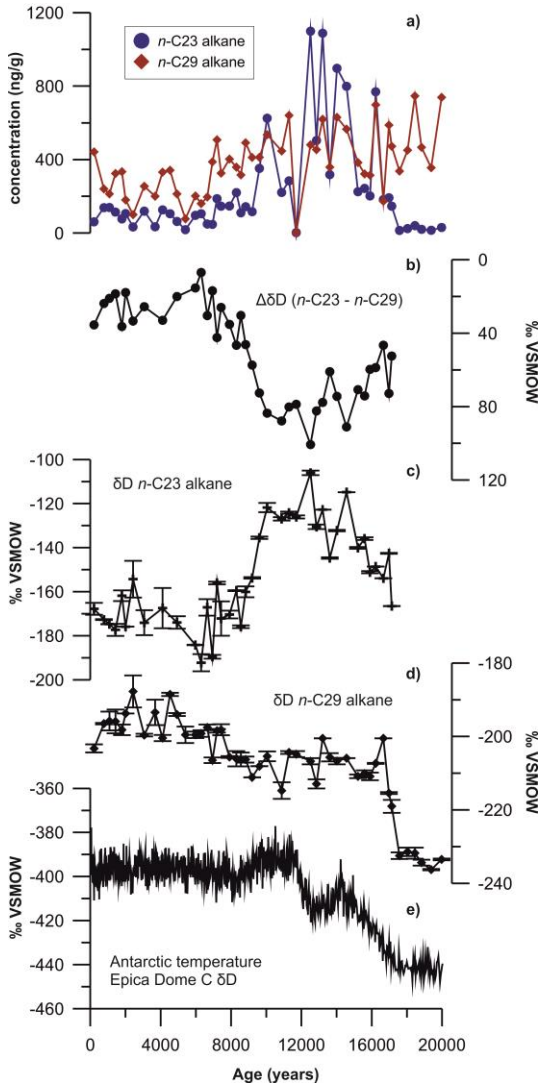

Fig. 2: a) concentration of n-C_{23} and n-C_{29} downcore **b)** isotopic lake water balance of Laguna Potrok Aike, which is determined by the difference of n-C_{23} and n-C_{29} **c)** variations in δD compositions of n-C_{23} alkane indicating isotopic changes of lake water **d)** variations in δD compositions of n-C_{29} alkane reflecting isotope precipitation changes **e)** deuterium isotope changes of ice in Antarctica representing Antarctic temperature changes (Jouzel et al., 2007)

230 ‰ VSMOW) before 17,500 years before present (BP) consistent with cool glacial conditions. Starting at 17,500 years BP, parallel to Antarctic warming (Barbante et al., 2006) (Fig. 2e), *n*-C_{29} δD values increase sharply to -200 ‰ VSMOW and range around -210 ‰ VSMOW afterwards (Fig. 2d). As the isotopic composition of precipitation at latitudes of about 50°S is largely controlled by temperature (Dansgaard, 1964) a change of about 20 ‰ in δD would correspond to a temperature increase of about 5°C during deglaciation. The *n*-C_{29} δD values remain at around -210 ‰ VSMOW until about 8,000 years ago and increased to values of around -190 to -200 until 200 years BP. This trend is different than the temperature trend observed in Antarctic ice cores (Barbante et al., 2006). Therefore, we ascribe this shift to a change in predominant moisture source. Atlantic-sourced rainfall events were found to be linked to enriched isotopic composition relative to Pacific-sourced precipitation in the LPTA region (Mayr et al., 2007a). We thus infer that from 8,000 years BP onward, the relative influence of Atlantic-derived moisture increased and that the relative influence of Pacific-derived moisture was higher before 8,000 years ago. This finding contradicts earlier interpretations of increasing westerly wind speeds over the Holocene (Mayr et al., 2007b). δD compositions of the *n*-C_{23} alkane (Fig. 2c) range from -190 to -106 ‰ V-SMOW (Fig. 2d). Since *n*-C_{23} is derived from aquatic macrophytes (Ficken et al., 2000), its δD values indicate isotopic changes of the lake surface water with the latter driven by isotopic changes of precipitation and evaporation. The difference in isotope values between these two compounds reflects the isotopic lake water balance, i.e., the hydrologic balance of the lake, mainly driven by evaporative processes (Fig. 2b).

Results of GDGT distributions in the top soil samples as well as a series of lake surface samples (Fig. 1) confirm a correlation between GDGT index parameters (MBT/CBT indices) and soil temperature and pH in the study area. The predicted temperatures based on the global calibration (Weijers et al., 2007) are, however, lower than measured temperatures. Therefore, we developed a new calibration for the use of GDGT-based proxies in southern Patagonia based on the published MBT/CBT indices. The MBT-based reconstructed temperature values, however, differ (+/-2°C) from the measured mean annual temperatures in our study area (Fig. 2). The temperature estimates from the analysed lake surface sediments overestimate regional mean annual air temperatures by almost 10°C (Fig. 3). In situ production of several of the GDGTs used in the calibration appears to compromise the signals. For that reason, we are trying to avoid the questionable components for the new regional calibration. Therefore, additional samples covering a wider temperature range will be analysed to identify suitable temperature sensitive components and thus develop a calibration appropriate for Southern Patagonia. 30 additional top soil samples from a north-south transect and a few samples from the Andean region are provided for this purpose from our cooperation partners from Argentina and Germany involved in the PASADO project.

40 further PASADO core samples are currently being processed to measure abundance and compound-specific isotope compositions (δD, $\delta^{13}C$) of *n*-alkanes as well as temperature- and pH-sensitive abundance ratios of GDGTs covering a period from 20,000 to 55.000 years.

References:

Barbante, C., Barnola, J.M., Becagli, S., Beer, J., Bigler, M., Boutron, C., Blunier, T., Castellano, E., Cattani, O., Chappellaz, J., Dahl-Jensen, D., Debret, M., Delmonte, B., Dick, D., Falourd, S., Faria, S., Federer, U., Fischer, H., Freitag, J., Frenzel, A., Fritzsche, D., Fundel, F., Gabrielli, P., Gaspari, V., Gersonde, R., Graf, W., Grigoriev, D., Hamann, I., Hansson, M., Hoffmann, G., Hutterli, M.A., Huybrechts, P., Isaksson, E., Johnsen, S., Jouzel, J., Kaczmarska, M., Karlin, T., Kaufmann, P., Kipfstuhl, S., Kohno, M., Lambert, F., Lambrecht, A., Lambrecht, A., Landais, A., Lawer, G., Leuenberger, M., Littot, G., Loulergue, L., Luthi, D., Maggi, V., Marino, F., Masson-Delmotte, V., Meyer, H., Miller, H., Mulvaney, R., Narcisi, B., Oerlemans, J., Oerter, H., Parrenin, F., Petit, J.R., Raisbeck, G., Raynaud, D., Rothlisberger, R., Ruth, U., Rybak, O., Severi, M., Schmitt, J., Schwander, J., Siegenthaler, U., Siggaard-Andersen, M.L., Spahni, R., Steffensen, J.P., Stenni, B., Stocker, T.F., Tison, J.L., Traversi, R., Udisti, R., Valero-Delgado, F., van den Broeke, M.R., van de Wal, R.S.W., Wagenbach, D., Wegner, A., Weiler, K., Wilhelms, F., Winther, J.G., Wolff, E., Members, E.C., 2006. One-to-one coupling of glacial climate variability in Greenland and Antarctica. Nature 444, 195-198.

Dansgaard, W., 1964. Stable isotopes in precipitation. Tellus 16, 436-468.

Ficken, K.J., Li, B., Swain, D.L. and Eglinton, G., 2000. An n-alkane proxy for the sedimentary input of submerged/floating freshwater aquatic macrophytes. Organic Geochemistry, 31: 745-749.

Garreaud, R., Lopez, P., Minvielle, M., Rojas, M., 2013. Large-Scale Control on the Patagonian Climate. Journal of Climate 26, 215-230.

Haberzettl, T. et al., 2007a. Lateglacial and Holocene wet-dry cycles in southern Patagonia: chronology, sedimentology and geochemistry of a lacustrine record from Laguna Potrok Aike, Argentina. Holocene, 17: 297-310.

Haberzettl, T. et al., 2005. Climatically induced lake level changes during the last two millennia as reflected in sediments of Laguna Potrok Aike, southern Patagonia (Santa Cruz, Argentina). Journal of Paleolimnology, 33: 283-302.

Haberzettl, T. et al., 2008. Hydrological variability in southeastern Patagonia and explosive volcanic activity in the southern Andean Cordillera during Oxygen Isotope Stage 3 and the Holocene inferred from lake sediments of Laguna Potrok Aike, Argentina. Palaeogeography Palaeoclimatology Palaeoecology, 259: 213-229.

Jouzel, J., Masson-Delmotte, V., Cattani, O., Dreyfus, G., Falourd, S., Hoffmann, G., Minster, B., Nouet, J., Barnola, J.M., Chappellaz, J., Fischer, H., Gallet,J.C.,Johnsen,S.,Leuenberger,M.,Loulergue,L.,Luethi, D.,Oerter,H., Parrenin,F.,Raisbeck,G.,Raynaud, D.,Schilt, A.,Schwander,J.,Selmo, E., Souchez, R., Spahni, R., Stauffer, B., Steffensen, J.P., Stenni, B., Stocker, T.F., Tison, J.L., Werner, M., Wolff, E.W., 2007. Orbital and millennial Antarctic climate variability over the past 800,000 years. Science 317 (5839), 793-796.

Kilian, R. and F. Lamy (2012). "A review of Glacial and Holocene paleoclimate records from southernmost Patagonia (49-55˚S)." Quaternary Science Reviews 53: 1-23.

Mayr, C., Wille, M., Haberzettl, T., Fey, M., Janssen, S., Lücke, A., Ohlendorf, C., Oliva, G., Schäbitz, F., Schleser, G., Zolitschka, B., 2007a. Holocene variability of the Southern Hemisphere westerlies in Argentinean Patagonia (52_S). Quat. Sci. Rev., 26, 579–584.

Mayr, C., Lücke, A., Stichler, W., Trimborn, P., Ercolano, B., Oliva, G., Ohlendorf, C., Soto, J., Fey, M., Haberzettl, T., Janssen, S., Schäbitz, F., Schleser, G.H., Wille, M., Zolitschka, B., 2007b. Precipitation origin and evaporation of lakes in semi-arid Patagonia (Argentina) inferred from stable isotopes (δ18O, δ2H). Journal of Hydrology, 334, 53-63.

Weijers, J.W.H., Schouten, S., van den Donker, J.C., Hopmans, E.C. and Damste, J.S.S., 2007a. Environmental controls on bacterial tetraether membrane lipid distribution in soils. Geochimica et Cosmochimica Acta, 71: 703-713..

IODP

Early to middle Miocene climate evolution: New insights from IODP Sites U1337 and U1338 (eastern equatorial Pacific Ocean)

A. HOLBOURN[1], W. KUHNT[1], M. LYLE[2], L. SCHNEIDER[3], O. ROMERO[4], K.G.D. KOCHHANN[1], N. ANDERSEN[5]

1 Institute of Geosciences, Christian-Albrechts-University, D-24118 Kiel, Germany
2 CEOAS, Oregon State University, Corvallis, OR 97331-5503, USA
3 International Ocean Drilling Program, Texas A&M University, College Station, Texas 77845-9547, USA
4 MARUM, University of Bremen ,Leobenerstrasse, Bremen 28359, Germany
5 Leibniz Laboratory for Radiometric Dating and Stable Isotope Research, Christian-Albrechts-University, D-24118 Kiel, Germany

The Miocene climatic optimum (MCO, ~17-14.7 Ma) represents an intriguing phase of global warming, which interrupted the long-term Cenozoic cooling trend for more than 2 Myr. At the end of the MCO, Earth's climate transitioned back into a colder mode with re-establishment of permanent ice sheets on Antarctica after 14 Ma, thus marking a fundamental step in Cenozoic cooling. We present high-resolution (~1-5 kyr time resolution) benthic foraminiferal isotopes in two exceptional, continuous, carbonate-rich sedimentary archives from the eastern equatorial Pacific Ocean (IODP Sites U1337 and U1338), which offer a new view of climate evolution over the onset and development of the MCO and the transition into the "Icehouse" climate.

Orbitally tuned chronologies (20-13 Ma)

Building on the shipboard stratigraphies, we developed new chronologies in Sites U1337 (20-14.8 Ma) and U1338 (16-13 Ma) by correlating the benthic foraminiferal $\delta^{18}O$ series to computed variations of the Earth's orbit (Laskar et al., 2004). As tuning target, we constructed an eccentricity-tilt-precession (ETP) composite with no phase shift and with equal weight of eccentricity and obliquity and only 1/3 (U1338) and 1/5 (U1337) precession. We correlated $\delta^{18}O$ minima to ETP maxima, generally following a minimal tuning approach in order to preserve original spectral characteristics. Comparison of the $\delta^{18}O$ and $\delta^{13}C$ curves plotted against depth and age shows that original spectral characteristics are retained following the tuning procedure. In particular, the 400 and 100 kyr eccentricity cycles are prominently encoded in the $\delta^{13}C$ records, supporting the age models, based on tuning of the $\delta^{18}O$ series.

Global perturbation of the carbon cycle at the onset of the MCO

High-resolution (~5 kyr) benthic and bulk carbonate isotope records combined with carbonate data in Site U1337 allow unsurpassed resolution over the inception and development of the MCO (Figure 1; Holbourn et al., 2015). A notable feature of the benthic and bulk carbonate $\delta^{18}O$ curves is the sharp decrease (~1 ‰) at ~16.9 Ma, marking the start of the MCO. This $\delta^{18}O$ drop coincides with the onset of a pronounced (~0.6 ‰) and relatively long-lasting (~200 kyr) negative shift in the benthic and bulk carbonate $\delta^{13}C$, indicating a contemporaneous intense perturbation of the carbon cycle. The comparable amplitude of the benthic and bulk carbonate (mainly derived from surface waters) $\delta^{18}O$ and $\delta^{13}C$ decreases at ~16.9 Ma implies that they were driven by a major climate transition and fundamental changes in the global carbon reservoir, and are not solely attributable to regional changes in deep ocean circulation or in surface productivity. Our records additionally reveal that the rapid global warming at ~16.9 Ma, possibly associated with polar ice melting, was coupled to a massive increase in carbonate dissolution, indicated by sharp drops in carbonate percentages and accumulation rates and by the fragmentation or complete dissolution of planktonic foraminifers. This substantial shoaling of the carbonate compensation depth (CCD), which persisted for ~80 kyr, is the most prominent event in a series of dissolution episodes within the initial negative $\delta^{13}C$ shift**.** The CCD continued to behave in a highly dynamic manner through the MCO and fluctuations were intricately coupled to marked changes in ocean geochemistry ($\delta^{13}C$) and climate ($\delta^{18}O$), supporting a crucial role for the marine carbon cycle as climate regulator.

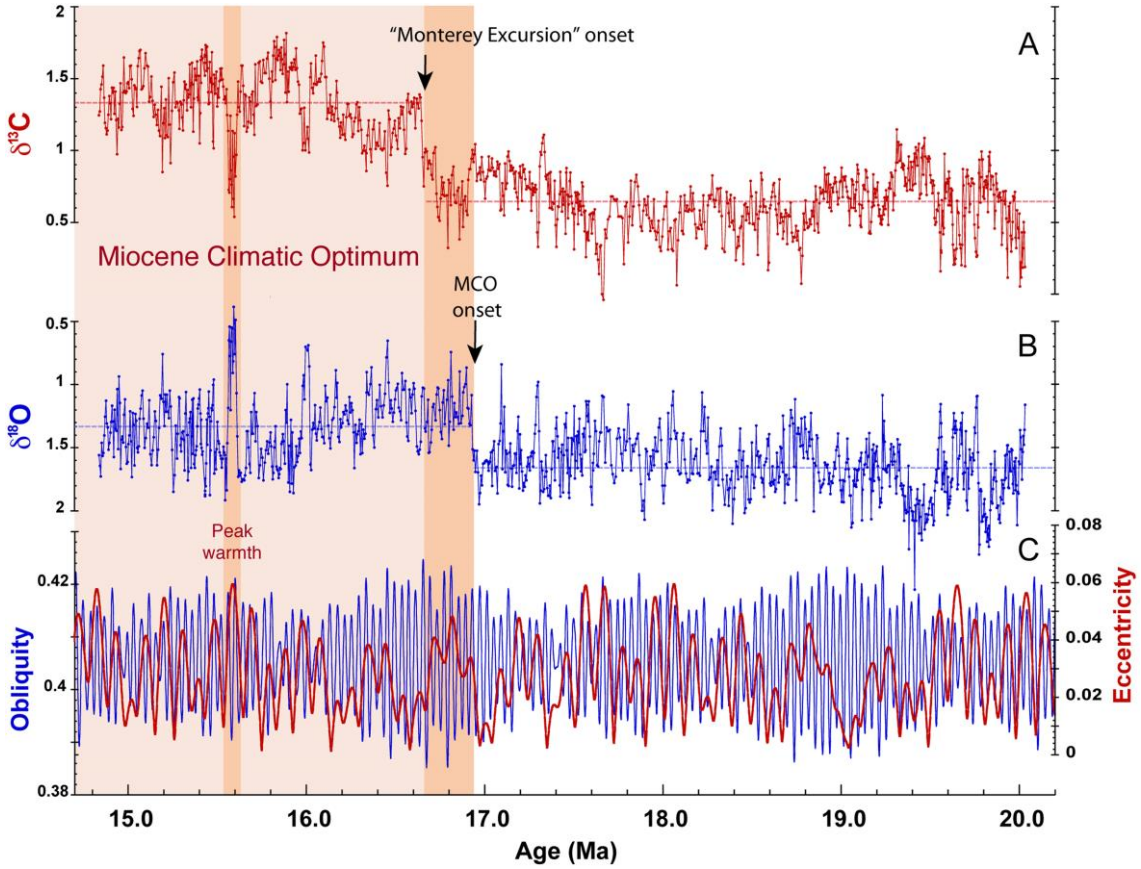

Fig.1. Early to middle Miocene paleoceanographic records from IODP Site U1337 (Holbourn et al., 2015). (a) Benthic foraminiferal $\delta^{13}C$ (‰ versus VPDB). (b) Benthic foraminiferal $\delta^{18}O$ (‰ versus VPDB). (c) Eccentricity and obliquity from Laskar et al. (2004). Stippled lines indicate mean $\delta^{18}O$ and $\delta^{13}C$ values.

Middle Miocene climate cooling linked to intensification of equatorial Pacific upwelling

High-resolution benthic stable isotope records (~1-3 kyr time resolution) in Site U1338 track climate evolution in unprecedented resolution through the development of the MCO and transition to a glaciated mode with permanent polar ice (Figure 2; Holbourn et al., 2014). We integrated the U1338 benthic stable isotope data with XRF-scanner derived biogenic silica and carbonate accumulation estimates to reconstruct eastern equatorial Pacific productivity variations and to investigate temporal linkages between high- and low-latitude climate change over the interval 16-13 Ma. Our records show that the climatic optimum (16.9-14.7 Ma) was characterized by high amplitude climate variations, marked by intense perturbations of the carbon cycle (Figure 2). Episodes of peak warmth at (southern hemisphere) insolation maxima coincided with sharp drops in $\delta^{13}C$ and transient shoaling of the carbonate compensation depth. These extreme events did not coincide with increased opal accumulation, indicating that equatorial Pacific upwelling was either suppressed or limited by nutrient availability during global warming episodes. The high-amplitude $\delta^{18}O$ and $\delta^{13}C$ variations poses a challenge, however, implicating massive switches in ocean heat transfer, ice volume and carbon cycling over relatively short timescales (on the order of a few kyrs). Further model-data comparisons are required to quantitatively evaluate controlling mechanisms and to elucidate the drivers of high-amplitude climate/carbon cycle fluctuations. A switch to obliquity-paced climate variability after 14.7 Ma concurred with a general improvement in carbonate preservation and the onset of stepwise global cooling, culminating with extensive ice growth over Antarctica at ~13.8 Ma. Two massive increases in opal accumulation at ~14.0 and ~13.8 Ma occurred just before and during the final and most prominent cooling step (Figure 2), supporting the hypothesis that enhanced siliceous productivity in the eastern equatorial Pacific contributed to CO_2 drawdown and fostered global cooling.

References:

Holbourn, A.E., Kuhnt, W., Lyle, M., Schneider, L., Romero, O., and Andersen. N., 2014. Middle Miocene climate cooling linked to intensification of eastern equatorial Pacific upwelling. Geology, 42, 19–22, doi:10.1130/G34890.1.

Holbourn, A.E., Kuhnt, W., Kochhann, K.G.G., Andersen. N., and Meier, K.J.S., 2015. Global perturbation of the carbon cycle at the onset of the Miocene climatic optimum. Geology, doi:10.1130/G36317.1.

Laskar, J., Robutel, P., Joutel, F., Gastineau, M., Correia, A., and Levrard, B., 2004, A long-term numerical solution for the insolation quantities of the Earth: Astronomy and Astrophysics, 428, 261-285, doi:10.1051/0004-6361:20041335.

Lyle, M., Olivarez Lyle, A. Gorgas, T., Holbourn, A., Westerhold, T., Hathorne, E., Kimoto, K., and Yamamoto, S., 2012. Data report, *in* Pälike, H., Lyle, M., Nishi, H., Raffi, I., et al., Proc. IODP, 320/321: Tokyo (Integrated Ocean Drilling Program Management International, Inc.), doi:10.2204/ iodp.proc.320321.203.2012.

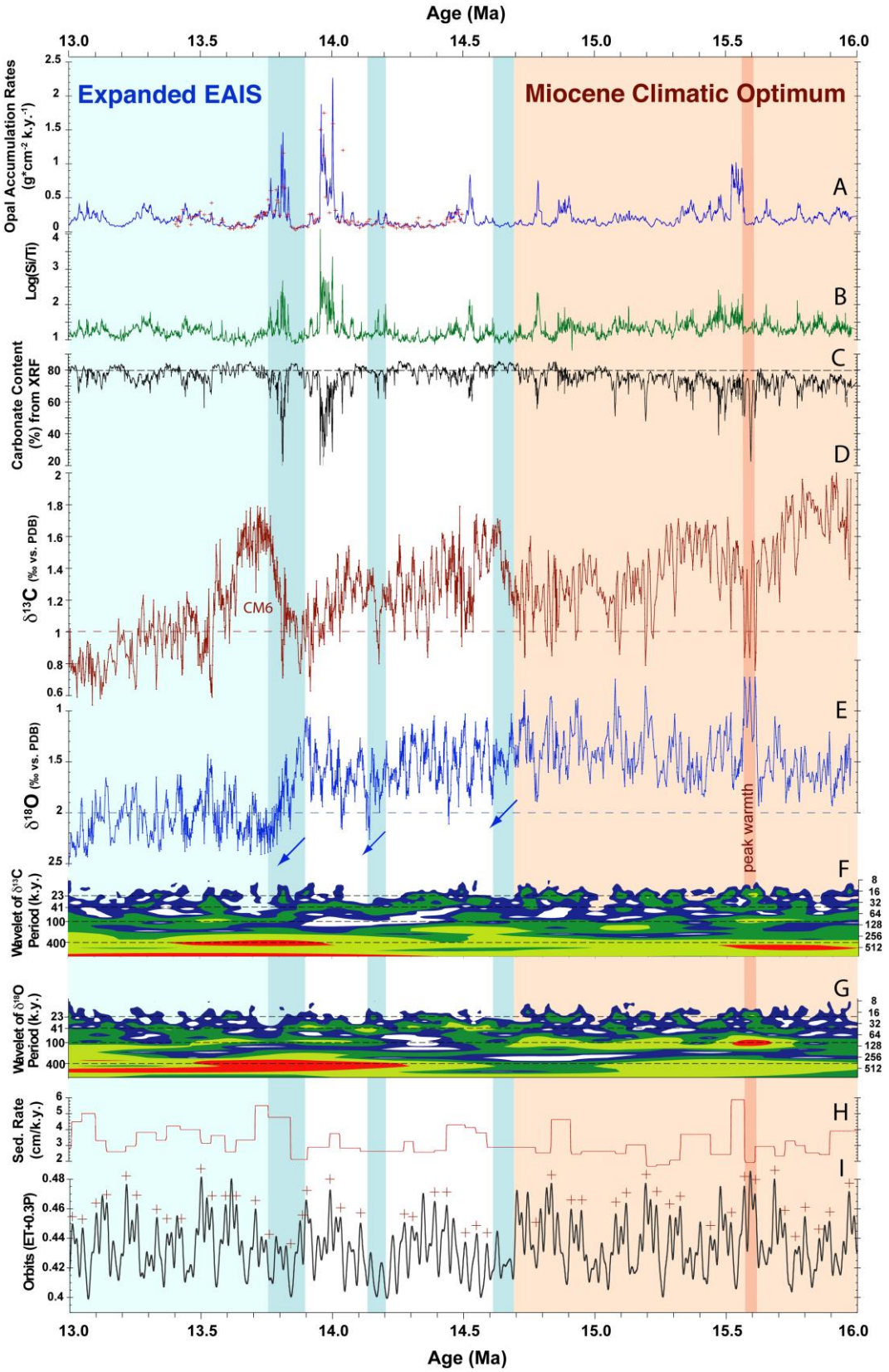

Fig. 2. Miocene paleoceanographic records from IODP Site U1338 (Holbourn et al., 2014). (a) Opal accumulation rates. (b) Silica content expressed as Log(Si/Ti) from Lyle et al. (2012). (c) Carbonate % calculated from XRF and GRAPE density data from Lyle et al. (2012); dashed line indicates 80 % $CaCO_3$. (d) Benthic foraminiferal $\delta^{13}C$; CM6 represents last and most prominent 400 kyr $\delta^{13}C$ maximum of "Monterey Excursion". (e) Benthic foraminiferal $\delta^{18}O$. (f) Wavelet power spectrum of $\delta^{13}C$ time series. (g) Wavelet power spectrum of $\delta^{18}O$ time series; dashed lines in f-g indicate main Milankovitch periodicities. (h) Sedimentation rates. (i) Eccentricity-tilt-precession tuning target (ET+0.3P) from Laskar et al. (2004); crosses indicate age correlation points; blue bars and arrows mark major $\delta^{18}O$ increases associated with high-latitude cooling; EAIS: East Antarctic Ice Sheet; XRF: X-Ray Fluorescence Spectrometry; PDB: PeeDee Belemnite.

IODP

Cryosphere expansion and East Asian monsoon variability during the Miocene (16.5-5 Ma): Insights from ODP Site 1146 (South China Sea)

A. HOLBOURN[1], W. KUHNT[1], S.C. CLEMENS[2], W. PRELL[2], N. ANDERSEN[3]

1 Institute of Geosciences, Christian-Albrechts-University, D-24118 Kiel, Germany
2 Department of Geological Sciences, Brown University, Box 1846, Providence, RI 02912, USA
3 Leibniz Laboratory for Radiometric Dating and Stable Isotope Research, Christian-Albrechts-University, D-24118 Kiel, Germany

The continuous, carbonate-rich, hemipelagic sedimentary succession recovered at ODP Site 1146 (South China Sea, water depth: 2091 m) provides an exceptional archive of middle to late Miocene climate evolution. We generated high-resolution (1-2 kyr) benthic *(C. wuellerstorfi)* and planktic *(G. sacculifer)* stable isotopes over the enigmatic Miocene interval 7-5 Ma and integrated these new data with published records from the same site, spanning the interval 16.5 to 7 Ma. Our methodology-consistent reference curves provide new insights into the pacing and magnitude of Miocene climate change, highlighting pivotal forcing and feedback processes. Our extended records show that the Miocene Climatic Optimum (16.9- 14.7 Ma) was characterized by high-amplitude climate variability with intense warming pulses associated with major perturbations of the carbon cycle and transient declines in deep-water ventilation (Holbourn et al., 2013). On the basis of $\delta^{18}O$ amplitudes, we find that climate variability decreased substantially after ~13 Ma, except for a remarkable warming episode at ~10.8-10.7 Ma during eccentricity maxima (100 and 400 kyr). This intense warming, reminiscent of Climatic Optimum warming spikes, suggests transient melting of polar ice and deep ocean warming at peak insolation. Dampened $\delta^{18}O$ variability after 13 Ma indicates a more stable ice cover following Antarctic glacial expansion, leading us to speculate that latitudinal moisture transfer rather than radiative forcing became the dominant control of ice volume variations. This long-term climate perspective also reveals that high-latitude cooling and glaciation progressed in a series of incremental steps at ~14.6, 13.9, 13.1, 10.6, 9.9 and 6.5 Ma. In the South China Sea, Antarctic ice growth episodes coincided with surface warming and freshening, implying high sensitivity of tropical rain belts to the inter-hemispheric temperature gradient (Holbourn et al., in prep). Comparable, high-resolution records from IODP Expeditions 346 (Asian Monsoon), 353 (Indian Monsoon) and forthcoming IODP Expeditions in the Indian Ocean and West Pacific Ocean will provide new insights into the inter-linkages of individual monsoonal subsystems and into the main controls of their long-term evolution through the Miocene.

Holbourn, A.E., Kuhnt, W., Clemens, S.C., Prell, W., and Andersen, N., 2013. Middle to late Miocene stepwise climate cooling: Evidence from a high-resolution deep-water isotope curve spanning 8 million years. *Paleoceanography*, 28, doi:10.1002/2013PA002538.

IODP

Denundation history of the St. Elias orogen: working programme of a provenance study of sediments from the Surveyor Fan, Gulf of Alaska

B. HUBER, H. BAHLBURG, C. DREWER

Institut für Geologie und Paläontologie, Westfälische Wilhelms-Universität Münster, Germany
barbara.huber@uni-muenster.de

The St. Elias orogen is the highest coastal mountain range on Earth, reaching an altitude of c. 5500 m at 55 km distance from the coast of the Gulf of Alaska. The onset of the formation of the mountain range in the middle Miocene was driven by the collision of the Yakutat terrane with the North American Plate. At c. 1 Ma, during the Mid-Pleistocene Transition (MPT), exhumation rates at the Gulf of Alaska side (windward side) of the orogen increased dramatically. Changing climate conditions are strongly linked to the high relief and the exhumation history of the mountain range. Large ice-sheets in the Pleistocene, temperate erosive glaciers in the Holocene and high precipitation rates today on the Gulf of Alaska side of the orogen characterise the setting. Erosion of the evolving St. Elias orogen supplied sediment for the formation of the Surveyor Fan depositional system. Onshore exhumation and denudation rates as well as glacial extent are reflected in the stratigraphy, accumulation rates and petrographic composition of the Surveyor Fan, making it a recorder of tectonic and climatic signals.

By applying diverse tools of provenance analysis on samples from the Surveyor Fan, we aim to constrain locations and rates of erosion, exhumation, denudation, tectonics and sedimentation pathways on the Alaska Margin. Based on this framework we will analyse the interplay of spatial and temporal interactions between erosion and mountain building, removal of mass at different locations and exhumation and uplift of the coastal St. Elias orogen to ultimately test if rapid erosion has the potential to cause a positive feedback on the exhumation rates in an active orogen.

During Integrated Ocean Drilling Program (IODP) Expedition 341 sites U1417 and U1418 were drilled on the distal and proximal Surveyor Fan in the Gulf of Alaska. At site U1417 over 750 m of Miocene to Holocene sediments were recovered. A 30 m-thick interval of diamict close to the Pliocene-Pleistocene boundary represents the first occurrence of ice rafted debris (IRD). Mud interbedded with turbidite sand and silt characterise the early Pleistocene, being overlain by intervals of diatom ooze and grey mud with lonestones representing IRD. At site U1418 early Pleistocene to Holocene sediments were recovered with mud and interbedded sand and silt representing 90 % of the sediments. Early to middle Pleistocene sediments are characterized by diamicts overlain by interbedded silt and mud with lonestones.

Sampling focused on sands and silts representing the complete stratigraphy recovered. Additionally core section length halfrounds of diamicts were sampled for analysis of heavy mineral content and populations of granule-sized larger clasts. The sand and silt samples will be analysed concerning grain size, petrographic composition and geochemistry of heavy minerals. Clasts with granule size or

coarser will be described under the microscope and analysed for provenance affiliations.

For more diverse distinction of mineral groups, in-situ single grain geochemical analysis of amphiboles, zircons, hornblende as well as of other heavy minerals will be performed using electron microprobe and LA-ICP-MS. By calculating their mineralogical formula amphiboles will be classified. ^{40}Ar-^{39}Ar age dating of sands rich in brown hornblende, which happen to be found especially at Site U1417, will be attempted in cooperation with Dr. J. Pfänder, Freiberg, for determination of origin and geochronological significance. Potential sources are the Wrangell volcanics that were active since 26 Ma, the Chugach Metamorphic Complex and the granitoids in the Wrangellia terranes. Geochemistry of pyroxenes will be analysed for deciphering the plate tectonic setting of their source rocks. Pyroxenes are reported from cobbles from the Chugach Metamorphic Complex and granitoids in the Wrangellia terranes Rutile analyses will be performed using an electron microprobe, providing high spatial resolution and being less invasive than LA-ICP-MS. Rutile geochemistry, preserving primary information even in mature sediments, is a promising tracer for material from the Chugach terrane which is an important source for mafic magmatic, metamorphic and metasedimentary rocks. Nb and Cr concentrations of rutile will be analysed to distinguish metamafic and metafelsic source rocks. Temperature dependence of Zr in rutile coexisting with quartz and zircon will be used as geothermometer giving information about the thermal history of the source rocks. By grouping rutiles according to geochemical data and optical rutile colour, combined with U-Pb isotopic age dating by LA-ICP-MS of individual rutile grains, the provenance of different grain populations will be identified. Additionally, analysis of turmaline geochemistry will give information of the geochemistry of the source rock, being expressed in the Mg, Fe and Al content of turmaline. U-Pb isotopic age dating of zircon by in-situ LA-ICP-MS will be applied to constrain the age of source rocks.

The results will contribute to the identification of regions under erosion at specific times, changes in size of the areas under erosion and the volume of the redistributed sediments. Combining these data with thermochronological data, to be obtained by the working group of K. Ridgeway at Purdue University, USA, will allow for considerations of spatial and temporal interplay between erosion and mountain building, the influence of mass removal at different locations and times of exhumation and uplift of the St. Elias orogen.

IODP

Friction properties of rocks sampled from a fossil accretionary prism

A. HÜPERS, S. TRÜTNER, M.J. IKARI, A.J. KOPF

MARUM - Center for Marine Environmental Sciences, University of Bremen, P.O. Box 330440, 28334 Bremen, Germany.

The exact cause for the updip limit of earthquake nucleaction in subduction zones is still subject to debate, because the seismogenic zone of an active megathrust zone has not been sampled so far. One of the most accepted hypotheses is the lithification of subduction zone sediments at depth. To test this hypothesis we aim to investigate changes in mechanical and hydrogeological properties of sediments that have undergone various degrees of diagenesis and low-T metamorphism. We utilize a unique sample set that comprises (1) samples from the Nankai Trough subduction zone, obtained via the Integrated Ocean Drilling Program (IODP) from up to 3 km depth below the seafloor, and (2) onshore samples from the Shimanto Belt (Japan), a fossil accretionary prism in the hinterland of the active Nankai subduction zone. The sample suite has experienced a wide range of in situ and paleo-temperatures, as high as those appropriate for the downdip limit of the seismogenic zone, and covers the different tectonic segments of pre-subduction, outer and inner wedge. Here, we focus on frictional behavior of samples from the Shimanto Belt. These samples experienced paleo-temperatures of ~100-290°C and represent sediments that have undergone substantial lithification during diagenesis and low-T metamorphism.

The 17 Shimanto Belt samples comprise the entire former oceanic-plate stratigraphy including oceanic crust, which were identified as dacites, red shales, black shales and sandstones (arkoses). Cylindrical samples of 63mm diameter were drilled from the specimens and cut to a height of at least 30 mm for the experiments. The shear behavior of the samples was tested under water-saturated conditions in a single-direct shear apparatus. In each experiment, the cohesion was determined first by breaking the intact samples by shearing at applied normal stress of $\sigma_n = 0$. Samples were then loaded to applied normal stresses σ_n of 81 to 117 MPa, which correspond to the depth range of the paleo-temperatures, and then sheared along the created fracture surfaces at a constant velocity of 10 µm/s until steady state shear strength (τ) wasreached. In order to calculate the velocity dependence of friction, as quantified by the parameter a-b, we increased the velocity (V) in one-order of magnitude steps within the range 0.1-100 µm/s. Velocity-strengthening materials (a-b>0) are expected to exhibit stable slip, whereas velocity-weakening behavior (a-b<0) is required for slip instability that results in earthquake nucleation.

We measured a cohesion of ~0.75 to ~21.26 MPa, and observed during the subsequent shearing an rapid increase in the friction coefficient μ ($= \tau/\sigma_n$) until reaching a maxima (μ_{max}), ranging from 0.42 to 0.93, followed by a drop in μ to a residual value μ_{res} (0.79-0.42). Both velocity-strengthening and velocity-weakening is observed for the tested lithologies, with values of a-b ranging from -0.025 to 0.015. Despite the great variety in frictional parameter, we observed several lithologically independent trends. For

example, a positive correlation between μ_{max} and the cohesion can be observed. Because cohesion is most likely a direct result of the lithification process, our tests verify that lithification increases rock strength. This is further corroborated by the fact that residual friction coefficients are greater than those measured in previous tests on unlithified powders of similar mineralogical composition. We further notice that the frictional parameter a-b correlates with frictional strength. a-b is mainly positive, with values ranging from 0 to 0.015 for weaker samples having residual friction coefficients of $\mu_{res}<0.5$. For stronger samples with friction coefficients $\mu_{res}>0.7$, the a-b parameter decreases and becomes mainly negative. Thus, lithification may also cause a transition from stable to unstable sliding.

These results will be complemented by future friction experiments using the IODP samples, which experienced lower temperature conditions to better constrain the effects of incipient lithification. In addition, detailed X-ray diffraction and secondary electron microscopy analyses will be conducted to identify the underlying key diagenetic to low-T metamorphic processes.

IODP

Controlling factors of Ca isotope fractionation in Porites corals evaluated by culture experiments and downcore records

M. INOUE[1,2], N. GUSSONE[1], Y. KOGA[3], A. IWASE[3], A. SUZUKI[4], K. SAKAI[3], H. KAWAHATA[2]

1 Institut für Mineralogie, Corrensstr. 24, 48149 Münster
2 Ocean Research Institute, The University of Tokyo, 1-15-1 Minamidai, Nakano, Tokyo 164-8639, Japan
3 Sesoko Station, Tropical Biosphere Research Center, University of the Ryukyus, 3422 Sesoko, Motobu, Okinawa 905-0227, Japan
4 Geological Survey of Japan, National Institute of Advanced Industrial Science and Technology (AIST), 1-1-1 Higashi Tsukuba, AIST Tsukuba Central 7, Ibaraki 305-8567, Japan

Geochemical tracers such as $\delta^{18}O$ and Sr/Ca ratios in the skeleton of massive *Porites* coral are well established environmental proxies for sea surface temperature and/or salinity changes through time. For instance, paleoclimate during the last glacial termination has been reconstructed using fossil *Porites* corals collected from Tahiti by IODP Exp. 310 (e.g., Felis et al., 2012). Knowing the mechanism of skeletal growth of *Porites* coral is consequently of great importance for the use of geochemical tracers as precise environmental proxies. Furthermore, to understand the controlling factors responsible for calcium isotope fractionation in marine calcifying organisms including scleractinian corals is critical to investigate the past evolution of Ca^{2+} concentrations in the ocean precisely. In this study, we cultured multiple colonies of *Porites* coral under temperature, pH and light controlled environments and investigated the relationship between $\delta^{44}Ca$ in skeleton grown during the cultured period and each environmental parameters. We also determined Ca isotope ratios of natural corals from the Great Barrier Reef collected during IODP expedition 325 (Yokoyama et al., 2011). Variation of fractionation pattern of $\delta^{44}Ca$ in skeleton of cultured and natural corals reveals information to understand coral biomineralization .

Culture experiments on *Porites* coral have been conducted at Sesoko Station, Tropical Biosphere Research Center, University of the Ryukyus, Okinawa, Japan. Temperature and pH controlled experiments were conducted inside for 6 and 3 months, respectively and settings of water temperature and pH were, 21, 23, 25, 27, 29˚C and 7.4, 7.6, 8.0, respectively. The light experiment was conducted in an outdoor tank of Sesoko Station for 18 months and light levels were maintained with high, middle and dark adjusted by partial shading with a sun-screen mesh. Skeletal samples grown during the culture experiment, mostly < 1 mm from the surface of each colony, were taken after the experiments by micro-milling. For isotope measurements, 300-400 ng Ca were loaded on Re-single filaments with a tantalum activator after addition of a ^{42}Ca-^{43}Ca double spike. Calcium isotope ratios were determined on a Finnigan TRITON TI TIMS follwing the method described in Gussone et al. (2011). The isotope values are expressed relative to NIST SRM 915a as $\delta^{44}Ca=((^{44}Ca/^{40}Ca)_{sample}/(^{44}Ca/^{40}Ca)_{SRM915a}-1) \times 1000$.

As a result of culture experiments, skeletal growth rate varied with the variation of each environmental parameter, typically higher growth rate at higher temperature, pH and light conditions with a colony-specific variation especially in the temperature experiment. However, $\delta^{44}Ca$ showed negligible variation related to these variations of growth rate generated by differences of pH and light level, indicating that there are little or no relationships between pH and light and $\delta^{44}Ca$ in *Porites* coral. On the other hand, the temperature dependence of isotope fractionation of 0.02 ‰/˚C which is similar to inorganic aragonite was found in this study, but the degree of isotope fractionation is about +0.4 ‰ offset in corals. Due to coral-specific biomineralization processes, the overall mean $\delta^{44}Ca$ of scleractinian corals including results from previous studies are different from other biogenic aragonites like screlosponges and pteropods, which resemble inorganic aragonite. Apparently, coral Ca isotope ratios are more similar to those of calcitic coccolithophores.

We sudied fossil corals from IODP expedition 325 drilled from the shelf edge seaward of the modern Great Barrier Reef, covering the time between 24 and 11 ka. Our results show a gradual increasing shift of $\delta^{44}Ca$ from the LGM towards the Holocene. This trend might reflect variations of temperature, weathering and/or other, previously unconsidered factors.

These results are important for the understanding of biomineralisation related Ca isotope fractionation in corals and in order to investigate the evolution of Ca isotope in seawater during the Phanerozoic, as corals contribute significantly to the Ca export production.

References:

Felis, T., Merkel, U., Asami, R., et al. (2012) Pronounced interannual variability in tropical South Pacific temperatures during Heinrich Stadial 1. Nat. Commun. 3:965, doi: 10.1038/ncomms1973.

Gussone, N., Nehrke, G., Teichert, B.M.A. (2011) Calcium isotope fractionation in ikaite and vaterite. Chem. Geol. 285, 194–202.

Yokoyama, Y., Webster, J. M., Cotterill, C., Braga, J. C., Jovane, L., Mills, H., Morgan, S., Suzuki, A. and the IODP Expedition 325 Scientists (2011) IODP Expedition 325: Great Barrier Reefs Reveals Past Sea-Level, Climate and Environmental Changes Since the Last Ice Age. Scientific Drilling 12, 32-45. doi:10.2204/iodp.sd.12.04.2011.

ICDP

The history of the Campi Flegrei (Napoli, Italy) magma system through time: the key to understand present and future volcanic processes.

R.S. IOVINE[1], G. WÖRNER[1], S. PABST[1,2], ITALIAN COLLABORATORS: I. ARIENZO[3], L.CIVETTA[3,5], M. D'ANTONIO[5], G. ORSI[5]

1 Geowissenschaftliches Zentrum, Georg-August-Universität, Göttingen, Germany
1 Project Geologist, BHP Billiton, Perth, Australia
3 Istituto Nazionale di Geofisica e Vulcanologia – sezione di Napoli Osservatorio Vesuviano, Naples, Italy
4 Istituto Nazionale di Geofisica e Vulcanologia – sezione di Palermo, Italy
5 Department of Earth, Environmental and Resources Science, University Federico II of Naples, Italy

We compile new and published geochemical and isotopic data on Campi Flegrei (CF) volcanic products (Napoli, South Italy) within a well-constrained stratigraphic framework. The goal of our project is to better understand the processes of (1) initial evolution of the Campi Flegrei magma system from the study of its oldest deposits, and (2) to characterize patterns of further evolution by identifying distinct magma batches throughout the entire history from ca. 60 ka ago to the 1538 A.D Monte Nuovo eruption. In particular, we aim to further study the processes that drive the CF magma system from one regime (many small eruptions) to the two major eruptions, Campanian Ignimbrite (CI) and Neapolitan Yellow Tuff (NYT) and back. Phenocryst zonation profiles provide time scales of petrogenetic processes such as fractional crystallisation, crystal growth and crystal residence times crucial for understanding magma emplacement, remobilisation, transport and eruption.

Major and trace elements bulk rocks analysis have been performed by XRF and ICMPS, respectively. Back scattered electron (BSE) images and secondary electron images (SEI) have been acquired on the selected crystals by electron microprobe. Sr-isotope analysis have been carried out by using a Thermal Ionization Mass Spectrometery.

XRF results show the oldest rocks of the CF volcano (pre Campanian Ignimbrite, >39 ky BP) to be phonolitic, samples from Campanian Ignimbrite (39 ky BP) to Neapolitan Yellow Tuff (14.90 ka) eruption are trachytic, while the youngest post Neapolitan Yellow Tuff volcanic products (12.8 ka - 1538) range in composition from rare shoshonite, to trachyte and phonolite. Thus there appears to be a systematic secular trend in the erupted magmas and/or proportions of magma batches during the life time of the magma system.

Rare Earth Element patterns are fractionated, with significant negative Eu anomalies. Incompatible trace element patterns normalised to primordial mantle show positive Pb and U spikes and relatively high concentration of HFSE. systematic changes in the trace element ratios will be explored to characterize distinct magma bachtes and evolutionary trends.

Plagioclase are always close to An60 but some show strong core-rim zonation in Pre CI, post CI/pre NYT and Agnano Monte Spina (Post NYT), deposits. Pyroxenes (mostly salite/diopside) and show weak oscillatory zoning.

Sr-isotopic composition of feldspar varies from ~0.7069 to ~0.7079, with Minopoli 2B upper (post NYT) showing the widest range (~0,7067 to ~0,7095). However, the majority of the analysed feldspar have a more narrow Sr-isotopic ratios between ~0,7073 and ~0,7075. The least radiogenic Sr in Minopoli feldspar phenocrysts (87Sr/86Sr ~0.7067) possibly derive from pre Campanian Ignimbrite volcanic activity which is the only product with similar low 87Sr/86Sr in feldspar.

Diffusion calculations based on Sr zonation in strongly contrasting core-rim in feldspar results in crystal residence times of hundreds to a maximum of a few thousands of years. Given the frequency of eruptions, it is likely that most crystals represent residues from previous magma batches and either became re-entrained by recharge, or crystal cargo from different mixed magmas and/or they represent crystal mushes from which the evolved magmas were extracted. These alterantive models will be evaluated further in future studies based on Sr- and O- isotope mineral analysis.

IODP

Deciphering early Pleistocene sea level variability and millennial-scale climate fluctuations in the eastern equatorial Pacific

K. JAKOB, O. FRIEDRICH, J. PROSS

University of Heidelberg, Institute of Earth Sciences, Im Neuenheimer Feld 234-236, 69120 Heidelberg
Kim.Jakob@geow.uni-heidelberg.de

This project aims at deciphering the rate of sea level variability and its effect on millennial-scale climate fluctuations during the final phase of the intensification of northern hemisphere glaciation (iNHG) between 2.6 and 2.4 Ma.

Millennial-scale climate fluctuations appear to have changed significantly at glacial-interglacial (G-IG) time scales during the late Pliocene and Pleistocene. Thereby, millennial-scale climate fluctuations under a warmer climate during late Pliocene and early Pleistocene show markedly lower amplitudes compared to the well-known fluctuations of the late Pleistocene. Numerous Pleistocene proxy records (e.g. McManus et al., 1999; Schulz et al., 1999) suggest that this difference can be explained by an ice-volume/sea level threshold that amplifies millennial-scale climate fluctuations and was not reached prior to the Mid-Pleistocene Transition (MPT). However, new records question the existence of this threshold, showing that the proposed threshold value was clearly reached and even surpassed during several glaciations around 2.5 Ma without amplification of climate fluctuations (Bolton et al., 2010). These observations suggest that either the amplification of millennial-scale climate fluctuations before the MPT required a higher ice-volume threshold than in the late Pleistocene, that ice-volume had no significant effect on the amplitude of climate fluctuations, and/or the available sea level estimates for the early Pleistocene are inaccurate.

For identifying the mechanisms underlying the dynamics of early Pleistocene ice sheets, material from the eastern equatorial Pacific (EEP, ODP Site 849) has been studied over a time interval from 2.6 to 2.4 Ma (marine isotope stages (MIS) 104 to 96). First, ODP Site 849

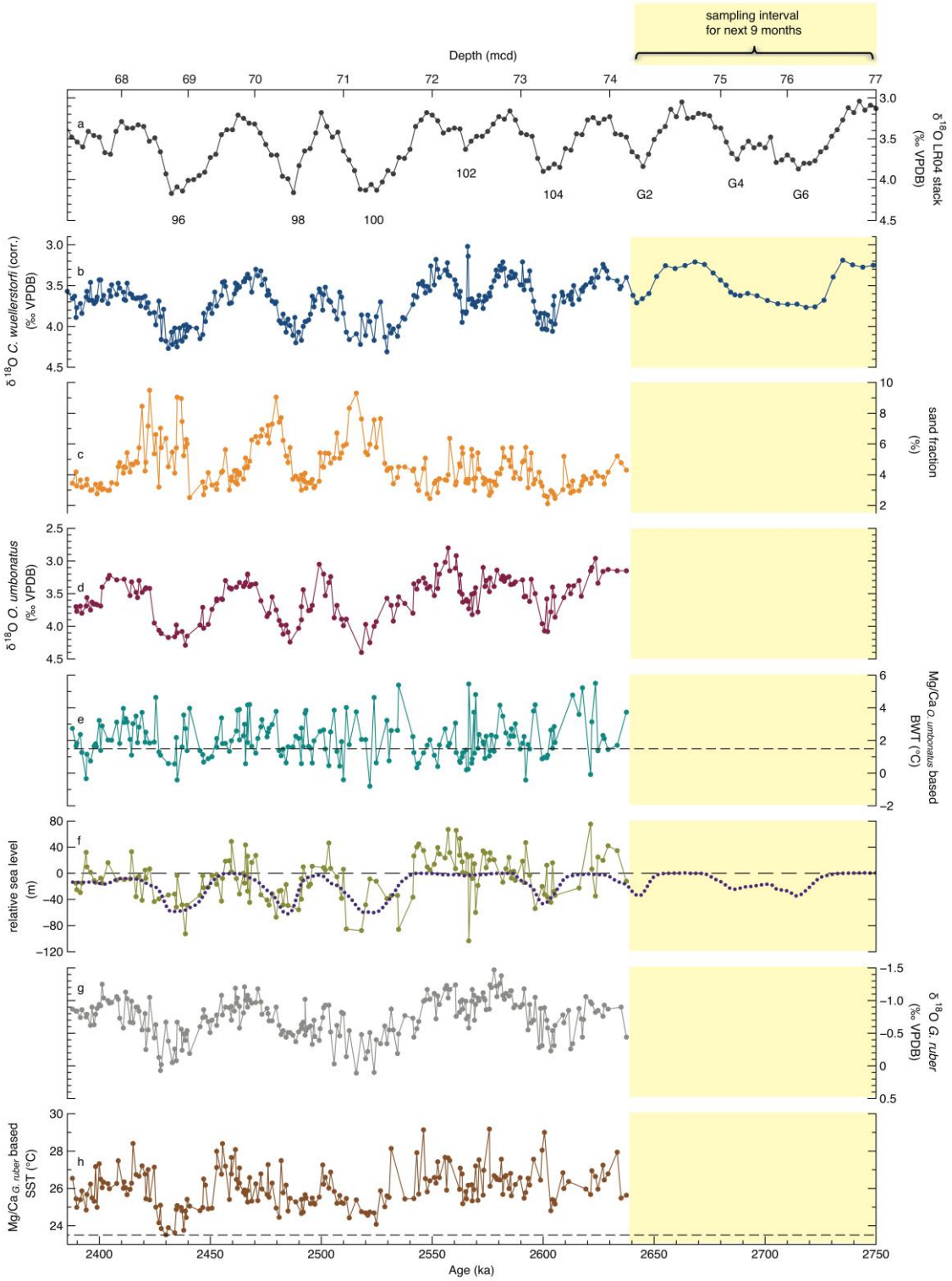

Fig. 1. High-resolution proxy records from ODP Site 849 for MIS 104 to 96 (2640 to 2385 kyr) tuned to the LR04 stack (Lisiecki and Raymo, 2005). Yellow boxes indicate the interval worked on within the next 9 months. **(a)** LR04 stack for G6 to MIS 96 (Lisiecki and Raymo, 2005). **(b)** $\delta 1^8O_{C.\ wuellerstorfi}$ from Site 849; high-resolution record from G1 to MIS 95 contains a combination of own measurements and data from Mix et al. (1995); low-resolution record from G7 to G2 only implies data of Mix et al. (1995). **(c)** Percentage of sand fraction (> 63 µm) for Site 849. **(d)** $\delta^{18}O_{O.\ umbonatus}$ from Site 849. **(e)** *O. umbonatus* Mg/Ca based BWT estimates from Site 849; black dashed line indicates recent modern mean BWT (Locarnini et al., 2013). **(f)** Sea level estimates relative to present for Site 849 and modelled global sea level relative to present (dotted blue line, Bintanja and van de Wal (2008)); black dashed line represents modern sea level. **(g)** $\delta^{18}O_{G.\ ruber}$ from Site 849. **(h)** *G. ruber* Mg/Ca based SST estimates from Site 849; black dashed line indicates recent modern mean annual SST (Locarnini et al., 2013).

sample depths have been converted to age by tuning the generated high-resolution $\delta^{18}O$ dataset of the benthic foraminifera *Cibicidoides wuellerstorfi* to the LR04 benthic oxygen isotope stack (Lisiecki & Raymo, 2005). Secondly, both bottom-water and sea-surface high-resolution (~700 years) Mg/Ca and $\delta^{18}O$ datasets have been established by

using the benthic foraminifera *Oridorsalis umbonatus* and the planktonic foraminifera *Globigerinoides ruber*. With this combined geochemical approach the following research questions are adressed:

(1) Quantification of sea level change from 2.6 to 2.4 Ma and comparison to model-based sea level estimates. The reconstructed dataset (Figure 1) indicates sea level lowstands of ~0-30 m below present for MIS 104 and 102, ~45-60 m below present for MIS 98 and 96, and up to 80 m below present for MIS 100, matching nicely to the global sea level model of Bintanja & van de Wal (2008). Sea level highstand estimates during interglacials before iNHG display values slightly above present day sea level and decreased during iNHG to values slightly below present day sea level. In summary, sea level decreased with increasing NHG. However, sea level lowstand estimates from N-Atlantic IODP Site U1313 and DSDP Site 607 for MIS 104 to 96 indicate much lower values than the estimates from Site 849 (up to 100 m below present for MIS 100 (Friedrich et al., unpublished), 70 and 90 m below present for MIS 98 and 96 (Sosdian & Rosenthal, 2009), respectively). In comparison to sea level estimates of Site 849 and the global sea level model (Bintanja & van de Wal, 2008), N-Atlantic sea level estimates seem to be overestimated.

(2) Reconstruction of sea-surface temperatures (SSTs) and bottom-water temperatures (BWTs) and comparison to other Sites. SSTs fluctuate between ~23.5 °C during glacials and ~29 °C during interglacials, which can be correlated in trend and amplitude to SST records of nearby EEP ODP Site 846 (Lawrence et al., 2006) and ODP Site 1241 (Groeneveld et al., 2014). The first significant cooling of SSTs during the analysed time interval occured during MIS 100, which can be correlated to iNHG. MIS 96 seems to be the most pronounced glacial with SSTs less than 24 °C. This is a great difference to N-Atlantic Site U1313, indicating MIS 98 as the strongest glacial (Bolton et al., 2010), which is in turn only sligthly visible in the SST record of EEP sites 849 and 846 (Lawrence et al., 2006). Other distinct features in the SST record are two intervals during MIS 96, indicating SSTs of ~25 °C between 2435 and 2450 kyr, followed by a prominent shift towards SSTs less than 24 °C between 2425 and 2435 kyr. Maybe the latter is representing the most southward extension of Laurentide Ice Sheet.

Reconstructed BWTs, which reflect the temperature of the Antarctic Bottom Water (AABW), range between ~ -1 °C and ~5.5 °C, with an average value of ~2.1 °C. The dataset shows great short-term BWT fluctuations up to 4 °C, which are independent to the 41 kyr G-IG cyclicity of the early Pleistocene. Such short-term temperature fluctuations within the same temperature range and the same time interval can also be recognized at N-Atlantic DSDP Site 607 (Sosdian & Rosenthal, 2009). Moreover, BWTs at Site 849 do not show significant G-IG patterns before iNHG. After iNHG only a slight trend towards lower BWTs during glacials is apparent. It seems that G-IG variations before iNHG were not strong enough to induce changes in BWT. This pattern is also visible in the SST record, indicating that significant G-IG fluctuations are much more pronounced after iNHG.

The gradient between SSTs and BWTs (ΔSST-BWT) seems to be slighty lower during glacials than during interglacials, which may suggest stronger upwelling during glacials. This idea is supported by productivity proxy data (C_{37}) from EEP Site 846, indicating enhanced productivity/upwelling during glacials (Lawrence et al., 2006). Moreover, a general shift towards lower ΔSST-BWT with iNHG potentially displays stronger upwelling since 2.5 Ma.

Generally, both mean BWT and SST are 0.5 °C and accordingly 3 °C higher than present day temperatures of the EEP (Locarnini et al., 2013), which supports the idea of a warmer climate during early Pleistocene.

(3) Critically assess the hypothesis of an ice-volume threshold for millennial-scale climate amplification during the early Pleistocene. Reconstructed BWT and SST estimates show no evidence for amplification during MIS 96, 98 and 100. However, these glacials clearly reached the proposed threshold (either a $\delta^{18}O_{benthic}$ value of 4.14 ‰ as proposed for the late Pleistocene (McManus et al., 1999), respectively 3.7 ‰ to 3.9 ‰ as proposed for the late Pliocene to early Pleistocene (Bailey et al., 2010), or a sea level drop of ~45-50 m below present (Schulz et al., 1999)), supporting the findings of N-Atlantic Site U1313, which question the existence of this threshold (Bolton et al., 2010). A possible explanation for this observation is the fact that potentially the proposed thresholdes are only slightly reached (and not clearly surpassed) in a time interval too short for triggering the amplification of climate. Furthermore, a higher ice-volume threshold than proposed might be required for climate amplification during early Pleistocene, or other factors influence millennial-scale climate fluctuations (McManus et al., 1999).

Further research work within the framework of this study will focus on the following deliverables:

(1) Expansion of the Site 849 record from MIS G7 to G2 (2.75 – 2.6 Ma). Moreover, Mg/Ca and $\delta^{18}O$ analyses of the thermocline-dwelling planktonic foraminifera *Globorotalia crassaformis* will be performed to deliver information about the development of the thermocline from MIS G7 to 95 in the EEP.

(2) Expansion and verification/falsification of already existing records from N-Atlantic Site U1313 (Bolton et al., 2010; Friedrich et al., unpublished) for the time interval from MIS G7 to 95 and comparison to EEP Site 849. High-resolution sea-surface records based on *G. ruber* for MIS 102 to 95 are already available (Bolton et al., 2010) and will be expanded by C. Bolton to MIS G7. Simultaneous, we will focus on the expansion of a high-resolution bottom-water record, based on *O. umbonatus*, which already exists for MIS 100 (Friedrich et al., unpublished). Working with the same species at Site 849 and U1313 will allow perfect preconditions for comparing the EEP with the N-Atlantic early Pleistocene record.

References:

Bailey, I., C.T. Bolton, R.M. DeConto, D. Pollard, R. Schiebel, P.A. Wilson (2010): A low threshold for North Atlantic ice-rafting from 'low-slung slippery' late Pliocene ice-sheets. Paleoceanography, 25, doi:10.1029/2009PA001736.

Bintanja, R. & van de Wal, R. (2008): North American ice-sheet dynamics and the onset of 100,000-year glacial cycles. Nature, 454 (7206): 869-872.

Bolton, C.T., P.A. Wilson, I. Bailey, O. Friedrich, C.J. Beer, J. Becker, S. Baranwal, R. Schiebel (2010): Millennial-scale climate variability in the subpolar North Atlantic Ocean during the late Pliocene. Paleoceanography, 25, doi:10.1029/2010PA001951.

Groeneveld, J., E.C. Hathorne, S. Steinke, H. DeBey, A. Mackensen, R. Tiedemann (2014): Glacial induced closure of the Panamanian Gateway during Marine Isotope Stages (MIS) 95–100. Earth and Planetary Science Letters, 404: 296-306, 10.1016/j.epsl.2014.08.007.

Lawrence, K.T., Z. Liu, T.D. Herbert (2006): Evolution of the eastern tropical Pacific through Plio-Pleistocene glaciation. Science, 312 (5770): 79-83.

Lea, D.W., D.K. Pak, H.J. Spero (2000): Climate impact of late Quaternary equatorial Pacific sea-surface temperature variations. Science, 289 (5485): 1719-1724.

Lisiecki, L.E. & Raymo, M.E. (2005): A Pliocene-Pleistocene stack of 57 globally distributed benthic $\delta^{18}O$ records. Paleoceanography, 20, doi:10.1029/2004PA 001071.

Locarnini, R.A., A.V. Mishonov, J.I. Antonov, T.P. Boyer, H.E. Garcia, O.K. Baranova, M.M. Zweng, C.R. Paver, J.R. Reagan, D.R. Johnson, M. Hamilton, D. Seidov (2013): World Ocean Atlas 2013, vol. 1, Temperature. Levitus, S., Ed., Mishonov, A., Technical Ed., NOAA Atlas NESDIS 73, pp. 40.

McManus, J., D.W. Oppo, J.L. Cullen (1999): A 0.5-Million-Year Record of Millenial-Scale Climate Variability in the North Atlantic. Science, 283, 971-975.

Mix, A.C., N.G. Pisias, W. Rugh, J. Wilson, A. Morey, T.K. Hagelberg (1995): Benthic foraminiferal stable isotope record from Site 849 (0-5 Ma): local and global climate changes. Proceedings of the Ocean Drilling Program, Scientific Results, 138, 371-412.

Schulz, M., W.H. Berger, M. Sarnthein, P.M. Grootes (1999): Amplitude variation of 1470-year climate oscillations during the last 100,000 years linked to fluctuations of continental ice mass. Geophysical Research Letters, 26, 3385-3388.

Sosdian, S. & Rosenthal, Y. (2009): Deep-sea temperature and ice volume changes across the Pliocene-Pleistocene climate transitions. Science, 325 (5938): 306-310.

IODP

The paleoenvironmental impact of the Latest Danian Event and response of planktic foraminifera at ODP Site 1210 (Shatsky Rise, Pacific Ocean)

SOFIE JEHLE[1], ANDRÉ BORNEMANN[1,2], ARNE DEPREZ[3], ROBERT P. SPEIJER[3]

1 Institut für Geophysik und Geologie, Universität Leipzig, Germany
2 Bundesanstalt für Geowissenschaften und Rohstoffe, Stilleweg 2, 30655 Hannover, Germany
3 Department of Earth and Environmental Sciences, KU Leuven, Belgium.

The marine ecosystem has been severely disturbed by several transient paleoenvironmental events (<200 ky) during the early Paleogene, of which the Paleocene-Eocene Thermal Maximum (PETM, ~56 Ma) is the most prominent one. Over the last decade a number of similar events of Paleocene and Eocene age have been discovered. Potential Paleocene events, bracketed by the Cretaceous/Paleogene boundary (66 Ma) and the Paleocene-Eocene thermal maximum (PETM, 56 Ma) are the Dan-C2 Event (65.2 Ma ago), the Latest Danian Event (LDE) or Top Chron 27n Event (62.15 Ma, e.g. Bornemann et al., 2009, Westerhold et al., 2011), and the Early Late Paleocene Event (ELPE, 58.9 Ma, e.g. Petrizzo, 2005).

However, relatively little attention has been paid to the LDE, specifically from an open ocean perspective. The LDE is characterized by a prominent negative carbon isotope excursion (CIE) of <2‰ in different marine settings like the southern Tethyan shelf (Egypt, Bornemann et al., 2009), the eastern North Atlantic (Zumaia, Spain, Dinarès-Turell et al., 2010), South Atlantic (Walvis Ridge,

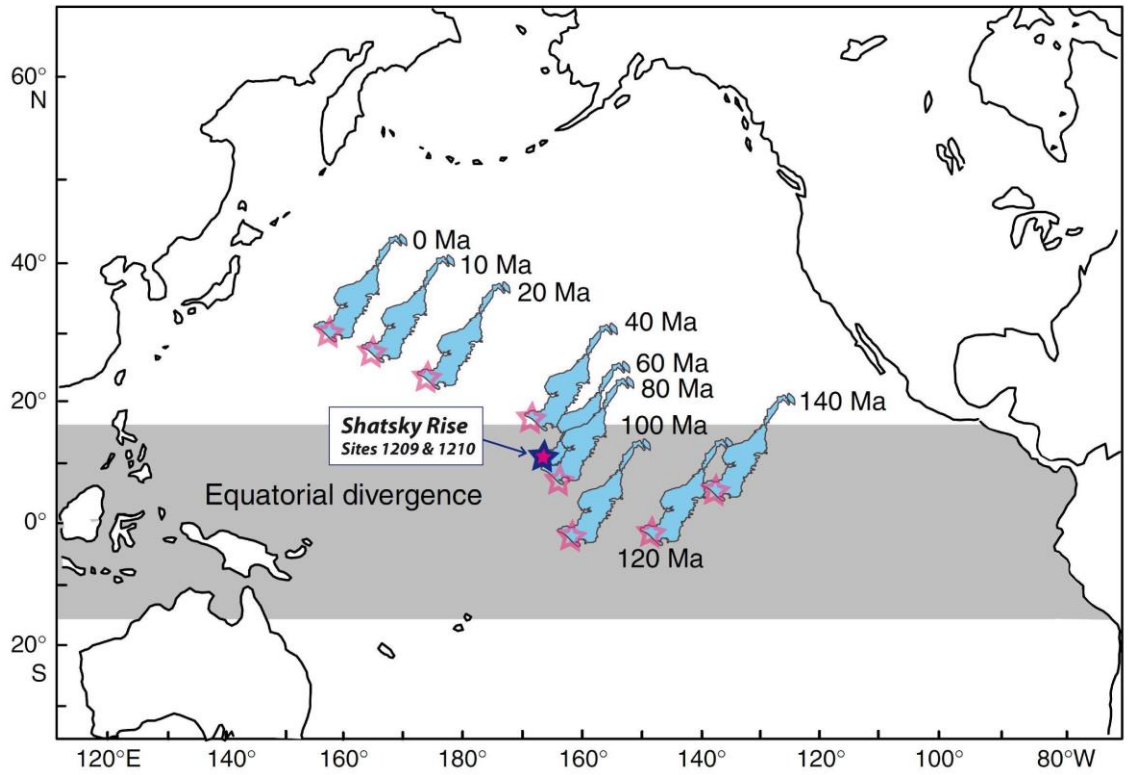

Fig. 1. Map of the Shatsky Rise centered Pacific Ocean. Redrawn after Bralower et al. (2002). ODP Sites 1209 and 1210 are marked by orange circles. Due to plate tectonic movements Shatsky Rise Plateau shifted north-westwards through over the last 140 My. Circled in bright orange shows the studied site during the Mid-Palaeocene (~60 Ma).

own unpublished data), and the Peri-Tethys (Bjala, Bulgaria, Dinares-Turell et al., 2012) . Moreover, the LDE is characterized by the most negative $\delta^{13}C$ values for the entire Paleocene, thus, representing an extreme position in the secular changes of the global carbon cycle (Westerhold et al., 2011). In various ODP cores this event is marked by two prominent peaks in Fe intensities based on XRF core scanning as well as magnetic susceptibility. Due to the supra-regional nature of the LDE and the associated paleoenvironmental changes that resemble those of the PETM (Bornemann et al., 2009) it has been hypothesized that the LDE may represent an additional Paleocene hyperthermal. So far, there are no detailed paleoecological faunal data available for the LDE from an open ocean setting. The overall objectives of studying a deep-sea record of the LDE were (1) to test the hyperthermal hypothesis, by analyzing the $\delta^{18}O$ of surface and subsurface water inhabiting planktic foraminifera, and (2) to assess the biotic response to the event of planktic foraminiferal assemblages.

Shatsky Rise Plateau (Fig. 1) is a large igneous province that is situated on a triple-junction in the Pacific Ocean, formed between the Late Jurassic and the Early Cretaceous (149 Ma – 135 Ma; Sager, 2005). Drilled sedimentary successions are up to 1000 m thick representing a remarkable long-term record of Cretaceous to Neogene age. Site 1210 was drilled in a water depth of 2573 mbsl in the southern part of the Plateau. Paleodepth has been estimated as upper abyssal to lower bathyal based on benthic foraminiferal faunas. The latest Danian is made up by homogeneous carbonate ooze, usually coloured in bright pale beige. Two prominent dark brown horizons are intercalated into this monotonous sequence that represent the LDE as indicated by stratigraphic correlation with other ODP sites based on Fe XRF core scanning and magnetic susceptibility data (Westerhold et al., 2008).

The study interval covers about five metres of core (231.2–236.6 rmcd) that represent ~900 ky according to cyclostratigraphy (Westerhold et al., 2008). From this interval 73 samples, collected at a resolution of 2 to 15 cm steps, have been investigated for $\delta^{13}C$ and $\delta^{18}O$ of planktic foraminiferal calcite, calcium carbonate content, planktic foraminiferal assemblages, planktic/benthic foraminifera ratio (%P) and other parameters like fragmentation, coarse fraction (CF) and absolute abundances. Faunal analysis was carried out at a size fraction >125 µm and P/B-ratio at >63 µm.

The diagenetic alteration of the sample material appears to be rather limited. Only slight indications for dissolution have been observed during the event horizons, %P never drops below 95.5% and %F never reaches values above 17% in the selected samples, thus, indicating minor alterations in the test structure due to dissolution and recrystallisation. However, more severe changes of the assemblages are indicated before and after this event. Few samples have been removed from the faunal analysis due to a potential preservational bias of the assemblage data from the intervals below and above the LDE. In these intervals $CaCO_3$ values are rather high in the samples, therefore we suspect that recrystallisation which is quite common in these intervals, has led to the observed changes in fragmentation and subsequently in CF and %P. Before and after the LDE, the sedimentation rate (SR) tends to be low between 0.2 and 0.35 cm/kyr. The decrease in cycle size during the LDE is hinting towards a sinking SR or increased dissolution, or a combination of both. This fact might be related to a rising CCD during the LDE horizons, and is supported by the dark event horizons, enhanced Fe counts and low carbonate content. Fe counts are largely anti-correlated to short-eccentricity derived SR.

Planktic foraminiferal $\delta^{13}C$ and $\delta^{18}O$ of surface (*Morozovella angulata*, *M. praeangulata*) and subsurface dwellers (*Parasubbotina pseudobulloides*/*variospira*) show abrupt negative excursions for both isotope species of different amplitudes. $\delta^{13}C$ shows a drop of ~0.7‰ during LDE main peak for planktic surface dwellers, whereas subsurface ones decrease by ~0.9‰ and benthics by ~0.6‰. For surface dwelling taxa $\delta^{18}O$ decreases by ~0.6‰, at a subsurface position by ~0.5‰ and on the sea-floor by 0.4‰, which is interpreted as temperature changes of 2.5°, 2° and 1.5°C, respectively. Benthic foraminifera (Westerhold et al., 2011) of neighbouring Site 1209 show similar magnitudes as observed at Site 1210.

Our isotope data, especially $\delta^{13}C$, suggest a stronger

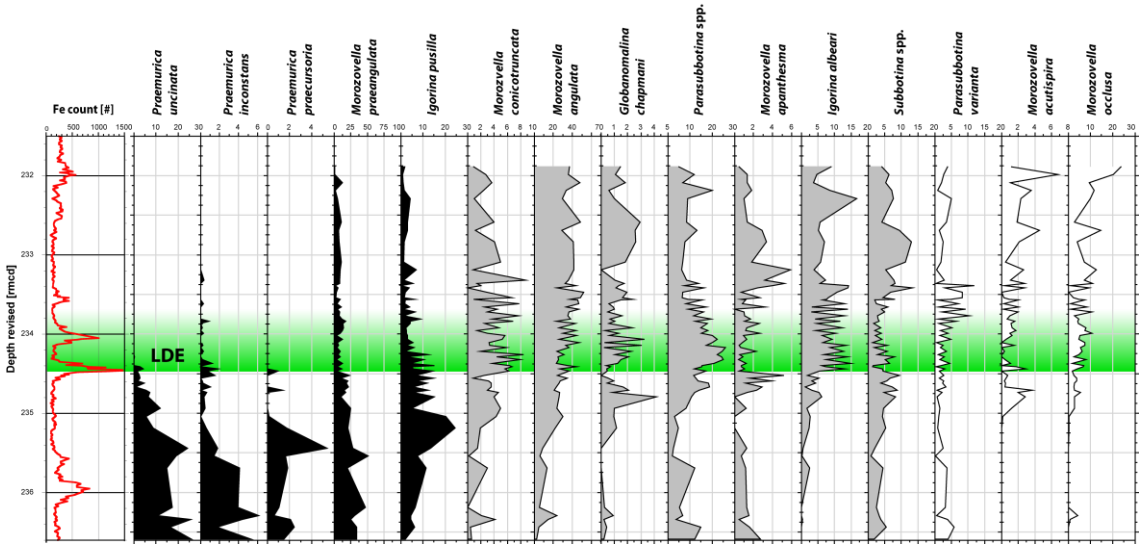

Fig. 2. Fe XRF core scanning data for chemostratigraphy and species abundance data (percentages). Species are sorted by the stratigraphic order of their abundance maxima. The LDE is marked by a grey bar.

gradient between surface and subsurface dwellers after the event, indicating a better stratified upper water column during and after the LDE. The difference in the offset between before and after the LDE is 0.5‰ for $\delta^{13}C$ and 0.4‰ for $\delta^{18}O$. Therefore a shallow thermocline during this time is assumed which is fostering the life-style of non-photosymbiotic species. This idea is further supported by changes in the planktic assemblage: these changes in the isotope gradients go along with relative abundance changes of subsurface dwelling Parasubbotina indicating that this taxon benefits from a thermocline shallowing.

Simple diversity varies between 13 and 23 species per sample, Shannon diversity H' ranges from 1.64–2.47 with a mean of 2.08. The lowest diversity is found at the beginning of the second peak. Planktic foraminiferal faunas are dominated by nine taxa that make up ~86% of the total assemblage (Fig. 2). *Morozovella angulata*, being the most abundant species, is constantly rising from 2 to 40% over the study interval with peaks of 52% and a strong increase during the LDE. *M. praeangulata* decreases from 35 to 10% in pre-event time and shows a massive break-down at the beginning of the event. The LDE might have affected these two opposite appearances in enforcing evolutionary or morphological trends or adaptation capability of the two species to environmental changes. *Praemurica uncinata* was a common component of planktic foraminifera faunas (c. 26%) before the LDE, but virtually disappears with the first LDE horizon, similar to *P. inconstans* and *P. praecursoria*, which suggests that this taxon is strongly affected by LDE-related environmental stress. The disappearance of this group at this level has previously been documented in shelf successions from Tunisia (Guasti et al., 2005). Abundance of *Parasubbotina spp*. shows a belly-shaped event-phase tipping 26% with 5–10% before and after the LDE. Highest values were found between the two LDE horizons which makes them important profiteers of LDE-linked oceanic changes. *Igorina albeari* is the base marker species for the subzone P3b and occurs throughout the entire study interval, which implies that the base of P3b is well below the LDE at Shatsky Rise or the species has no temporally consistant global appaerance. The surface mixed-layer water inhabitant *I. albeari* starts with 0.2–6%, to rise with the onset of the LDE to 14.8%. *I. pusilla* mainly peaks at 24.5% during pre-event phase to decrease with the onset of the LDE. Having strong oscillations like *I. albeari*, values rapidly go down from 15 to around 2% and disappears only shortly later.

In conclusion, the high-resolution quantitative analysis of planktic foraminiferal assemblages and foraminiferal $\delta^{13}C$ and $\delta^{18}O$ provide new insights into paleoceanographic conditions and planktic foraminiferal responses during the Latest Danian Event at Shatsky Rise. The entire water column has been warmed by ~1.5 to 2.5°C during the LDE, supporting the idea that this event represents a Paleocene warming, albeit temperature variability is generally of a similar magnitude throughout the latest Danian. However, this is the only warming phase in this interval that is accompanied by a negative CIE of 0.7‰. The isotope gradient between surface and subsurface dwellers point to an enhanced stratification of the upper water column towards the LDE, strongly enhanced during it and followed by a weakening thereafter, mainly driven by subsurface dwelling non-photosymbiotic *Parasubbotina spp*. We observed major changes in the faunal assemblages specifically in photosymbiont-bearing taxa like the disappearance of *Praemurica* during the first LDE horizon and the gradual evolution of new *Morozovella* taxa. Multivariate statistics (NMDS) indicate rather distinct faunal communities before, during and after the event suggesting a significant control of the subsurface dwelling isotope changes and its paleoenvironmental cause on the faunal community.

References:

Bornemann, A., Schulte, P., Sprong, J., Steurbaut, E., Youssef, M., Speijer, R.P., 2009. Latest Danian carbon isotope anomaly and associated environmental change in the southern Tethys (Nile Basin, Egypt). J. Geol. Soc. 166, 1135-1142.

Dinares-Turell, J., Pujalte, V., Stoykova, K., Baceta, J.I., Ivanov, M., 2012. The Palaeocene "top chron C27n" transient greenhouse episode: evidence from marine pelagic Atlantic and peri-Tethyan sections. Terra Nova 24, 477-486.

Dinarès-Turell, J., Stoykova, K., Baceta, J.I., Ivanov, M., Pujalte, V., 2010. High-resolution intra- and interbasinal correlation of the Danian-Selandian transition (Early Paleocene): The Bjala section (Bulgaria) and the Selandian GSSP at Zumaia (Spain). Palaeogeogr. Palaeoclimatol. Palaeoecol. 297, 511-533.

Guasti, E., Kouwenhoven, T.J., Brinkhuis, H., Speijer, R.P., 2005. Paleocene sea-level and productivity changes at the southern Tethyan margin (El Kef, Tunisia). Marine Micropaleontol. 55, 1-17.

Petrizzo, M.R., 2005. An early late Paleocene event on Shatsky Rise, northwest Pacific Ocean (ODP Leg 198): Evidence from planktonic foraminiferal assemblages. Proc. Ocean Drill. Program Sci. Res. 198, doi:10.2973/odp.proc.sr.2198.2102.2005.

Sager, W.W., 2005. What built Shatsky Rise, a mantle plume or ridge tectonics? Geol. Soc. Am. Spec. Pap. 388, 721-733.

Westerhold, T., Röhl, U., Donner, B., McCarren, H.K., Zachos, J.C., 2011. A complete high-resolution Paleocene benthic stable isotope record for the central Pacific (ODP Site 1209). Paleoceanography 26, doi:10.1029/2010PA002092.

Westerhold, T., Röhl, U., Raffi, I., Fornaciari, E., Monechi, S., Reale, V., Bowles, J., Evans, H.F., 2008. Astronomical calibration of the Paleocene time. Palaeogeogr. Palaeoclimatol. Palaeoecol. 257, 377-403.

IODP

Degradation of complex organic matter by methanogenic microbial communities in deep subsurface systems

N. JIMÉNEZ, M. KRÜGER

Bundesanstalt für Geowissenschaften und Rohstoffe - BGR. Geomikrobiologie. Stilleweg 2, 30655 Hannover

Organic matter constitutes the main source of energy for microbial communities in subsurface environments, which contain on the order of 10^{22} g carbon [1]. This includes carbohydrates, hydrocarbons, nitrogen-containing compounds, lipids and other complex, non-characterized and relatively recalcitrant organic matter. After sulfate-reduction, methanogenesis is the second most important organic matter degradation pathway, particularly relevant in the deep subsurface.Although the degradation kynetics are very slow, it is estimated that about 10% of the global organic matter is converted to methane by methanogens [2]. In marine environments around 80% of the methane is biogenic [3]. So methanogenic deep subsurface microbial communities have a great influence on global cycling of carbon and nutrients, affecting the composition of the atmosphere and thus impacting the planetary climate.

Despite the huge relevance of these microbial communities, the fundamental processes driving complex organic substrates turnover in deep subsurface environments and the identity and physiology of the microorganisms involved are still poorly understood. It is

known that the complete transformation of complex organic matter to methane requires syntrophic associations between a first group of fermentative microorganisms, generally Bacteria, and the methanogenic Archaea. Fermenters transform complex substrates into smaller substances (such as short-chain fatty acids, alcohols, amines, H_2) that can be further used by methanogenic microbiota.

In the light of this, our study will focus on the microbial networks carrying out the complete mineralization of complex organic matter in deep subsurface environments. As most of the microbiota inhabiting those environments lack cultivated relatives, our first specific objective is to cultivate a variety of deep subsurface microbial community samples to carry out subsequent studies that will allow us to: assess the use (extent and rate) of different complex substrates by distinct deep subsurface microbial communities and determine the influence of factors such as the temperature, organic load and pressure on the transformation processes; to identify the key microbial players on the initial hydrolisis and the subsequent transformation steps of the organic matter, ending in methane production; to identify metabolites that will help to reconstruct biodegradation pathways.

For this purpose, sediment samples from various deep subsurface marine (IODP 337, 347) and terrestrial environments with different temperatures and different organic loads are incubated with a variety of complex substrates (hydrocarbons, lipids, polymers, algaeal and microbial cell fragments), including ^{13}C-labelled compounds for SIP analysis. Incubations are carried out in the dark at *in situ* temperatures and high *in situ* or atmospheric pressures. Head space samples are regularly taken to assess methane and CO_2 production. Subsequent DNA, RNA and protein-SIP analysis will provide insight on the key microbial players. Supernatant metabolite analysis will be carried out by LC-ESI-QTOF.

References:
1. Hedges, J.I. and R.G. Keil, Sedimentary organic matter preservation: an assessment and speculative synthesis. Marine Chemistry, 1995. 49(2-3): p. 81-115.
2. Claypool, G.E., Methane and other hydrocarbon gasses in marine sediments. Ann. Rev. Earth Planet. Sci., 1983. 11: p. 299-327.
3. Kvenvolden, K.A. and B.W. Rogers, Gaia's breath - global methane exhalations. Marine and Petroleum Geology, 2005. 22(4): p. 579-590.

ICDP

Microbial abundance in lacustrine sediments, a case study from Lake Van, Turkey

JENS KALLMEYER[1*], SINA GREWE[2], CLEMENS GLOMBITZA[3], J. AXEL KITTE[1]

1 GFZ German Research Centre for Geosciences, Telegrafenberg, 14473 Potsdam, Germany
2 University of Potsdam, Earth and Environmental Sciences, Karl-Liebknecht Straße, 14476 Potsdam, Germany
3 Center for Geomicrobiology, Aarhus University, Ny Munkegade 114, 8000 Aarhus C, Denmark

The ICDP "PaleoVan" drilling campaign at Lake Van, Turkey provided a long (>100 m) record of lacustrine subsurface sedimentary microbial cell abundance. After the ICDP campaign at Potrok Aike, Argentina, this is only the second record ever produced.

During the PaleoVan drilling campaign, two sites were cored and quantification of microbial abundance revealed that the two sites have a strikingly similar cell distribution despite differences in organic matter content and microbial activity. Although shifted towards higher values, cell counts from Lake Potrok Aike, Argentina reveal very similar distribution patterns.

Although the records from Lake Van and Potrok Aike show rather similar cell distributions, they are significantly different to published marine records. Apparently the mechanisms that control microbial distribution in lacustrine sediment are different from those in the marine realm.

Long parts of Lake Van drill cores are finely laminated. On samples from the Ahlat Ridge site at Lake Van, we sampled individual millimetre to sub-millimetre sized microlayers for a detailed look at microbial distribution on the microscale. The results indicate that there are in fact large differences in microbial abundance between the different microlayers, a feature that is normally overlooked due to much larger sampling intervals that integrate over several centimetres. This is the first study that looked at microbial stimulation at interfaces on the microscale.

IODP

The magmatic and geochemical evolution of oceanic intraplate volcanoes: constraints from the Louisville Seamounts and other Pacific hotspots

F. KEMNER, C. BEIER, K. HAASE

GeoZentrum Nordbayern, Universität Erlangen-Nürnberg, Schlossgarten 5, D-91054 Erlangen, Germany

The formation of long-lived seamount trails by hotspots or mantle plumes has been questioned and alternative hypotheses mostly involving plate tectonics have been proposed in several settings that had previously been associated with the presence of a mantle hotspot. Most oceanic intraplate volcanoes show changes of magma compositions with time where major elements and trace element concentrations and radiogenic isotope ratios change considerably over time scales of 1-2 Myr. The geochemical evolution of volcanism along the Hawaiian-Emperor Chain is relatively well known from analysis of drilled and dredged sample material. In the case of Hawaii four stages of volcano evolution have been defined, namely a preshield stage, shield stage, postshield stage and a rejuvenated stage. According to the plate tectonic and deep mantle plume model these stages are believed to reflect variations of partial melting and plume-asthenosphere/lithosphere mixing depending on the relative situation of the plume centre to the overriding lithosphere.

According to the plate tectonic and plume models all oceanic intraplate volcanoes formed above a mantle plume should follow these patterns but only few volcanoes have been studied systematically with respect to their magmatic evolution. Here we present a compilation of published data from several Pacific volcanic chains in order to compare the evolutionary paths.

In the Pacific the two longest lived trails are the Hawaiian-Emperor and Louisville Seamount Trails that both represent >70 Ma of volcanic history. Only little is

known about the Louisville Seamount Trail as it is less well sampled and characterized than the Hawaiian-Emperor Chain. We use fresh glasses of five drilled Louisville volcanoes during IODP Leg 330 to determine the melting dynamics and mantle sources both along chain (from Site U1377 to the oldest Site U1372) and within a single seamount using major elements, trace elements and radiogenic isotopes of about 200 glass samples. Additionally, we compare the data on shield and postshield lavas of relatively well-studied volcanoes from the Society, Austral, Marquesas, and Samoa volcano chains. First results show that the duration of volcanic activity varies considerably between 1 and 2 Ma but is generally about 1.2 Ma. A few volcanoes show much longer periods of activity but some of these may be due to inaccurate age determinations. Hawaiian and Tahiti volcanoes show distinct trends of decreasing SiO_2 with decreasing age in agreement with a continuous transition from tholeiitic shield to alkaline postshield stage magmas. Lava compositions of the studied volcanoes also vary but there are systematic correlations between SiO_2 contents and rare earth element enrichment reflecting variable degree and depth of melting. For example, the Tahiti lavas show higher $(Ce/Yb)_N$ for a given SiO_2 content compared to the Hawai and Louisville lavas. This variation probably reflects lower degrees of partial melting at Tahiti than beneath the Hawaiian and Louisville volcanoes and it appears not to reflect changes in lithospheric age and thickness but may rather reflect variable temperature of the mantle source.

IODP & ICDP

Amphibious drilling projects maximise benefits from ICDP and IODP initiatives: The example of the Ligurian slope near Nice

A.J. KOPF

MARUM - Center for Marine Environmental Sciences, University of Bremen, P.O. Box 330440, 28334 Bremen, Germany.

Submarine landslides, followed by tsunamis, represent a major geohazard and an exciting research target given the wealth of trigger mechanisms and their dynamic interaction. The Ligurian margin, western Mediterranean, is known for its steep topography with numerous landslide scars, however, the cause of these landslides is incompletely understood. Given the geodynamic situation adjacent to the western Alps (with seismicity ranging up to M>6) and the large discharge of water and sediment through the Var River, the lithological variability (coarse sand and conglomerate interbedded with sensitive clay) and different hydrological regimes (coupled to precipitation and seasonal melt-water discharge), as well as the profound human impact on the coast (e.g. collapsed landfill area and construction site in 1979, followed by a tsunami in the Gulf of Antibes), the French portion of the Riviera is an area where various triggers can be studied in a locally confined region.

The fact that the margin comprises permeable delta deposits that underwent transgression calls for an amphibious approach that addresses both the onshore portion of a charged aquifer as well the area into which the fluids are funneled, thus causing elevated pressure in the shallow submarine slope. We here propose to drill two onshore and four offshore holes at the Ligurian margin (Figure 1) to characterise the strata of the Plio-Quaternary Var aquifer, and the marine metastable slope E and W of the 1979 collapse structure and its redeposited material downslope. The target depth at each site will provide reconnaissance data to portions already sampled (onshore groundwater wells, offshore gravity/piston coring) as well as characterisation of the underlying strata down to the Pliocene puddingstones. Since we propose mission-specific amphibious drilling and borehole instrumentation, drill cores and downhole-logging information will identify mechanically weak vs. strong layers, hydraulically active horizons, and zones of overpressure owing to groundwater-charging or rapid vertical loading in the Var delta deposits. The related hypotheses may be tested by drilling, and will be comprehensively answered by long-term monitoring of the physical parameters affecting slope failure. Borehole observatory installation is effortless given water depths of <50 m and will include multi-parameter instruments.

This first joint ICDP-IODP proposal is designed to unambiguously test multiple-triggers for landslides at the French Riviera by a suite of state-of-the-art methods concerning drilling and time series acquisition. Given that the drill sites are in shallow water, with favourable logistics and good infrastructure at the French Riviera and an EMSO seafloor-cabled node, scuba diving operations to facilitate borehole installations are a feasible way to maximise the success and use the drill holes as a hydrogeophysical monitoring and fluid sampling facility and real-time landslide observatory. Only an amphibious approach can set up an appropriate network of observation points to allow researchers a comprehensive landslide understanding and hazard assessment. Boreholes on land will help characterising the inputs and discharge rates of fluids as

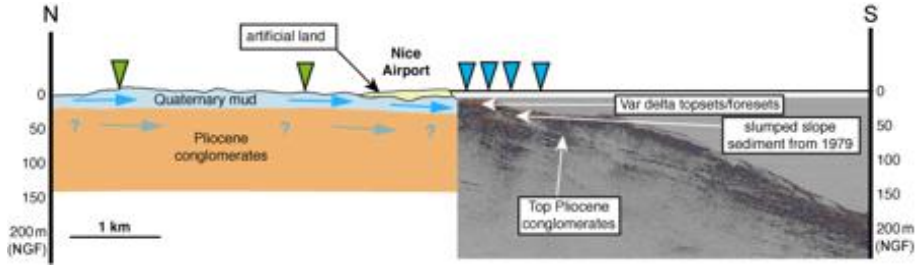

Fig. 1. Composite cross section of the Ligurian amphibious drilling profile, combining geological information onshore with marine seismic profiles. Black vertical lines indicate locations of existing groundwater wells. Triangles represent the (sometimes projected) sites proposed for amphibic scientific drilling (Green = ICDP, blue = IODP). Marine seismic reflection profile with top of Pliocene conglomerates underlying the slumped as well as deltaic sediments composed of permeable Holocene sand interbedded with clay. Blue arrows mark Var river discharge and groundwater flow in Quaternary and Pliocene (?) units.

well as the permeability and strength of the sediment/rock in the aquifer system. Offshore boreholes will then serve to monitor how sediment properties and fluid flow change as a function of the inputs. Although locally restricted, the complexity of the area makes this landslide-prone ocean margin a primary site for time- and cost-efficient amphibious drilling and monitoring at a glacially affected margin in the NEAM (North-East Atlantic / Mediterranean) region.

Acknowledgements:
The team of co-proponents of this joint ICDP-IODP full proposal comprises P. Henry (F), S. Garziglia (F), A. Camerlenghi (I), P. Pezard (F), Y. Yamada (J), A. Solheim (N), S. Stegmann (GER), A. Deschamps (F), G. Unterseh (NL), V. Spiess (GER), J.F. Rolin (F), S. Davies (UK), and C. Mangan (F).

IODP

Reconstructing palaeo-environmental and climatic conditions in the Baltic region: A multi-proxy comparison from IODP Site M0059 (Little Belt)

ULRICH KOTTHOFF[1], THOMAS ANDRÉN[2], THORSTEN BAUERSACHS[3], ANNE-SOPHIE FANGET[4], WOJCIECH GRANOSZEWSKI[5], JEROEN GROENEVELD[6], NADINE QUINTANA KRUPINSKI[7], ODILE PEYRON[8], ANNA STEPANOVA[9], CAROL COTTERILL[10], EXPEDITION 347 SCIENCE PARTY

1 Institute of Geology and Centre of Natural History, University Hamburg, Germany
2 School of Life Sciences, Södertörn University, Sweden
3 Christian-Albrechts-University, Kiel, Germany
4 Department of Geoscience, Aarhus University, Denmark
5 Polish Geological Institute-National Research Institute, Krakow, Poland
6 MARUM, University Bremen, Germany
7 Department of Geology, Lund University, Sweden
8 Laboratoire Chrono-Environnement, Université de Franche-Comté, Besançon, France
9 Oceanography, Texas A&M University, US
10 British Geological Survey, Edinburgh, UK

The ongoing global climate change has a particularly strong impact on ecosystems in continental shelf seas and enclosed basins. Presently, these ecosystems are influenced by oxygen depletion, intensifying stratification, and increasing temperatures. In order to predict future changes in water mass conditions, it is essential to reconstruct how these conditions have changed in the past and which factors drove the respective changes. The brackish Baltic Sea provides a unique opportunity to analyse such changes because it is one of the largest semi-enclosed basins worldwide. The Baltic Sea region is also of particular interest for the reconstruction of past changes in terrestrial ecosystems, since it is adjacent to different vegetation zones, from cool temperate forest with mixed coniferous and deciduous trees in the South to closed boreal forest with taiga-like conditions in the North. Among other goals, IODP expedition 347 to the Baltic Sea aims at the reconstruction of ecosystem, climate, and sea level dynamics and the underlying forcing in different settings in the Baltic Sea region from the Marine Isotope Chrone 5 until today. During Expedition 347, a unique set of long sediment cores from the Baltic Sea Basin was recovered, which allow new high-resolution reconstructions.

The application of existing and development of new proxies in a setting like that of the Baltic Sea is complicated, as environmental changes often occur on very fast time scales with large variations. Therefore, we present a comparison of commonly used proxies to reconstruct palaeoecosystems, -temperatures, and -salinity from IODP Site M0059 in the Little Belt. The age model for Site M0059 is based on ^{14}C dating and biostratigraphic correlation with neighbouring terrestrial pollen records. The aim of our study is to reconstruct the development of the terrestrial and marine ecosystems in the research area and the related environmental conditions, and to identify potential limitations for specific proxies.

Pollen grains are used as proxies for vegetation development in the hinterland of the southern Baltic Sea and as land/air-temperature proxies. By comparison with dinoflagellate cysts and green algae remains from the same samples, a direct land-sea comparison is provided. The application of the modern analogues technique to pollen assemblages has previously yielded precise results for late Pleistocene and Holocene datasets, but pollen-based reconstructions for Northern Europe may be hampered by plant migration effects. Chironomid remains are used where possible as indicators for surface water conditions during the warm season. Analyses of palynomorphs and chironomids are complemented with the analysis of lipid palaeothermometers, such as TEX86 and the long chain diol index (LDI), which both allow reconstructing variation in sea surface temperatures (SST) of the Baltic Sea. In addition, the MBT/CBT proxy is used to infer past changes in mean annual air temperatures and the diol index (DI) to determine variation in salinity of the Baltic Sea's surface waters over the investigated time period.

The low salinity (25 psu) of the Little Belt is a potential limitation for several of the used proxies, which could lead to under-estimation of paleo-temperatures. To estimate the impact of salinity, $\delta^{18}O$ measurements (monospecific) and faunal assemblage analyses are performed on benthic foraminifera as well as ostracod faunal assemblages.

The results of this inter-comparison study will be useful for the reconstruction of gradients between different settings, e.g. how water column stratification developed, possibly if and how changes in seasonality occurred, and to identify the circumstances under which specific proxies may be affected by secondary impacts.

IODP

Understanding slow-slipping submarine landslides: 3D seismic investigations of the Tuaheni landslide complex as support for IODP Ancillary Project Letter 841APL

S. KRASTEL[1], J. MOUNTJOY[2], G. CRUTCHLEY[3], S. KOCH[4], A. DANNOWSKI[4], I. PECHER[5], J. BIALAS[4]

1 Institut für Geowissenschaften, Chrisian-Albrechts-Universät zu Kiel, skrastel@geophysik.uni-kiel.de
2 National Institute of Water and Atmospheric Research (NIWA), Wellington
3 GNS Science, Lower Hutt, New Zealand
4 GEOMAR Helmholtz-Zentrums für Ozeanforschung Kiel
5 School of Environment; The University of Auckland

The dynamics of submarine landslides is only poorly understood. While some landslides rapidly disintegrate others may stay as coherent blocks. Recently, it has been proposed that submarine landslides could also be characterized by very slow (creeping) deformation. The Tuaheni landslide complex off the east coast of New Zealand may acts as key site for investigating such slow-slipping landslides. We collected a 3D-seismic data set covering different parts of the slide complex by means of the so-called P-cable system using the research vessel Tangaroa in April/May 2014. The P-cable system is a cost-efficient, low-fold, high resolution 3D-seismic acquisition system, which can be deployed on relatively small vessels. Main objectives of the proposed project include the development of a model for landslide evolution, the investigation of the methane hydrate system in the working area with special emphasis on its role for landslide dynamics, and the analysis of the deformations style for the Tuaheni landslide complex. Two competing hypotheses have been postulated to explain the deformation style: i) The Hydrate Valve suggest build-up of overpressure at the base of the gas hydrate stability zone beneath a shallow gas hydrate zone, which causes hydro-fracturing and induces small scale episodic mobility. ii) The Hydrate-Sediment Glacier postulates plastic behavior of gas hydrate bearing sediments resulting in continuous downslope creep. Gas hydrates are known to strengthen sediments during short-term deformation but it is unclear whether they may exhibit plastic behavior during slow deformation, similar to ice.

The new data also supports IODP Ancillary Project Letter 841APL (Pecher et al, Creeping Gas Hydrate Slides: Slow Deformation of Submarine Landslides on the Hikurangi Margin). The aim of the APL is the recovery of undisturbed pressure cores for shore-based laboratory analyses and determination of in-situ pressure from logging-while-drilling (LWD) and pressuretemperature penetrometer stations. The proposal is currently in the 'holding bin' as some minor data issues have to be adressed.

ICDP

Zero-Offset VSP in the COSC-1 borehole

F. KRAUß[1], H. SIMON[2], R. GIESE[1], S. BUSKE[2], P. HEDIN[3], C. JUHLIN[3], H. LORENZ[3]

1 Scientific Drilling, GFZ German Research Centre for Geosciences, Helmholtz Centre Potsdam
2 Institute of Geophysics and Geoinformatics, TU Bergakademie Freiberg
3 Dept. of Earth Sciences, Uppsala University

As support for the COSC drilling project (Collisional Orogeny in the Scandinavian Caledonides), an extensive seismic survey took place during September and October 2014 in and around the newly drilled borehole COSC-1. The main aim of the COSC project is to better understand orogenic processes in past and recently active mountain belts (Gee et al. 2010). For this, the Scandinavien Caledonides provide a well preserved example of Paleozoic plate collision. Surface geology and geophysical data provide knowledge about the geometry of the Caledonian structure. The COSC project will investigate the Scandinavian Caledonides with two approximately 2.5 km deep boreholes, located near Åre and Mörsil, in western Jämtland. (http://ssdp.se/projects/COSC). The geometry of the upper crust was imaged by regional seismic and magnetotelluric data and was refined by seismic pre-site surveys in 2010 and 2011 to define the exact position of the first borehole (Hedin et al. 2012).

The approximately 2.5 km deep borehole COSC-1 was drilled close to the town of Åre between April and August 2014. The borehole was drilled with an Atlas Copco CT20, a slim-hole core drilling rig. The core recovery was nearly 100%. The borehole is completely open hole, except from the first 102 m at which a conductor casing with 102 mm inner diameter was installed. The inner diameters of the borehole are 96 mm from 102 m to 1616 m driller's depth and 76 mm from 1616 m driller's depth to the bottom.

The seismic survey consisted of a high resolution zero-offset VSP (vertical seismic profiling) and a multi-azimuthal walkaway VSP experiment with receivers at the surface and in the borehole. For the zero-offset VSP (ZVSP) a hydraulic hammer source (VIBSIST 3000) was used and activated over a period of 20 seconds as a sequence of impacts with increasing hit frequency, the so-called 'swept impact seismic technique' (SIST, Park et al. 1996). For each source point, 25 seconds of data were recorded. The wavefield was recorded in the borehole by 15 three-component receivers using a Sercel Slimwave geophone chain with an inter-tool spacing of 10 meters. The ZVSP was designed to result in a geophone spacing of 2 meters over the whole borehole length. The source was about 30 meters away from the borehole and thus, provides a poor geometry to rotate 3C-data in greater depths. For this reason, a check shot position was defined in about 1.9 km distance to the borehole. With this offset shots, it is possible to rotate the components of the 3C-receivers and to concentrate the P- and S-wave energy each on one component and thus, increase the signal-to-noise ratio of P- and S-wave events. This offset source point was activated periodically for certain depth positions of the geophone chain.

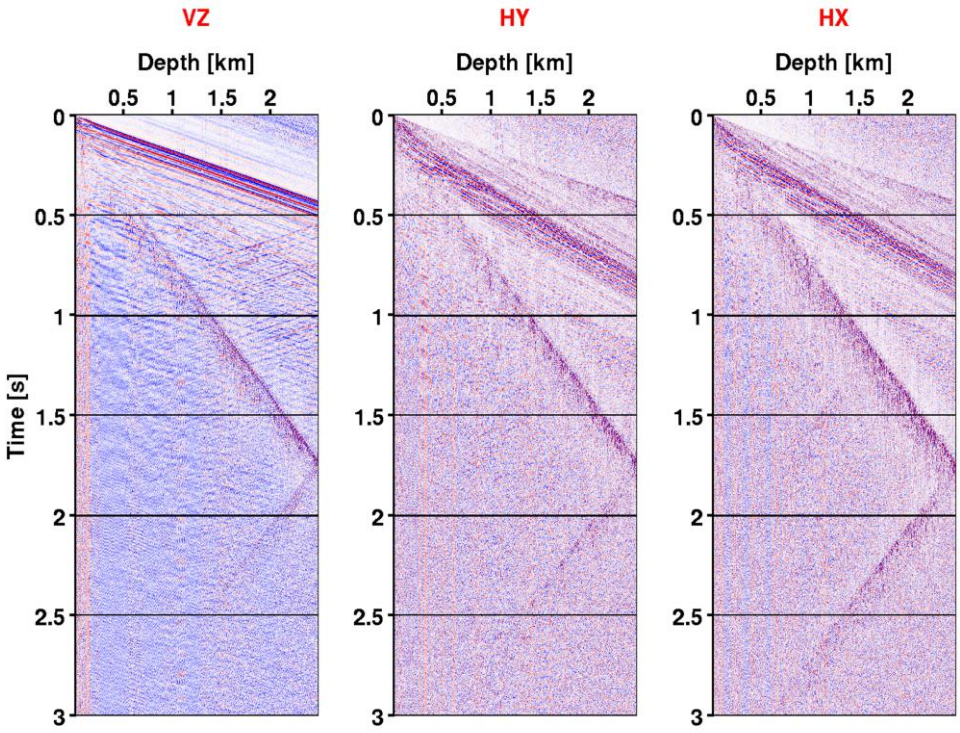

Fig. 1. Unrotated ZVSP-data sorted by component (automatic gain control applied). From left to right: vertical and the two horizontal components of the recorded wavefield.

As a first pre-processing step, the data from the hammer source were decoded, using a shift-and stack algorithm (Park et al. 1996), and the repetitive shots were stacked together. Afterwards, the shots were merged to get two continuous shotgathers, containing the ZVSP-data and the check-shot data (CS-data), respectively.

The merged ZVSP-data show a high signal-to-noise ratio and good data quality (Fig. 1). Signal frequencies up to 150 Hz were recorded. On the vertical component, clear direct P-wave arrivals are visible. Several P-wave

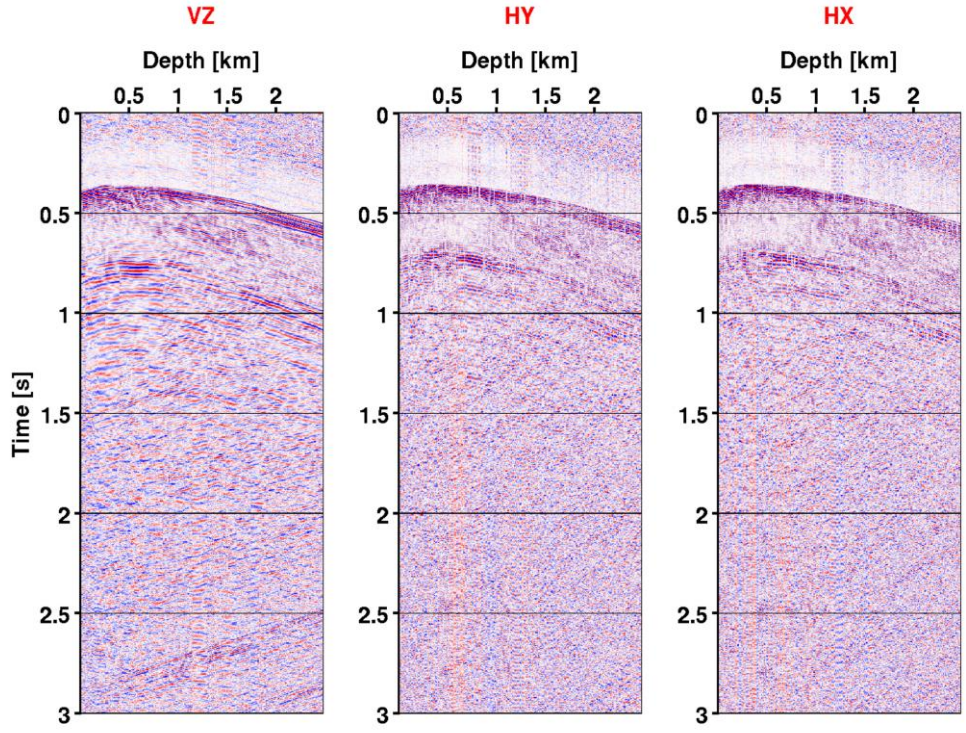

Fig. 2. Unrotated CS-data sorted by component (automatic gain control applied). From left to right: vertical and the two horizontal components of the recorded wavefield.

reflections occur below 1600 meters logging depth. On both horizontal components, clear direct S-wave arrivals are visible. Additionally, two downgoing PS-converted waves can be identified.

The merged CS-data show a clear P-wave arrival in all three components (Fig. 2). On the vertical component the deflection point of the P-wave is observable at about 370 m logging depth. At this point the P-wave arrives perpendicular to the vertical component and thus, the P-wave amplitude decreases. The phase of the direct P-wave on the vertical geophone component is switched at the deflection point.

In a next step, the CS-data will be used to rotate the ZVSP-data to concentrate P- and S-wave arrivals on one component, each. A signal deconvolution will be applied to sharpen the signal shape and to suppress multiple arrivals. Furthermore, the wavefield will be separated in upgoing and downgoing wavefield by f-k-filtering. P- and S-wave velocities as well as reflection events will be compared to available information from logging and geological interpretation of the drilled cores.

The ZVSP-data will be used as reference for depth correlation of the surface seismic data and will provide a 1D velocity profile for both P- and S-wave, respectively.

References:
Gee, D.G. et al. (2010). Collisional Orogeny in the Scandinavian Caledonides (COSC). GFF, 132(1), 29-44.
Hedin, P., Juhlin, C. & Gee, D.G., 2012. Seismic imaging of the Scandinavian Caledonides to define ICDP drilling sites. Tectonophysics, 554-557(0), 30–41.
Park C.B. et al. (1996). Swept impact seismic technique (SIST), Geophysics, 61(6), 1789-1803.

ICDP

Approaching Q factor tomography of Western Bohemia using a master and slave event method

M. KRIEGEROWSKI[1], S. CESCA[1,2]

1 University of Potsdam, Institute for Earth and Environmental Sciences; E-mail: kriegero@uni-potsdam.de
2 Helmholtz Centre Potsdam, GFZ German Research Centre for Geosciences, Department 2.1, D-14473 Potsdam, Germany; E-mail: simone@gfz-potsdam.de

Western Bohemia shows frequent earthquake swarm activity which culminated in magnitudes of up to Mw 4.6 in recent years. Isotope analysis of gas exhalations showed that the seismic activity can hypothetically be related to migrating magmatic fluids [Bräuer et al., 2005]. A compact and potentially impermeable body at the top a the seismogenic zone is assumed to act as a fluid seal blocking uprising fluids. A major hypothesis which can be drawn from this is that fluids gather beneath the compact body leading to increasing pore pressure. This can eventually cause fracturing of the focal zone beneath [Alexandrakis et al., 2014].

However, the origin of the seismic swarms remains a point of discussion. Given that the seismic swarm cycle is triggered by fluid migration, attenuation provides a key information helping to answer the question regarding the origin. Fluids strongly influence the acoustic attenuation properties of the contaminated rock. Hence, an area of high fluid content and high brittleness is likely to be identifiable by means of attenuation tomography. This effect is targeted by the developed method.

Attenuation properties of Western Bohemia are, in comparison to wave propagation velocity anaylsis, rarely discussed or quantified. We address the problem of Q factor estimation based on t* analysis of event couples comparable to the double difference algorithm by [Waldhauser et al. 2000]. Given that the distance between two events is small compared to the distance between events and the recording station, the ray paths between events and station are nearly identical. This, in turn implies that differences in both event's waveform result from the inter-event rock properties, as e.g. the attenuation.

In order to test this newly developed technique Western Bohemia provides us with a favorable testing environment. This is due to a comparably good station coverage and long term recordings. Furthermore, the great number of preceding investigations concerning seismicity of Western Bohemia have contributed to great general knowledge of that area.

Synthetic tests based on 1 dimensional velocity and Qp and Qs factor models show the applicability of the developed method for local to regional epicentral distances. These tests involve the calculation of synthetic seismograms based on realistic moment tensor components. In order to reduce the effect of the source term in the Q factor anaylsis we focus on events with similar focal mechanisms. A semi-automated moment tensor inversion routine is set up to identify moment tensors of recent earthquake swarms on a large scale using data from the West Bohemia seismic monitoring network (WEBNET).

References
Bräuer et al., 2005: Evidence for ascending upper mantle-derived melt beneath the Cheb basin, central Europe, 2005
Alexandrakis et al., 2014: , Velocity structure and the role of fluids in theWest Bohemia Seismic Zone, 2014
Waldhauser et al. [2000]: , A Double-Difference Earthquake Location Algorithm: Method and Application to the Northern Hayward Fault, California, 2000

ICDP

Sedimentology of the Middle Buntsandstein in the INFLUINS Scientific Deep Drilling in the Thuringian Syncline: Implications for Aquifer Characteristics

C. KUNKEL, M. AEHNELT, R. GAUPP, M. ABRATIS, N. KUKOWSKI, K.U. TOTSCHE AND THE INFLUINS SCIENTIFIC DRILLING TEAM

Friedrich Schiller Universität Jena, Institut für Geowissenschaften, Burgweg 11, 07749 Jena
Cindy.Kunkel@uni-jena.de

In the framework of the joint project "Integrated Fluid Dynamics in Sedimentary Basins" (INFLUINS) a scientific deep drilling was carried out from June to September 2013. The drill site is located in the center of the Thuringian Syncline in the north of Erfurt. To the present, subsurface data in the syncline center close to Erfurt is sparse, as there was no drilling or rock material was barely sampled and/or archived. Major goals of deep drilling were to gather substantial knowledge of subsurface fluid dynamics and fluid rock interaction in the permo-triassic sedimentary succession. The main focus of the INFLUINS scientific drilling campaign was on coring potential aquifers and their surrounding aquitards, i.e. parts of the Upper Muschelkalk (Trochitenkalk), the Middle Muschelkalk, the Upper Buntsandstein (Pelitrot and Salinarrot) and the Middle Buntsandstein.

In this study, we focus on the Middle Buntsandstein, which is a major aquifer in Thuringia and adjacent areas. The cored material comprises 219 m of excellently preserved sandstones and mudstones with 100 % core recovery. Surprisingly, drilling discovered very poor hydraulic parameters and connectivity at this site which was also substantiated by geophysical borehole measurements and macroscopically very compact appearance of the rocks. To understand the controlling mechanisms of the Buntsandstein aquifer system a facies and diagenesis study was carried out including permeability measurements on 50 plug samples from the core material.

Four depositional environments (fluvial, sandflat, lacustrine, aeolian) could be distinguished and studied from the macroscopic to the microscopic scale. First results show a high dependence of hydraulic parameters not only on different facies and depositional environments, but also on compaction and cementation during burial history. Good hydraulic connectivity, which controls fluid dynamics, is due to an interaction of sedimentary facies, their spatial allocation, the diagenetic development and secondary dissolution processes as well as vertical connectivity via faults, fractures and fissures.

IODP

Earthquake nucleation in calcareous sediments from offshore Costa Rica triggered by a combined temperature and pore fluid pressure increase, Costa Rica Seismogenesis Project (CRISP)

R.M. KURZAWSKI[1], M. STIPP[1], A. NIEMEIJER[2], C.J. SPIERS[2] , J.H. BEHRMANN[1]

1 Department of Marine Geodynamics, GEOMAR Helmholtz Centre for Ocean Research Kiel, Kiel, Germany, (rkurzawski@geomar.de)
2 HPT Laboratory, Faculty of Geosciences, Utrecht University, Utrecht, The Netherlands

Mechanical properties of subducted sediments strongly influence the nucleation and propagation of seismic rupture on subduction zone megathrust faults. The Costa Rica Seismogenesis Project (CRISP) is the first drilling program established to investigate the genesis of megathrust earthquakes and related tsunamis at an erosive active continental margin. Subduction erosion, i.e. the basal tectonic removal of overriding plate material, occurs along the entire Middle America Trench (MAT), where the oceanic Cocos plate is subducted beneath the continental Caribbean plate. At Costa Rica increased tectonic erosion along the MAT is caused by subduction of the Cocos Ridge. This extensive topographic high originates from Galapagos hotspot volcanism and is oriented approximately perpendicular to the trench. Cocos Ridge subduction induces a steepening of the geothermal gradient and results in a shift in seismicity towards shallower levels. The localization of the décollement within frictionally unstable material is a crucial prerequisite for the nucleation of a megathrust earthquake. Calcareous sediment has recently been recognized to potentially become frictionally unstable. At the same time, however, such material is found to exhibit markedly high shear strength. Experimentally determined friction coefficients at low sliding velocities are around $\mu \approx 0.8$, thereby favouring the localization of slip within much weaker and predominantly velocity-strengthening clayey sediments.

Here we report on friction experiments performed on fault gouges prepared from incoming plate sediments. Four samples from the CRISP drilling site U1414 with variable calcite contents were experimentally deformed in a rotary shear apparatus (Niemeijer et al., 2008) under hydrothermal conditions. Experimental parameters were defined according to the expected conditions at the updip limit of seismogenesis in approximately 5-6 km depth. In each experiment temperature was held constant at room temperature, 70 °C or 140 °C together with a fixed pore fluid pressure of 20 MPa, 60 MPa or 120 MPa. Effective normal stress was stepped from 30 MPa to 90 MPa in increments of 20 MPa. At each effective normal stress step, a velocity-stepping sequence was performed following the scheme 10-1-3-10-30-100 µm/s. The velocity dependence of friction was explored at several temperature and effective normal stress combinations to cover a wide range of natural conditions and, particularly, to simulate an increasing geothermal gradient towards the Cocos Ridge. Additionally, effects of pore fluid pressure variations were tested.

Our results indicate important differences in the frictional behaviour of different sediments. Low-calcite hemipelagic sediments show velocity weakening, i.e. potentially unstable behaviour at low effective normal stresses of 30-50 MPa and low sliding velocities of 1-10 μm/s independently of given temperatures. Domains of such low effective normal stress are typical of shallow levels of subduction near the updip limit of seismogenesis, but can also occur in greater depths at near-lithostatic pore fluid pressures. In contrast, calcareous ooze with high calcite contents (> 80 vol.-%) shows a dramatic change in frictional behaviour as a function of temperature. This material is frictionally strong at room temperature with no significant dependency on effective normal stress or sliding velocity. At 140 °C, however, it exhibits unstable slip, i.e. "stick-slip" events. Moreover, our experiments reveal a dramatic weakening effect linked to increasing pore fluid pressures: At P_f = 60 MPa, i.e. the hydrostatic pore pressure in 6 km depth, internal friction drops to $\mu_{int} \approx 0.6$ ($0.54 < \mu_{int} < 0.58$). At the highest tested pore pressures of P_f = 120 MPa calcareous ooze becomes even weaker than hemipelagic clayey sediment, indicated by an internal friction coefficient of as low as μ_{int} = 0.27.

Based on our experiments nucleation of shallow earthquakes at the updip limit of the seismogenic zone can be explained by frictional properties of subducted sediments. The shear strength of calcareous sediments eventually falls below that of clayey sediments, potentially allowing for slip localization. Frictional instability, however, is triggered by increasing temperatures, in our experiments between 70 and 140 °C in line with previous findings. Such temperatures are usually reached at the average updip limit of seismogenesis, but can also occur on the shallowmost portion of megathrust fault planes if the local thermal gradient is sufficiently high. We propose that the combined effects of thermally induced frictional instability and fluid pressure related weakening of highly calcareous sediments might be a fundamental mechanism of earthquake nucleation on subduction zone megathrust faults.

References:

Niemeijer, A.R., Spiers, C.J. and Peach, C.J. (2008). Tectonophysics, 460, 288-303.

ICDP

Paleoclimate, Paleoenvironment, and Paleoecology of Neogene Central America: Bridging Continents and Oceans (NICA-BRIDGE)

S. KUTTEROLF[1], M. BRENNER[2], A. FREUNDT[1], S. KRASTEL[3], A. MEYER[4], A. MUÑOZ[5], L. PÉREZ[6], A. SCHWALB[7]

1 GEOMAR Helmholtz Center for Ocean Research Kiel, Germany
2 Department of Geo-logical Sciences and Land Use and Environmental Change Institute (LUECI), University Florida, USA
3 Institute of Geosciences, Christian-Albrechts-Universität zu Kiel, Germany
4 Directora general de Geofísica, INETER, Managua, Nicaragua
5 Institute of Zoology and Evolutionary Biology, University of Konstanz, Germany
6 Instituto de Geología, Universidad Nacional Autónoma de México (UNAM), Mexico
7 Institute for Geosys-tems und Bioindication (IGeo), Technische Universität Braunschweig, Germany

We seek support for a workshop to develop a scientific drilling project focused on Lakes Nicaragua and Managua, in Nicaragua. Several factors make the Nicaraguan lakes uniquely suited for scientific investigation with globally important objectives: 1) their long history of basin (lake) development, 2) their interactions with marine environments in the past, 3) their proximity to the volcanic arc, 4) their significance as an endemic hot spot, 5) their strategic location for the study of an important paleozoogeographic event, the great American biotic interchange, 6) the recently initiated canal construction, connecting the Pacific Ocean and the Caribbean Sea via Lake Nicaragua, and 7) the ability to combine seismology, volcanology, paleoclimate, paleoecology, and paleoenvironment in one project. Connection and relation to the marine Sandino Basin in the fore arc of Nicaragua may facilitate a second project phase regarding a complementary IODP proposal.

We will address important global scientific hypotheses under the general themes of Paleoclimate, Paleoenvironment, and Paleoecology that will include investigation into the region's geology (volcanology, geophys-ics (earthquakes) and tectonics) and biology. Additionally, the prerequisite seismic imaging survey will yield valuable information about the deeper structure of western Nicaragua, which is also highly relevant to the proposed Pacific-Caribbean canal construction. All data obtained will be accessible to local authorities, who will be able to better assess possible hazards and risks.

We will collect long continuous sediment profiles from multiple sites in Lakes Managua and Nicaragua to provide a unique archive of past subtropical climate and environmental changes extending over several millions of years. The lake sediment records are key to understanding past climatological and ecological variability, earthquake and volcanic eruption magnitudes and frequencies, the processes leading up to these natural hazards, and their socio-economic impacts. Understanding long-term paleoclimate variability will help to predict future climate scenarios and thus guide future agricultural strategies in Nicaragua and other tropical regions. In contrast to paleoclimate data from the marine environment the lacustrine high-resolution sediment data will also allow us to directly connect past climate shifts to terrestrial paleoenvironmental and paleoecological changes. We will also use these records to infer the frequency and amplitude of past natural hazards (volcanic eruptions, earthquakes, large landslides, hurricanes) and evaluate changes in the environment that stemmed from these natural causes (including climate changes and tectonic movements), as well as human influences (agriculture, pollution). The seismic imaging survey will not only provide the data necessary to select drill sites, but will also yield information about basin development. In the past, tectonic processes caused repeated flooding with seawater, which undoubtedly influenced the lake biota. These fresh/saltwater phases will yield insights into what may occur during and after construction of the new Nicaragua canal that will connect the Pacific Ocean and the Caribbean Sea through Lake Nicaragua.

The proposed drilling project in the large lakes of Nicaragua will have broad scientific and socio-economic impacts. It will benefit the Nicaraguan and broader science communities and will enhance the reputation of Nicaragua on many levels. In addition it will lead to world-wide recognition of Nicaragua's natural resources, will open new opportunities for project-related short courses and outreach programs, and will establish exchange programs between institutions in Nicaragua and those in other participating countries.

We assembled an international team to organize the workshop on drilling the Nicaraguan lakes, including PIs from Germany (Kutterolf, Schwalb, Freundt, Krastel, Meyer), Nicaragua (Muñoz), the USA (Brenner) and Mexico (Pérez). We will extend workshop invitations to scientists from other nations, especially in Latin America, the USA, Europe (Switzerland, Great Britain, France), China, and Japan, to broaden the scope of expertise represented. Our plan is to foster collaborative interactions during the workshop and to refine scientific hypotheses to be tested by future drilling and scientific investigations of the Nicaragua lakes.

Drilling of the Nicaragua lakes, under the broad umbrella of Paleoclimate, Paleoenvironment, and Paleoecology will involve two major societal challenges the ICDP initiative wants to address: Climate & Ecosystems and Natural Hazards.

IODP

Plio-Pleistocene paleoceanography of the Subantarctic Southeast Pacific linked to Drake Passage throughflow (SUBANTPAC)

FRANK LAMY[1], ANDREA ABELMANN[1], ROBERT ANDERSON[2], HELGE ARZ[3], GIUSEPPE CORTESE[4], OLIVER ESPER[1], MARTIN FRANK[5], KARSTEN GOHL[1], IAN HALL[6], NAOMI HARADA[7], DIERK HEBBELN[8], ROLF KILIAN[9], GERHARD KUHN[1], CARINA LANGE[10], LESTER LEMBKE-JENE[1], ANDREAS MACKENSEN[1], ALFREDO MARTINEZ-GARCIA[11], ULYSSES NINNEMANN[12], DIRK NÜRNBERG[5], KATHARINA PAHNKE[13], ALINA POLONIA[14], JOSEPH STONER[15], RALF TIEDEMANN[1], GABRIELE UENZELMANN-NEBEN[1], GISELA WINCKLER[2]

1 Alfred-Wegener-Institut Helmholtz-Zentrum für Polar- und Meeresforschung, Bremerhaven, Germany
2 Lamont-Doherty Earth Observatory, Columbia University, Palisades, NY, USA
3 Leibniz Institute for Baltic Sea Research, Rostock-Warnemünde, Germany
4 GNS Science, Lower Hutt, New Zealand
5 GEOMAR Helmholtz-Zentrum für Ozeanforschung, Kiel, Germany
6 School of Earth and Ocean Sciences, Cardiff University, Cardiff, CF10 3AT, UK
7 Japan Agency for Marine-Earth Science and Technology, Yokosuka 237-0061, Japan
8 MARUM – Center for Marine Environmental Sciences, Bremen, Germany
9 Universität Trier, Trier, Germany
10 Department of Oceanography and Center for Oceanographic Research in the eastern South Pacific (COPAS), University of Concepción, Concepción, Chile
11 Geologisches Institut, ETH Zürich, Zürich, Switzerland
12 University of Bergen, Norway
13 Institute for Chemistry and Biology of the Marine Environment (ICBM), University of Oldenburg, Germany
14 ISMAR/CNR - Institute of Marine Sciences, Bologna, Italy
15 Oregon State University, Corvallis, USA.

The Subantarctic Southeast Pacific (SEP) is a particularly sensitive region where atmosphere-ocean changes between high-, mid- and low latitudes are strongly coupled. The SEP provides a unique opportunity to obtain exceptionally highly-resolved sediment records to document millennial and orbital-scale Plio/Pleistocene changes and their implications for global climate. Within our pre-proposal SUBANTPAC, we propose two drilling areas: the central Subantarctic Pacific at the western and eastern flanks of the East Pacific Rise (primary sites SEP-1A and SEP-2A, and alternate site SEP-3A), and the eastern Subantarctic Pacific on the Chilean Margin at the entrance to the Drake Passage (primary sites CHI-1A and CHI-4A, and alternate sites CHI-2A and CHI-3A). Both areas have high sedimentation-rates that allow resolving orbital and millennial-scale variations throughout the Pleistocene and at least parts of the Pliocene.

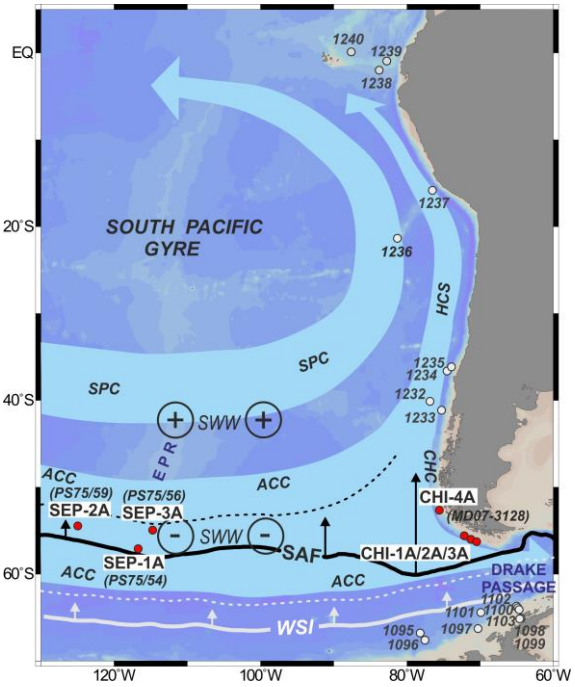

Fig. 1. Map showing the location of the proposed drilling sites (CHI and SEP primary and alternate sites; red dots) and of previously collected cores during various expeditions in the eastern Pacific referred to in text (white dots; ODP Leg 202 Sites 1232–1240; IMAGES MD159/PACHIDERME core MD07-3128; ODP Leg 178 Sites 1095–1102) in context of the inferred LGM paleoceanography of the Southeastern Pacific (SEP) and Drake Passage (DP). Reduced core of the Southern Westerlies (SWW) and extended sea-ice diminish the wind-forcing on the Antarctic Circumpolar Current (ACC) and thus the DP transport. Drake Passage throughflow is further reduced by a northward shifted Subantarctic Front (SAF) and enhanced export of surface and intermediate waters into the HCS. Stronger winds in the northern SWW enhance the SEP Gyre. Background shows bathymetry. WSI=winter sea-ice; SAF=Subantarctic Front; dotted lines show inferred LGM positions; SPC= South Pacific Current; HCS= Humboldt Current System; CHC= Cape Horn Current; EPR= East Pacific Rise.

We expect to recover up to 600–1000-m long Plio/Pleistocene sediment sequences, which will allow us to reconstruct, in unprecedented stratigraphic detail, surface, subsurface/intermediate, and deep ocean variations and their relation to atmospheric changes through stadial-to-interstadial, glacial-to-interglacial and warmer than present time intervals. We identify six major scientific goals:

1) To resolve past changes in the flow of circumpolar water masses through the Drake Passage (DP), which is crucial for our understanding of the Southern Ocean's (SO) role in affecting ocean and climate change on a global scale;
2) To estimate changes in the surface to intermediate water coupling between the Antarctic Circumpolar Current (ACC) and the tropical Pacific over various time-scales and during warmer-than-present climate states;
3) To extend our knowledge of Plio/Pleistocene Subantarctic temperature evolution and corresponding atmospheric variations of the Southern Westerlies and their coupling to the ACC, the relation to Antarctic Ice Sheet variability, especially to WAIS stability, and during warmer-than-present time periods critical to assess the SO's role under future warming;
4) To reconstruct past changes in the latitudinal position of the Subantarctic Front and related changes in ACC transport, intra-basinal mixing, and Antarctic Mode and Intermediate Water production over a wide range of climate states;
5) To reconstruct Subantarctic export production and its relationship to nutrient consumption and dust fluxes in the SEP and compare them to the Subantarctic Atlantic, in order to construct a more global picture of the SO's role in nutrient distribution/ utilization, biogenic export production, and their impact on CO2 variations;
6) To provide a history of Patagonian Ice Sheet variability at orbital and sub-orbital time-scales throughout the Plio/Pleistocene to evaluate its role in controlling dust availability for the transport to the Atlantic SO and Antarctica.

Pre-proposal SUBANTPAC falls within the main theme "Climate and Ocean Change: Reading the Past, Informing the Future" of the IODP Science Plan 2013-2023, and the scientific objectives relate to Challenge 1 and Challenge 2.

ICDP

Seismic site characterization for the Deep-Fault-Drilling-Project Alpine Fault

V. LAY[1], S. BUSKE[1], A. KOVACS[2], A. GORMAN[2]

1 TU Bergakademie Freiberg, Institute of Geophysics and Geoinformatics, 09596 Freiberg, vera.lay@geophysik.tu-freiberg.de

2 University of Otago, Department of Geology, Dunedin 9054, New Zealand

The Alpine Fault in New Zealand (South Island) is one of the largest active plate-bounding continental fault zones on earth. It accommodates most of the Australian and Pacific plate motion on the South Island with 37 mm/year strike-slip movement parallel to the fault and 11 mm/year perpendicular (Norris and Cooper, 1995). The Alpine Fault fails in large earthquakes (moment magnitude $M_W > 7$) occurring every 329 ± 68 years (Berryman et al., 2012). The last earthquake ruptured in 1719 so that the fault is late in its earthquake cycle.

Due to the surface exposure and the shallow depth of mechanical and chemical transitions, it is a globally significant natural laboratory. Within the ICDP Deep-Fault-Drilling-Project Alpine Fault (Townend et al., 2009), a drill hole shall give insight into the geological structure of the fault zone and its evolution. This is to understand the related deformation and earthquake processes, especially for a fault prior to a great earthquake.

During the first phase of the DFDP Project two shallow boreholes (DFDP-1A and DFDP-1B) have been drilled. Sutherland et al. (2012) clearly show that the principal slip zone (PSZ) and the surrounding alteration zone (ca. 50 m thick) can be distinguished from the hanging wall and footwall by petrophysical properties. Especially from the low permeability of the PSZ it is concluded that the Alpine Fault plays a hydrologically important role. Furthermore,

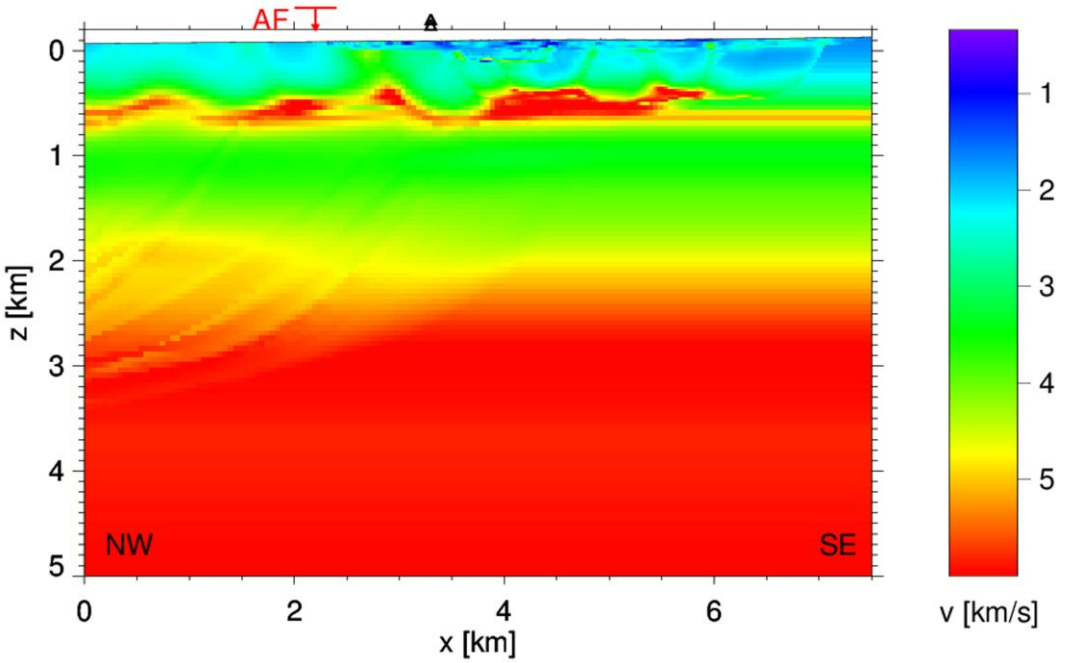

Fig. 1. Combined 3D velocity model obtained by first arrival tomography of the WhataDUSIE and the Whataroa98 data sets.

geophysical wireline-logging reveals particularly low seismic P-wave velocities (v_p=2500 m/s) for the PSZ in addition to higher v_p for the hanging wall than the footwall in general (Carpenter et al., 2014 and Townend et al., 2014).

Within the second project phase starting in autumn 2014 a deeper borehole DFDP-2 shall intersect the Alpine Fault at a depth of approximately 1 km. Due to technical complications, the drilling reached only a final depth of ca. 900 m. The Alpine Fault has not yet been reached.

With the help of advanced seismic imaging techniques, the shallow structure of the Alpine Fault shall be imaged around the drill site location. A seismic reflection profile has been acquired in 2011 by the WhataDUSIE project team consisting of partners from the University of Otago (New Zealand), TU Bergakademie Freiberg (Germany) and the University of Alberta (Canada). The reflection profile, located in the Whataroa river valley, has a total length of about 5 km. Up to 643 geophones with spacings between 4-8 m recorded 182 shots at 99 shot point locations along the profile line.

The data set needed extensive, time-consuming pre-processing to obtain shot gathers usable for imaging. Due to the field conditions, the profile was divided into 5 parts with different features concerning geophone spacing and frequency characteristics. To combine the single stations to one shot gather, overlapping geophones were used to derive the relative time corrections by crosscorrelation of these particular traces. Additionally, three Reftek 130 stations were recording continuously. By correlating the absolute Reftek time and the adjacent geophone trace the absolute shot time was extracted and the resulting time-shift was applied to the corresponding traces. Finally, the merged single shot gathers were further processed including basic trace editing, deconvolution, bandpass filtering, trace equalization, FK-filtering and automatic gain control.

The single shot gathers already show various indicators of the Alpine Fault and the surrounding geology. Strong reflections and distorted first-arrival wavefields are clearly visible. A first-arrival tomography based on this data set delivered a near-surface (< 0.5 km) macro-velocity model. Moreover, a velocity model was derived independently by first arrival tomography of an older seismic reflection data set (Whataroa98). Due to its larger offsets of up to 25 km, this data set allowed to derive velocity information down to greater depths of up to 4 km. Both models were merged and extrapolated to create a velocity model of the subsurface down to 5 km depth. As shown in Figure 1, the velocities increase from about 2300 m/s at the surface to 6000 m/s at 5 km depth. Velocities of around 3500 – 5500 m/s for depths greater than 500 m are realistic for the expected rock type of (cataclastic) schist.

Particularly interesting is the high-velocity layer at approximately 500 m depth with velocities being more than 2000 m/s higher than the surrounding. This layer is not an artefact as it can be seen in both tomography results of the WhataDUSIE and Whataroa98 data set. Furthermore, a similar high-velocity layer was also derived independently by Oelke (2010) from the Whataroa98 data set. Although there is no straight-forward explanation, there might be a correlation to the regional fault structure.

The obtained velocities fit previous analysis. Seismic velocities were recorded by Garrick & Hatherton (1974) on a seismic profile close to Whataroa. They interpret P-wave velocities of 4800 – 5200 m/s as the basement consisting of schist that is overlain by a sediment layer with 2100 m/s. Additionally, rock samples from the schist garnet zone analysed by Christensen & Okaya (2007) at a concealing pressure of 20 Mpa have a mean velocity of 4000 – 5000 m/s. Within the DFDP-1 boreholes, Carpenter et al. (2014) measured v_p values of 3300 m/s for cataclasite samples above the PSZ. P-wave velocities of 3500 – 4500 m/s were reported by Townend et al. (2014) from geophysical

logging results with single values being as high as 6000 m/s.

This newly derived velocity model is currently used for 3D Kirchhoff prestack depth migration as well as the application of focusing prestack depth migration techniques (Cohereny-Migration, Fresnel-Volume-Migration). The images obtained so far show several highly reflecting areas that indicate a more complex setting than originally expected.

Further work will also concentrate on improving the image by choosing optimal migration and stacking parameters. As the drilling for the DFDP borehole has stopped in late 2014, the found structures will be very valuable to link their findings with the local seismic image of the geology. Additionally, the high resolution seismic images themselves allow a better understanding of the tectonic and geodynamic settings.

References:

Berryman, K. R., Cochran, U., Clark, K., Biasi, G.P., Langridge, R. M., and Villamor, Pilar: Major earthquakes occur regularly on an isolated plate boundary fault. Science 336 (6089), 1690-3 (2012).

Carpenter, B. M., Kitajima, H., Sutherland, R., Townend, J., Toy, V. G. and Saffer, D.M.: Hydraulic and acoustic properties of the active Alpine Fault, New Zealand: Laboratory measurements on DFDP-1 drill core. Earth Planet. Sci. Lett. 390, 45-51 (2014).

Garrick, R. A. & Hatherton, T.: Seismic refraction profiles across the Alpine Fault. Otago University, internal report (1974).

Norris, R. J. & Cooper, A. F. Origin of small-scale segmentation and transpressional thrusting along the Alpine fault, New Zealand. Geol. Soc. Am. Bull. 107, 231-240 (1995).

Oelke, A.: Seismic Imaging of the Whataroa'98 Reflection Profile across the Alpine Fault, South Island, New Zealand. Diploma Thesis, FU Berlin (2010)

Townend, J., Sutherland, R. & Toy, V. G. Deep Fault Drilling Project — Alpine Fault, New Zealand. Scientific Drilling 82 (2009).

Townend, J. Sutherland, R., Toy, V. G., Eccles, J. D., Boulton, C. J., Cox, St. and Mcnamara, D: Late-interseismic state of a continental plate-bounding fault: analysis, Alpine Fault, New Zealand 1 petrophysical results from DFDP-1 wireline logging and core. Geochemistry, Geophys. Geosystems 14, 3801-3820 (2013).

Sutherland, R., Toy, V. G., Townend, J., Cox, St., Eccles, J. D., Faulkner, D., Prior, D. J., Norris, R. J., Mariani, E., Boulton, C. J., Carpenter, B. M., Menzies, C. D., Little, T. A., Hasting, M., De Pascale, G. P., Langridge, R. M., Scott, H. R., Lindroos, Z. R., Fleming, B. and Kopf, A.J. Drilling reveals fluid control on architecture and rupture of the Alpine fault, New Zealand. Geology 40, 1143-1146 (2012).

IODP

Cenozoic plankton evolution: a tale of young and old oceans, old and young clades?

DAVID LAZARUS

Museum für Naturkunde, Invalidenstrasse 43, 10115 Berlin.
david.lazarus@mfn-berlin.de

Marine microfossils from deep-sea sediments hold perhaps the most complete record of evolution in paleontology. Most marine microfossil research to date has been for biostratigraphy or paleoenvironmental reconstruction, and our knowledge of diversity change over the Cenozoic is still incomplete. Despite the provisional nature of available data, some patterns in the diversity histories that have been published have implications for biotic vs abiotic controls on large-scale patterns of evolution.

Cenozoic diversity histories for low and high latitude members of several different plankton groups have been published in the last years, including the planktonic foraminifera (Ezard et al, 2011; Lloyd et al., 2012; Cermeno et al., 2013), coccolithophores and discoasters (Bown et al., 2004; Rabosky and Sorhannus, 2009; Lloyd et al., 2011) and marine planktonic diatoms (Rabosky and Sorhannus, 2009; Lazarus et al., 2014). I present here new provisional estimates of radiolarian diversity for both low and high latitudes, based on a newly revised radiolarian taxonomy and the NSB version of the Neptune database (Lazarus, 1994; Spencer-Cervato, 1999, earlier versions of Neptune used by Rabosky and Sorhannus, 2009; Cermeno et al., 2013 and Lazarus et al., 2014). Key features of diversity change over time frequently differ between authors (e.g. Ezard et al., 2011 vs Cermeno et al., 2013 or Rabosky and Sorhannus, 2009 vs Lazarus et al., 2014) but, if we accept, for sake of discussion, the results of Bown et al., 2004; Ezard et al., 2011 and Lazarus et al., 2014 as broadly correct the following observations are possible:

- Plankton has increased strongly in diversity over the Cenozoic, primarily by diversification of siliceous plankton in polar regions.
- Diversity has been nearly static in low latitudes for most groups, dipping temporarily only in the early Oligocene. This is true for coccolithophores, planktonic foraminifera and radiolarians. Only low-latitude diatoms show a different pattern, of strong, nearly continual diversity increase over the Cenozoic.

Planktonic diatoms are unique in being the only clade among the 4 main groups that is evolutionarily young: they first unquestionably appeared in open-ocean plankton in the early Cenozoic. The other groups extend back to the early Mesozoic or (radiolarians) the base of the Phanerozoic.

The low-latitude surface ocean is probably the oldest persistent environment on earth, having been continuously present since the late pre-Cambrian, despite changes in absolute conditions, such as extensive epipieric oceans in the pre-Cenozoic, and extreme warmth at the P/Tr boundary. Cenozoic polar environments by contrast are essentially new, despite similar environments in geologically much older times: in the early Paleogene and much of the Mesozoic there were no strongly differentiated polar water masses or endemic biotas.

I propose that in low latitudes, evolutionarily old clades have had time to fully diversify into the environment and thus, in the absence of major physical change in the Cenozoic, show static diversity. In geologically young environments (high latitudes) or for evolutionarily young clades (diatoms) in the low latitudes Cenozoic diversification has not yet reached equilibrium even after 65 my. This is in accord with the long diversification times of old clades at their origin: the coccolithophores for example required ca 80 my from their origin in the early Mesozoic to reach, in the mid Mesozoic, the diversity levels typical of the Cenozoic (Bown et al., 2004). Recovery of coccolithophores and planktonic foraminifera from partial extinction at the K/T boundary did not reset their evolutionarily ancient status: the recovery was very rapid (ca 10 my) and reflects the ca 100 my of prior planktonic adaptations retained by surviving taxa. I

conclude that physical environmental history, with contrasting patterns and evolutionary results in different latitudes, and a biotic factor - clade age - together may have largely determined patterns of evolution in Cenozoic marine plankton. This conclusion however definitely needs testing against better data than currently available.

References:
Bown, P. R., Lees, J. A., & Young, J. R. (2004). Calcareous nannoplankton evolution and diversity through time. In H. R. Thierstein & J. R. Young (Eds.), Coccolithophores: From Molecular Processes to Global Impact (pp. 481-508). Berlin: Springer.
Cermeño, P., Castro-Bugallo, A., & Vallina, S. M. (2013). Diversification patterns of planktic foraminifera in the fossil record. Marine Micropalaeontology, 104, 38-43.
Ezard, T. H. G., Aze, T., Pearson, P. N., & Purvis, A. (2011). Interplay between changing climate and species' ecology drives macroevolutionary dynamics. Science, 332, 349-351.
Lazarus, D. B. (1994). The Neptune Project - a marine micropaleontology database. Mathematical Geology, 26(7), 817-832.
Lazarus, D., Barron, J., Renaudie, J., Diver, P., & Türke, A. (2014). Cenozoic diatom diversity and correlation to climate change. PLoS One, 9(1), 1-18.
Lloyd, G. T., Smith, A. G., & Young, J. R. (2011). Quantifying the deep-sea rock and fossil record bias using coccolithophores. In A. J. McGowan & A. G. Smith (Eds.), Comparing the Geological and Fossil Records: implications for biodiversity studies (pp. 167-178). London: Geological Society.
Lloyd, G. T., Pearson, P. N., Young, J. R., & Smith, A. G. (2012). Sampling bias and the fossil record of planktonic foraminifera on land and in the deep sea. Paleobiology, 38(4), 569-584.
Rabosky, D. L., & Sorhannus, U. (2009). Diversity dynamics of marine planktonic diatoms across the Cenozoic. Nature, 247, 183-187.
Spencer-Cervato, C. (1999). The Cenozoic deep sea microfossil record: explorations of the DSDP/ODP sample set using the Neptune database. Palaeontologica Electronica, 2(2), web.

ICDP

A Lower–Middle Ordovician composite $\delta^{13}C$ record for central Sweden based on drillcores from the Siljan impact structure

O. LEHNERT[1,2,3], G. MEINHOLD[4], R. WU[2], M. CALNER[2], M.M. JOACHIMSKI[1]

1 GeoZentrum Nordbayern, Lithosphere Dynamics, University of Erlangen-Nürnberg, Schlossgarten 5, D-91054, Erlangen, Germany; oliver.lehnert@fau.de
2 Department of Geology, Lund University, Sölvegatan 12, SE-223 62 Lund, Sweden
3 Institute of Geology, Tallinn University of Technology, Ehitajate tee 5, Tallinn 19086, Estonia
4 Geowissenschaftliches Zentrum der Universität Göttingen, Abteilung Sedimentologie/ Umweltgeologie, Goldschmidtstraße 3, D-37077 Göttingen, Germany

General aspects of the Lower–Middle Ordovician sedimentary successions of Baltoscandia were discussed in various publications. The aspects on its origin in temperate water environments within a slowly subsiding, shallow epicontinental basin located at middle palaeolatitudes, was briefly summarised by Calner et al. (2014). In central Sweden, marine sediments spanning this interval have only been preserved from erosion in the ring-like depression around the more than 30 km wide central uplift area of the Siljan impact structure exposing Precambrian basement. This structure is of late Devonian age (e.g., Jourdan et al. 2012) and shows a present-day diameter of about 52 km (Grieve 1988). It is of particular palaeogeographical significance since it preserves marine Ordovician–Silurian strata in a region dominated by Precambrian basement rocks (Lehnert et al. 2012, 2013).

Latest Tremadocian and Floian units are extremely condensed and contain large stratigraphic gaps. Multiple hard grounds, sometimes even with karstic overprint, display times of erosion and/or non-deposition. Like in other parts of Sweden, the Dapingian and Darriwilian succession in this area, located palaeogeographically within the Central Baltoscandian Confacies Belt (Fig. 1), is characterised by a relatively complete sedimentary record

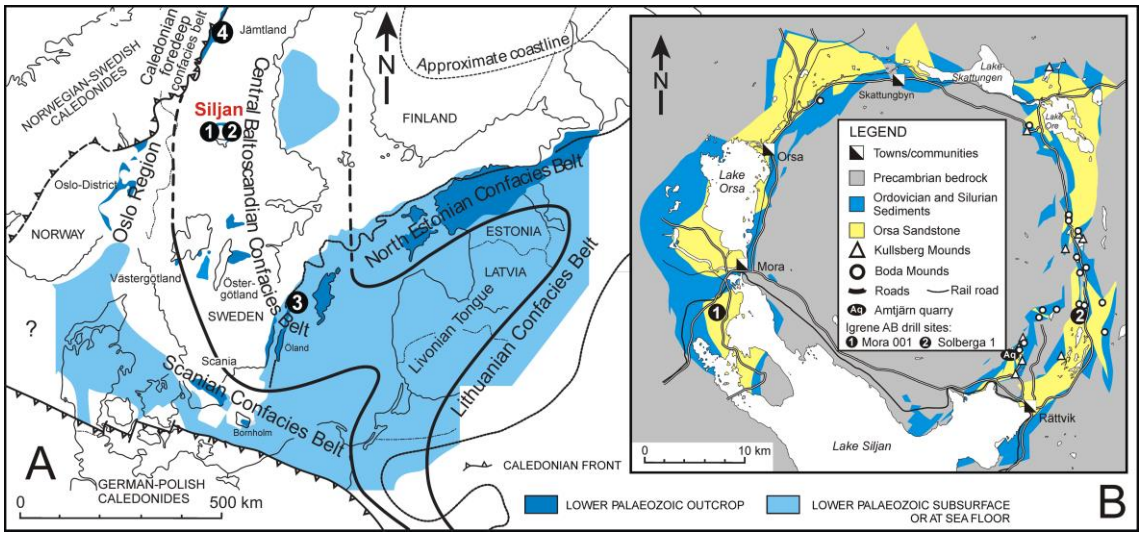

Fig. 1. . A – Swedish core and outcrop locations mentioned in the text and shown on a map of Baltoscandia modified from Pärnaste et al. (2013) and Bergström et al. (2013) showing their modified concept of regional confacies (bio-lithofacies) belts. 1 – Mora 001 core; 2 – Solberga 1 core; 3 – Tingskullen core, Öland; 4 – Brunflo 1 core, Jämtland. B – Drillhole locations of the cores studied for the Ordovician $\delta^{13}C$ record in the Siljan district, Dalarna, central Sweden. 1 – Mora 001; 2 – Solberga 1.

and low sedimentation rates. The Lower Ordovician portion of the cores virtually displays more gaps than record which is also reflected by our $\delta^{13}C$ data. $\delta^{13}C$ is a partly a good tool to detect hiatuses in the sections reflected by incomplete isotope excursions in more condensed settings. It became more and more evident during the last two decades, that there is in general a strong potential of the $\delta^{13}C$ record for regional and global correlations of ancient marine strata (see Saltzman & Thomas 2012 for a summary). Bergström et al. (2009) compiled a generalised $\delta^{13}C$ curve for the Ordovician System, which serves as a good overview of the period (for a simplified version in Fig. 2, upper right). The strong excursions in the late Middle and Upper Ordovician are most likely coupled with climatic changes and have been rather well studied on a global scale. Especially, the $\delta^{13}C$ record of the Upper Ordovician is characterised by a series of high-amplitude positive excursions culminating in the

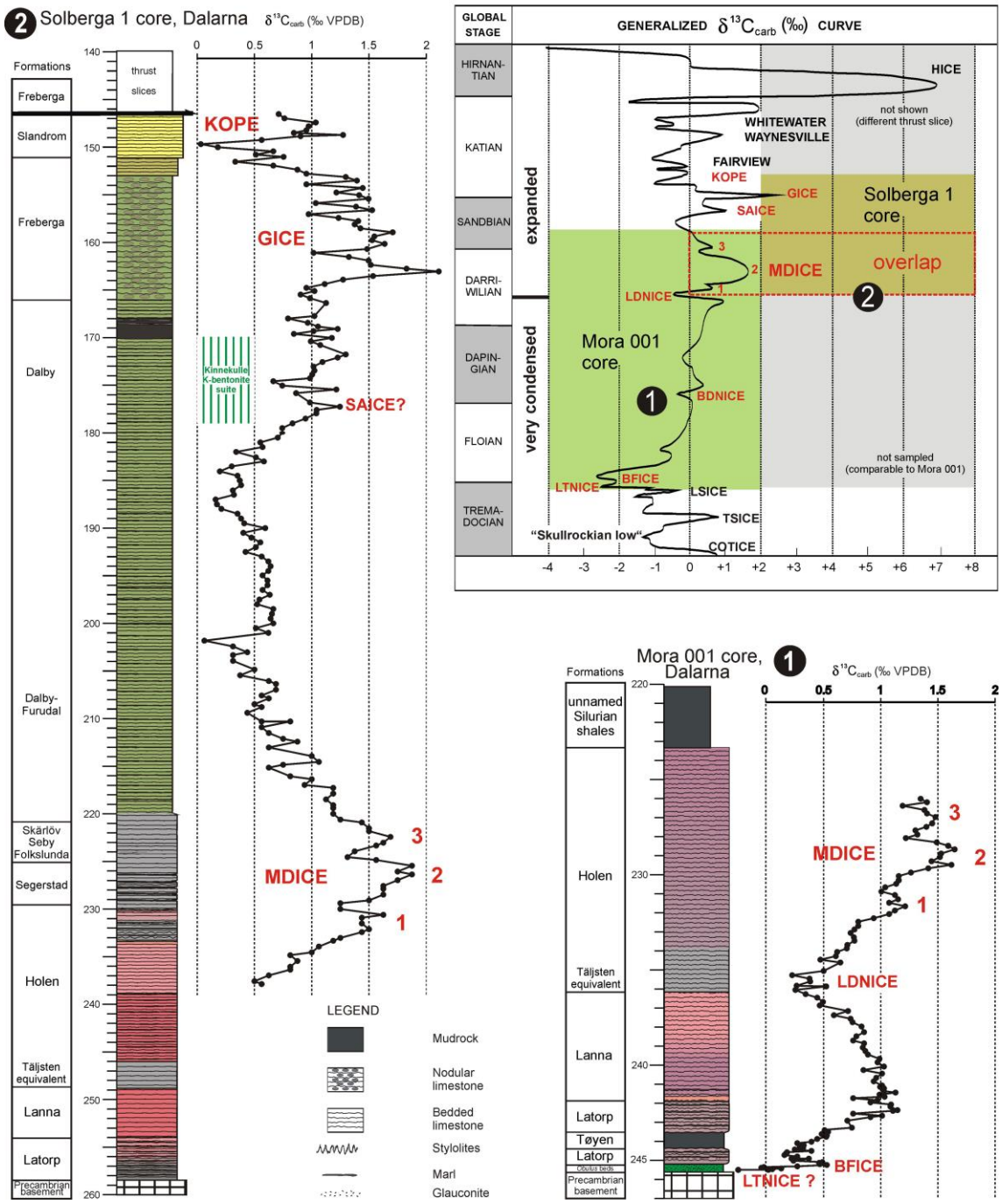

Fig. 2. Stratigraphy, $\delta^{13}C$ chemostratigraphy and sedimentary profiles of the upper Tremadocian through lower Katian succession in the Siljan core sections (Mora 001 and Solberga 1). The MDICE is characterised by a tripartite subdivision indicated by numbers 1–3 for the individual smaller peaks. The generalised $\delta^{13}C$ curve for the Ordovician System (upper right) is modified from Bergström et al. (2009) by the addition of the SAICE (Leslie et al. 2011), and the $\delta^{13}C$ events named COTICE, TSICE, LSICE, TNICE, BFICE, DNICE, plus the informal terms "Skullrockian Low" and "Floian–Darriwilian rise" by Lehnert et al. (2014);. The two darker grey blocks show the stratigraphic range of the sedimentary record in the Mora 001 and Solberga 1 cores (the lower part of the succession in Solberga which is comparable to that in the Mora section was not sampled for this study and is indicated in pale grey), the encircled numbers refer to the corresponding location numbers shown on Figure 1.

Hirnantian Isotopic Carbon Excursion (HICE) that are interpreted to relate to strong shifts in palaeoclimate during the Early Palaeozoic Ice-house.

The less pronounced excursions in the Early and Middle Ordovician have received far less attention and for about a decade stable isotope workers usually referred to the curve published by Buggisch et al. (2003) from the Argentine Precordillera. Just a few additional studies have been undertaken in Lower and Middle Ordovician strata since then (e.g., Ainsaar et al. 2010, Munnecke et al. 2011, Edwards & Saltzman 2014) and until 2014 only one positive $\delta^{13}C$ excursion was formally named from this interval by Schmitz et al. (2010), i.e. the middle Darriwilian Isotope Carbon Excursion (MDICE). Based on $\delta^{13}C$ data from two drillcores in the Late Devonian Siljan impact structure, we present a continuous carbon isotope record from the latest Tremadocian (?) glauconitic limestones resting on Precambrian basement to the early Katian Slandrom Formation of central Sweden. The densely sampled Lower–Middle Ordovician succession in the Mora 001 core (127 samples; WGS 84 coordinate system: N 60º58.855, E 14º31.870) widely overlaps with the record from the Middle–early Upper Ordovician strata in the Solberga 1 core (210 samples; WGS 84 coordinates: N 60 59.296, E 15 12.735), which was sampled up to the base of a major thrust zone 4.84 m above the base of the Slandrom Formation. Both cores (locations shown in Fig. 1) were drilled by the Swedish private company Igrene AB for exploration of geothermal energy and natural gas, and the recorded Lower Palaeozoic successions have been documented by Lehnert et al. (2012).

We used the isotopic data from the thick Early Palaeozoic carbonate platform succession of the Argentine Precordillera (Buggisch et al. 2003) to define some of the Lower Ordovician stable isotope events for discussing the possible presence of these peaks in Swedish sections (Lehnert et al. 2014; Fig. 2). With respect to one of our goals, to investigate the Lower to Middle Ordovician carbon isotope record in Baltoscandia for comparison, a first standard reference section for southern Sweden (Tingskullen-1 core on northern Öland, Fig. 1) was recently published by Calner et al. (2014).

In the Siljan area, there is a latest Tremadocian (?) positive $\delta^{13}C$ excursion, which needs to be dated by conodonts, followed by the known long-term rise of $\delta^{13}C$ values during the Floian and Dapingian culminating in the uppermost part of the Latorp and basal part of the Lanna formations. Then, values decrease towards the Lower Darriwilian during the deposition of the lower Täljsten interval displaying a negative $\delta^{13}C$ excursion observed in various sections on Baltica. In our $\delta^{13}C$ analysis, this is termed as the Darriwilian Negative Isotopic Carbon Excursion (DNICE, minimum $\delta^{13}C$ value 0.23 ‰), which represents a characteristic intrabasinal chemostratigraphic marker and includes the most negative $\delta^{13}C$ values measured in the Baltoscandian Darriwilian $\delta^{13}C$ curves. It is less obvious in the published records of pre-MDICE strata from Laurentia (including the Argentine Precordillera) and South China. In the upper transgressive part of the Täljsten interval, $\delta^{13}C$ values start to rise and shift into the famous and expanded middle Darriwilian Isotopic Carbon Excursion (MDICE, maximum $\delta^{13}C$ value 1.84 ‰). The MDICE is well developed and displays a tripartite subdivision in its peak interval. This, was also observed also in the Tingskullen-1 core from northern Öland. The deposition of the upper Holen Formation through the top of the interval including the Skarlöv, Seby and Folkslunda limestones spans the peak interval of the MDICE comprising three smaller "positive excursions" separated by two small "negative excursions". Between the pronounced positive excursions of the MDICE and the GICE, the latter located in the Freberga Formation, there are two smaller positive excursions which have to be investigated for their potential to correlate on an intrabasinal scale. The highest $\delta^{13}C$ value of the GICE is 2.10 ‰. The KOPE $\delta^{13}C$ excursion is at the transition of the Freberga Formation to the Slandrom Formation and within the latter unit reflected by a maximum $\delta^{13}C$ value of 1.07 ‰. Its falling limb is partly cut off by the basal fault of a major fault zone in the Solberga 1 core (see Lehnert et al. 2012).

The Siljan $\delta^{13}C$ record provides not only a composite for Central Sweden but also a correlation tool for intrabasinal (Baltoscandian) and intracontinental comparisons.

References:

Ainsaar, L., Kaljo, D., Martma, T., Meidla, T., Männik, P., Nõlvak, J. & Tinn, O. 2010. Middle and Upper Ordovician carbon isotope chemostratigraphy in Baltoscandia: a correlation tool and clues to environmental history. Palaeogeography, Palaeoclimatology, Palaeoecology, 294, 189–201.

Bergström, J., Pärnaste, H. & Zhou, Z-Y. 2013. Trilobites and biofacies in the Early–Middle Ordovician of Baltica and a brief comparison with the Yangtze Plate. Estonian Journal of Earth Sciences, 62, 205-230.

Bergström, S. M., Chen, X., Gutiérrez-Marco, J. C. & Dronov, A. 2009. The new chronostratigraphic classification of the Ordovician System and its relations to major regional series and stages and to $\delta^{13}C$ chemostratigraphy. Lethaia, 42, 1–11.

Buggisch, W., Keller, M. & Lehnert, O. 2003. Carbon isotope record of the Late Cambrian and Early Ordovician carbonates of the Argentine Precordillera. Palaeogeography, Palaeoclimatology, Palaeoecology, 195, 357–373.

Calner, M., Lehnert, O., Wu, R., Dahlqvist, P., & Joachimski, M. M. 2014. $\delta^{13}C$ chemostratigraphy in Lower-Middle Ordovician succession of Öland (Sweden) and the global significance of the MDICE. In Early Palaeozoic Global Change (Calner, M., Albanesi, G. L., Babcock, L. E., Harper, D. A. T., Lehnert, O. & Melchin, M., eds.), GFF, 136, 48–54.

Edwards, C. T. & Saltzman, M. R. 2014. Carbon isotope ($\delta^{13}C_{carb}$) stratigraphy of the Lower–Middle Ordovician (Tremadocian–Darriwilian) in the Great Basin, western United States: Implications for global correlation. Palaeogeography, Palaeoclimatology, Palaeoecology, 399, 1–20.

Grieve, R.A.F. 1988. The formation of large impact structures and constraints on the nature of Siljan. In Deep Drilling in Crystalline Bedrock; Vol. 1: The Deep Gas Drilling in the Siljan Impact Structure, Sweden and Astroblemes (Boden, A. & Eriksson, K. G., eds), Proceedings of the International Symposium, Springer Verlag, Berlin, 328–348.

Jourdan, F., Reimold, W. U. & Deutsch, A. 2012. Dating terrestrial impact structures. Elements, 8, 49–53.

Lehnert, O., Meinhold, G., Bergström, S. M., Calner, M., Ebbestad, J. O. R., Egenhoff, S., Frisk, Å. M., Hannah, J. L., Högström, A. E. S., Huff, W., Juhlin, C., Maletz, M., Stein, H. J., Sturkell, E. & Vandenbroucke, T. R. A. 2012. New Ordovician-Silurian drill cores from the Siljan impact structure in central Sweden: an integral part of the Swedish Deep Drilling Program. GFF, 134, 87–98.

Lehnert, O., Meinhold, G., Arslan, A., Ebbestad, J. O. R. & Calner, M. 2013. Ordovician stratigraphy and sedimentary facies of the Stumsnäs 1 core from the southern Siljan Ring, central Sweden. GFF, 135, 204–212.

Lehnert, O., Meinhold, G., Wu, R., Calner, M. & Joachimski, M. M. 2014. $\delta^{13}C$ chemostratigraphy in the upper Tremadocian through lower Katian (Ordovician) carbonate succession of the Siljan district, central Sweden. Estonian Journal of Earth Sciences, 63, 277–286.

Leslie, S. A., Saltzman, M. R., Bergström, S. M., Repetski, J. E., Howard, A. & Seward, A. M. 2011. Conodont biostratigraphy and stable isotope stratigraphy across the Ordovician Knox/Beekmantown unconformity in the central Appalachians. In Ordovician of the world (Gutiérrez-Marco, J. C., Rábano, I., Diego, G.-B., eds), Publicaciones del Instituto

Geológico y Minero de España: Serie: Cuadernos del Museo Geomin-Minero, 14, 301–308.
Munnecke, A., Zhang, Y., Liu, X., & Cheng, J. 2011. Stable carbon isotope stratigraphy in the Ordovician of South China, Palaeogeogr., Palaeoclimat., Palaeoecol., 307, 17–43.
Pärnaste, H., Bergström, J. & Zhou, Z-Y. 2013. High-resolution trilobite stratigraphy of the Lower–Middle Ordovician Öland Series of Baltoscandia. Geological Magazine, 150, 509–518.
Saltzman, M. R. & Thomas, E. 2012. Carbon isotope stratigraphy. In The Geologic Time Scale (Gradstein, F., Ogg, J., Schmitz, M. D. & Ogg, G., eds), Elsevier, Amsterdam, 207–232.
Schmitz, B., Bergström, S. M. & Wang, X. F. 2010. The middle Darriwilian (Ordovician) $\delta^{13}C$ excursion (MDICE) discovered in the Yangtze Platform succession in China: implications of its first recorded occurrences outside Baltoscandia. Journal of the Geological Society, London, 167, 249–259.

ICDP

First tephrostratigrahic results of the DEEP site record in Lake Ohrid, Macedonia

N. LEICHER[1], G. ZANCHETTA[2], R. SULPIZIO[3], B. GIACCIO[4], S. NOMADE[5], B. WAGNER[1], A. FRANCKE[1]

1 Institute of Geology and Mineralogy, University of Cologne, Zülpicher Str. 49a, 50674 Cologne, Germany
2 Dipartimento di Scienze della Terra, University of Pisa, via S. Maria 53, 56126 Pisa, Italy
3 Dipartimento di Scienze della Terra e Geoambientali, University of Bari, via Orabona 4, 70125 Bari, Italy
4 Istituto di Geologia Ambientale e Geoingegneria, CNR, Area della Ricerca di Roma1-Montelibretti, Via Salaria Km 29,300, Roma, Italy
5 Laboratoire des sciences du climat et de l'environnement, UMR 8212, CEA/CNRS/UVSQ, F-91190 Gif-Sur-Yvette, France

Explosive volcanism is usually investigated on proximal pyroclastic successions, providing the best context for depositional processes and eruptive dynamics. However, also distal archives can help to unravel even a more complex and often a longer history than near-vent successions do, as they are less affected by erosion and burial (Wulf et al., 2004; Paterne et al., 2008). The wider field of application of distal tephrostratigraphy comprises various Quaternary fields, such as dating or correlation/synchronisation of records from different regions. For both fields, distal tephrostratigraphy can be of great potential being a frontier subject between volcanology and Quaternary sciences (Giaccio et al., 2014).

In the Mediterranean region tephrostratigraphy has been proofed to be a suitable tool for dating and correlation of marine and terrestrial records, but most existing records are limited to the period < 200 ka. The knowledge of the Middle Pleistocene tephrostratigraphy, covering one of the periods, when the Italian Quaternary explosive volcanism was most active, is relatively poor. However, in recent years new proximal records from various Italian continental basins significantly improved the knowledge of volcanic activity. Active volcanic centres during the Middle-Pleistocene were i.a. the Roman Province (Sabaitini, Vulsini, Alban Hills, Vico), the Ernici-Roccamonfina province or the Vulture volcano (Petrosino et al. 2014 and references wherein). Promising information about this time is recorded e.g. in the Sulmona (Giaccio et al., 2013), the Acerno (Petrosino et al., 2014) or the Mercure basin (Giaccio et al., 2014) and other continental lacustrine successions in Italy. Some of these records and tephrostratigraphic events are very well dated ($^{40}Ar/^{39}Ar$) and helped to better understand our knowledge of geological processes, such as the paleomagnetic reversal at the Matuyama-Brunhes boundary (Sagnotti et al., 2014).

Distal archives downwind of the Italian volcanoes covering such an age range are rare in the eastern Mediterranean. However, the most promising terrestrial archive of the eastern Mediterranean is Lake Ohrid in Macedonia/Albania, which is supposed to be the oldest continuously existing lake of Europe (Wagner et al., 2014). Previous tephrostratigraphic studies on relatively short sediment cores of Lake Ohrid are summarized in Sulpizio et al. (2010) and cover the last 135 ka. Over this period, eleven tephra layers from Italian eruptions have been recognized and provide valuable information of tephra dispersal from Italian volcanoes. In spring 2013, the ICDP deep-drilling campaign SCOPSCO (Scientific Collaboration on Past Speciation Conditions in Lake Ohrid) was conducted on Lake Ohrid. The drilling campaign comprised four drill sites with the master drill site, DEEP, in the centre of the lake. At this site, the maximum drill depth was 569 m below the lake floor and pelagic sediments characterize the uppermost 430 m. Initial data from borehole logging, core logging and geochemical measurements indicate that the DEEP site record covers more than 1.2 Ma were continuously (Wagner et al., 2014). The recovered sediments are and will be analysed with different biological and geological methods. One of the foci is a detailed tephrostratigraphic study in order to provide more information on Italian volcanism from a distal site and to provide an independent chronological tie points for the establishment of an age model of the DEEP site record.

During core-opening only macroscopic tephra layers were identified so far, but XRF down core data give hope for more tephra horizons, i.e. cryptotephra layers, which are not visible by naked eye. So far, the uppermost 210 m of the DEEP site record, which represent the last ca. 510 ka, comprise 27 macroscopic tephra layers. Out of these, a set of 9 tephra layers was selected to provide information for a first age-depth model. Criteria for selection have been a good match with known Italian tephras and the availability and reliability of respective ages of these tephras. Except of one ^{14}C-date, all other ages are well constrained by $^{40}Ar/^{39}Ar$ dating. As known from the previous studies, the Y-3, the Campanian Ignimbrite, the X-6 and the P 11 tephra horizons were selected from the last 135 ka. In the older sediments, the Vico B, probably the Pitigliano Tuffs, the Pozzolane Rosse, the Sabatini Fall A and the tephra horizons A11-A12, from Acerno succession, were found and cover the period 162 – 511 ka. The ages of these tephras are used as independent first order tie-points for a robust age model for the Lake Ohrid record based on astronomical tuning. The tephrostratigraphic work forms thus the backbone to correlate and interpret borehole logging and sediment core data in the front of environmental change over time.

Over the next years, more analytical work will help to improve the proper correlation of tephras in the Ohrid core sequences with the relevant Italian volcanic provinces and their specific eruptions. In this way, the Lake Ohrid record will become a unique distal record of Italian volcanic activity and can be used for other distal records in the eastern Mediterranean as master record. The cross correlation with astronomical tuning, on the other hand, allows us to cross validate the proximal records and the

reliability of ages obtained from these records. For example, the cross correlation of the Sabatini Fall A deposit in Lake Ohrid implies that the existing ages of more proximal Sabatini Fall A deposits in Italy are probably several thousand years too young.

References:
Giaccio, B., Castorina, F., Nomade, S., Scardia, G., Voltaggio, M., and Sagnotti, L.: Revised Chronology of the Sulmona Lacustrine Succession, Central Italy, Journal of Quaternary Science, 28, 545-551, 2013.
Giaccio, B., Galli, P., Peronace, E., Arienzo I., Nomade, S., Cavinato, G. P., Mancini, M., Messina, P., and Sottili, G.: A 560-440 ka tephra record from the Mercure Basin, southern Italy: volcanological and tephrostratigraphic implications, Journal of Quaternary Science, 29, 232-248, 2014.
Petrosino, P., Jicha, B. R., Mazzeo, F. C., and Russo Ermolli, E.: A high resolution tephrochronological record of MIS 14–12 in the Southern Apennines (Acerno Basin, Italy), Journal of Volcanology and Geothermal Research, 274, 34-50, 2014.
Sagnotti, L., Scardia, G., Giaccio, B., Liddicoat, J. C., Nomade, S., Renne, P. R., and Sprain, C. J.: Extremely rapid directional change during Matuyama-Brunhes geomagnetic polarity reversal, Geophysical Journal International, 199, 1110-1124, 2014.
Sulpizio, R., Zanchetta, G., D'Orazio, M., Vogel, H., and Wagner, B.: Tephrostratigraphy and tephrochronology of Lakes Ohrid and Prespa, Balkans, Biogeosciences, 7, 3273-3288, 2010.
Wagner, B., Wilke, T., Krastel, S., Zanchetta, G., Sulpizio, R., Reicherter, K., Leng, M. J., Grazhdani, A., Trajanovski, S., Francke, A., Lindhorst, K., Levkov, Z., Cvetkoska, A., Reed, J. M., Zhang, X., Lacey, J. H., Wonik, T., Baumgarten, H., and Vogel, H.: The SCOPSCO drilling project recovers more than 1.2 million years of history from Lake Ohrid, Scientific Drilling, 17, 19-29, 2014.

ICDP

Integration and Correlation of geophysical data sets with sedimentological information of a long continuous sediment core: results from the SCOPSCO ICDP campaign

K. LINDHORST[1], S. KRASTEL[1], H. BAUMGARTEN[2], T. WONIK[2], A. FRANCKE[3], B. WAGNER[3]

1 Christian-Albrechts-Universität zu Kiel, Institut für Geowissenschaften, Abteilung Geophysik, Otto-Hahn-Platz 1, 24118 Kiel, Germany, klindhorst@geophysik.uni-kiel.de
2 Leibniz-Institute for Applied Geophysics (LIAG), Stilleweg 2, 30655 Hannover, Germany
3 Institute für Geologie und Mineralogie, Universität Köln, Germany

Lake Ohrid is located on the Balkan Peninsula shared by the Former Yougoslavia Republic Macedonia and Albania within the Dinaride-Helenide-Albanide mountain belt (Fig. 1). Lake Ohrid is surrouded by the Galicica Mountains (east) and Mokra Mountains (west, Fig. 1). Considering its size, Lake Ohrid contains a remarkable amount of endemic species with more than 212 described, which makes it to a hotspot of endemic biodiversity (Albrecht and Wilke, 2008).

The ICDP SCOPSCO project has been initiated in order to constrain the following targets : (1) to reveal a precise age and origin of Lake Ohrid, (2) to unravel the seismo-tectonic history of the lake area including effects of major earthquakes and associated mass wasting events, (3) to obtain a continuous record containing information on volcanic activities and climate changes in the central northern Mediterranean region, and (4) to better understand the impact of major geological/environmental events on general evolutionary patterns and shaping an extraordinary degree of endemic biodiversity as a matter of global significance. Interpretation of seismic lines that were collected during several pre-site surveys in between 2004 and 2009 revealed up to 700 m thick undisturbed sediments in the central basin providing a long and continuous sediment record for adressing the main questions of the SCOPSCO project. A successful deep drilling campaign took place in spring 2013. Opening of cores and data sampling and analyses is ongoing.

Processing and interpretation of hydroacoustic and seismic data in between 2004 and 2009 allowed a reconstruction of the initial formation of Lake Ohrid Basin as a pull-apart basin estimating a timing for the basin opening in late Miocene times (Lindhorst et al., 2014). After Lake Ohrid became a water filled body, the lake existed coninuously. In the central part of Lake Ohrid we found an undisturbed complete sedimentary succession. A striking feature of sediments within the basin is the cyclic change in amplitude from high to low or medium, respectively. It has been suggested that this pattern reflects climatic and/or environmental change of the area surrounding Lake Ohrid.

The internal structure of Lake Ohrid is complex and beside thick undisturbed sediment successions in the central part the sedimentary infill is represented by transparent units (slide deposits), clinoform structures, and offsets of reflectors indicating active tectonics. The southern region is characterized by a long history of mass wasting with several mass transport deposits stacked on top of each other (Fig. 2). Several stacked clinform structures are imaged along the southern shelf area indicating a

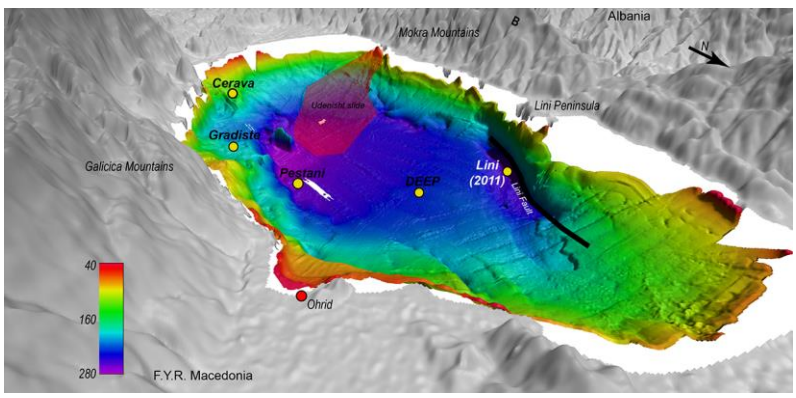

Fig. 1. A: Bathymetry map viewed from NE direction. Drill sites are marked with yellow dots. Offshore Lini Peninsula a black line marks the Lini Fault and the coring location of the Lini site from 2011. The area affected by the Udenisht slide is marked in red.

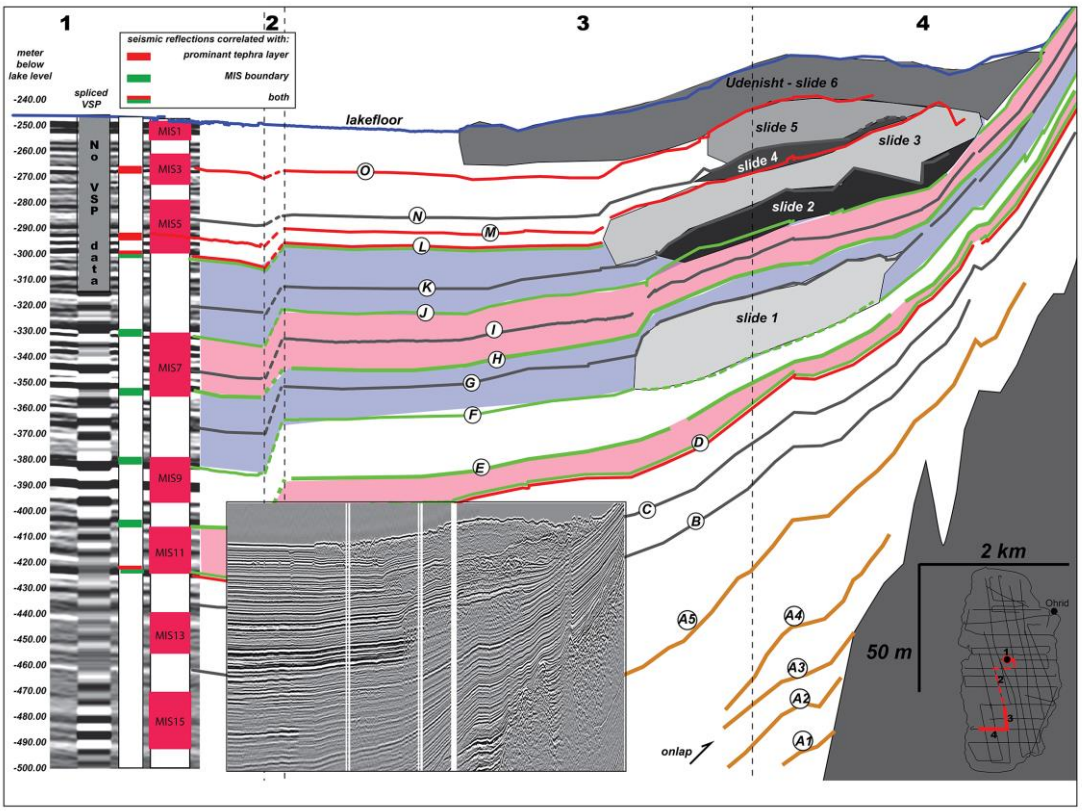

Fig. 2. Interpretation of arbitrary line of seismic cross sections showing the spliced VSP data (left), undisturbed central basin, and sliding deposits within the southern area. Six major slides have been marked in gray and labeled. Red lines (D, L,M, and O) mark seismic reflections associated with tephra layers found in the DEEP drill sediment core. Green lines (D – F, H, J, and L) are boundary of Marine Isotope Stages. Notice that reflector L and D are both. Gray lines (B, C, G, I, K, and N) are not correlated with the sediment core yet. They have been used to constrain an age model for the mass wasting history of Lake Ohrid. Some of them are most likely gliding planes. The interpreted data is shown as an inlet.

stepwise rise of lake level over time. Seismic cross sections show evidences for active seismic faulting along the sides of Lake Ohrid and in the northern area. A major fault entitled Lini Fault, located offshore the Peninsula Lini, is still active at present indicated by a prominent relief within the bathymetry. Deposition within the northern area is influenced by active tectonics and mass wasting.

More than 2000m of sediment were extracted in spring 2013 (Fig. 1, Wagner et al., 2014). In total four sites were drilled: (i) the main site DEEP in the central basin, (ii) CERAVA in the south, (iii) GRADISTE within a subbasin within the eastern major boundary fault area, and (iv) PESTANI in the deepest part of Lake Ohrid on the hanging wall of the major fault with a maximum sediment depth of ~569m, ~123m, ~91m, and ~195 m, respectively. Our work onsite included the measurment of Magnetic Susceptibility (MS) at all sections by using a Multi Sensor Core Logger (MSCL) device immediately after the 1m-long core sections were brought back from the drill barge. Down-hole logging was carried out at each site by the LIAG group from Hannover. In addition, we carried out a Vertical Seismic Profile (VSP) shot gather at site DEEP in Hole 1C enabling us to convert travel time into depth.

The resulting seismic trace of the VSP contains less multiple reflections compared to surface multichannel seismic data (Fig. 2). This is due to the fact that after separating the downgoing from the upgoing wave a deconvolved downgoing wave is used as an operator to attenuate multiple reflections within the upgoing wave. Main processing steps of VSP data includes (1) common depth stacking to reduce noise, first break picking to extract a time-depth-chart, wave field separation of the downgoing and upgoing wave, deconvolution using the downgoing wave as an operator, f-k-filtering. A so called corridor stack will then result in a seismic trace illustrating the sediment layers along the bore-hole. After adapting the amplitude to to the seismic data recorded in 2007, the seismic trace (multiplied by ten in order to imitate a seismic cross section) is spliced into surface multichannel seismic cross section across the bore location (Fig. 2). This approach allows a very solid correlation between seismic and drill data

A dense grid of seismic lines and sediment echosounder data is available for Lake Ohrid. Alle lines were converted into depth enabling us to integrate sediment physical properties into seismic lines. The analyses of sedimentological data is still ongoing today but information are available up to a sediment depth of 260m (~660ka).

As mentioned above, Lake Ohrid has a long history of mass wasting that can be seen on seismic cross section especially in the southern area (Fig. 2). With the new information from the sediment core DEEP, we reinterpreted the occurrence of sliding events. We correlated dominant seismic reflections (A to O on Fig. 2) with environmental conditions (e.g., Interglacials va. Glacial periods) reconsturcted from the drilling data (sediments anddownhole- logging data). Six reflectors could be associated to transitions from Glacial to Interglacial and vice versa (green lines on Fig. 2). Deposits older than ~670ka are clearly visible on seismic data but

have not been correlated with core data (orange lines on Fig. 2). Strong reflections directly overlaying the acoustic basement and are likely associated with fluvial material deposited in an early rift phase in shallow water depth (A1-A3 on Fig. 2). Furthermore, we could link four tephra layers with seismic reflectors. Two of them are most likely glide planes for sliding events (M and O, red lines on Fig. 2). No transparent mass wasting units have been detected older than horizon F that marks the transition from MIS 9 to MIS 8 (Fig. 2). One interesting fact is that no sliding event is imaged within Interglacial MIS 7. In contrast in Glacial period associated with MIS 6 several mass transport deposits could be found (Fig. 2). Mass wasting is ongoing since the warm period MIS5 and several large and mid-sized events have been detected, some of them are clearly visible on bathymetric data. Analyses of sediment echosounder data further show that slide deposits can be found not only in the southern area but distributed over the entire lake basin. One reason might be that for the time younger than ~130ka, a dense grid of high resolution sediment echosounder data is available allowing us to detect even small events in between two reflections that are most likely undetectable in multichannel seismic data due to the reduced lateral resolution. The Udenisht slide body in the southwestern part of the lake is detectable within acoustic data. A multibeam and sediment echo-sounder campaign was conducted in 2009 in order to constrain its age and potential to trigger a tsunami within Lake Ohrid. The Udenisht slide shows a retrogressive behavior meaning that it is the result of several sliding events which makes it more difficult to determine its age and assess the tsunamigenic potential. Nevertheless, the sediment cover on top of the Udenisht slide is very thin (< 10 cm) and hence we suggest that the slide has occurred in the Holocene. A recent study of a sediment core drilled in 2011 offshore the Peninsula Lini revealed a slide deposit within the uppermost sediment column that is overlying a prominent tephra layer (AD472/512). Wagner et al. (2012) argued that seismic shaking along the adjacent Lini Fault is responsible for triggering a slide within the last 1500 years. This event and the larger Udenisht slide may be triggered by the same seismic event; historical data document a major earthquake in the early 6th century AD that destroyed the city of Lychnidus (today: city of Ohrid Wagner et al., 2012).

Our future task are to continue the correlation of sedimentological information with seismic data as more and more data become available until we reach the end of the lacustrine succession. On the basis of the new age model we will be able to reconstruct the sedimentary history of Lake Ohrid as well as its subsidence and tectonic evolution in detail.

References

Albrecht, C. and Wilke, T. (2008) “Ancient Lake Ohrid: Biodiversity and Evolution.” Hydrobiologia, Vol. 615, p.103-140.

Lindhorst, K., S. Krastel, et al. (2014). "Tectonic and Sedimentary Evolution of Lake Ohrid (Albania/Macedonia)." Basin Research. 0, 1-18, 10.1111/bre.12063

Wagner, B., Francke, A., et al. (2012): Possible earthquake trigger for 6th century mass wasting deposit at Lake Ohrid (Macedonia/Albania), Clim. Past, 8, 2069-2078, 10.5194/cp-8-2069-2012

Wagner, B., Wilke, T., et al. (2014) “More than one million years of history in Lake Ohrid cores.” Eos, 95 25-26.

IODP

Mid-Cretaceous nannofossil biometry and assemblage characterisation and its relation to palecology

N. LÜBKE [1], J. MUTTERLOSE [1], C. BOTTINI [2]

1 Institut für Geologie, Mineralogie und Geophysik, Ruhr-Universität Bochum, Universitätsstraße 150, 44801 Bochum, Deutschland

2 Dipartimento Scienze della Terra, Università degli Studi di Milano, Via Mangiagalli 34, 20133 Milano, Italia

Introduction

Coccolith-bearing haptophyte algae, coccolithophores, have been one of the main marine primary producers and the main carbonate producers at least since their first fossil occurrence in Upper Triassic sediments. Species recognition is mainly based on the morphology of coccoliths, circular to elliptical calcite discs attached to the outer cell wall of these single-celled algae with sizes of only a few µm, preserved in the fossil record. Assemblage analysis have been conducted intensely throughout the last decades and shed light on the relation of the abundance of several species and ecological parameters, such as for example sea-surface temperature, nutrient levels and salinity. Biometric analyses of coccoliths of single species give valuable insight into intra-specific adaptations to ecological parameters or environmental changes. These additional information enable a better understanding of the past ocean-biosphere interactions. This project studies nannofossil assemblages preserved in mid-Cretaceous marine sediments from various locations covering open-oceanic to coastal settings and different latitudes.

Material and methods

The project is two-parted with one focus on the Upper Barremian – Lower Aptian sediments from the Lower Saxony Basin (Alstätte outcrop, northwest Germany) and the North Sea (North Jens-1 and Adda-2 cores), representing mid-latitude coastal and hemipelagic settings, respectively. Biometric studies on several coccolith species were conducted on this material. The results were compared to biometric data on the same species from two pelagic, low-latitude sections in the western Tethys and the Mid-Pacific obtained by Erba et al. (2010). The second focus of this project is on material from ODP core 763B (Leg 122, Exmouth Plateau), ODP core 1052E (Leg 171B, Blake Nose) and a composite record from northwest Germany (Kirchrode/Anderten cores, drilled by BGR Hannover). The recovered sediments cover the Upper Albian and Lower Cenomanian at various paleolatitudes. In addition, ODP core 763B exposes an entire succession of Upper Aptian to Lower Cenomanian sediments. The selected cores display good age control based on chemostratigraphy and nannofossil biostratigraphy, allowing for comparison of the sections. Nannofossil preservation and abundance are well suited for biometric studies and assemblage analyses.

Rock material is processed using the settling method by Geisen et al. (1999) resulting in plain-lying coccoliths, best suited for biometric measurements. Nannofossil assemblage analyses are based on counts of at least 300 individual specimens per sample using an Olympus BX51 transmitted light microscope mounted with a ColorView II camera. Nannofossil biometry was conducted on at least 50

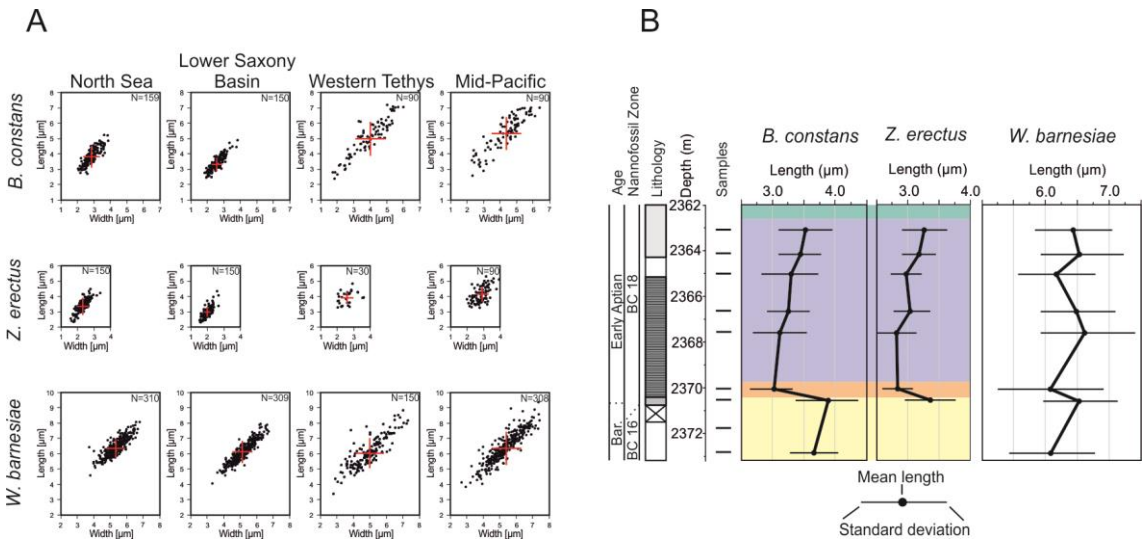

Fig. 1. (A) The size distribution data of *B. constans*, *Z. erectus* and *W. barnesiae* from the confined interval (C-isotope segment C2) in scatter plots of width versus length of the individual coccoliths. N is the number of measured specimens per data set. **(B)** Coccolith size evolution of *B. constans*, *Z. erectus* and *W. barnesiae* represented by coccolith length along the Adda-2 core (North Sea). Orange interval represents the initial phase of OAE 1a and the abrupt site decrease of *B. constans* and *Z. erectus*, purple interval comprises the coccolith size recovery phase. Yellow and green intervals indicate pre-OAE and post-OAE periods with similar sizes. The coccolith size of *W. barnesiae* remains stable along the section.

plain-lying individual specimens per species per sample at a magnification of x2000. Besides nannofossil data, carbonate content and stable isotopes are measured. The resulting data set is evaluated statistically.

First results

The Upper Barremian – Lower Aptian material from the North Sea and the Lower Saxony Basin has already been studied with respect to nannofossil biometry. Three species have been studied in three sections: *Biscutum constans*, *Zeugrhabdotus erectus* and *Watznaueria barnesiae*. These species represent the major components of the nannofossil assemblages accounting for 52 to 56 % on average (Bottini and Mutterlose, 2012; Mutterlose and Bottini, 2013). Length, width and ellipticity data were collected in 30 samples. The results from the three sites are two-parted: A comparison of coccolith size distribution from a confined interval (C-isotope segments C2; Menegatti et al., 1998) with literature data revealed a smaller coccolith size range in the North Sea and the Lower Saxony Basin for *B. constans* and *W. barnesiae* with respect to the western Tethys and the Mid-Pacific. In addition, *B. constans* coccoliths in the North Sea and Lower Saxony Basin samples only covered the small-sized endmeber of the entire size range, while the mean size of *W. barnesiae* was similar at all sites (Fig. 1). The size distribution of *Z. erectus* was most likely altered by dissolution due to its more delicate morphology compared to the placolith species *B. constans* and *W. barnesiae*. In a manuscript submitted to Marine Micropaleontology and currently under review, the results of this comparison are discussed in detail with respect to preservation and ecological factors. Besides this comparison, the response of coccolith sizes with regard to oceanic anoxic event 1a (OAE 1a) at the three sites was studied. A coccolith size decrease of *B. constans* and *Z. erectus* associated with

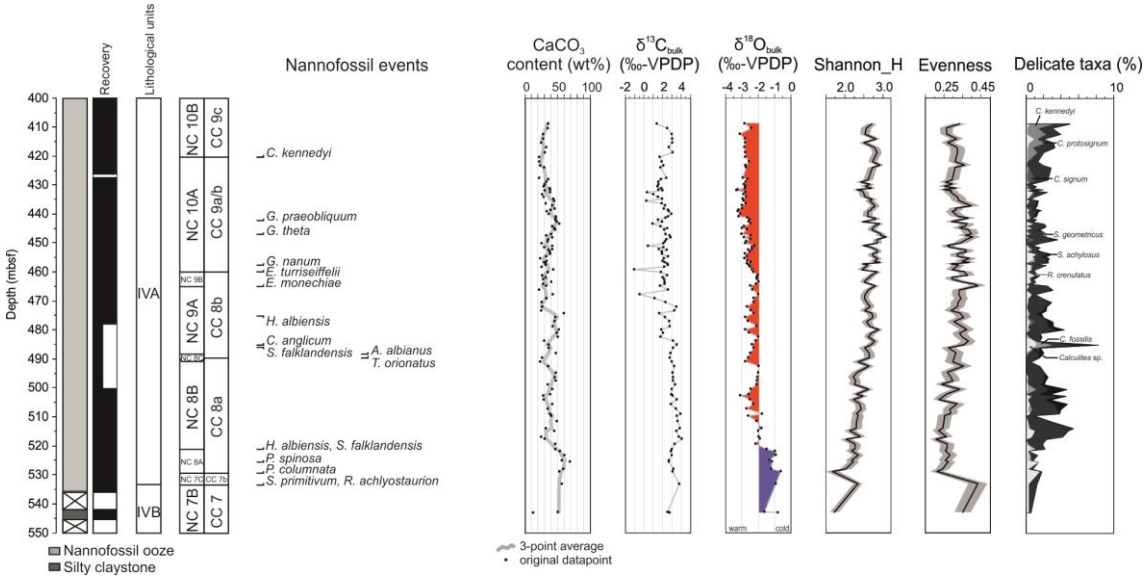

Fig. 2. A compilation of lithology, age, bulk rock and nannofossil-based data for ODP core 763B.

OAE 1a was detected and is similar to that reported from the western Tethys and the Mid-Pacific (Erba et al., 2010). This feature has now been described for the first time in Boreal sections.

Current work

The current work focuses on ODP core 763B. So far, the nannofossil assemblage has been studied in all 113 samples covering Late Aptian to the Early Cenomanian silty claystones and nannofossil oozes. Furthermore, carbonate content and stable isotope data were compiled. Stratigraphically, the core covers nannofossil zones NC7B or CC7 to NC10B or CC9c (Bown et al., 1998; Burnett, 1998) which is consistent with the dating of Bralower (1992). Based on the nannofossil assemblage data, the diversity indices Shannon Index and Evenness were calculated (Fig. 2). The Shannon index increases slightly towards the core top from 1.7 at the base to 3.1 in the upper 50m of the core indicating an increase in diversity, while Evenness remains fairly constant at roughly 3.1. Nannofossil preservation is good to excellent in most samples using visual criteria and based on the frequent to common and rather stable occurrence of delicate species throughout the section. No trend in preservation was detectable. The most abundant nannofossil species (> 1%) are in descending order *W. barnesiae, B. constans, Tranolithus orionatus, Z. erectus, Discorhabdus ignotus, Zeugrhabdotus howei, Seribiscutum primitivum, Watznaueria fosscincta, Eiffelithus turriseiffelii, Rhagodiscus asper, Rhagodiscus angustus, Repagulum parvidentatum* and *Eprolithus floralis.* The two former species are by the far most abundant. At the bottom of the section, *R. parvidentatum* accounts for 15 % of the entire nannofossil assemblage. Its presumed preference for cool sea-surface temperatures indicates a cooling event in the Latest Albian as it was reported by Mutterlose et al. (2009) for a number of sections from the northern and southern hemisphere. Oxygen isotope data display less negative values at the bottom of ODP core 763B which is in line with a cooling. However, oxygen isotope data are prone to diagenetic alteration and have to be taken cautiously.

Outlook

At the moment, the nannofossil-based data are treated statistically. Furthermore, nutrient and temperature index based on the inferred preference of specific taxa will be calculated. Based on the analysis of the nannofossil assemblage, suitable samples and species for a detailed biometric analysis will be selected; coccolith length and width will be measured. In addition, more detailed features will be used to characterize the morphology, including for example dimensions of the central area or thickness of bars.

References:

Bralower, T. J. (1992) Aptian-Albian Calcareous Nannonfossil Biostratigraphy of ODP Site 763 and the Correlation Between High- and Low-Latitude Zonations, in Synthesis of Results from Scientific Drilling in the Indian Ocean (Eds. Duncan, R.A.Rea, D.K., Kidd, R.B., von Rad, U. Weissel, J.K.), American Geophysical Union, Washington, D. C.

Bottini, C., Mutterlose, J., 2012. Integrated stratigraphy of Early Aptian black shales in the Boreal Realm: calcareous nannofossil and stable isotope evidence for global and regional processes. Newsletters on Stratigraphy, 45, 115–137.

Bown, P.R., Rutledge, D.C., Crux, J.A., Gallagher, L.T., 1998. Lower Cretaceous. In: Bown, P.R. (Ed.), Calcareous nannofossil biostratigraphy. Chapman and Hall, London, 86-131.

Burnett, J.A, 1998. Upper Cretaceous. In: Bown, P.R. (Ed.), Calcareous nannofossil biostratigraphy. Chapman and Hall, London, 132-199.

Erba, E., Bottini, C., Weissert, H., Keller, C.E., 2010. Calcareous Nannoplankton Response to Surface-Water Acidification Around Oceanic Anoxic Event 1a. Science, 329, 428–432.

Geisen, M., Bollmann, J., Herrle, J.O., Mutterlose, J., Young, J.R., 1999. Calibration of the random settling technique for calculation of absolute abundances of calcareous nannofossils. Micropaleontology, 45, 437–442.

Menegatti, A.P., Tyson, R.V., Farrimond, P., Strasser, A., Caron, M., 1998. High-resolution δ13C stratigraphy through the Early Aptian "Livello Selli" of the Alpine Tethys. Paleoceanography, 13, 530-545.

Mutterlose, J., Bottini, C., 2013. Early Cretaceous chalks from the North Sea giving evidence for global change. Nature Communications, DOI: 10.1038/ncomms2698.

Mutterlose, J., Bornemann, A., Herrle, J.O., 2009. The Aptian – Albian cold snap: Evidence for "mid" Cretaceous icehouse interludes. Neues Jahrbuch für Geologie und Paläontologie – Abhandlungen, 252, 217-225.

ICDP

First evidences of neotropical glacial/interglacial (220-85 ka BP) climate change based on freshwater ostracodes and geochemical indicators from Lake Petén Itzá, northern Guatemala

L. MACARIO[1], S. COHUO[1], L. PÉREZ[2], S. KUTTEROLF[3], J. CURTIS[4], A. SCHWALB[1]

1 Institut für Geosysteme und Bioindikation, Technische Universität Braunschweig, Langer Kamp 19c, 38106 Braunschweig, Germany
2 Instituto de Geología, Universidad Nacional Autónoma de México, Ciudad Universitaria, 04510 México, D.F. Mexico
3 GEOMAR Helmholtz-Zentrum für Ozeanfoschung, Kiel, Wischhofstr. 1-3, 24148 Kiel, Germany
4 Deparment of Geological Sciences and Land Use and Environmental Change Institute, University of Florida, Gainesville, FL.USA.

The northern Neotropics is a key region for understanding past climatic changes and their role in shaping the actual environment. Lake sediments from this region are highly sensitive recorders of such climatic variations but only a few have preserved continuous Pleistocene/Holocene-age deposits, because most of the lakes were dry during the last glacial period, especially at the end of the deglaciation (Hodell et al. 2008). Seismic reflection surveys in Lake Petén Itzá revealed its potential for obtaining high quality sedimentary records in the lowlands of Guatemala (Anselmetti et al., 2006). Therefore, seven long cores (PI-1, PI-2, PI-3, PI-4, PI-6, PI-7 and PI-9) were retrieved under the auspices of the Lake Petén Itzá Scientific Drilling Project (PISDP) in 2006. The complete sedimentary record of all drill sites was believed to extend back to 200 ka (Mueller et al., 2010). Established correlations by chemical fingerprinting to well-dated proximal tephras (e.g., L-Fall tephra from Amatitlán Caldera, Guatemala, 191 ka; W-Fall tephra from Atitlán Caldera, Guatemala, 159 ka) yielded new age constraints for the older sediment successions. The resulting tephrochronology of lacustrine ash layers from sites PI-1 and PI-7 (retrieved from water depths of 65 m and 46 m) suggests that the stratigraphic sequence in hole PI-1 and PI-7 extends back to 230 - 210 ka and at least to 280 - 260 ka, respectively; however, the establishment of the age model is still in progress. The paleoclimatic history of the last 85 ka in the northern Neotropics, inferred by multiproxy analysis (magnetic susceptibility, density,

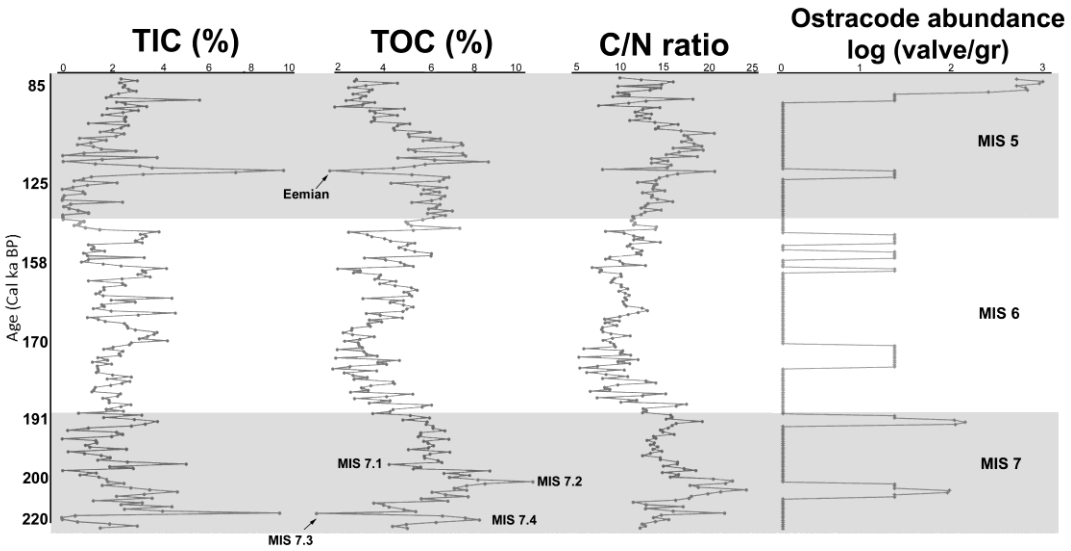

Fig 1. Geochemical parameters and ostracode abundance of core PI-1 from Lake Petén Itzá, Guatemala, with preliminary age assignments.

stable isotopes, pollen and ostracodes) suggests alternating environmental conditions, such as a cold and wet Last Glacial Maximum (LGM), a cold and dry Heinrich Stadial 1, warm and wetter conditions during the Bølling-Allerød, dry episodes during the Younger Dryas as well as warm and wetter conditions during the early Holocene. Hodell et al. (2012) found evidence of extreme cooling during Heinrich Stadial 1 in the Neotropics, being up to 10°C cooler in comparison of modern temperatures. Escobar et al. (2012) and Pérez et al. (2013) showed that the variations in oxygen and carbon isotope values registered in ostracode shells represent hydrological changes coinciding with Heinrich Stadials, LGM and the Deglacial. Previous work, however, was restricted to the past 85 ka and only very little information is available from aquatic organisms such as ostracodes, which react to climate and environmental changes faster than terrestrial proxies. Therefore, this work provides with first evidences of environmental change based on a combination of aquatic organisms (ostracodes) and geochemical indicators from the age window of 260 - 85 ka.

The main scientific objectives of this study are: (1) the quantitative inference of lake level changes during the past 260 ka by expanding the original training set and further refining transfer functions for ostracodes, (2) reconstruction of the ultrastructure of late Pleistocene climate extremes (for example 50, 85 and 150 ka) by using fossil ostracode assemblages and geochemical indicators from samples collected during a core sampling party at the National Lacustrine Core Facility (LacCore), University of Minnsota, Minneapolis, in August 2013.

Ostracode training set and transfer functions

The original training set consisted of autoecological information of 29 ostracode species from 50 aquatic ecosystems. This training set was extended by sampling 50 additional systems in the Yucatán Peninsula and northern Central America (Guatemala, El Salvador, Honduras and Nicaragua). To refine the transfer functions for water depth we sampled three large lakes (Bacalar, Chichancanab and Amatitlán). This sampling was conducted during the rainy season in summer/fall 2013, following a gradient of precipitation, conductivity and altitude. We found a total of 60 ostracode species in 2013, most of the species are endemic and nine species display a continental or worldwide distribution. Species optima and tolerances are being determined to identify species sensitivity to climatic and environmental changes. Transfer functions will be improved using the new species information.

Late Pleistocene climatic changes inferred by fossil ostracode assemblages and geochemical indicators

Results from geochemical analysis (total organic carbon, TOC; total inorganic carbon, TIC, C/N ratios), displays highest TIC concentrations during Marine Isotope Stage (MIS) 5 and MIS 7, while lower values of TIC characterize MIS 6. The TOC values exhibit several sudden changes during MIS 7 and MIS 5. These peaks correlate with the presence and absence of ostracode species, suggesting high environmental variability during these warm stages (see Figure 1).

Basal sediments of core PI-1, dated to approximately 220 ka, correspond to MIS 7. In general, MIS 7 was characterized by drastic fluctuations of TIC (0 to 8 %) and TOC values (2 to 10 %), these fluctuations were preliminarily assigned to the climatic interval variations (7.1 to 7.5) observed in Antarctica ice cores (Dome C) during the same period (Jouzel et al., 2007). The period identified as MIS 7.4 is characterized by a peak of TOC values of 8 % and C/N ratios of 15. This would suggest significant input of terrestrial organic matter, high lake productivity and humid climate. Both MIS 7.3 and 7.2 are characterized by maximum C/N ratios of up to 22, attesting to high input of terrestrial matter during wet periods. The ostracode assemblage is composed of two tropical species: *Cytheridella ilosvayi* and *Cypria petenensis*, suggesting that temperatures remained warm during this period. During MIS 7.1, the values of TOC (4 %), TIC (5.5 %) and C/N ratios (16) may suggest a short-lived dry and warm period. Further work, however, is needed to test these climatic correlations and assumptions.

During the cold stage MIS 6, decreasing C/N ratios attest to a decrease in terrestrial input and thus drier climate. Ostracode diversity during this period was low, with periods of exclusive presence of *C. petenensis* and periods with dominance of *Darwinula stevensoni*, *Candonidae* sp. and *Cyprididae* spp. At the beginning of the period *C. petenensis* was the dominant species, suggesting moderately warm conditions, because this species inhabits warm waters but can also tolerate temperate climates. At the end of MIS 6, the ostracode assemblage experienced a species replacement, characterized by absence of tropical species and presence of temperate species such as *Darwinula stevensoni*, *Candonidae* sp. and *Cyprididae* spp. This indicates a change to colder climate. During the entire period, however, most of the valves found were broken, probably caused by high energy levels during deposition.

During MIS 5 a peak of low TOC values (<2 %) around 120 ka, is tentatively correlated to the Eemain interglacial period (MIS 5.5). In this period TIC values reached 10 % and C/N ratios values of around 5, respectively. This suggests low input of terrestrial organic matter and thus dry conditions. Again, ostracode valves were mostly broken, probably due to the drastic changes in lake level during this period. Shortly after the Eemian period TOC values increase drastically up to 9 %, TIC values remain low (1.6 %) and C/N ratios were about 15, suggesting rather warm and humid conditions. Between 100 and 85 ka TOC values decrease (4.5 to 2 %), TIC values increase (from 2 to 6 %) and C/N ratios decrease (from 15 to 6), indicating a drying and cooling trend. Interestingly, at around 85 ka, ostracode abundance reaches a maximum of up to 1000 valves per gram with dominance of the nektobenthic species *C. petenensis* and the benthic species *Typhlocypris* sp., suggesting a significant input of littoral ostracodes. Our results are consistent with Mueller et al. (2010), who suggested a drastic lake level drop during this time based on lake sediment grain size composition (gravels, coarse sand) and abundance of gastropods. This work highlights the importance of multiproxy analysis, especially the complementarity of biological and geochemical records.

Acknowledgements

This work was supported by DFG-project SCHW 671/16-1 and CONACYT, Mexico, through scholarships 218639, 213456 to the first two authors.

References:

Anselmetti, F. S., D. A. Hodell, M.M. Hillesheim, M. Brenner, A. Gilli, J.A. McKenzie, Mueller, A.D., 2006. Late Quaternary climate-induced lake level varitions in Lake Petén Itzá, Guatemala, inferred from seismic stratigraphic analysis. Palaeoclimatology, Palaeoecology 230, 52-69.

EPICA COMMUNITY MEMBERS et al., 2004. Eight glacial cycles from an Antarctic ice core. Nature 249, 623-628.

Escobar, J., Hodell, D.A., Brenner, M., Curtis, J.H., Gilli, A., Müller, A.D., Anselmetti, F.S., Ariztegui, D., Grzesik, D.A., Pérez, L., Schwalb, A., Guilderson, T.J., 2012. A ~43-ka record of paleoenvironmental change in the Central American lowlands inferred from stable isotopes of lacustrine ostracods. Quaternary Science Reviews 37, 92-104.

Hodell, D.A., Anselmetti, F., Ariztegui, D., Brenner, M., Bush M. B., Correa-Metrio, A., Curtis, J.H., Escobar, J., Gilli, A.,Grzesik, D.A., Guilderson, T.P., Kutterolf, S., Mueller, A.D., 2008. An 85-ka Record of Climate Change in LowlandCentral America. Quatern. Sci. Rev. 27, 1152-1165.

Hodell , D. A., Turchyna, A.V., Wisemana, C.J., Escobar, J., Curtis, J.H., Brenner, M., Gilli, A., Mueller, A.D., Anselmetti F., Ariztegui D., Brown, E.T., 2012. Late Glacial temperature and precipitation changes in the lowland Neotropics by tandem measurement of δ18O in biogenic carbonate and gypsum hydration water. Geochimica et Cosmochimica Acta 77, 352-368.

Jouzel, J., Masson-Delmonte, V., Cattani, O., Dreyfus, G., et al. 2007. Orbital and millennial Antarctic climate variability over the past 800,000 years. Science 317, 793-796.

Mueller, A., F. Anselmetti, D. Ariztegui, M. Brenner, D. Hodell, J. Curtis, J. Escobar, A. Gilli, D. Grzesik, T. Guilderson, S. Kutterolf, Plötze, M., 2010. Late Quaternary palaeoenvironment of northern Guatemala: evidence from deep drill cores and seismic stratigraphy of Lake Petén Itzá, Sedimentology 57, 1220-1245.

Pérez, L., Curtis, J., Brenner, M., Hodell, D., Escobar, J., Lozano, S., Schwalb, A., 2013. Stable isotope values (δ18O & δ13C) of multiple ostracode species in a large Neotropical lake as indicators of past changes in hydrology. Quaternary Science Reviews 66, 96-111.

ICDP

INFLUINS Deep Drilling Campaign: Data of borehole geophysical and multi sensor core logger measurements

P. METHE, A. GOEPEL, N. KUKOWSKI

Friedrich Schiller Universität Jena, Institut für Geowissenschaften, Burgweg 11, 07749 Jena, pascal.methe@uni-jena.de

In the framework of INFLUINS (INtegrated FLUid dynamics IN Sedimentary basins), we aim for the coupled dynamics of near surface and deep fluids in a sedimentary basin on various scales, ranging from the pore scale to the basin scale. This is essential to understand the functioning of sedimentary basins' fluid systems and therefore e.g. drinking water supply or subsurface storage. INFLUINS is focusing on the Thuringian Basin, a well-confined, easily accessible intra-continental sedimentary basin, serving as a natural geo laboratory. Therefore it is also a perfect candidate for deep drilling.

In 2013, drilling a 1179 m meter deep scientific borehole in the center of the Thuringian Basin (Germany) was a central target. In order to characterize rock physical properties on samples, coring was done in the potential aquifers and aquitards of the Muschelkalk and Buntsandstein. Furthermore, extensive borehole geophysical measurements (e.g. caliper, density, porosity, acoustic borehole televiewer, sonic and more) were undertaken along the whole depth to determine the borehole characteristics and in-situ rock geophysical properties in the open hole. Immediately after the drilling campaign, all core samples were petrophysically characterized with a multi sensor core logger (MSCL).

From the borehole geophysical logs, small embedded layers with a thickness of a few cm were resolvable in the rock salt of the Salinarrot formation in the Upper Buntsandstein, due to the high sampling rates during wireline logging. The Salinarrot formation consists of primarily rock salt with thin layers of claystone, anhydrite and sometimes dolomitic rocks. Density and sonic log values of the INFLUINS bore hole are suitable for the cluster analysis, due to their significant change between the lithostratigraphic units. The combined petrophysical datasets allow to resolve rock properties on the cm scale. The aim for this attempt is to obtain a lithologic description by downhole logs including the benefit of the high spatial resolution offered by the MSCL measurements, but independent from core descriptions. We test if this strategy enables to estimate lithologic informations of borehole sections where no coring was done. Since core descriptions are available for sections of Muschelkalk and Buntsandstein, it is possible to directly evaluate these estimates.

ICDP

Wet Glacials and Dry Interglacials in the Southern Levant? Preliminary Evidence from Pollen Analyses

C. CHEN, A. MIEBACH, T. LITT

Steinmann Institute of Geology, Mineralogy, and Paleontology, University of Bonn, Nussallee 8, 53115 Bonn, Germany

The Dead Sea is located at the lowest place on earth between the Mediterranean and Arabian-Sahara climate zones. It serves as a valuable archive for understanding the climate, vegetation, and settlement history of the southern Levant. Current vegetation territories converge in this area because of the steep precipitation gradient. Hence, pollen assemblages in the Dead Sea sediment document shifting of the vegetation belts. A previous study confirms sensitive response of Holocene Levantine vegetation to climate change and human activities (Litt et al., 2012). It further quantitatively reconstructs climate parameters based on botanical-climatological transfer functions.

Deep drilling cores were retrieved from the northern Dead Sea Basin in the framework of the International Continental Scientific Drilling Program (ICDP) in 2010/2011. These cores enable a long sedimentary record through glacial-interglacial cycles (Stein et al., 2011). Changes in the lithology suggest wet glacials and dry interglacials (Neugebauer et al., 2014). The major goal of our study is to reconstruct the vegetation history with a detailed time resolution and shed light on the environmental conditions of Levantine hominin dispersal.

Our preliminary results suggest in general steppe is the prevailing vegetation, and deciduous oaks are the most common trees. The MIS 6/5 transition is characterized by an increase of desert elements. The early MIS 5 shows higher woodland density with frequent occurrence of sclerophylls. A gravel layer occurs between 109.99 and 116.65 ka BP (Torfstein et al., 2015) and suggests a depositional hiatus. The remaining Last Interglacial witnesses a gradual steppe expansion. During most of the Last Glacial, only patches of thermophilous trees are growing in the region, and semiarid conditions prevail. Our results from Lake Kinneret (Sea of Galilee) in the upstream of the Dead Sea also suggest there is no Mediterranean vegetation belt in the vicinity (unpublished). During the late MIS 2, temperate pioneer trees occur in the open landscape. Most arid periods are indicated during Termination I and II.

Our study provides independent evidences of Levantine climate changes in terms of paleobotany. Combining with other paleoenvironmental proxies and lake level reconstructions of the Dead Sea Basin (e.g., Bookman et al., 2006), we will contribute to a more comprehensive understanding of the paleoenvironment. Pollen-based quantitative investigations will be carried out in light of the Holocene counterpart.

References:

Bookman, R., et al., 2006. Quaternary lake levels in the Dead Sea basin: Two centuries of research. Geological Society of America special papers 401, 155-170.

Litt, T., et al., 2012. Holocene climate variability in the Levant from the Dead Sea pollen record. Quaternary Science Reviews 49, 95-105.

Neugebauer, I., et al., 2014. Lithology of the long sediment record recovered by the ICDP Dead Sea Deep Drilling Project (DSDDP). Quaternary Science Reviews 102, 149-165.

Stein, M., et al., 2011. Dead Sea Deep Cores: A Window Into Past Climate and Seismicity. Eos, Transactions, American Geophysical Union 92 (49), 453-454.

Torfstein, A., et al., 2015. Dead Sea drawdown and monsoonal impacts in the Levant during the last interglacial. Earth and Planetary Science Letters 412, 235-244.

ICDP

Archean spherule layers in the Barberton Greenstone Belt, South Africa: Discovery of extra-terrestrial component carrier phases

T. MOHR-WESTHEIDE[1], D. HÖHNEL[1], J. FRITZ[1], R.T. SCHMITT[1], W.U. REIMOLD[1,2], T. SALGE[3,4], C. KOEBERL[5,6], A. HOFMANN[7]

1 Museum für Naturkunde - Leibniz Institute for Evolution and Biodiversity Science, Invalidenstrasse 43, 10115 Berlin, Germany.
2 Humboldt-Universität zu Berlin, Unter den Linden 6, 10099 Berlin, Germany.
3 Bruker Nano GmbH, Berlin, Germany.
4 Science Facilities, Natural History Museum, London, UK.
5 Department of Lithospheric Research, University of Vienna, 1090 Vienna, Austria.
6 Natural History Museum, 1010 Vienna, Austria.
7 Department of Geology, University of Johannesburg, Johannesburg, South Africa.

Introduction

The oldest known remnants of large bolide impacts onto Earth are represented by ca. 3.47-3.2 Ga old Archean spherule layers of the Barberton Greenstone Belt (BGB) in South Africa and the Pilbara craton in West Australia [1,2]. The spherules are interpreted as molten impact ejecta and condensation products from impact plumes or ejecta that were melted during atmospheric reentry [2,3]. Therefore, the primary signatures preserved in the spherule layers may give insights regarding Archean impact event(s) and the nature of the extraterrestrial projectiles involved. Selected samples of these spherule layers contain ultra-high concentrations of Platinum Group Elements (PGE), which are in many cases in excess of chondritic abundances. These enrichments are caused by an anomalously high amount of an extra-terrestrial component (ETC) deposited in these layers, and were used to propose very large projectile sizes responsible for these impact layers [e.g., 1,2].

Cores drilled within the framework of the 2011 “Barberton Drilling Project: Peering into the Cradle of Life”, supported by the International Continental Scientific Drilling Program (ICDP), penetrated mid-Archean supracrustal rocks. The BARB5 drill core, containing parts of the 3.26 Ga old Fig Tree Group, hosts several spherule layers in the depth interval 511 - 513 m. These spherule layers are investigated by a multidisciplinary and multinational consortium comprising working groups at the Museum für Naturkunde Berlin, University of Johannesburg, University of Vienna, University of Cardiff, and CRPG-CNRS-Nancy. The research conducted by the working groups in Berlin and Vienna focuses on the identification of the carrier phases of the extraterrestrial component.

Analytical methods

The samples were investigated at the Museum für Naturkunde Berlin by transmitted and reflected light microcopy, electron microprobe analysis (EMPA), and scanning electron microscopy (SEM), including energy dispersive X-ray spectroscopy (EDX) at low voltage (6kV). The BRUKER QUANTAX EDS system was applied for automated feature analysis. This method combines chemical data with morphological features in order to detect and classify minerals [4]. The necessary EDX spectra were acquired by point measurements in the center of each grain or by scanning the complete grain area. Bulk material of the spherule layers was studied by XRD. Instrumental neutron activation analysis (INAA) at the University of Vienna was used to determine trace elements for the spherule layers. Therefore, a continuous section of the depth interval from 511.29 - 511.51 m was cut into 22 individual subsamples and analyzed.

Results

In the BARB5 drill core, five spherule layers were found in the depth interval 511 to 513 m. This depth interval fits stratigraphically into the sequence hosting the previously studied spherule layers S3/S4 [e.g., 5,7]. Nevertheless, the spherule layers in BARB5 could also represent a so far unknown spherule layer. For clarification we termed the spherule layers with letters A to E from bottom to top. The lowermost spherule layer A occurs at 512.30 m depth and is up to 10 cm thick. Following a sequence of cm- to dm-wide shale and chert layers, the further spherule layers B to E (from bottom to top) were observed in the core interval 511.29 - 511.51 m depth. In this interval four ca. 4 cm thick spherule layers are recognized, which are separated by <1.5-cm-thick shale bands. Between spherule layers B and C cross-lamination is observed. All spherule layers comprise densely packed, 0.3 - 2 mm sized spherules. At a depth of ~511.0 m some individual spherule grains were found embedded in chert. Although the chemical compositions of the spherules have been almost completely changed by alteration, some primary characteristics, including the total amount of spherules, the spherule sizes, their shapes, and some mineralogical features are preserved.

Spherule layers A and C to E are composed of generally undeformed or only slightly deformed spherules. In contrast, the spherules on top of layer B are strongly sheared. The apparent spherule size determined by statistical analysis did not indicate sorting of the individual spherule beds. The average values of spherule size are for A: 0.99 mm, B: 0.75 mm, C: 0.72 mm, D: 0.79 mm, and E: 0.87 mm. The average spherule size in the lowermost layer A is, at best, only marginally increased in comparison to spherule layers B to E above. Overall, spherules in all layers are invariably diverse in size (0.27-2.03 mm) and do not show gradation – in contrast to previous studies of spherule occurrences in this stratigraphic interval from other locations [6].

The microscopic investigation of the spherule layers reveals quartz - phyllosilicate - K-feldspar - Mg-siderite - barite - calcite assemblages are indicative of pervasive alteration. XRD analysis confirmed these observations and determined quartz, muscovite, K-feldspar, chlorite, siderite, dolomite/ankerite, and - in some subsamples - pyrite as main minerals in the BARB5 spherule layers. Local sulfide mineralization is clearly of secondary origin. A rare but important relict of the primary mineral composition is the occurrence of nickel-rich chromium-spinel (Ni-Cr-spinel). Only the upper layers C to D contain Ni-Cr-spinel, whereas Ni-Cr-spinel is missing in layers A and B. These Ni-Cr-spinels show distinct zonation with respect to Fe, Ni, Zn, and Cr contents, as indicated by SEM-EDX analysis. Spinel fragments of shattered crystals frequently show marginal Zn-enrichment on all fragments – indicative of post-depositional alteration. Previous research reported Ni-Cr-spinels from S3 [e.g., 5].

Siderophile elements (Ni, Co, Ir, and Os), as well as Cr and Au, have distinctly elevated contents over the depth interval from 511.31 to 511.51 m (i.e., in spherules and interbeds), as indicated by INAA data of spherule layer and shale samples. The trace element measurement of spherule layer A by INAA is in progress. The layer B has the lowest contents of siderophile elements with ca. 0.3 - 10 ppb Ir, 7 - 22 ppm Co, 80 - 730 ppm Cr, and 120 - 470 ppm Ni. In contrast, the highest amounts were detected in spherule

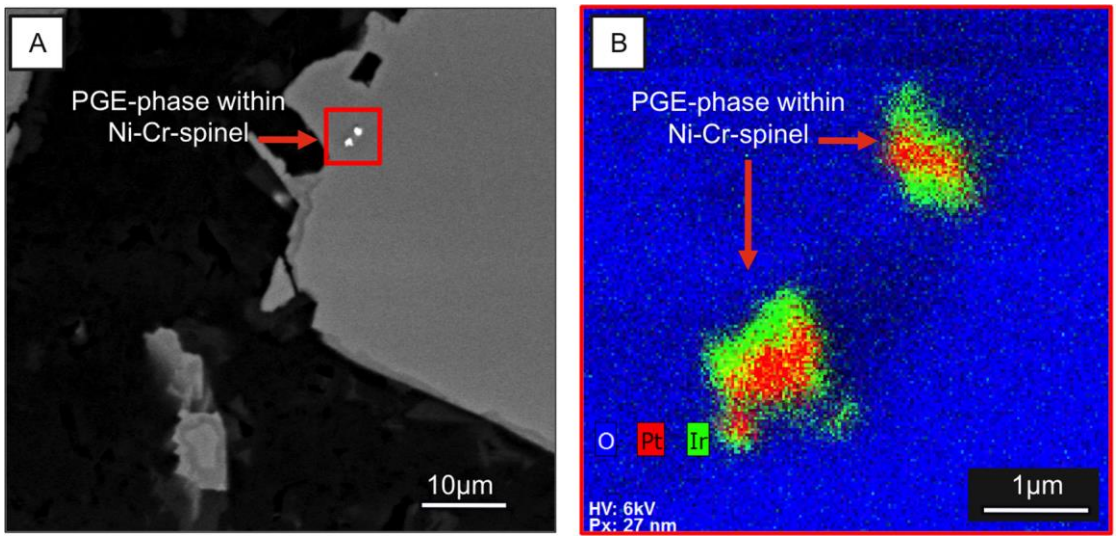

Fig. 1A. Back-scattered electron image of two PGE metal alloy grains within a Ni-Cr-spinel grain, BARB5 drill core, ~511.44 m depth, top of spherule layer D. **Fig. 1B.** Composite element map of heterogeneous composed PGE- and Ni-rich metal alloy grains, enlarged part of Fig. 1A.

layer C with ca. 600 ppb Ir, 250 ppm Co, 3500 ppm Cr and 3800 ppm Ni, and at the top of layer D with 730 ppb Ir, 530 ppm Co, 3200 ppm Cr and 5400 ppm Ni. Generally, in other parts of this section, the Ir content is in the range from 150 to 400 ppb. The high abundances of the siderophile elements including the PGE are caused by an extraterrestrial component, which locally exceeds significantly the contents of these elements in chondritic meteorites.

Clusters of Ni-Cr-spinel contain very small local areas of PGE enrichment as shown by SEM-EDX at high spatial resolution (e.g., Fig. 1A). Two different types of PGE enrichments were found: (i) PGE- and Ni-rich metal alloys in the form of micro-nuggets with sizes of 600-1400 nm (e.g., Fig. 1A). These metal alloys are composed mainly of Pt and Ni, which dominate the alloys with more than 40 at% each. Additional significant amounts of Ir, Os, Ru, Pd, and/or Rh, and Fe were recognized by low voltage EDX measurements (Fig. 1B). (ii) PGE sulfarsenide phases with sizes of 600-3000 nm occur mainly in the matrix, between internally broken Ni-Cr-spinel grains, have varied amounts of sulfur and arsenic, and are possibly the result of secondary overprint.

Interpretation

The BARB5 drill core contains in the depth interval 511 - 513 m five closely spaced spherule beds, which are separated by beds of fine-grained siliciclastic sediment. One of these sedimentary intervals (between spherule layers B and C) shows cross-lamination. The complete spherule-bearing interval could have been formed after a single impact event within an aquatic depositional environment with multiphase currents affecting/interrupting sedimentation. A strong hydrothermal overprint of all lithologies in this interval is indicated by our petrographic and geochemical investigations. In the main part the primary mineralogical composition of the spherule layers is completely altered. The only remnants of the primary mineral content observed so far are zircon and Ni-Cr-spinel. The Ni-Cr-spinel contains systematic variations in major element composition from core to rim (see also [5]) and unusually high Ni (and also V) concentrations compared to terrestrial chromium-spinel (see also [5,7]). An individual cluster of Ni-Cr-spinel has a more or less identical appearance and chemical composition. Nevertheless, the complete population of Ni-Cr-spinel clusters displays significant variation, which indicates that the Ni-Cr-spinels of these clusters have crystallized or condensed from phases of different compositions.

The Ni-Cr-spinels contain PGE- and Ni-rich metal alloys identified by high resolution SEM-EDX studies with feature analysis. These alloys are interpreted as a primary phase directly derived from the projectile or to represent condensates from the impact plume. Therefore, the Ni-Cr-spinels with their PGE- and Ni-rich metal alloy inclusions are the long-sought carrier phase for the extraterrestrial signature in Archean spherule layers from the Barberton Greenstone Belt. In contrast, the additionally observed PGE sulfarsenides could be the result of secondary alteration by S and As rich solutions. The local enrichment of Ni-Cr-spinel with the PGE- and Ni-rich metal alloy inclusions causes a micro-nugget effect that is responsible for the local, anomalous enrichment of siderophile elements and PGE in excess of meteoritic abundances.

The Ir abundance in spherule layer samples from the Barberton Greenstone Belt varies from 0.1 to 1518 ppb for S2 (avg. 116 ppb), 0.6-2730 ppb for S3 (avg. 164 ppb), and 7-450 ppb (avg. 128 ppb) for S4 samples, based on a comprehensiveliterature review. Our investigation of the BARB5 drill core reveals 0.3-735 ppb (avg. 290 ppb) Ir for spherule layers B - E. These Ir concentrations are of similar magnitude as those in layers S1 - S3/S4 and still suggest a 30-40% chondrite component, on average, for these layers. However, the present study has indicated that Ir concentrations in the spherule layers of the BARB5 core are the result of a heterogeneously distributed carrier phase (Ni-Cr-spinel with PGE- and Ni-rich metal alloys), and are also affected by secondary processes, as indicated by the occurrence of PGE sulfarsenides.

The identification of the ETC has major implications for the further evaluation of the Archean impact record. The heterogeneous incorporation of the meteoritic component in the spherule layers and the influence of secondary processes (e.g., hydrothermal alteration and mobilization of PGE) must be taken into consideration for the investigation and interpretation of the PGE contents of these layers. The estimation of the global fallout of ETCs and, thus, to constrain the sizes of projectiles and the impact magnitude for these Archean events [8], needs carefully determined PGE concentrations over the complete interval of the respective unit, excluding a local increase in thickness of the unit due to sedimentary focusing or repetitions.

Acknowledgements

Financial support from the Deutsche Forschungsgemeinschaft (DFG RE 528/15-1) is gratefully acknowledged.

References:
[1] Lowe D. R. et al. (1989) Science, 245, 959-962.
[2] Lowe D. R. et al. (2003) Astrobiology, 3, 7-47.
[3] Johnson B. C. and Melosh H. J. (2014) Icarus, 228, 347-363.
[4] Salge T. et al. (2013) Proc. 23rd IMCET, Turkey. 357-367.
[5] Byerly G. R. and Lowe D. R. (1994) Geochim. Cosmochim. Acta, 58, 3469-3486.
[6] Koeberl C. and Reimold W. U. (1995) Precambrian Research, 74, 1-33.
[7] Krull-Davatzes et al., (2012) Precambrian Research, 196-197, 128-148.
[8] Kyte et. al. (2003) Geology, 31, 283-286.

ICDP

Investigation of probable fluid pathways in NW Bohemia/Vogtland (German-Czech border region) by seismic travel-time tomography

S. MOUSAVI[1], K. BAUER[2], M. KORN[1]

1 Institut für Geophysik und Geologie, Universität Leipzig, Talstraße 35, 04103 Leipzig, Germany
2 Deutsches Geoforschungszentrum Helmholtz-Zentrum Potsdam, Germany

The West Bohemia/Vogtland region is one of the seismically most interesting areas in Europe because of magmatic processes in the intra-continental lithospheric mantle. This region is characterized by a series of phenomena distributed over a relatively large area, like occurrence of repeated swarm earthquakes, surface

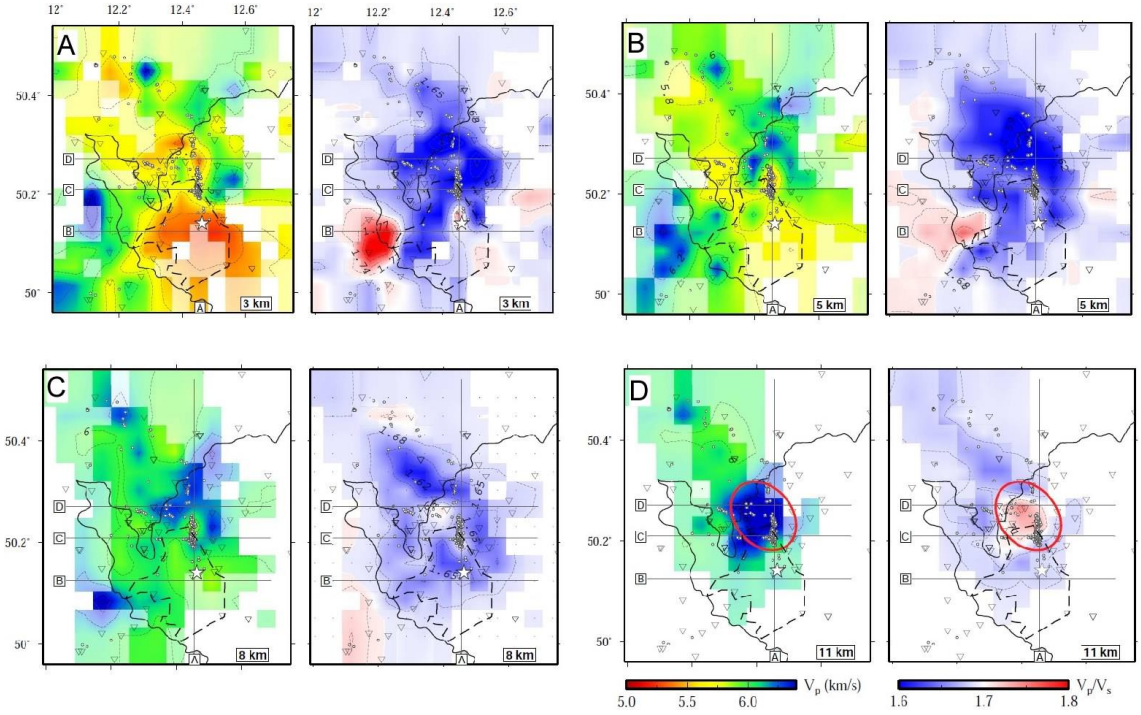

Fig. 1. Horizontal slices show Vp and Vp/Vs distribution at **(a)** 3 km, **(b)** 5 km, **(c)** 8 km and **(d)** 11 km depth. The location of profiles A, B, C and D are given for orientation. Seismic event locations are plotted as gray circles. The outline of the Cheb basin is shown as a dashed line. The white star indicates the location of the Bublák/Hartoušov mofette fields. Seismic event locations are plotted as gray circles. The outline of the Cheb basin is shown as a dashed line. The white star indicates the location of the Bublák/Hartoušov mofette fields.

exhalation of mantle-derived and CO_2-enriched fluids, mofettes, mineral springs, presence of mantle derived He isotopes and increased heat flow. Bohemian Massif is subdivided into three main zones Saxothuringian(ST) Zone, Moldanubian(MD) and Teplá-Barandian(TB). The tectonic structure of this region is rather complex. Cheb Basin, Eger Rift and Márianské Lázně Fault zone(MLF) are the main geological features of West Bohemia. Quaternary volcanoes are located close to Cheb Basin.

We present a local earthquake tomography study undertaken to image the Vp and Vp/Vs structure in the broader area of earthquake swarm activity. In comparison with previous investigations, more details of the near-surface geology, potential fluid pathways and features around and below the swarm focal zone could be revealed. In the uppermost crust, for the first time the Cheb basin and the Bublák/Hartoušov mofette fields were imaged as distinct anomalies of Vp and Vp/Vs. The well-pronounced low Vp anomaly of the Cheb basin is not continuing into the Eger rift indicating a particular role of the basin within the rift system (Fig. 1,a-d). A steep channel of increased Vp/Vs is interpreted as the pathway for fluids ascending from the earthquake swarm focal zone up to the Bublák/Hartoušov mofette fields (Fig. 2). As a new feature, a mid-crustal body of high Vp and increased Vp/Vs is revealed just below and north of the earthquake swarm focal zone (Fig. 1d). It may represent a solidified magmatic body which intruded prior or during the formation of the rift system. Fluids could propagate from the magmatic body along faults and rift-related structures into the focal zone and trigger earthquakes. We consider the intrusive structure as a heterogeneity leading to higher stress particularly at the junction of the rift system with the basin and prominenent fault structures. This may additionally contribute to the triggering of earthquakes.

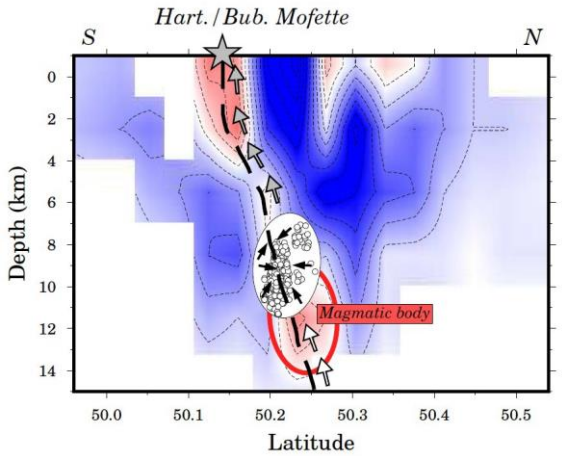

Fig. 2. Conceptual model showing major crustal features as imaged and interpreted in this study. The colored background represents the Vp/Vs distribution along profile A (Fig. 1). The indicated magmatic body was first identified and interpreted within the 11 km depth slices of Vp and Vp/Vs (Fig. 1d). Potential fluid pathways are identified based on a channel-like increased Vp/Vs structure. Crustal fluids and supercritical fluids from greater depths may trigger earthquakes and are mixed before their ascend to the Bublák/Hartoušov mofette fields.

References:

Mousavi, S., Bauer, K., Korn, M. & Hejrani B., 2015. Seismic tomography reveals a mid-crustal magmatic body, fluid pathways and their relation to the earthquake swarms in West Bohemia/Vogtland. Geophysical Journal International (submitted).

IODP

The Mid Pleistocene Transition in the Gulf of Alaska (NE Pacific): A multi-proxy record of palaeoenvironmental and climatic changes

J. MÜLLER[1], O. ROMERO[2], E. COWAN[3], E. MCCLYMONT[4], R. STEIN[1], K. FAHL[1], K. MANGELSDORF[5], H. WILKES[5]

1 Alfred Wegener Institute Helmholtz Center for Polar and Marine Research, Bremerhaven, Germany
2 MARUM - Center for Marine Environmental Sciences, Universität Bremen, Germany
3 Department of Geology, Appalachian State University, Boone, USA
4 Department of Geography, Durham University, UK
5 Department of Organic Geochemistry, GFZ Potsdam, Germany

A remarkable sedimentary record that extends from the Miocene to the late Pleistocene has been drilled during IODP Expedition 341 (May - July 2013) in the Gulf of Alaska (Expedition 341 Scientists, 2014). The recovery and examination of sediments along a transect of five drill sites (U1417 - U1421) from the deep ocean towards the continental slope and shelf offshore the St. Elias Mountains enables the reconstruction of the palaeoceanographic and environmental development in the NE Pacific during a period of significant global cooling and directly addresses the overall climate research objectives of the IODP programme.

The knowledge about palaeo sea surface conditions and their relation to climate changes in the subpolar NE Pacific is relatively scarce and mainly confined to the past 17 ka BP (Addison, 2012; Davies, 2011; Barron, 2009). Within

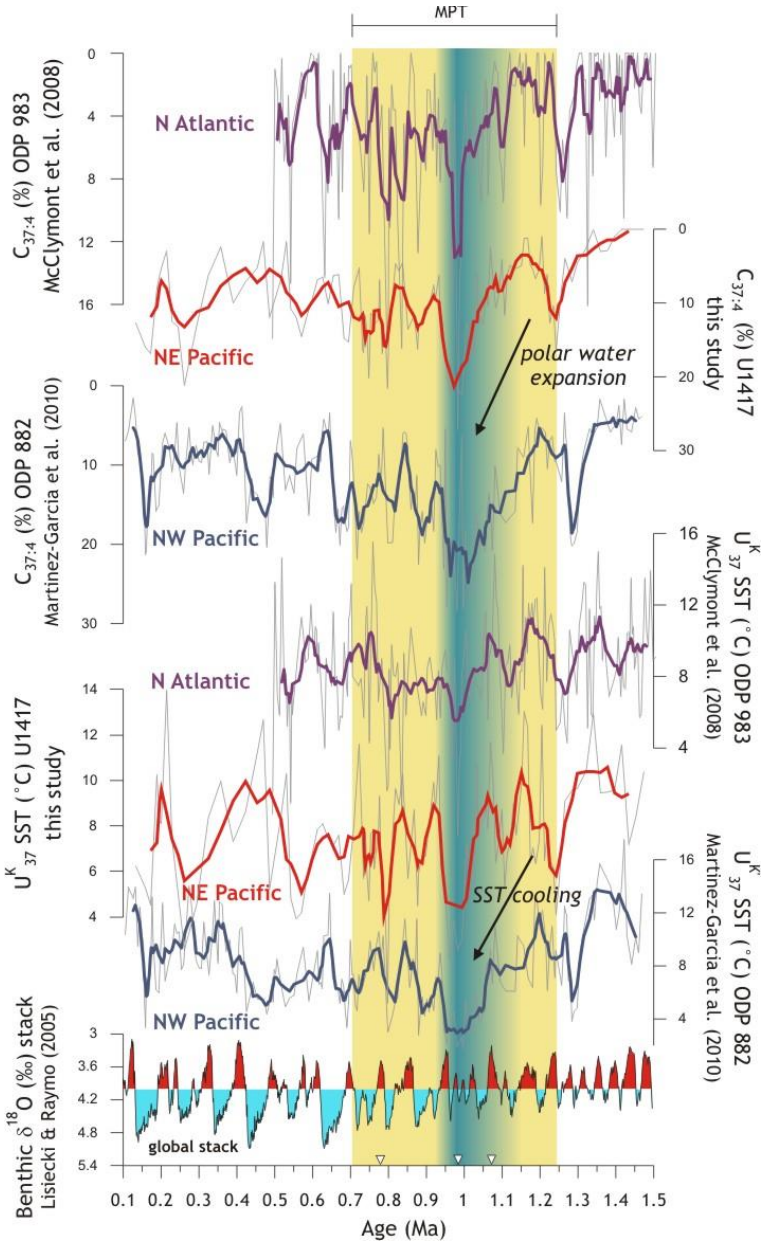

Fig. 1. Comparison of Mid to late Pleistocene (CI-MS) UK37 sea surface temperatures and C37:4 alkenone percentages for IODP site U1417 (Gulf of Alaska) with published records for ODP site 882 in the NW Pacific and ODP site 983 in the North Atlantic. The preliminary age model for site U1417 is based upon shipboard biostratigraphy and palaeomagnetic data. Colour shading indicates the transition from 41 ka (low-amplitude) to 100 ka (high-amplitude) glacial oscillations in the global benthic $\delta^{18}O$ record and the 1 Ma cooling event (blue).

the **PECA** project (Plio-**P**leistocene **E**nvironmental and **C**limatic conditions in the Gulf of **A**laska), Expedition 341 sediments are investigated for their biomarker inventory to reconstruct the sea surface conditions (i.e. sea surface temperature (SST), sea ice coverage, marine primary productivity) that characterised the subpolar NE Pacific during critical time intervals of Plio- and Pleistocene climate change. These data provide new information on oceanic and atmospheric feedback mechanisms and they further allow the identification of teleconnections between the palaeoceanographic evolution in the North Pacific and the North Atlantic.

The Mid Pleistocene Transition (MPT) between 1.25 Ma and 0.7 Ma ago constitutes a fundamental shift in Earth's climate system from a 41 ka to a 100 ka periodicity in glacial oscillations (Elderfield et al., 2012). The exact timing and the mechanisms that caused this shift from a low- to a high-amplitude glacial variability are still under debate. Most studies targeting the MPT are based on Atlantic sediment records whereas only few data sets are available from the North Pacific (see Clark et al., 2006 and McClymont et al., 2013 for reviews). IODP Expedition 341 distal deep-water site U1417 now provides a continuous sediment record for reconstructing Pleistocene changes in the sea surface conditions and their linkage to ice-sheet fluctuations on land. Here we present organic geochemical biomarker data covering the 1.5 Ma to 0.1 Ma time interval with special focus on the MPT. To fully exploit the environmental information archived within these sediments and to complement the biomarker results we integrated microfossil and sedimentological data.

Variability in the distribution and abundance of alkenones, sterols, C_{25}-highly branched isoprenoids (HBIs), and short- and long-chain *n*-alkanes is interpreted to reflect changes in SST, marine primary productivity, and the input of terrigenous organic matter via iceberg, sea ice, meltwater or aeolian transport. Previously, Rowland et al. (2001) documented that not only the degree of unsaturation in C_{25}-HBIs but also the *E*- to *Z*-isomerisation in the C_{25}-HBI trienes increases with increasing water temperature. Based on this observation we suggest that the ratio of the *Z*-isomer to the *E*-isomer in the C_{25}-HBI trienes might reflect SST changes and could be used as an additional qualitative SST proxy. The applicability of this approach, however, needs further evaluation. The diatom concentration and the species composition of the diatom assemblage allow estimates of palaeoproductivity and nutrient (silicate) availability. Information about ice-sheet dynamics (and associated iceberg calving) and sea ice coverage is derived from ice rafted detritus (IRD) data.

The SST record of site U1417 is in remarkably close agreement with published records from ODP site 882 in the NW Pacific and ODP site 983 in the North Atlantic. All records depict significant temperature fluctuations and a pronounced cooling and expansion of polar water at about 1 Ma ago (Fig. 1). This synchronous Northern Hemisphere ocean cooling event seems to be associated with the relatively weak interglacials during Marine Isotope Stages 29 and 27. Interestingly, at site U1417 the onset of the cooling about 1.03 Ma ago coincides with a peak deposition of IRD, whereas during the following temperature minimum (1.02 Ma - 0.96 Ma) only moderate or even minimum amounts of IRD reach the core site (Fig. 2). This observation of a reduction in IRD deposition along with decreasing ocean temperatures may point to the formation of landfast sea ice that hampers the calving of icebergs and their export from coastal to distal ocean areas in the Gulf of Alaska. An alternative explanation could be a change in the oceanic and/or atmospheric circulation (governing iceberg drift patterns). The abundance of diatoms, however, seems to be decoupled from SST changes and clearly coincides with short-term maxima in terrigenous organic matter deposition (high TAR values) and IRD minima (Fig. 2). The inverse relationship between IRD content and TAR values suggests that a high portion of terrigenous biomarker lipids is transported towards the core site by wind or meltwater rather than by icebergs. In this context, aeolian dust (and land-plant biomarker) input is a probable mechanism to stimulate diatom productivity through the supply of iron.

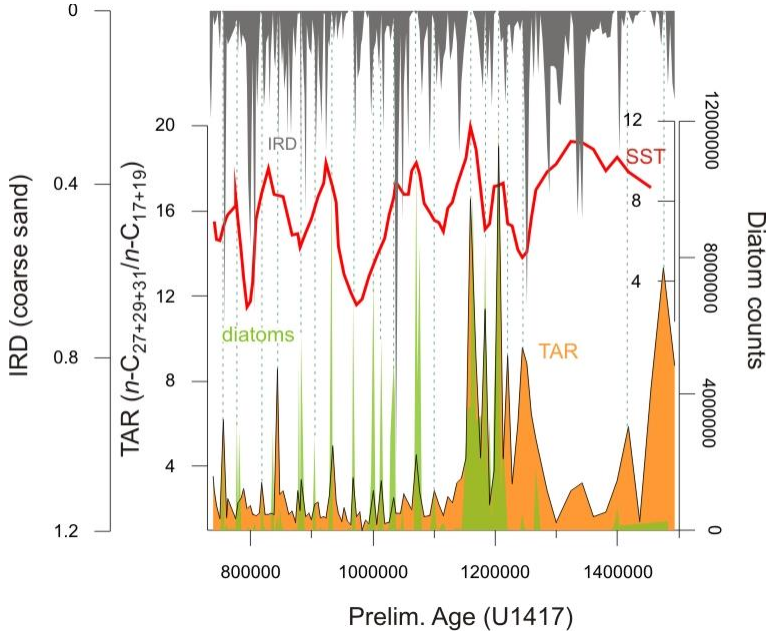

Fig. 2. Mid Pleistocene diatom counts, ice rafted detritus (IRD) abundance, ratio of terrigenous vs. aquatic biomarker lipids (TAR) and U^{K}_{37} sea surface temperatures for site U1417. Dashed lines indicate coincident diatom and TAR maxima during intervals of minimum IRD deposition.

We further examined the distribution of the *Z*- and *E*-isomers of the C_{25}-HBI triene and the applicability of the *Z*/*E* ratio as potential SST proxy. Apart from maximum *Z*/*E* ratios during the 1 Ma cooling event we observe only a weak relationship between U^{K}_{37} derived SSTs and the *Z*/*E* record. However, a distinct correlation exists between the *Z*/*E* record and compound-specific $\delta^{13}C$ values of the land-plant biomarker alkane *n*-C_{31}. Shifts in the carbon isotopic composition of land-plant biomarkers are often referred to as indicators of changes in the precipitation conditions (with high/low $\delta^{13}C$ values characterstic for dry/wet periods). The minimum $\delta^{13}C$ values, suggestive of wet conditions during the 1 Ma cooling event, thus might be an important hint for an elevated atmospheric moisture transport promoting Cordilleran ice-sheet growth during the MPT.

References:

Addison, J.A., Finney, B.P., Dean, W.E., Davies, M.H., Mix, A.C., Stoner, J.S., Jaeger, J.M., 2012. Productivity and sedimentary $\delta^{15}N$ variability for the last 17,000 years along the northern Gulf of Alaska continental slope. Paleoceanography, 27 (1), PA1206.

Barron, J.A., Bukry, D., Dean, W.E., Addison, J.A., Finney, B., 2009. Paleoceanography of the Gulf of Alaska during the past 15,000 years: Results from diatoms, silicoflagellates, and geochemistry. Marine Micropaleontology, 72 (3–4), 176-195.

Clark, P.U., Archer, D., Pollard, D., Blum, J.D., Rail, J.A., Broken, V., Mix, A.C., Pisias, N.G., Roy, M., 2006. The middle Pleistocene transition: characteristics, mechanisms, and implications for long-term changes in atmospheric pCO2. Quaternary Science Reviews, 25, (23–24), 3150-3184.

Davies, M.H., Mix, A.C., Stoner, J.S., Addison, J.A., Jaeger, J., Finney, B., Wiest, J., 2011. The deglacial transition on the southeastern Alaska Margin: Meltwater input, sea level rise, marine productivity, and sedimentary anoxia. Paleoceanography, 26 (2), PA2223.

Elderfield, H., Ferretti, P., Greaves, M., Crowhurst, S., McCave, I.N., Hodell, D., Piotrowski, A.M., 2012. Evolution of Ocean Temperature and Ice Volume Through the Mid-Pleistocene Climate Transition. Science, 337, (6095), 704-709.

Expedition 341 Scientists, 2014. Southern Alaska Margin: interactions of tectonics, climate, and sedimentation. IODP Prel. Rept., 341. doi:10.2204/iodp.pr.341.2014

Lisiecki, L.E., Raymo, M.E., 2005. A Pliocene–Pleistocene stack of 57 globally distributed benthic d18O records. Paleoceanography 20, PA1003.

Martínez-Garcia, A., Rosell-Melé, A., McClymont, E.L., Gersonde, R., Haug, G.H., 2010. Subpolar Link to the Emergence of the Modern Equatorial Pacific Cold Tongue. Science, 328, (5985), 1550-1553.

McClymont, E.L., Sosdian, S.M., Rosell-Melé, A., Rosenthal, Y., 2013. Pleistocene sea-surface temperature evolution: Early cooling, delayed glacial intensification, and implications for the mid-Pleistocene climate transition. Earth-Science Reviews, 123, 173-193.

McClymont, E.L., Rosell-Melé, A., Haug, G.H., Lloyd, J.M., 2008. Expansion of subarctic water masses in the North Atlantic and Pacific oceans and implications for mid-Pleistocene ice sheet growth. Paleoceanography, 23, (4), PA4214.

Rowland, S.J., Allard, W.G., Belt, S.T., Masse, G., Robert, J.M., Blackburn, S., Frampton, D., Revill, A.T., Volkman, J.K., 2001. Factors influencing the distributions of polyunsaturated terpenoids in the diatom, Rhizosolenia setigera. Phytochemistry, 58 (5), 717-728.

ICDP

Petrological and geochemical investigation related to the “Wadi Gideah” cross-section in the southern Oman ophiolite: constraints on fast-spreading crust accretion processes in the frame of the ICDP project "The Oman drilling project"

T. MÜLLER[1], J. KOEPKE[1], D. GARBE-SCHÖNBERG[2], H. STRAUSS[3], B. ILDEFONSE[4]

1 Institut für Mineralogie, Leibniz Universität Hannover, Germany (t.mueller@mineralogie.uni-hannover.de)
2 Institut für Geowissenschaften, Christian-Albrechts-Universität zu Kiel, Germany
3 Institut für Geologie und Paläontologie, Westfälische Wilhelms-Universität zu Münster, Germany
4 Géosciences Montpellier, Université Montpellier 2, France

Fast-spreading oceanic crust, which covers a large part of our planet, is regarded as layered and relatively homogenous, in contrast to oceanic crust generated at slow-spreading ridges. Theoretical models on magmatic accretion, thermal models, mass balance calculations or general alteration models of and for the oceanic crust therefore only exist for fast-spreading systems. In spite of tremendous efforts by ship-based research, a complete modern chemical/petrological profile based on natural samples is still missing due to a lack of exposures and drilled sections of the deeper parts of fast-spread crust. The Oman ophiolite is regarded as the best analogue of fast-spreading oceanic lithosphere on land. Its southern massifs are regarded as the best area for studying “normal” fast-spreading crust where the so-called "late-stage magmatism" related to subduction zone processes being widely absent.

For this study we undertook three detailed field campaigns in the Wadi Gideah, which is located in the Wadi-Tayin Massif in the southern part of the Oman ophiolite, to sample a complete section of fast-spreading oceanic crust. The project focuses on (1) petrography and major element studies, (2) trace and rare earth element studies, (3) quantification of variations of the crystallographic preferred orientations (CPO) with depth, (4) characterization of the evolution of hydrothermal alteration with depth by the use of Sr and O isotopes, and (5) quantification of sulfur cycling. Our concept of performing different analytical and structural investigations on the same sample enabled us to create a coherent data set. Hence, it is well suited for advancing our understanding of crustal accretion processes at fast-spreading mid-ocean ridges. The Wadi Gideah profile represents a reference section through fast-spreading oceanic crust in order to provide scientific support for the ICDP "Oman drilling project" (lead PI Peter Kelemen and 38 co-proponents), which aims to drill at three sites in the Wadi Gideah, focusing on the layered gabbro, the transition between layered and foliated gabbro, and the gabbro/dike transition. The analytical work within the project focuses on: electron probe micro analyses (EPMA) in Hannover; inductive coupled plasma optical emission spectroscopy for bulk and trace elements (ICP-OES; ICP-MS) in Kiel; multi-collector mass spectrometry for Sr, Nd, and Hf isotopes (MC-ICP-MS) in Hannover; electron

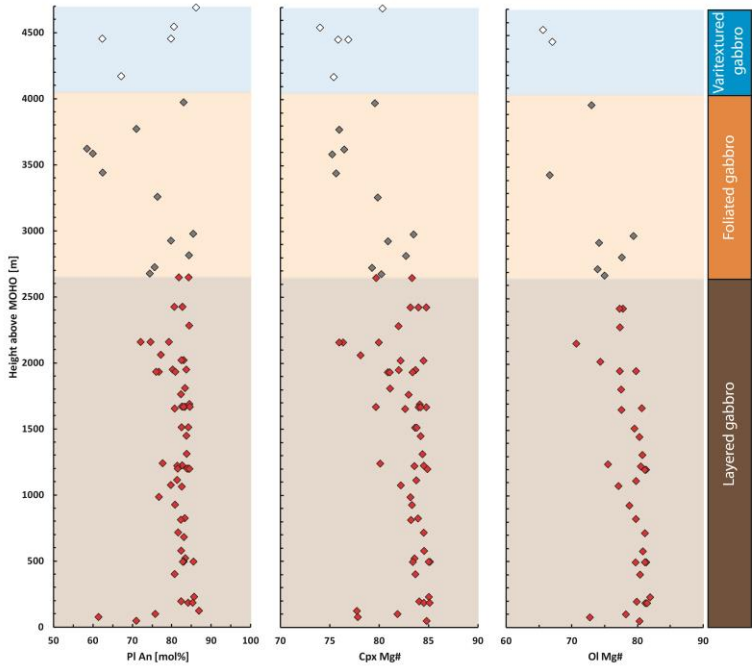

Fig. 1. Mineral major element concentration vs. depth with **a:** Plagioclase anorthite content. **b:** Clinopyroxene magnesium number (MgO/(MgO+FeO) molar). **c:** Olivine magnesium number

backscatter diffraction (EBSD) in Montpellier (France); sulfur isotopes in Münster.

The thickness of the layered and virtually undeformed oceanic crust was recalculated to approximately 6km, containing pillow lavas (~600m) and sheeted dikes (~1300m) as well as varitextured (~400m), foliated (~1600m), and layered (~2200m) gabbros resting on a relatively thin MOHO transition zone. Samples from the layered gabbro sequence show modal compositions of ~50 vol% plagioclase, ~40 vol% clinopyroxene and ~10 vol% olivine in average. In very few samples up to 10 vol% of orthopyroxene is present. Samples from the foliated gabbro sequence display a slightly higher amount of plagioclase with little lower amount of clinopyroxene and olivine. In few samples up to 10 vol% of oxides are present. Samples from the varitextured gabbro and sheeted dike sequences show modal compositions of ~50 vol% plagioclase, ~45 vol% clinopyroxene, ~5 vol% oxides, and were highly pervasively altered into minerals of the amphibolite to greenschist facies.

The layered gabbro sequence compositions typical for cumulates with bulk Mg# 44-68, An% in plagioclase of 71-87 mol%, Mg# 76-85 for clinopyroxene, and Mg# 71-82 for olivine (Fig. 1). The foliated gabbro sequence displays composition characteristics for cumulates with bulk Mg# 27-58, An% in plagioclase of 59-85 mol%, Mg# 75-83 for clinopyroxene, and Mg# 67-79 for olivine. The varitextured gabbro sequence can be regarded as frozen basaltic to basaltic andesitic melts with bulk Mg# 25-51, An% in plagioclase of 60-86 mol%, and Mg# 74-80 for clinopyroxene. The sheeted dike sequence shows a basaltic to basaltic andesitic compositions with bulk Mg# 29-45, An% in plagioclase of 22-70 mol%, and Mg# ~70 for clinopyroxene. The generally evolving trends in mineral and bulk major element composition from bottom to top of the profile and implications for a possible change in differentiation process especially in the layered to foliated gabbro transition zone are also observed for bulk rock trace element data. While layered gabbro cumulates show only minor variability for most trace elements over the entire thickness, systematic trends in La/Sm, La/Yb, Zr/Hf, Nb/Ta, Cr/Zr etc. can be observed in the transition from foliated gabbros and varitextured gabbros towards sheeted dikes and basalts. Petrological modeling using the program PETROLOG (Danyushevsky & Plechov, 2011) in a chemical system corresponding to the bulk crust composition calculated for the Wadi Gideah profile, shows that the overall XMg trend with depth can be well produced by fractionation crystallization in combination with replenishments with fresh parental melt in the layered gabbro, and pure fractional crystallization for the upper part of the gabbroic crust.

Crystallographic preferred orientation of plagioclase in samples from all sequences of Wadi Gideah reveal a magmatic deformation type independent from depth and with only very few samples tending to plastic deformation.

The average Sr^{87}/Sr^{86} ratio is 0.7033 ± 0.0002 for the entire gabbro sequence which is significantly higher than modern EPR crust (~0.7025, White at al., 1987), but which is in accord with Sr^{87}/Sr^{86} estimations for the lower crust in the Oman ophiolite from other locations (~0.7030, McCulloch et al., 1980; ~0.7031, Lanphere et al., 1981). Significantly higher Sr^{87}/Sr^{86} was estimated for samples from hydrothermal fault zones cutting the gabbros at all crustal level. We interpret these zones as possible hydrothermal pathways for an effective cooling of the deep crust at very high temperatures. This is a requirement for a model based on in-situ crystallization within the deep crust, which is indicated by our geochemical/petrological results, which clearly show crystallization/fractionation in the lower crust (see above).

Summarizing, the major and trace element bulk rock trends and the mineral compositional trends combined with modeling, possible convectional cooling enabled by deep hydrothermal zones, and little evidence for of mineral (depth dependent) plastic deformation indicate an accretion model of the lower Oman paleocrust based on significant in-situ crystallization eventually established by sill intrusions (according to the "sheeted sill model" of Kelemen et al., 1997).

References:

Danyushevsky L.V., and Plechov P., Petrolog3: Integrated software for modeling crystallization processes, Geochem. *Geophys. Geosyst.*, 12

Kelemen P.B., Koga K., Shimizu N., Geochemistry of gabbro sills in the crust-mantle transition zone of the Oman ophiolite: implications for the origin of the oceanic lower crust, *Earth Planet. Sci. Lett.*, 146, 475-488, 1997

Lanphere M.A., Coleman R.G, and Hopson C.A., Sr Isotopic Trace Study of the Samail Ophiolite, Oman, *J. Geophys. Res.*, 86, 2709-2720, 1981

McCulloch M.T., Gregory R.T., Wasserburg G.J., and Taylor H.P., A Neodymium, Strontium, and Oxygen Study of the Cretaceous Samail Ophiolite and Implications for the Petrogenesis and Seawater-Hydrothermal Alteration of Oceanic Crust, *Earth Planet. Sci. Lett.*, 46, 201-211, 1980

White W.M., Hofman A.W., and Puchelt H., Isotope Geochemistry of Pacific Mid-Ocean Ridge Basalt, *J. Geophys. Res.*, 92, 4881-4893, 1987

ICDP

Interglacial climate variability recorded in the Dead Sea sediments

I. NEUGEBAUER, M.J. SCHWAB, A. BRAUER, R. TJALLINGII, P. DULSKI, U. FRANK AND DSDDP SCIENTIFIC PARTY*

GFZ German Research Centre for Geosciences, Section 5.2 Climate Dynamics and Landscape Evolution, Telegrafenberg, D-14473 Potsdam, Germany

* The complete list of scientists involved in the DSDDP can be found at http://www.icdp-online.org

Introduction

In order to estimate the impact of global warming on natural systems, it is crucial to understand the natural climate variability in the past, especially during warm periods like the Holocene and the last interglacial. Lake sediments from the Dead Sea basin provide high-resolution records of climatic variability in the eastern Mediterranean region, which is considered being especially sensitive to changing climatic conditions. In the study presented here, we aim to reconstruct palaeoclimatological changes during the last two interglacials as archived in the ICDP Dead Sea Deep Drilling Project (DSDDP) sediment cores and in exposed profiles from the lake's margin, using a combination of high-resolution sedimentological-mineralogical and geochemical analyses. Micro-facies analyses on large-scale petrographic thin sections, magnetic susceptibility measurements and µXRF element scanning allow depicting even single flood or drought

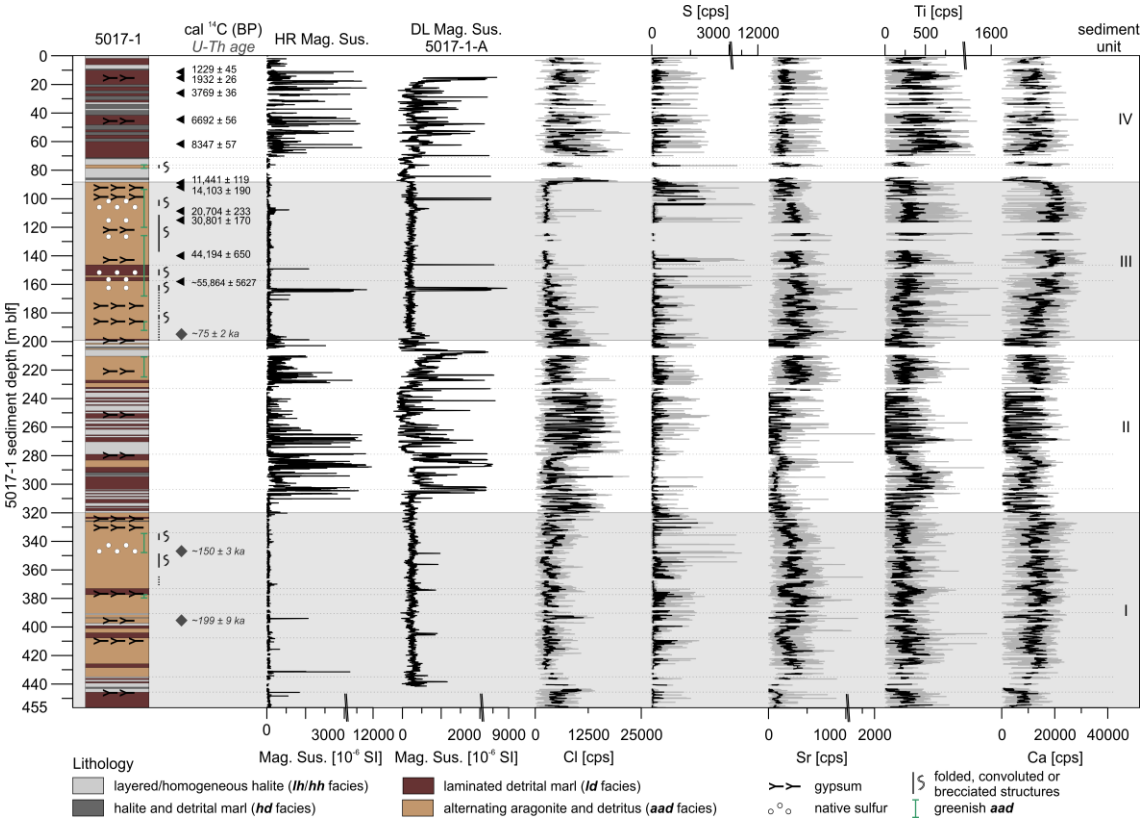

Fig. 1. Lithological profile of 5017-1 (water depth 297 m, composite profile) with radiocarbon and U-Th ages; magnetic susceptibility data, measured with high resolution (HR; 1 mm resolution) on the splitted core surface and with low resolution (10 cm) by downhole logging (DL, hole 5017-1-A): both curves are in good agreement, excluding any depth shifts during the drilling process; µXRF profiles of Cl, S, Sr, Ti and Ca in counts per second (cps): grey curves are measured values in 1 mm steps, black overlying curves are 101-values running means (10.1 cm); gaps in the HR magnetic susceptibility curve and µXRF data are due to lacking core recovery, insufficiently smooth core surface and folded or slumped - not measured – sections, respectively.

events.

Lithology of the deep-basin core 5017-1

The ca 460 m long sediment profile 5017-1 from the deep Dead Sea basin (water depth ~300 m; Fig. 1) is estimated to comprise about 220,000 years and hence two glacial-interglacial cycles (Neugebauer et al., 2014). The record covers the upper part of the Amora (parts of MIS 7 and MIS 6; sediment unit I in Fig. 1), the last interglacial Samra (broadly corresponding to MIS 5; sediment unit II in Fig. 1), the last glacial Lisan (MIS 4-2; sediment unit III in Fig. 1) and the Holocene Ze'elim (sediment unit IV in Fig. 1) formations, including their transitions. Sediments composed of alternating aragonite and detrital marl (*aad*) characterize the more humid periods during glacials, whereas laminated detrital marl has been deposited during relatively drier and partly laminated halite during driest conditions. The latter is found within the interglacial Samra and Ze'elim formations, as well as at the MIS 6/5, 5/4 and 2/1 transitions, which are denoted as hiatuses in sediments outcropping on the present-day lake shores.

Several different gravel layers were identified in the deep core; one of them was previously interpreted as a shore line deposit which implicates a drawdown (Torfstein et al., 2015). Here we provide results of petrological investigations (composition, grain size, grain shape) of additional gravel layers.

Last interglacial

The Samra Formation that corresponds to the marine isotope stage 5 encompasses ca 120 m in the deep 5017-1 profile (Fig. 1). The lower ~85 m of the formation are mostly composed of laminated or homogeneous massive halite deposits that fingerprint a long period of aridity during the last interglacial MIS 5e. The finding of the thickest halite sequence (ca 40 m thick) of the entire 5017-1 profile at the upper part of this interval suggests the driest conditions at the end of MIS 5e.

The upper part of the stratigraphically defined Samra Formation in the 5017-1 profile has been deposited from ca 100,000 to 75,000 yrs BP, based on U/Th ages of primary aragonite layers (Torfstein et al., 2015). High-resolution sedimentological and µXRF element scanning data of the 5017-1 sediment core allow tracing lake level fluctuations of this interval during the early phase of the last glaciation. Detailed reconstruction of these fluctuations was feasible by distinguishing six micro-facies types and assigning a relative lake level to each of these types. Greenish sediments of alternating aragonite and detrital marl laminae build the highest lake level end-member, whereas massive laminated halite represents lowest lake levels. While a gradual increase of the lake level is described from ca 100 to 85 ± 3 ka BP, a sharp decline and following millennial-scale low-stand is marked by a several meter thick

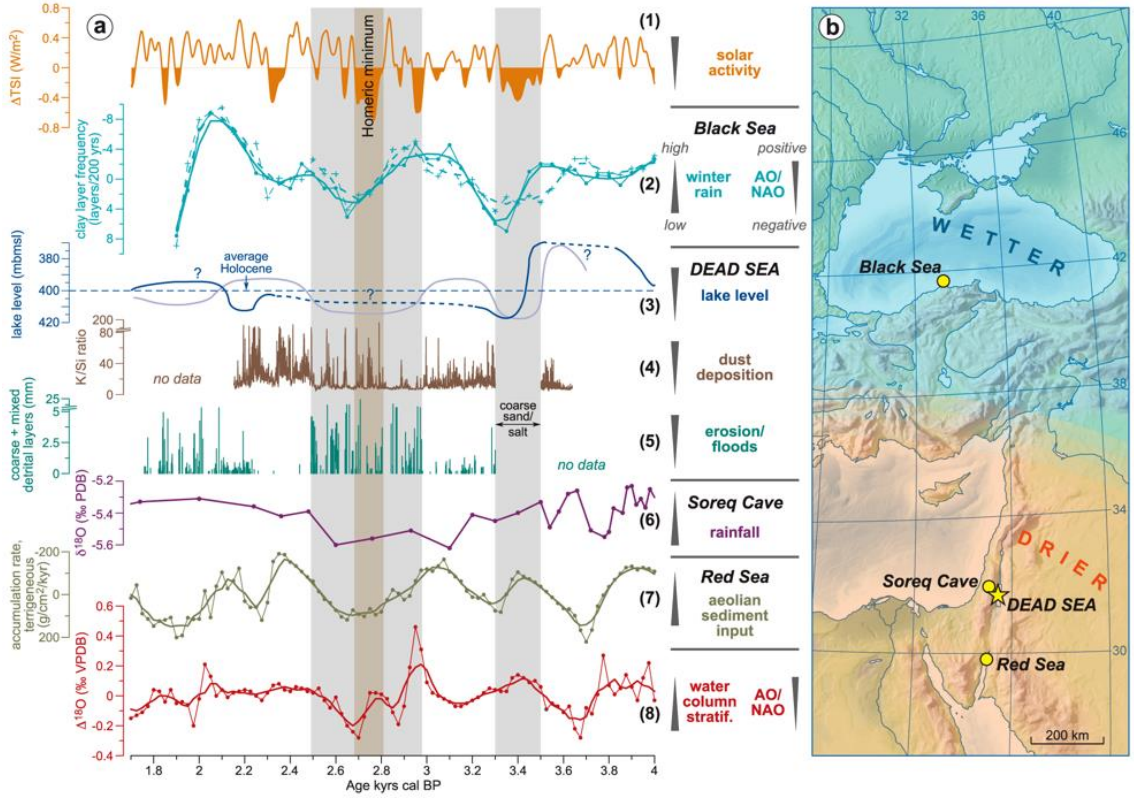

Fig. 2: (a) Comparison of the late Holocene Dead Sea data to other records: (1) difference of the total solar irradiance ΔTSI from the year 1986, 1365.57 W/m² (Steinhilber et al., 2009); (2) clay layer frequency record from the Black Sea, cores GeoB7622 (solid lines) and GeoB7625 (dashed lines), thick lines: 3-point moving average, reversed scale (Lamy et al., 2006); (3-5) Dead Sea: (3) lake level reconstruction based on core DSEn (Migowski et al., 2006), light blue line: this study, (4) K/Si ratio from µXRF element scanning (this study), (5) coarse and mixed detrital layer thickness (this study), both (4) and (5) from core DSEn and on radiocarbon-based age-scale; (6) Soreq Cave $\delta^{18}O$ speleothem record (Bar-Matthews et al., 2003); Red Sea: (7) terrigeneous sand accumulation rate, reversed scale, and (8) stable oxygen isotope difference $\Delta\delta^{18}O$ between planktic and epibenthic foraminifera, both core GeoB5804-1, thick lines: 5-point moving average (Lamy et al., 2006). Vertical bars indicate the two dry periods detected in this study. AO/NAO: Arctic Oscillation/ North Atlantic Oscillation. **(b)** Inferred humidity changes in the eastern Mediterranean during the two dry periods at the Dead Sea, discussed here (~3500-3300 yrs BP and ~2900-2400 yrs BP).

sequence of mainly layered halite that was dated to 85-82 ± 3ka BP during the early part of MIS (marine isotope stage) 5a. Subsequently, lake level increased again and achieved high glacial-like values at the MIS 5-4 transition and thereafter. The early MIS 5a low-stand of the lake is forced by an orbital insolation maximum and coincides with a period of increased humidity and vegetation cover in the Sahara region, the formation of sapropel S3 in the Mediterranean and Greenland interstadial 21. We demonstrate that the Mediterranean and Sahara regions experienced overall humid climate during that time, while pronounced aridity was restricted to the south-eastern Levantine region. A possible explanation that monsoon-driven humidity could not reach this area during MIS 5a is the southward shift of the polar front due to the growing ice sheets during the early last glacial, which had a major influence on the climatic conditions in the eastern Mediterranean.

The last interglacial Dead Sea (i.e. Lake Samra) experienced strong droughts in its watershed recorded by its low lake levels and by deposition of thick sequences of halite. Analyses of these halite sequences present intercalations of halite laminae with fine-grained clastics brought to the lake primarily by floods (Palchan et al., in review). Geochemical characterization of these sediments complemented by statistical analyses indicates an annual depositional cycle of 7.5 yr, as it is also identified by other recent regional archives. Thus, we propose a common climatic mechanism behind the modern and last interglacial periodicities. We suggest that the 7.5 yr cycle had possibly been affecting the Eastern Mediterranean region during past interglacial intervals for a long time, possibly also during glacial intervals. This cycle has been proposed to be synchronized with the North Atlantic Oscillation and is induced by the 7-8 yr oscillation in the position of the Gulf Stream front. We anticipate that this expression of North Atlantic control will result in a similar periodicity in other annual sequences in the region.

Holocene

For the Holocene, we aim on detailed reconstruction of climatic fluctuations and related changes in the frequency of flood and dust deposition events at ca 3500 and especially at 2800 years BP (Neugebauer et al., in review). A ca 4 m thick, mostly varved sediment section from the western margin of the Dead Sea (DSEn - Ein Gedi profile) was analysed and correlated to the ICDP core 5017-1 from the deep basin. To detect even single event layers, we applied a multi-proxy approach of high-resolution microscopic thin section analyses, µXRF element scanning and magnetic susceptibility measurements, supported by grain size data and palynological analyses. Based on radiocarbon and varve dating two pronounced dry periods were detected at ~3500-3300 yrs BP and ~2900-2400 yrs BP which are differently expressed in the sediment records. In the shallow-water core (DSEn), the older dry period is characterised by a thick sand deposit, whereas the sedimentological change at 2800 yrs BP is less pronounced and characterised mainly by an enhanced frequency of coarse detrital layers interpreted as erosion events. In the 5017-1 deep-basin core both dry periods are depicted by halite deposits. The older dry period concurs with a cultural crisis in the region during the late Bronze Age. The younger dry period coincides with a cool and wet climate in widespread areas of Europe that has been related to a Grand Solar Minimum around 2800 BP (Fig. 2). Despite the overall dry climate during this time in the south-eastern Mediterranean region, the Dead Sea experienced an increase in flooding probably caused by a reduction and eastward migration of the dominant Cyprus Low weather pattern and/or by more frequent intrusions of the Active Red Sea Trough into the Negev desert and the southern Dead Sea catchment. Despite the contrasting climate signature in Europe (wet) and the Dead Sea region (dry) during this period, these changes might be linked through complex teleconnections of atmospheric circulation patterns.

Main conclusions

Sediments from the Dead Sea basin are valuable recorders of past climatic changes due to their sensitivity to varying lake levels and hence climate. The ICDP deep-basin core allowed, for the first time, studying exceptionally dry periods, when lake level declined below elevations of sediment sections that are exposed today at the margins of the lake. Strongest lake level drops occurred during the last and recent interglacial periods and were the focus of this study. We demonstrate that the combination of high-resolution micro-facies and µXRF analyses is a suitable instrument to investigate climatic fluctuations from millennial to annual time-scales.

References:

Neugebauer, I., Brauer, A., Schwab, M.J., Waldmann, N.D., Enzel, Y., Kitagawa, H., Torfstein, A., Frank, U., Dulski, P., Agnon, A., Ariztegui, D., Ben-Avraham, Z., Goldstein, S.L. and Stein, M., 2014. Lithology of the long sediment record recovered by the ICDP Dead Sea Deep Drilling Project (DSDDP). Quaternary Science Reviews 102, 149-165.

Neugebauer, I., Brauer, A., Schwab, M.J., Dulski, P., Frank, U., Hadzhiivanova, E., Kitagawa, H., Litt, T., Schiebel, V., Taha, N. and Waldmann, N.D., in review. Responses to the 2800 years BP climatic oscillation in shallow-water and deep-basin sediments from the Dead Sea. The Holocene.

Palchan, D., Neugebauer, I., Waldmann, N.D., Schwab, M.J., Dulski, P., Brauer, A., Naumann, R., Stein, M., Erel, Y. and Enzel, Y., in review. North Atlantic control over cyclic deposition of halite and clastic laminas during the Last Interglacial Dead Sea. Quaternary Research.

Torfstein, A., Goldstein, S.L., Kushnir, Y., Enzel, Y., Haug, G. and Stein, M., 2015. Dead Sea drawdown and monsoonal impacts in the Levant during the last interglacial. Earth and Planetary Science Letters 412, 235-244.

IODP

Three component borehole magnetometrie in the Amami Sankaku Basin during IODP Expedition 351

MARTIN NEUHAUS[1], LAUREEN DRAB[2], SANG-MOOK LEE[3], CHRISTOPHER VIRGIL[1], SEBASTIAN EHMANN[1], ANDREAS HÖRDT[1], MARTIN LEVEN[4] AND IODP EXPEDITION 351 SCIENTISTS

1 Technical University of Braunschweig
2 Lamont Doherty Earth Observatory
3 Seoul National University
4 University of Göttingen

By the use of reliable three component magnetic data we are able to constrain the paleomagnetic history in the subsurface as it allows us to determine the vector of the remanent magnetization of formations distant from the borehole and of near borehole regions of drilled layers. The magnetization vector is usually characterized by its

inclination and declination. While it is possible to derive the inclination from core magnetization data too, it is only possible to assess the declination from azimuthally oriented cores, which is very rarely done. However, since the declination can be used to derive information about the history, especially the rotation, of a tectonic plate, it becomes more and more interesting in modern geosciences to derive a reliable estimation of the full remanent magnetization vector.

In summer 2014 IODP Expedition 351 drilled 1611 m of sediment and basement in the Amami Sankaku Basin west of the Kyushu-Palau Ridge in order to contribute to the questions of when and how subduction processes are initiated. To provide supplementary information, like the rotational history of the host plate, the Philippine Sea Plate (PSP), we successfully investigated 600 m of sediment between 600 mbsf and 1200 mbsf with the Göttinger Borehole Magnetometer (GBM).

In a preliminary processing of the data, we calculated the horizontal and vertical component of the magnetic flux density inside the borehole by the use of the data of the GBM's orientational sensors.

By comparing the magnetic susceptibility to the components of the magnetic flux density and by comparing the components of both down- and uplog to each other we have been able to provide an initial assessment of the data quality of the measurement. It becomes clear that we successfully resolved small but spatially coherent magnetic structures clearly related to a remanent magnetization. The resolution is considerable, since the measurements were taken in a weakly magnetized sedimentary environment, whereas until now, three component borehole magnetic anomalies were only resolved in stronger magnetic igneous environments.

IODP

Revealing crystal growth and diffusion processes with Fe-Mg chemical and isotopic zoning in MORB olivine

M. OESER[1], R. DOHMEN[2], I. HORN[1], S. SCHUTH[1] AND S. WEYER[1]

1 Leibniz Universität Hannover, Institut für Mineralogie, Callinstr. 3, D-30167 Hannover

2 Ruhr-Universität Bochum, Insitut für Geologie, Mineralogie und Geophysik, Universitätsstr. 150, D-44780 Bochum

Introduction

Since the 1980s, several studies have used the chemical zoning of olivines in mid-ocean ridge basalts (MORBs) to estimate the magma residence time of these crystals by diffusion modeling (Nabeleck and Langmuir, 1986; Humler and Whitechurch, 1988; Danyushevsky et al., 2002; Pan and Batiza, 2002). Nabeleck and Langmuir (1986) and Humler and Whitechurch (1988), who modeled the diffusive re-equilibration of Ni in olivines from the slow-spreading Mid-Atlantic Ridge (MAR) and the intermediate-spreading Central Indian Ridge, respectively, interpreted their modeled diffusion times to represent the time interval between a magma mixing event and the eruption of the MORBs. Pan and Batiza (2002) used a similar assumption, based on Fe-Mg zoning in olivines from the fast-spreading East Pacific Rise (EPR). In contrast, the time interval obtained by modeling Fe-Mg zoning in melt inclusions and olivines from the EPR in the study by Danyushevsky et al. (2002) was interpreted to represent the time between olivine crystallization and eruption. Nevertheless, all of these studies point to rather short magma residence times of olivines in MORBs (i.e., between 1 day and 4 years), with shorter time intervals being prevalent. This is also consistent with the findings of Costa et al. (2010) who modeled diffusion-generated Mg zoning in plagioclase in MORBs from the MAR and the intermediate-spreading Costa Rica Rift (CRR) and found time spans of <1.5 years between magma mixing and eruption. However, as pointed out in recent studies (Dauphas et al., 2010; Teng et al., 2011; Sio et al., 2013), diffusion-driven zoning may be difficult to distinguish from zoning that is mainly produced by prolonged crystal growth in an evolving melt during magmatic differentiation („growth zoning"), and the latter provides only limited information on time scales.

Recent studies have demonstrated that a determination of Fe-Mg isotopic variations in olivine provides a powerful means to reliably trace Fe-Mg inter-diffusion occurring on the mineral scale during magma evolution (e.g. Teng et al.,

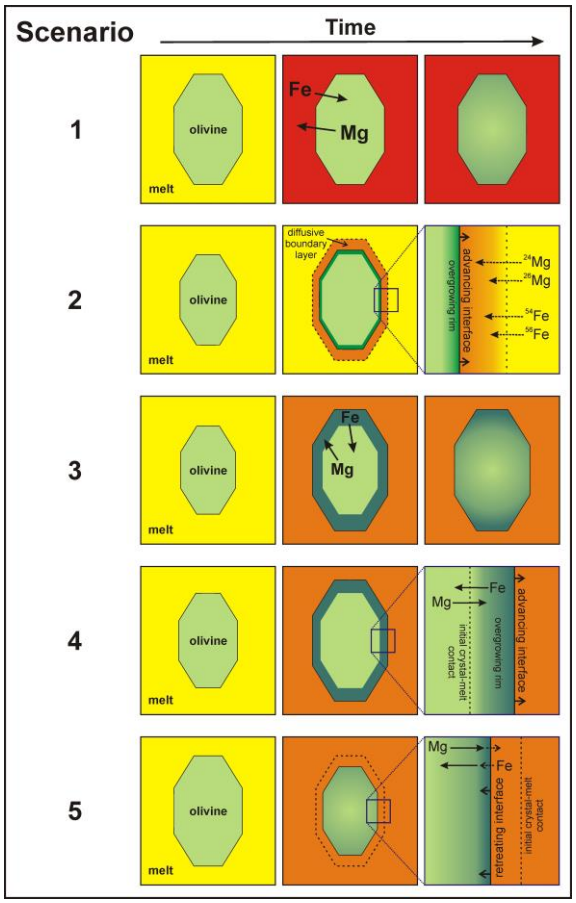

Fig. 1. Illustration of the five scenarios explored in this study in order to theoretically investigate the effects of Fe-Mg inter-diffusion, crystal growth and dissolution on chemical and isotopic zoning of olivines. Scenario 1: pure Fe-Mg inter-diffusion due a compositional contrast between olivine and melt. Scenario 2: rapid (diffusion-limited) crystal growth producing a diffusive boundary layer around the growing crystal. Scenario 3: Fe-Mg inter-diffusion after two crystal growth episodes. Scenario 4: olivine growth and simultaneous Fe-Mg inter-diffusion. Scenario 5: olivine dissolution and simultaneous Fe-Mg inter-diffusion. Cartoon for scenario 1 is modified after Teng et al. (2011).

2011; Sio et al., 2013; Oeser et al., 2014a), because diffusion results in large kinetic isotope fractionations even at magmatic temperatures (e.g. Richter et al., 2003). Modeling of clearly diffusion-generated zoning in olivine can then yield constraints on the time scales of magma differentiation processes. In order to examine possible processes that can produce chemically and isotopically zoned olivines, we simulated the effects of Fe-Mg inter-diffusion, crystal growth and crystal dissolution on chemical and isotopic zoning of olivines in general. In a next step, we investigated whether we can reproduce observed Fe-Mg chemical and isotopic variations in natural olivines from MORBs, which were determined by *in situ* Fe-Mg isotope analyses using femtosecond-LA-MC-ICP-MS (Oeser et al., 2014a and 2014b).

Theoretical Approach

The following 5 scenarios were investigated in order to simulate the effects of various proccesses occurring during magma evolution which may generate and/or modify chemical and isotopic zoning in natural olivines (Fig. 1): 1) Pure Fe-Mg inter-diffusion: diffusive Fe-Mg exchange between olivine and melt is driven by a compositional contrast between crystal and melt; 2) Rapid (diffusion-limited) growth of olivine in a melt on top of a homogeneous olivine core producing a diffusive boundary layer around the growing crystal (e.g. Watson and Müller, 2009); 3) Internal homogenization of olivine after two growth episodes producing chemical step profiles but homogeneous Fe and Mg isotopic compositions across the

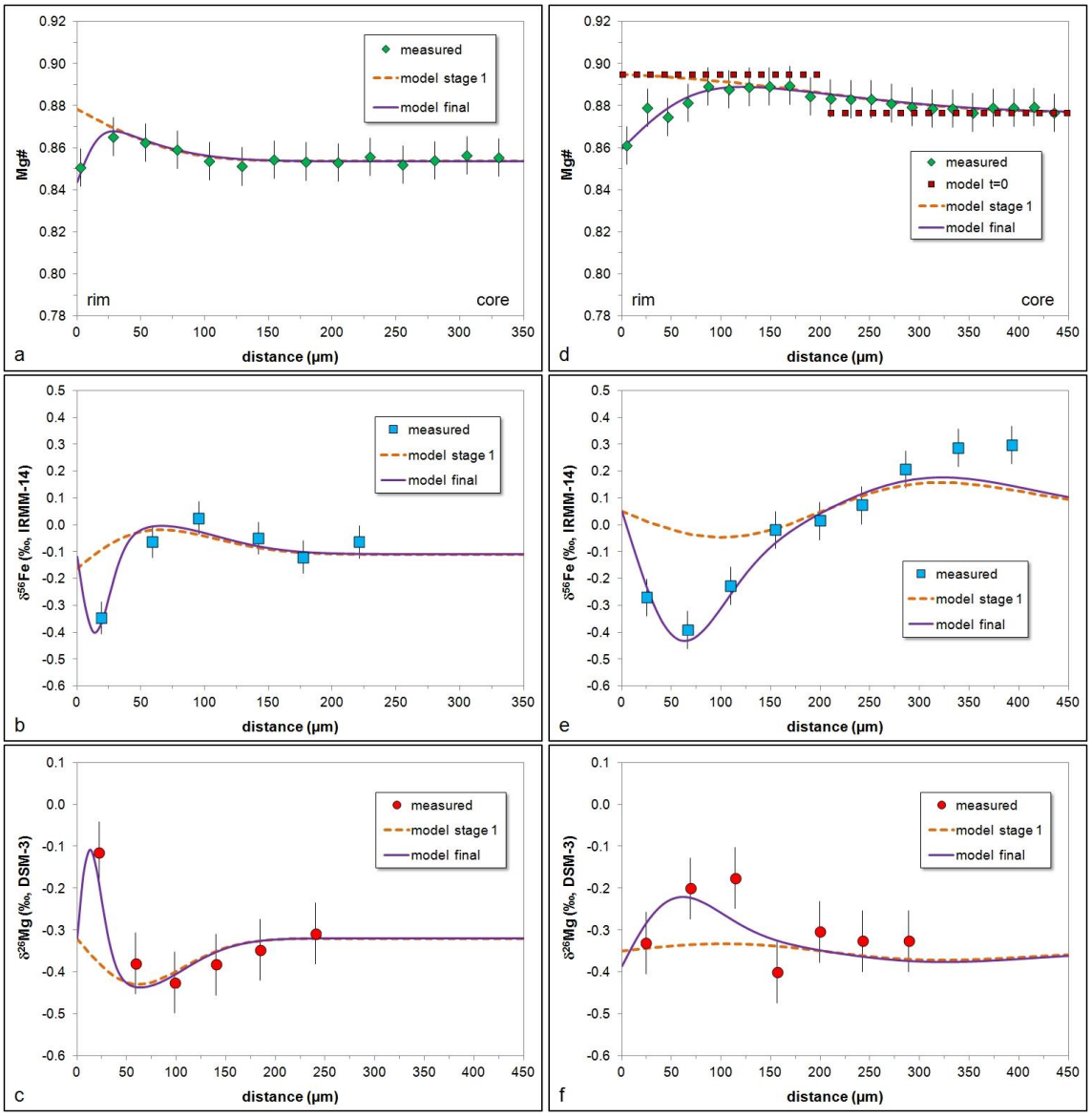

Fig. 2. Modeling of Fe-Mg chemical **(a,d)** and isotopic **(b,c,e,f)** diffusion profiles for two multiply zoned olivines in MORBs from the MAR and the CRR. **(a-c):** Zoned olivine from the MAR; the model includes two stages: during the first stage (lasting ~490 days at 1205°C) Mg diffuses from the melt into the olivine while Fe diffuses in the opposite direction (e.g. after magma mixing with a more primitive melt); the modeled chemical and isotopic profiles at the end of stage 1 are shown as a dashed line. In the second stage (lasting 45 days at 1175°C) Fe diffuses from the melt into the olivine while Mg diffuses out of the olivine (e.g. due to cooling and differentiation of the host magma, potentially during magma ascent in dikes). **(d-f):** Zoned olivine from the CRR; this model also includes two stages; however, prior to the first diffusion episode, a chemical step function (red squares in d) was established due to two episodes of crystal growth. Subsequent Fe-Mg inter-diffusion smoothes out this step; the modeled chemical and isotopic profiles at the end of stage 1 (lasting 6.1 years at 1205°C) are shown as a dashed line. In the second stage (lasting 2.1 years at 1175°C) Fe diffuses from the melt into the olivine while Mg diffuses out of the olivine (e.g. due to cooling and differentiation of the host magma).

olivine; 4) Olivine growth and simultaneous Fe-Mg inter-diffusion; 5) Olivine dissolution and simultaneous Fe-Mg inter-diffusion.

Results of these simulations demonstrate that Fe-Mg inter-diffusion, in general, leads to inversely correlated Fe-Mg isotopic profiles (cf. Dauphas et al., 2010). However, the specific shapes of such profiles differ considerably from each other depending on whether (and when) episodes of crystal growth or dissolution played a major role in modifying the chemical and isotopic zoning of olivine. For example, scenario 3 would generate Fe-Mg isotopic profiles that resemble a (symmetric) sine function, while the isotopic profiles of Fe and Mg obtained in scenario 4 are asymmetric, i.e., the isotope fractionation is always higher in the initial part of the olivine than in the newly formed rim. In contrast to Fe-Mg inter-diffusion in olivine, rapid crystal growth (generating a diffusive boundary layer in the melt; scenario 2) would lead to a strong fractionation of Mg isotopes (1-2‰ in $^{26}Mg/^{24}Mg$) and a very small Fe isotope fractionation (<0.1‰ in $^{56}Fe/^{54}Fe$). Hence, our theoretical examination shows that combining the information of chemical and isotopic zoning in olivine allows to distinguish between diverse proccesses occurring during magma evolution.

Observations in Natural Samples

Apart from several "normally zoned" olivine phenocrysts in MORBs from the MAR (Sites 332A and 396B) and the CRR (Site 896A; see Oeser et al., 2014a), two multiply zoned olivines from these locations are of special interest as they show pronounced zoning in $\delta^{56}Fe$ and $\delta^{26}Mg$ (up to 0.7‰ and 0.3‰, respectively). In the olivine from the MAR (Site 332A) heavy Fe and light Mg isotopes appear to be relatively enriched in a zone where Mg may have diffused from the crystal's rim, i.e. from the melt, towards the core (and Fe in the opposite direction). This process could be triggered if the olivine came into contact with a more primitive melt (compared to the one it had grown in). Furthermore, the crystal rim has light Fe and heavy Mg isotopic compositions, indicating diffusion of Fe from the melt into this domain during a second, shorter diffusion event (Fig. 2a-c). This may be explained by a chemical gradient that was generated by magma differentiation during the magma ascent in dikes, or by a second mixing event with a more evolved magma (which finally also triggered the eruption). A model with pure diffusive Fe-Mg exchange between olivine and melt (scenario 1) in two stages is suitable to simulate the chemical zoning as well as the Fe-Mg isotopic zoning. The first stage lasts ~490 days at 1205°C, possibly representing the time span between a magma mixing event (with a primitive melt) and either a second mixing event with a more evolved magma or the start of the final magma ascent in dikes associated with cooling and differentiation of the magma. In the latter case, the second stage (lasting 45 days at 1175°C) could represent the duration of magma transfer from the magma chamber to the seafloor.

The other multiply zoned olivine comes from the CRR. Its apparently homogeneous core (in terms of Mg#) shows a relatively heavy Fe isotopic composition ($\delta^{56}Fe \approx 0.30$‰ relative to IRMM-014), indicating that the core was affected by Mg diffusion into and Fe diffusion out of the olivine, potentially due to contact with a hotter, more primitive melt. The lightest Fe isotopic composition is observed near the Fe-rich crystal rim (Fig. 2d-f). This domain may also be characterized by a relatively heavy Mg isotopic composition (although the precision of the *in situ* analyses is insufficient to unambiguously resolve Mg isotope variations here). Nevertheless, the chemical and isotopic zoning of this olivine points to at least two diffusion episodes, analogous to the other multiply zoned olivine. Simple diffusive Fe-Mg exchange between olivine and melt (scenario 1) is suitable to reproduce the chemical zoning, if Mg diffuses into and Fe out of the olivine during a first diffusion episode, which is followed by a second, shorter diffusion event where Fe diffuses into the olivine (and Mg into the opposite direction). However, such a scenario does not satisfactorily reproduce the observed isotopic zoning, especially for Fe. Alternatively, a chemical step function may be assumed for the first diffusion episode (Fig. 2d), which may develop due to two episodes of crystal growth (scenario 3). These steps in the concentrations of Fe and Mg are subsequently smoothed out by intra-mineral Fe-Mg inter-diffusion resulting in Fe-Mg isotopic zoning (Fig. 2e and 2f). The second diffusion event is characterized by diffusion of Fe into and Mg out of the olivine due to magma differentiation / cooling. The time scales obtained with such a model (that adequately reproduces the chemical *and* isotopic zoning of this olivine) are about 6 years for the first diffusion episode at ~1205°C and 2 years for the second one at ~1175°C.

In summary, our findings demonstrate that a combined investigation of Fe-Mg chemical and isotopic zoning in olivine provides more detailed and reliable information on magma evolution than chemical zoning alone.

Outlook

As some MORB samples from the CRR investigated in this study contain large, fresh clinopyroxene phenocrysts we want to apply our developed technique to these crystals as well in order to address the following questions:

- Is the zoning of Fe and Mg isotopes in cpx comparable to that observed in olivines and correlated with the chemical zoning?
- If we identify diffusion-generated chemical and isotopic zoning in cpx, can we model the inter-diffusion of Fe and Mg in cpx and thus receive additional time information on magmatic processes?
- How do these information compare to the time constraints we have received by modeling of the diffusion zoning in olivine?

Pure Fe-Mg inter-diffusion data for cpx have just recently been determined (Müller et al., 2013). The findings of this study indicate that Fe-Mg inter-diffusion in cpx is about an order of magnitude slower than in olivine. Accordingly, diffusion zoning in cpx may cover different time scales than diffusion zoning in olivine.

References:

Costa F., Coogan L. A. and Chakraborty S. (2010) The time scales of magma mixing and mingling involving primitive melts and melt–mush interaction at mid-ocean ridges. Contrib. to Mineral. Petrol. 159, 371–387.

Danyushevsky L. V, Sokolov S. and Falloon T. J. (2002) Melt Inclusions in Olivine Phenocrysts: Using Diffusive Re-equilibration to Determine the Cooling History of a Crystal, with Implications for the Origin of Olivine-phyric Volcanic Rocks. J. Petrol. 43, 1651–1671.

Dauphas N., Teng F.-Z. and Arndt N. T. (2010) Magnesium and iron isotopes in 2.7 Ga Alexo komatiites: Mantle signatures, no evidence for Soret diffusion, and identification of diffusive transport in zoned olivine. Geochim. Cosmochim. Acta 74, 3274–3291.

Humler E. and Whitechurch H. (1988) Petrology of basalts from the Central Indian Ridge (lat. 25°23′S, long. 70°04′E): estimates of frequencies and

fractional volumes of magma injections in a two-layered reservoir. Earth Planet. Sci. Lett. 88, 169–181.
Müller T., Dohmen R., Becker H. W., Heege J. H. and Chakraborty S. (2013) Fe–Mg interdiffusion rates in clinopyroxene: experimental data and implications for Fe–Mg exchange geothermometers. Contrib. to Mineral. Petrol. 166, 1563–1576.
Nabeleck P. I. and Langmuir C. H. (1986) The significance of unusual zoning in olivines from FAMOUS area basalt 527-1-1. Contrib. to Mineral. Petrol. 93, 1–8.
Oeser M., Weyer S., Dohmen R., Horn I. and Schuth S. (2014a) Time scales of magma evolution derived from diffusion modeling of Fe-Mg chemical and isotopic zoning in natural olivines. In IODP/ICDP-Kolloquium Erlangen, Germany. pp. 104–106.
Oeser M., Weyer S., Horn I. and Schuth S. (2014b) High-Precision Fe and Mg Isotope Ratios of Silicate Reference Glasses Determined In Situ by Femtosecond LA-MC-ICP-MS and by Solution Nebulisation MC-ICP-MS. Geostand. Geoanalytical Res. 38, 311–328.
Pan Y. and Batiza R. (2002) Mid-ocean ridge magma chamber processes: Constraints from olivine zonation in lavas from the East Pacific Rise at 9°30′N and 10°30′N. J. Geophys. Res. - Solid Earth 107, 9–13.
Richter F. M., Davis A. M., DePaolo D. J. and Watson E. B. (2003) Isotope fractionation by chemical diffusion between molten basalt and rhyolite. Geochim. Cosmochim. Acta 67, 3905–3923.
Sio C. K. I., Dauphas N., Teng F.-Z., Chaussidon M., Helz R. T. and Roskosz M. (2013) Discerning crystal growth from diffusion profiles in zoned olivine by in situ Mg–Fe isotopic analyses. Geochim. Cosmochim. Acta 123, 302–321.
Teng F.-Z., Dauphas N., Helz R. T., Gao S. and Huang S. (2011) Diffusion-driven magnesium and iron isotope fractionation in Hawaiian olivine. Earth Planet. Sci. Lett. 308, 317–324.
Watson E. B. and Müller T. (2009) Non-equilibrium isotopic and elemental fractionation during diffusion-controlled crystal growth under static and dynamic conditions. Chem. Geol. 267, 111–124.

IODP

Gulf Stream hydrography during the Late Pliocene and Early Pleistocene: low versus high latitude forcing of the Atlantic Meridional Overturning Circulation

A. OSBORNE, M. FRANK

GEOMAR Helmholtz Centre for Ocean Research Kiel, Kiel, Germany

This is a new project proposal to investigate the strength and variability of the Gulf Stream during the Late Pliocene and Early Pleistocene. ODP Site 1006A, on the western slope of the Great Bahama Bank, is ideally situated to examine the history of the Gulf Stream, but has so far been vastly under-utilised. For the project we propose to first produce a high resolution age model for the site using benthic foraminifera stable isotope stratigraphy, given that the age model is currently only based on magnetostratigraphy and biostratigraphy [Kroon et al., 2000; Spezzaferri et al., 2002]. The age model would be established in collaboration with Prof. Dick Kroon [University of Edinburgh, UK]. Subsequently, the hypothesis that Central American Seaway closure directly affected the salinity and temperature of the Gulf Stream on glacial/interglacial and shorter time scales will be tested by measuring $\delta^{18}O$ and $\delta^{13}C$ in mixed layer and thermocline dwelling planktonic foraminifera and by comparing these to records from the Caribbean warm pool and the eastern equatorial Pacific [De Schepper et al., 2013; Groeneveld, 2005; Groeneveld et al., 2006; 2008, 2014; Steph et al., 2006]. It is not possible to use Mg/Ca to reconstruct seawater temperature at this location, as recrystallization of the foraminiferal calcite has altered the original ratio but has not overprinted the original $\delta^{18}O$ signal [Reuning et al., 2005]. The third part of the proposed project would be to reconstruct intermediate depth ocean circulation at high temporal resolution at both ODP Site 1006A and ODP Site 1000 using ε_{Nd} and rare earth element patterns in the early diagenetic coatings of uncleaned planktonic foraminifera. A coarse 12.5 Myr record of εNd at Site 1006A has already been produced which is broadly consistent with long-term million year trends in the intermediate and deep Caribbean [Newkirk and Martin, 2009; Osborne et al., 2014], suggesting that Site 1006A is perfectly suitable for a high resolution investigation and reconstruction of the history of intermediate waters exiting the Caribbean.

References:

De Schepper, S., J. Groeneveld, B.D.A. Naafs, C. Van Renterghem, J. Hennissen, M.J. Head, S. Louwye, and K. Fabian (2013) PLOS ONE 8, e81508.
Groeneveld, J. (2005) PhD thesis, Faculty of Mathematics and Natural Sciences, Christian Albrechts University, Kiel, Germany.
Groeneveld, J., E.C. Hathorne, S. Steinke, H. DeBe, A. Mackensen, and R. Tiedemann (2014) Earth and Planetary Science Letters 404, 296-306.
Groeneveld, J., D. Nürnberg, R. Tiedemann, G. J. Reichart, S. Steph, L. Reuning, D. Crudeli, and P. Mason (2008) Geochemistry Geophysics Geosystems, 9, doi:Q01p23/10.1029/2006gc001564.
Groeneveld, J., S. Steph, R. Tiedemann, D. Garbe-Schoenberg, D. Nürnberg, and A. Sturm (2006) Proc. ODP, Scientific Results, 202, 1-27.
Kroon, D., T. Williams, C. Primez, S. Spezzaferri, T. Sato, and J. D. Wright (2000) Proc. ODP Sci. Res., 166, 155-166.
Newkirk, D. R., and E. E. Martin (2009) Geology, 37(1), 87-90.
Osborne, A.H., D.R. Newkirk, J. Groeneveld, E.E. Martin, R. Tiedemann, and M. Frank (2014) Paleoceanography 29, 715-729.
Reuning, L., J.J.G. Reijmer, C. Betzler, P. Swart, and T. Bauch (2005) Sedimentary Geology 175, 131-152.
Spezzaferri, S., J. A. McKenzie, and A. Isern (2002) Marine Geology, 185, 95-120.
Steph, S., R. Tiedemann, M. Prange, J. Groeneveld, D. Nürnberg, L. Reuning, M. Schulz, and G. H. Haug (2006) Paleoceanography, 21(4), doi:Pa4221/4210.1029/2004pa001092.

IODP

Benthic Foraminifers as Archive for Changes in the Paleogene Ca Budget and Investigations on Benthic Foraminifer Test Preservation using Raman and EBSD Techniques

ST. PABICH[1], N. GUSSONE[1], K. RABE[2], CHR. VOLLMER[1], B.M.A. TEICHERT[3]

1 WWU Münster, Institut für Mineralogie, Corrensstr. 24, 48149 Münster
2 LUH Hannover, Institut für Mineralogie, Callinstr. 3, 30167 Hannover
3 WWU Münster, Institut für Geologie und Paläontologie, Correnstr. 24, 48149 Münster

Understanding the Earth´s climate as well as the oceanic chemical and isotopic evolution in the past is one of the main aims in Earth Science. In this context, Ca as one of the major elements in the ocean is especially important because its variation in concentration is controlled by different factors including the CO_2 concentration of the atmosphere, continental weathering and Ca carbonate sedimentation. Imbalances in input and output of Ca to the ocean will cause a shift in the Ca isotopic composition of the ocean (cf. Zhu and MacDougall 1998, Skulan et al. 1997). We used samples from IODP Exp. 320/321 to establish a $\delta^{44/40}Ca$ paleo-seawater record between 45 and 25 Ma and model changes in the Ca budget through time. Our results show differences in the Eocene and Oligocene Ca isotope record of benthic foraminifers. The $\delta^{44/40}Ca$ values during the Eocene are relatively

constant with no significant fluctuations during phases of large short term CCD fluctuations (Pälike et al. 2012). The Oligocene is characterized by sediments with uniformly high carbonate content and increasing $\delta^{44/40}$Ca towards the late Oligocene. Past seawater $\delta^{44/40}$Ca values were calculated from the measured benthic foraminifer record applying the calibration for *Gyroidinoides* spp. (Gussone and Filipsson 2010). The Ca budget during the Eocene is relatively constant and not affected by short term CCD fluctuations, indicating that they are too small to alter the isotopic Ca budget. The Oligocene, in contrast is characterized by a general increase in $\delta^{44/40}$Ca seawater values and a continuously deep CCD (Pälike et al. 2012). This is consistent with a massive long term (>1Ma) $CaCO_3$ deposition and decreasing Ca concentration in the ocean water.

Two different quantitative scenarios were modelled. The first scenario shows the effect of changing the fractionation between seawater and oceanic Ca sink in response to a shift from a calcite to an aragonite ocean. The second scenario shows the Ca flux (input/output ratio) vs. time with constant boundary conditions (today's isotope composition of oceanic Ca sources and fractionation factor of the dominant Ca sink). Consequently, a shift in isotope fractionation caused by a change from a calcite to an aragonite ocean is not a likely explanation for the increase in Ca_{sw} isotope values during the Oligocene. Therefore, the Ca isotope record is most likely reflecting changes in the input/output ratio of Ca.

To verify, if the fossil carbonate shell structure and crystal orientation remains intact over the 45 Ma PEAT record, we studied the crystallization behavior and re-crystallization effects of benthic foraminifer shells using Raman spectroscopy and EBSD analysis.

References:
Gussone N. and Filipsson H.L. (2010): Calcium isotope ratios in calcitic tests of benthic Foraminifers. Earth and Planetary Science Letters 290, 108–117.
Pälike H., Mitchell W. Lyle, Hiroshi Nishi, Isabella Raffi, Andy Ridgwell, Kusali Gamage, Adam Klaus et al. (2012): A Cenozoic record of the equatorial Pacific carbonate compensation depth. Nature 488, 609–614.
Skulan J., DePaolo D. and Owens T.L. (1997): Biological control of calcium isotopic abundances in the global calcium cycle. Geochimica et Cosmochimica Acta 61, 2505 – 2510.
Zhu P. and MacDougall J.D. (1998): Calcium Isotopes in the marine environment and the oceanic calcium cycle. Geochimica et Cosmochimica Acta 62, 1691 – 1698.

ICDP

The lacustrine species flocks in the ancient lakes of Sulawesi (Indonesia): Linking organismic diversification and key environmental Events

J. PFAENDER[1], F. HERDER[2], B. STELLBRINK[3], T. VON RINTELEN[1]

1 Museum für Naturkunde, Invalidenstraße 43, 10115 Berlin
2 Zoologisches Forschungsmuseum Alexander Koenig, Adenauerallee 160, 53113 Bonn
3 Department of Animal Ecology & Systematics, Justus Liebig University, Heinrich-Buff-Ring 26-32 IFZ, D-35392 Giessen

Understanding the distribution and origin of the Earth´s biodiversity is still a major task in evolutionary biological research. Ancient lakes are known for their outstanding endemic biodiversity, including some of the world´s most famous species flocks. Therefore, these lakes serve as prime models to study ecological adaptation and its genomic consequences during species flock formation. According to their estimated age and fauna, the Malili lakes and Lake Poso in the central highlands of Sulawesi (Indonesia) are the only ancient lakes in Southeast Asia. Harboring endemic radiations of several animal taxa, like e.g. gastropods, atyid shrimps, parathelphusid crabs and fishes, these lakes offer the rare opportunity to compare timescales of species flock formation between different organisms, evolving within the same environmental setting. Here, we present the first results of the reconstructed evolutionary history of the major species flocks in the Malili lakes and Lake Poso, based on metaanalyses and molecular clock estimates of the timing of diversification and adaptive evolution. In a next step, the molecular clock data will be calibrated, based on age estimations for Lake Towuti, resulting from the ICDP drilling project (scheduled for 2015), to provide important information about the rates of biological evolution and diversification of the endemic species flocks.

ICDP

Comparative approach of the past two interglacials at Lake Van, Turkey

N. PICKARSKI[1,*], T. LITT[1], O. KWIECIEN[2], G. HEUMANN[1] AND THE PALEOVAN SCIENTIFIC TEAM

1 University of Bonn, Steinmann-Institute of Geology, Mineralogy and Paleontology, Nussallee 8, D-53115, Bonn, Germany
2 Ruhr-University Bochum, Institute for Geology, Mineralogy & Geophysics, Universitätsstrasse 150, D-44801 Bochum, Germany
* corresponding author: pickarski@uni-bonn.de

Lake Van (38.6°N, 42.8°E) is located on the high plateau of eastern Anatolia in Turkey. With a surface area of 3,574 km², a maximum water depth of ~460 m, and with an extention of about 130 km WSW-ENE, Lake Van is the largest soda lake (pH 9.8, salinity 21.4 ‰) and the fourth largest terminal lake (volume: ~607 km³) in the world. The Lake Van sediments yield the longest continental paleoclimate record in the entire Near East encompassing the last 600 ka (Stockhecke at al., 2014). Palynological and stable oxygen isotope data were extracted from a 220 m partly laminated sequence (composite profile) obtained at the 357 m deep Ahlat Rigde (AR) site during the drilling campaign in summer 2010.

The high-resolution pollen sequence documents several interglacial-glacial cycles until MIS 15 expressed as changes in thermophilous oak steppe-forest expansion (Litt et al., 2014). In general, the glacial/stadial vegetation is characterized by cold-adapted dwarf-shrub steppe/desert steppe (*Ephedra*, *Artemisia*, chenopods, grasses and forbs), whereas the climax vegetation of past interglacials starts with an oak steppe-forest along with pistachio and juniper. In particular, the expansion of warm-temperate steppe-forest suggests a more favorable environment with increased moisture availability.

Here we combine paleovegetation (pollen record) and geochemical data (oxygen isotopes composition of bulk carbonates and XRF measurements) to yield a comprehensive view of vegetation and climate dynamics of last two interglacials seeking for potential analogue conditions for the current interglacial. It documents a general feature of relatively dryer glacials and relative

wetter interglacial conditions. However, the $\delta^{18}O$ values pointing to a different view of dry interglacials (Kwiecien et al., 2014), which is also evident due to the relative high amounts of *Pinus*. As an additional arboreal pollen (AP) component, pine played an important role during the last (MIS 5e; Pickarski et al., subm.) and the penultimate interglacial (MIS 7e; Litt et al., 2014). It indicates an even stronger continentality during these interglacials compared to the Holocene. Apart from several palynological differences between interglacial periods, we also find similaries, in particular, at the beginning of interglacial periods (e.g. expansion of warm-temperate species *Pistacia*).

One major results of our study is that the observation of cooler MIS 7 interglacials made in southern Europe is contrary to the Lake Van pollen record where the vegetation development during all three warm intervals (MIS 7a, 7c and 7e) reach the level of the last interglacial (MIS 5e) and the Holocene.

References:
Kwiecien, O., Stockhecke, M., Pickarski, N., Heumann, G., Litt, T., Sturm, M., Anselmetti, F., Kipfer, R., Haug, G.H., 2014. Dynamics of the last four glacial terminations recorded in Lake Van, Turkey. QSR 104, 42–52.

Litt, T., Krastel, S., Sturm, M., Kipfer, R., Örcen, S., Heumann, G., Franz, S.O., Ülgen, U.B., Niessen, F., 2009. "PALEOVAN", International Continental Scientific Drilling Program (ICDP): site survey results and perspectives. QSR 28, 1555–1567.

Litt, T., Pickarski, N., Heumann, G., Stockhecke, M., Tzedakis, P.C., 2014. A 600,000 Year Long Continental Pollen Record from Lake Van, Eastern Anatolia (Turkey). QSR 104, 30-41.

Pickarski, N., Kwiecien, O., Djamali, M., Litt, T., subm. Vegetation and environmental changes during the last interglacial in eastern Anatolia (Turkey): a new high-resolution pollen record from Lake Van.

Stockhecke, M., Kwiecien, O., Vigliotti, L., Litt, T., Pickarski, N., Schmincke, H.-U., Çağatay, N., 2014. Chronology of the 600 ka old long continental record of Lake Van: climatostratigraphic synchronization and dating. QSR 104, 8-17.

IODP

Vegetation and climate development on the Atlantic Coastal Plain during the late Mid-Miocene Climatic Optimum (IODP Expedition 313)

SABINE PRADER[1,2], ULRICH KOTTHOFF[1,2], FRANINCE M.G. MCCARTHY[3], DAVID R. GREENWOOD[4], GERHARD SCHMIEDL[2]

1 Centre of Natural History, University Hamburg, Germany
2 Institute of Geology, University Hamburg, Germany
3 Department of Earth Sciences, Brock University, 500 Glenridge Avenue, St. Catharines, Ontario, L2S 3A1, Canada
4 Department of Biology, Brandon University, 270 18th Street, Brandon, MB Manitoba, R7A 6A9, Canada

The major aims of IODP Expedition 313 are estimating amplitudes, rates and mechanisms of sea-level change and the evaluation of sequence stratigraphic facies models that predict depositional environments, sediment compositions, and stratal geometries in response to sea-level change. In addition, the sediments retrieved during Expedion 313 allow assessing palaeoecosystem and -climate dynamics via microfossil-based studies. Cores from three Sites (313-M0027, M0028, and M0029) from the New Jersey shallow shelf (water depth approximately 35 m) were retrieved during May to July 2009, using an ECORD "mission-specific" jack-up platform. These cores comprise sediments from the Eocene until today. Several intervals during the Oligocene and Miocene, including the Mid-Miocene Climatic Optimum (MMCO) are particularly well represented in the retrieved material and allow palynology-based reconstructions.

We have investigated the palynology of sediment cores from Site M0027, 45 km off the present-day coast of New Jersey. For the study presented here, we have focused on pollen studies for the second half of the MMCO and the subsequent transition to cooler conditions (ca. 15 to 13 million years before present). Transport-caused bias of the pollen assemblages was identified via the analysis of the terrestrial/marine palynomorph ratio and the results were considered when interpreting palaeo-vegetation from the pollen data. Pollen preservation in the interval analyzed herein was generally very good. Pollen grains were analyzed via both light and scanning electron microscopy.

The most abundant taxa through all samples are *Quercus* (oak) and *Carya* (hickory). Wetland elements like Cyperaceae, *Taxodium* (cypress), *Nyssa* (tupelo tree) and taxa today growing in the tropics and subtropics like Sapotaceae, Symplocaceae, Arecaceae (palm trees), Buxaceae, and *Alangium*, which indicate particularly warm climate conditions, were only sporadically found, but indicate warmer phases during the second half of the MMCO. Herbal pollen was generally rare, but members of the Asteraceae, Apiaceae, and Ericaceae families, together with infrequent occurences of Poaceae pollen indicate the presence of areas with open vegetation.

The Mid-Miocene pollen assemblages reflect an ecosystem which was reminiscent of Oligocene and early Miocene ecosystems analyzed in previous studies for the hinterland of the New Jersey shelf (e.g. Kotthoff et al. 2014). Oak-hickory forests probably dominated in the lowlands, while frequent occurrence of conifer pollen (*Pinus*, *Picea*, *Abies*, *Sciadopitys*, and *Tsuga canadensis*) indicate that conifer forests prevailed in higher altitudes during the MMCO. Our data imply that vegetation and regional climate in the hinterland of the New Jersey shelf may not have reacted as sensitive to climate changes during MMCO as other regions in North America or Europe. We assume that this is partially caused by a Miocene uplift of the Appalachian Mountains (e.g. Gallen et al., 2013), which led to reduction of suitable areas for thermophilous species and to the proliferation of mountainous taxa and thus to an increase of related pollen taxa in the palynological record.

As next step, we will analyze samples from the onset and the first half of the MMCO in order to examine if the hinterland of the New Jersey shelf experienced warmer or more humid conditions during these phases. This is of particularly interest since the timing of the Miocene uplift of the Appalachian Mountains which could have diluted the impact of global climate change in the research region is still dubious. In this context, we aim at a particularly precise differentiation between highland and lowland pollen taxa in order to develop an highland/lowland index which could then be used to identify topographic changes.

References:
Gallen, S. F., Wegmann, K. W., Bohnenstieh, D. W. R.: Miocene rejuvenation of topographic relief in the southern Appalachians, GSA Today, 23, 4–10, 2013.

Kotthoff, U., McCarthy, F.M.G., Greenwood, D.R., Müller-Navarra, K., Prader, S., Hesselbo, S.P., (2014): Vegetation and climate development on the Atlantic Coastal Plain from 33 to 13 million years ago (IODP expedition 313). Climate of the Past 10, 1523-1539.

ICDP

Limitations of decompression experiments using a trachytic Campi Flegrei composition

O. PREUSS, H. MARXER, M. NOWAK

Eberhard Karls Universität Tübingen, Department of Geosciences, Wilhelmstr. 56, 72076 Tübingen, Germany

Pressure (*P*) decrease during magma ascent accompanied with volatile supersaturation in the melt initiates bubble nucleation and growth. These processes act as driving forces for increased ascent rates in deeper parts of the crust and are important factors for different eruption styles (e.g. Gonnermann and Manga, 2007). Bubble nucleation and growth cause a substantial density decrease and an increase in viscosity by volatile exsolution of the ascending magma (Gonnermann and Manga, 2007). Homogeneous bubble nucleation during decompression can be delayed significantly due to high surface tension of the silicate melt. Such melts will tend to erupt explosively (Gardner, 2012). This may lead to potentially catastrophic eruptions threatening millions of people in highly populated areas like Naples (Italy) located in the middle-southern part of the Campanian plain between the Campi Flegrei (CF) and the Vesuvius stratovolcano. The CF are an active volcanic field characterized by both, magmatic and hydromagmatic episodes with explosive activity (Mastrolorenzo and Pappalardo, 2006). The main structural feature of CF is a nested caldera that formed during two main collapses (Orsi et al., 1992), related to very powerful eruptions, the 39 ka Campanian Ignimbrite (CI) and the 14 ka Neapolitan Yellow Tuff events.

The dynamic degassing processes beneath volcanic systems occurring during magma ascent cannot be observed directly in nature. Therefore, simulation of magma ascent in the lab realized by decompression of volatile containing melts is essential to understand these processes. In this study, the H_2O degassing behavior of a trachytic magma composition of the CI super-eruption was investigated during continuous decompression. The aim of this study is to determine the degree of super-saturation (ΔP) needed for a homogeneous bubble nucleation and to estimate the surface tension of the trachytic melt. These results may provide valuable information for eruption models that rely upon assumptions of magma degassing systematics during ascent (Neri et al., 2003).

Marxer et al. (accepted) have clearly shown that continuous decompression (CD) for simulating magma ascent from a deeper magma chamber into more shallow areas in the crust with ascent rates between 0.17 and 0.024 $MPa \cdot s^{-1}$ is much more realistic than single-step (SSD) or multi-step decompression (MSD) experiments with unrealistic high decompression rates of 2.5 – 10 $MPa \cdot s^{-1}$ during each decompression step. Additional factors may control the results of CD experiments and thereby homogeneous bubble nucleation of a volatile containing melt. In previous studies glass cylinders or pieces of volcanic glass were used as starting material and silicate melts coexisting with a free H_2O fluid phase were decompressed (Gardner and Ketcham, 2011; Mangan and Sisson, 2000; Marxer et al., accepted). As a result of excess H_2O prior to decompression, a big fluid filled bubble forms inside the capsule, which collapse during isobaric rapid quench due to the significant decrease of molar volume of H_2O (Marxer et al., accepted). Bubble shrinkage induces the melt to flow until it is too viscous to relax. Therefore, the bubbles in decompressed quenched samples are often deformed and dented, which lead to flow textures of the bubbles. Bubble size distributions and porosities derived from such samples may thus be erroneous. In other studies glass- or natural rock powder was used as starting material (e.g. Mastrolorenzo and Pappalardo, 2006; Suzuki et al., 2007). Experiments with excess vapor using glass powder as starting material produce numerous small hydration bubbles in the melt, which would inhibit the nucleation of bubbles due to decompression. The growth of such pre-existing hydration bubbles effects nucleation and growth of bubbles during decompression (Gardner et al., 1999). On the contrary, H_2O undersaturated starting conditions are suggested to produce nitrogen rich bubbles in the melt prior to decompression (Mourtada-Bonnefoi, 2002) due to entrapped air in the pore space of the powder during preparation. Nevertheless, the advantage of using glass powder is the short time for H_2O to dissolve homogeneously in the melt depending on grain sizes. Additionally, the sample size is not limited, due to short H_2O diffusion paths in contrast to massive glass cylinders.

This study is focused on (1) hydration experiments at 1300 °C and 200 MPa to investigate the melt conditions prior to decompression and (2) isothermal CD experiments

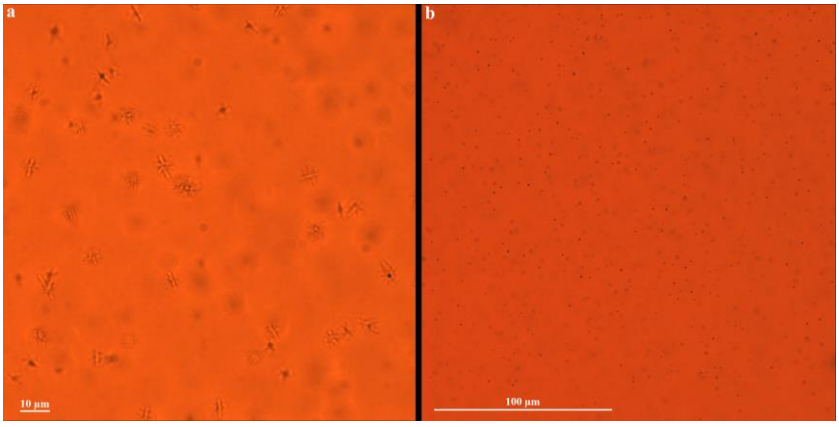

Fig. 1. Optical light microscopy images illustrating details of starting materials equilibrated at 200 MPa, 1300 °C, hydrated with 4.7 wt% H_2O. **(a)** hydrated glass cylinder quenched with a cooling rate of about 150 K min^{-1} with 10 µm sized radial shaped quench crystals, **(b)** glass powder sample with numerous objects on a µm scale despite rapid quench

at 1050 °C. Decompression started at 200 MPa with two different decompression rates (0.024 and 0.17 MPa·s^{-1}) and two different target pressures (P_{final} = 100, 75 MPa). For both experimental sets, massive glass cylinders and glass powder were used as starting material. The CI glass was synthesized by mixing oxides and carbonates that were fused at 1600 °C and subsequently quenched rapidly. 6 - 7 mm long cylinders with 5 mm in diameter were drilled out of the glass. The glass powder is based on a grain size mixture in a 1:1 weight proportion (500 – 200 µm and below 200 µm) to minimize the free intergranular volume and thus to minimize the amount of entrapped air during preparation. $Au_{80}Pd_{20}$ was chosen as capsule material. 13 mm long capsules with an inner diameter of 5 mm (wall thickness 0.2 mm) and a welded lid at the bottom and a crimped and welded star on top were used. Marxer et al. (accepted) showed for the applied decompression rates that 5 mm capsules provide enough space for homogeneous bubble nucleation and growth unaffected by heterogeneous bubble nucleation processes at the capsule melt interface and diffusional loss of H_2O to the capsule wall.

The experiments were conducted in a vertically operated internally heated argon pressure vessel (IHPV) at intrinsic oxygen fugacity conditions (QFM +3.5, Berndt et al., 2002). The autoclave is equipped with a rapid quench device ensuring a sample cooling rate of approximately 150 K s^{-1} (Berndt et al., 2002) depending slightly on the size of the capsule, heat conductivity of the sample and *P*. Rapid cooling causes tension and cracks in the quenched glass samples. To obtain complete unbroken samples, a 40 mm ceramic rod was inserted into the quench zone to lower moderately the cooling rate of the samples.

Fanara et al. (pers. communication) determined a H_2O solubility of about 5.2 wt% at 200 MPa and 1100 °C. Three hydration experiments were conducted slightly H_2O undersaturated (4.7 wt%) at 200 MPa and 1300 °C to test whether 96 hours for massive glass cylinders and 24 or 96 hours for glass powder is sufficient to dissolve H_2O homogeneously within the melt by diffusion. This high temperature (*T)* equilibration was chosen to keep the run time as short as possible, because H_2O diffusion increases exponentially with *T* (e.g. Nowak and Behrens, 1997). The FTIR measurements of the quenched samples showed that 96 h for cylinders and 24 h for powder are sufficient to dissolve H_2O in the melt homogeneously. Furthermore, 4.7 wt% H_2O was dissolved in the melts prior to decompression at 200 MPa, 1300 °C and 96 h using glass cylinders and 24 h as well as 96 h for hydration of melts using glass powder. Isothermal decompression took place at a superliquidus *T* of 1050 °C to ensure a crystal free melt and thus homogeneous bubble nucleation. The continuous pressure decrease was realized by using a high-pressure low-flow metering valve equipped with a piezoelectric nano-positioning system (Nowak et al., 2011). After decompression, the melt was rapidly quenched isobarically. One half of each sample was embedded in epoxy resin racks. The surface was ground and polished for analysis by EMPA and SEM to generate high-resolution backscattered electron (BSE) images. The other half of the cylinder was carefully removed from the capsule, embedded, double-sided ground and polished down to a thickness of 150 - 200 µm for FTIR transmission spectroscopy and optical light microscopy.

Detailed observation of the starting materials using optical light microscopy revealed that the dry starting glass is crystal and bubble free. In contrast, the glass cylinder and powder samples equilibrated with H_2O at 200 MPa, 1300 °C and 1050 °C contain numerous objects on a µm scale despite rapid quench (Fig. 1b). We suggest that these objects are quench crystals due to the observation that these objects formed using both equilibration temperatures. The number densities of crystals in the vitrified samples (*CND*) ranges between $1 \cdot 10^5$ and $4 \cdot 10^5$ mm^{-3}. These *CND* values range within error in the same order of magnitude with µm sized objects found in the decompressed samples quenched at 100 MPa indicating that this problem affects also decompressed samples. Samples quenched after equilibration with a lower cooling rate of about 150 K min^{-1} showed 10 µm sized radial shaped quench crystals (Fig. 1a) with a *CND* of $7 \cdot 10^4$ mm^{-3}. These results indicate that the formation of quench crystals in hydrous CI melt is very sensitive to the cooling rate.

The transmitted light microscopy images of the samples from the experiments with a P_{final} of 100 MPa and both decompression rates reveal significant differences in degassing behavior between samples derived from massive glass cylinders and glass powder, which was equilibrated for 24 h. Two samples starting from powder with both decompression rates (0.024 MPa·s^{-1}, 0.17 MPa·s^{-1}) show high porosities and are characterized by a low population density of big bubbles (~250 mm^{-3}) whereas the equivalent glass cylinder samples reveal very high population densities of objects ($2 \cdot 10^5$ - $6 \cdot 10^5$ mm^{-3}) with much smaller size (1 – 4 µm). We suggest that these objects are small bubbles nucleated heterogeneously at quench crystals during cooling due to the supersaturation of H_2O of the melt at P_{final} of 100 MPa. One glass powder sample was equilibrated for 96 h and shows the same characteristics like both glass cylinder samples. This indicates that 96 h equilibration time is sufficient for entrapped nitrogen rich bubbles to ascend to the top of the capsule; hence a homogeneous nucleation of H_2O bubbles after 96 h of equilibration using powder is possible.

In general, the same observations of differences in degassing behavior can be made with BSE images (Fig. 2), but bubbles or objects < 4 µm as well as crystals in the rapid quenched starting materials are not visible in these

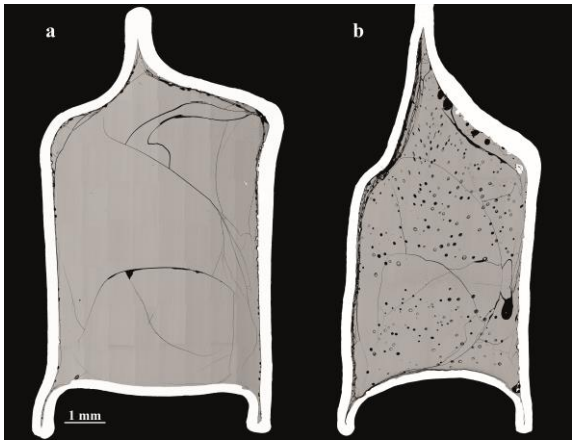

Fig. 2 BSE images of comparing decompression experiments starting from (a) glass cylinder equilibrated for 96 h and (b) glass powder equilibrated for 24 h both decompressed with 0.17 MPa·s^{-1} to a P_{final} of 100 MPa.

images due to limitations in resolution of BSE images and the low intersection probability to cut e.g. bubbles.

BSE images of samples decompressed to a P_{final} of 75 MPa with both decompression rates using cylinders are characterized by higher porosities than samples with a P_{final} of 100 MPa, but the bubble number densities are lower. The slower decompressed sample (0.024 MPa·s^{-1}) illustrates that bubbles nucleated at the capsule-melt interface are more numerous and bigger than using a faster decompression rate of 0.17 MPa·s^{-1}. The huge bubbles in the center of the sample are suggested to have ascended from the bottom of the capsule into the center of the melt during decompression. This is evident by the fact that smaller bubbles only appear above these big bubbles, which have a rim free of smaller bubbles around them. If the duration of the decompression experiment is increased depending on decompression rate then the ascended bubbles will erase homogeneously nucleated bubbles.

The experiments of this study reveal that at a equlibration time of 96 h prior to decompression the starting material will not influence the results of decompression experiments. However, there is no advantage in equilibration time by using glass powder as starting material so H_2O undersaturated massive glass cylinders for decompression experiments should be used. The formation of quench crystals is critical, if the melt is quenched around the supersaturation pressure initiating bubble nucleation and growth during quench. Therefore, the cooling rate has to be increased to prevent cryztallization during the quench process. According to the experiments, it can be demonstrated that the ΔP for the trachytic CI melt range between 100 and 125 MPa.

References:

Berndt, J., Liebske, C., Holtz, F., Freise, M., Nowak, M., Ziegenbein, D., Hurkuck, W., and Koepke, J. (2002) A combined rapid-quench and H2-membrane setup for internally heated pressure vessels: Description and application for water solubility in basaltic melts. American Mineralogist, 87(11-12), 1717-1726.

Gardner, J.E. (2012) Surface tension and bubble nucleation in phonolite magmas. Geochimica et Cosmochimica Acta, 76, 93-102.

Gardner, J.E., Hilton, M., and Carroll, M.R. (1999) Experimental constraints on degassing of magma: isothermal bubble growth during continuous decompression from high pressure. Earth and Planetary Science Letters, 168(1-2), 201-218.

Gardner, J.E., and Ketcham, R.A. (2011) Bubble nucleation in rhyolite and dacite melts: temperature dependence of surface tension. Contributions to Mineralogy and Petrology, 162(5), 929-943.

Gonnermann, H.M., and Manga, M. (2007) The Fluid Mechanics Inside a Volcano. Annual Review of Fluid Mechanics, 39(1), 321-356.

Mangan, M., and Sisson, T. (2000) Delayed, disequilibrium degassing in rhyolite magma: decompression experiments and implications for explosive volcanism. Earth and Planetary Science Letters, 183(3-4), 441-455.

Marxer, H., Bellucci, P., and Nowak, M. (accepted) Degassing of H2O in a phonlitic melt: A closer look at decompression experiments. Journal of Volcanology and Geothermal Research.

Mastrolorenzo, G., and Pappalardo, L. (2006) Magma degassing and crystallization processes during eruptions of high-risk Neapolitan-volcanoes: Evidence of common equilibrium rising processes in alkaline magmas. Earth and Planetary Science Letters, 250(1-2), 164-181.

Mourtada-Bonnefoi, C.C. (2002) Homogeneous bubble nucleation in rhyolitic magmas: An experimental study of the effect of H2O and CO2. Journal of Geophysical Research, 107(B4).

Neri, A., Papale, P., Del Seppia, D., and Santacroce, R. (2003) Coupled conduit and atmospheric dispersal dynamics of the AD 79 Plinian eruption of Vesuvius. Journal of Volcanology and Geothermal Research, 120(1-2), 141-160.

Nowak, M., and Behrens, H. (1997) An experimental investigation on diffusion of water in haplogranitic melts. Contributions to Mineralogy and Petrology, 126(4), 365-376.

Nowak, M., Cichy, S.B., Botcharnikov, R.E., Walker, N., and Hurkuck, W. (2011) A new type of high-pressure low-flow metering valve for continuous decompression: First experimental results on degassing of rhyodacitic melts. American Mineralogist, 96, 1373-1380.

Orsi, G., Dantonio, M., Devita, S., and Gallo, G. (1992) The Neapolitan Yellow Tuff, a Large-Magnitude Trachytic Phreatoplinian Eruption - Eruptive Dynamics, Magma Withdrawal and Caldera Collapse. Journal of Volcanology and Geothermal Research, 53(1-4), 275-287.

Suzuki, Y., Gardner, J.E., and Larsen, J.F. (2007) Experimental constraints on syneruptive magma ascent related to the phreatomagmatic phase of the 2000AD eruption of Usu volcano, Japan. Bulletin of Volcanology, 69(4), 423-444.

ICDP

Hydrologic cycles in Pliocene North America and their climate teleconnections - Initial study of newly recovered drill core from paleo-lake Idaho

A. PROKOPENKO

University of Cologne, Mathematisch-Naturwissenschaftliche Fakultät, Geologie und Mineralogie, Zuelpicher str. 49, 50674Köln

The mid-Pliocene warm period some 3 Myr ago is the most recent time in the Earth's history with 'mature' equilibrium-state warmer global climate. Estimated by GCM simulations to be 2-3°C warmer than the pre-industrial Holocene climate, the mid-Pliocene warm period thus may serve as the most recent analog to the projected 2-3°C warmer climate at the end of the 21st century. Because Pliocene geography was similar to that today, understanding the nature of Pliocene warm climate with similar principal boundary conditions and the ability to portray it in climate models are essential for the development of tools for simulating future climate change. An important feature of the Pliocene climate is the apparently lower latitudinal gradients in sea-surface temperatures (SSTs); models suggest that lower gradients are associated with weaker atmospheric circulation, the poleward expansion of Hadley cells, and zonal increases in mid-latitude humidity. There also exists a dramatic mismatch between the simulated temperatures and those based on pollen/biome reconstructions. Studies of continental records of Pliocene paleoclimate are important and timely in this context. Few records, however, are available worldwide, and most compilations of Pliocene climate in terrestrial settings derive paleodata from discontinuous sections. Here a plan is presented for an upcoming DFG proposal aimed at developing new continental Pliocene paleoclimate record based on the drill core already recovered, but not yet studied.

Pliocene sequences from the Great Basin in mid-latitude North America are among the key sites providing boundary conditions for the Pliocene climate simulations and for testing the paleodata/model convergence (e.g., PRISM0-PRISM3). Cyclic variations in sediment properties, pollen and diatom composition driven by past variations in humidity in this sensitive semi-arid region have been recognized before, yet none of the records so far has recognized orbital cycles and/or provided time scales compatible with those of marine records. As a part of the Project HOTSPOT (2010-2012, supported by ICDP and the US DOE), a drill core at the Mountain Home location (HOTSPOT site 3) recovered the lacustrine sediment sequence of the Western Snake River Plain (WSRP) rift basin, previously occupied by the presently extinct deep paleo-Lake Idaho. This was the first scientific drilling of

the Pliocene lacustrine sequences in the Great Basin area since the 1980s to 1991. The core was obtained by DOSECC, Inc. with nearly 100% recovery and now offers an unprecedented opportunity to develop the first complete well-resolved Pliocene continental archive from North America. The sequence, penetrated to the depth of 1821 m, consists of ca. 60 m of basalt, underlain by 730 m of lacustrine sediments (silts and fine sands) with minor intercalated basalt flows. The lower 867 m of the hole comprises hydrothermally altered basalts, basalt hyaloclastites, and basaltic sands. For this upcoming project, the proposal will be made to log and process the presently unopened lacustrine portion of this core, stored at UMN LacCore facility (USA), and make a detailed study of the 300-meter portion of fine lacustrine mud representing the highstand of paleo-Lake Idaho corresponding to the mid-Pliocene warm period. The results of the study will allowing testing of a series of hypotheses on climate teleconnections and meridional heat transport during the mid-Pliocene, zonal humidity changes in the Northern Hemisphere (NH) associated with changing SST gradients, and on the role of moisture transport to continental North America in initiating NH glaciations ca. 2.7 Ma.

ICDP

A multiple isotope and trace element approach to constrain the oxygenation and metal cycling of 3.5 to 3.2 Ga paleo-oceans

P. RAMMENSEE[1], A. MONTINARO[2], H. STRAUSS[2], R. CREASER[3], I. HORN[4], S. WEYER[4], N.J. BEUKES[5], S. AULBACH[1]

1 Goethe-Universität Frankfurt, Institut for Geowissenschaften, Frankfurt, Germany
2 Westfälische Wilhelms-Universität Münster, Institut für Geologie und Paläontologie, Münster, Germany
3 University of Alberta, Department of Earth and Atmospheric Sciences, Edmonton, Canada
4 Universität Hannover, Institut für Mineraloge, Hannover, Germany
5 University of Johannesburg, Department of Geology, Johannesburg, South Africa

The complex redox evolution of the terrestrial atmosphere and hydrosphere prior the Great Oxidation Event at ca. 2.45 Ga has become a highly active field of research with regard to multiple aspects. This is also owing to the recent development of analytical techniques allowing the acquisition of non-traditional stable isotope ratios that are sensitive recorders of various biogenic and abiogenic redox reactions [1,2]. The evolution of early life forms is closely linked to the redox state and availability of metabolically cycled elements. For example, oxygenic photosynthesis has been established long before the rise of oxygen levels in the atmosphere. The ICDP Project "Barberton Drilling Project: Peering into the Cradle of Life" has provided drill core covering successions of the 3.5 to 3.2 Ga Barberton Greenstone Belt and has attracted >50 scientists from 12 countries, with aims to resolve the details of environmental conditions on early Earth that led to the emergence and evolution of life [3]. At three of the project's drilling sites (BARB3, BARB4 and BARB5) sedimentary successions of deep to shallow marine environments were retrieved, consisting mostly of carbonaceous siltstone, chert and banded iron formation (BIF), spanning ca 300 Ma of Palaeo-Archaean deposition. We are investigating selected samples of theses cores by (a) platinum group element (PGE) and Re-Os isotopic compositions, (b) U isotope compositions and (c) Fe isotope compositions to fingerprint metal sources to the early oceans, to decipher modes of stable isotope fraction and for age constraints using the Re-Os radiogenic isotope system.

Rhenium and PGE are variably redox-sensitive and have been successfully exploited to identify detrital vs. hydrogenous sources and the presence of oxic, suboxic or euxinic conditions in marine sediments [4]. As ^{187}Re decays to ^{187}Os, the Re-Os isotope system can – under favorable circumstances - additionally be used to date the deposition of sediments, and to obtain the initial Os isotope composition, which is a tracer for continental input of radiogenic Os [5].

We are in the process of acquiring Re-Os isotope data for 8+ samples from narrow intervals (~1 m, to avoid initial Os isotope heterogeneity) of carbonaceous siltstone from BARB3 (one interval) and BARB5 (two intervals), using a high-pressure/high-temperature Carius tube digestion technique followed by isotope dilution thermal ionisation mass spectrometry at the University of Alberta [6]. This will be complemented by information on PGE concentrations (Frankfurt University), carbon and sulphur contents, Fe speciation and multiple S isotope compositions (Muenster University). Our aim is to determine whether any short-scale changes occur in the sources and processes of incorporation of these various elements into the sediments that will allow constraints to be placed on the palaeo-depositional environment.

To assess the differences between hydrogenous and detrital PGE content we are investigating sample powders with (1) digestion in PFA vials on hotplate and (2) low-temperature leaching of presumably hydrogenous, acid-soluble components. Both are spiked with mixed isotope tracers, processed through cation exchange chromatography to isolate PGE-Re from the residue, further purification with BPHA (organic solvent) and measurement of Ru-Pd-Ir-Pt by ICPMS. Prior work [7] has shown that PGE-Re abundance patterns of BGB sediments resemble those of komatiites, indicating an ultramafic, detrital source. Given the age of the BGB (3.5 – 3.2 Ga) and the absence of oxidative weathering, we expect to see low concentrations and no resolvable difference between the two digestion approaches that would be attributable to the variable redox behavior of Re and PGE.

The small scale intervals may not be representative of the complete history of deposition in the sedimentary basin. To constrain basin wide changes in PGE abundance and pattern, we are currently examining samples of the reference sample suite of BARB5 core ranging from 205 to 760 m depth. At this time, sample powders are ready and lab work started to be carried out. This will follow the procedure described above, with the exception that the high-pressure digestion will be carried out with the high-pressure asher and Re-Os isotopes will be acquired by MC-ICPMS at Frankfurt university.

Uranium is a redox sensitive trace metal that is mobile under oxidic conditions. During U reduction, and the

deposition in sediments of anoxic environments, measurable fractionation of the U isotopes occurs [2]. In our study, we will perform U isotope analyses to fingerprint potential U mobilization, that may have occurred under localy slightly enhanced oxygen levels. The underlying idea is that the subsequent reduction of any mobilized U under overall anoxic conditions in the oceans will result in U isotope fractionation which may be recorded in the investigated sediments, even if overall U enrichment is low [7]. Purification of U was carried out following the proccedure descriped in [2] subsequent to the chromatographic purification of PGEs. To show that no fractionation of U occurs on the cation columns used for the separation of PGEs, we processed a standard U solution with distinct isotopic composition and examined various eluant splits. Within the error of measurement we could not detect any fractionation of U. We will obtain isotopic compositions from low-temperature leaching of the small scale intervals of BARB3 and BARB5 and the reference suite samples of BARB5. Measurements of first samples were hindered by technical issues, but will be carried out in the near future.

As the formation processes of BIF are a matter of debate, the modes of Fe isotope fractionation in this setting are a topic of discussion [1]. We use pristine Fe-rich layers in thin sections of the BARB4 core from depths of 230 to 354 m with the aim to determine the pathways of Fe isotope fractionation until early diagenesis.

In situ Fe isotope measurements were performed at Institut für Mineralogie at University of Hannover using a UV-femtosecond laser ablation system coupled with MC-ICP-MS [8]. A total of n = 172 valid $\delta^{56}Fe$ values (relative to the IRMM-14 standard) from six thin sections were obtained in two sessions in July and December 2013. The overall range of measured $\delta^{56}Fe_{IRMM}$ is -1.88 ‰ to +1.28 ‰ with an average precision of 0.1 ‰. The majority of data represent single phase measurements of magnetite (n = 95) and siderite (n = 52). Furthermore, analyses of ankerite and hematite were performed. Due to small grain size of hematite, the analysis of mixed phase could not be avoided (hematite and siderite, n = 4; hematite and magnetite, n = 1). Within errors, all measured values are consistent with mass-dependent fractionation.

Mean $\delta^{56}Fe_{IRMM}$ of magnetite at depths from 230 to 354 m is +0.53 ± 0.39 ‰ (standard deviation). The means of magnetite in each thin section are between +0.40 ± 0.08 ‰ (253 m) and +0.70 ± 0.07 ‰ (285 m, student-t distribution 95 % confidence interval). Furthermore, significant variation within thin sections and between sets of siderite-magnetite lamination could be identified. Siderite $\delta^{56}Fe$ is on average lighter than magnetite, and ranges between -1.88 and +0.33 ‰ for single analyses. Hematite-siderite mixed analyses lead to $\delta^{56}Fe$ of +0.04 ± 0.14 ‰, indicating hematite $\delta^{56}Fe$ of more positive value. With an assumption of a likely range of siderite mass contribution to the analysis, the range for this primary hematite is calculated to be +0.27 to +0.78 ‰. In agreement, pure hematite analyses yield +0.58 ± 0.15 ‰. This contrasts with the expected composition in equilibrium with siderite of +2.20 ± 0.21 ‰, indicating disequilibrium. Secondary hematite replacing magnetite, as a mixed analysis, yields: +1.28 ± 0.13 ‰, suggesting that, hematite has a more positive composition than magnetite (+0.76 ± 0.08 ‰) in this case. An estimate for this secondary hematite is +1.66 to +2.55 ‰, which is in gross agreement with the equilibrium composition of hematite in a ferrous aqueous solution with the isotopic composition of siderite. As a conclusion, iron isotopic compositions of magnetite and primary hematite probably are similar and hematite is generally not in isotopic equilibrium with its surrounding siderite. Primary hematite shows the pristine signature and during magnetite formation no frationation in respect to hematite occurred. Hence also magnetite traces the same signature.

As siderite and magnetite concentrate almost the entire mass of Fe in many laminae and layers, a quantification of modal proportion is used to constrain bulk isotopic compositions of laminae and layers. Back scattered electron images of representative areas were processed and simplified through graphics software with the result of an estimate of iron mass distribution of a two-dimensional transect. Fe-rich chert layers and nodules may be equilibrated with ankerite. Hence, hematite in chert and ankerite as dominating Fe phases are keys to bulk isotopic composition of veins. Estimated bulk layer isotopic composition of siderite-chert-magnetite lamination is between -0.03 and +0.29 ‰ and averages at +0.06 ± 0.10 ‰ (SD). These numbers are in the range of a hydrothermal source of iron. As magnetite occurs in massive nodules, one expects those to be dominated by the isotopic composition of magnetite. Solution bulk isotopic compositions of equivalent rocks of the Manzimnyama IF show a range from +0.44 to +0.98 ‰ [9], suiting a mixture of magnetite, primary hematite and a potential minor contribution of sulfides or secondary hematite.

These early BIF show similar characteristics than those of late Archean BIF [1]. Our conclusion is, the principle of formation of the scarce early Archean BIFs might be similar to those of the massive abundant late Archean BIF.

References:
[1] Steinhoefel et al. (2010) Geochim Cosmochim Acta: 74, 2677-2696
[2] Weyer et al. (2008) Geochim Cosmochim Acta: 72, 345-359
[3] Arndt et al. (2013) Geophys Res Abstr 15: EGU2013-3909
[4] Siebert et al. (2005) Geochim. Cosmochim. Acta 69: 1787–1801
[5] Kendall et al. (2009) Geol. Soc. London Spec. Publ. 326: 85-107
[6] Creaser et al. (1991) Geochim Cosmochim Acta 55, 397-401
[7] Kendall et al. (2013) Chem. Geol. 362, 105-114
[8] Horn et al. (2006) Geochim Cosmochim Acta: 70, 3677-3688
[9] Planavsky (2012) Geochim Cosmochim Acta: 80, 158-169

IODP

Diatoms and the Si and C cycles

J. RENAUDIE

Museum für Naturkunde, Leibniz-Institut für Evolutions- und Biodiversitätsforschung, Invalidenstraße 43, 10115 Berlin.

Marine planktonic diatoms play an unique role as the main carbon exporter to the deep sea in the modern oceans, since they constitute the single largest component of the ocean biologic carbon pump (e. g. Ragueneau et al. 2000). Many authors (e. g. Pollock, 1997; Tréguer and Pondaven, 2000; Lazarus et al., 2014) have speculated or modeled that changes in the activity of diatoms as a carbon pump could have been strong enough to influence atmospheric pCO_2 on geological timescales, and thus affect the climate state.

In addition to this, diatoms are also, today, the main silica exporter to the deep sea. Biogenic opal deposition being the only output of the marine silica cycle (Tréguer et al., 1995) and weathering being the main input to the cycle, both should in principle balance each other on geological timescales.

A preliminary study (Renaudie, *subm.*), based on a review of the literature and a compilation of the smear slide descriptions from the Initial Reports of DSDP and ODP expeditions, highlighted several significant deposition events such as an increase of diatom relative abundance, mainly in the South Atlantic, near the Eocene/Oligocene boundary; the first appearance of the Southern Ocean diatom belt during a regional event in the Late Oligocene; and a complete change in the diatom geographical pattern at ca. 15 Ma (the 'Silica Switch'), coeval with a sustained increase in global relative abundance of diatoms in sediments. The first and third events seem to correlate well with both known drops in pCO_2 and shifts in strontium and osmium isotopes. It is also during the first event that diatoms seem to take over the biogenic silicon cycle to the detriment of radiolarians.

This preliminary study had however many limitations. The time scale resolution was too low to pinpoint events with precision and thus understand fully the sequence of events; the use of relative, instead of absolute abundance, prevented interpreting results in terms of rates and thus integration of results with oceanographic models; and finally the accuracy of smear slide data permitted only broad categories instead of a more finely divided silica abundance scale.

In a new project, I propose to count timeseries of absolute abundance of siliceous microfossils (with a focus on diatoms) in a selection of Cenozoic pelagic sections representing the various biogeographic provinces (as revealed during the preliminary study) and quantify the global deposition rate of biogenic silica. This new dataset will improve our understanding of how the rise of diatoms impacted the Cenozoic carbon cycle and better constrain changes in silica weathering rates during the Cenozoic.

References:

Lazarus, D. B., Barron, J., Renaudie, J., Diver, P., and Türke, A. (2014). Cenozoic diatom diversity and correlation to climate change. PLoS ONE, 9(1):e84857.

Pollock, D. E. (1997). The role of diatoms, dissolved silicate and Antarctic glaciation in glacial/interglacial climatic change: a hypothesis. Global and Planetary Change, 14: 113-125.

Ragueneau, O., Tréguer, P., Leynaert, A., Anderson, R. F., Brzezinski, M. A., DeMaster, D. J., Dugdale, R. C., Dymond, J., Fischer, G., Francois, R., Heinze, C., Maier-Reimer, E., Martin-Jézéquel, E., Nelson, D. M. and Quéguiner, B. (2000). A review of Si cycle in the modern ocean: recent progress and missing gaps in the application of biogenic opal as a paleoproductivity proxy. Global and Planetary Change, 26: 317-365.

Renaudie J., (submitted). A quantitative review of the Cenozoic diatom deposition history. Earth-Science Reviews, (invited).

Tréguer, P. J. and Pondaven, P. (2000). Silica control on carbon dioxide. Nature, 406: 358-359.

Tréguer, P. J., Nelson, D. M., Van Bennekom, A. J., DeMaster, D. J., Leynaert, A. and Quéguiner, B. (1995). The silica balance in the world ocean: a reestimate. Science, 268: 375-379.

ICDP

Preliminary results from the deep drilling at Chew Bahir, south Ethiopia

F. SCHÄBITZ[1], B. WAGNER[2], F.A. VIEHBERG[2], V. WENNRICH[2], J. RETHEMEYER[2], J. JUST[2], N. KLASEN[3], A. ASRAT[4], H. LAMB[5], V. FOERSTER[6], M.H. TRAUTH[6], A. JUNGINGER[7], A. COHEN[8] AND THE HSPDP SCIENCE TEAM[9]

1 University of Cologne, Seminar for Geography and Education, Gronewaldstr. 2, 50931 Cologne, Germany
2 University of Cologne, Institute of Geology and Mineralogy, Zülpicher Str. 49A, 50674 Cologne, Germany
3 University of Cologne, Institute of Geography, Otto-Fischer-Str. 4, 50674 Cologne, Germany
4 Addis Ababa University, School of Earth Sciences; P. O. Box 1176, Addis Ababa, Ethiopia
5 Aberystwyth University, Department of Geography and Earth Sciences, Aberystwyth SY23 3DB, U.K.
6 University of Potsdam, Institute of Earth and Environmental Science, Karl-Liebknecht-Str. 24-25 14476 Potsdam-Golm, Germany
7 Eberhard Karls Universität Tübingen, Department of Geosciences, Hölderlinstr. 12, 72074 Tübingen, Germany
8 Department of Geosciences, University of Arizona, Tucson AZ 85721, USA
9 http://hspdp.asu.edu/

Chew Bahir is one of the five sites drilled during 2013-14 in the framework of the *Hominin Sites and Paleolakes Drilling Project* (ICDP-HSPDP), in order to understand climatic and environmental influences on the evolution of hominins in eastern Africa during the last 4 million years. The Chew Bahir record will concentrate on the last 500 ka of that history and is supported by the Cologne Collaborative Research Centre (CRC-806), and the International Continental Scientific Drilling Program (ICDP).The site is a playa lake, today, within a tectonic basin located in the southern part of the Main Ethiopian Rift (MER) at about 500 m a. s. l. and lies close to the fossil sites of Omo Kibish and to Konso-Gardula. In a transect from west to east of this tectonic basin, six short cores (maximum depth of 19 m) recovered in 2009 and 2010 provided a basic understanding of sedimentation processes from the border to the centre of the paleolake, mainly by using XRF scanning data. The age-models for these cores were based on 32 AMS radiocarbon dates, which placed the base of the centremost core at about 45 ka BP. The potassium (K) record is one of the most promising proxies in all these cores allowing us to identify wet and dry climates (e.g., a dry climate during LGM times, a wet African Humid Period, a dry Younger Dryas equivalent, a wet early Holocene followed by a dry middle to late Holocene) possibly driven by solar insolation, causing shifts in the intensity and the position of the Intertropical Convergence zone (ITCZ) and the Congo Air Boundary

(CAB). In March 2014, a 41.5 m deep core was recovered from the centre of the basin. As with the short cores, the K counts measured by XRF scanning show variations probably caused by climate driven processes. Radiocarbon , OSL and paleomagnetic measurements on this core are still in progress, but preliminary results will be available by the time of the meeting. Preliminary stratigraphic indications suggest that this record may extend to marine oxygen isotope stages (MIS) 5 or 6. In Nov-Dec 2014 the HSPDP team drilled two parallel cores, ~260 and ~280 m long, that will allow paleoenvironmental reconstruction back to at least 500 ka BP, covering the transition into the Middle Stone Age and the timespan of origin and dispersal of *Homo sapiens*.

IODP

Izu-Bonin-Arc tephrostratigraphy- evolution, provenance, cyclicities (IODP Exp. 350&352)

J.C. SCHINDLBECK, S. KUTTEROLF, IODP EXPEDITION 350 AND 352 SCIENCE PARTIES

GEOMAR, Helmholtz Center for Ocean Research Kiel, Wischhofstraße 1-3, 24148 Kiel

The Izu-Bonin-Mariana arc (IBM) in the Western Pacific extends over 2800 km from Izu Peninsula (Japan) to Guam (USA) and has been the target of several, individual, drilling projects in the past. The current multiphase IBM drilling project is a synthesis of four closely related IODP Expeditions that started in March 2014. The project described here submitted in the proposal that we introduce here will focus on tephra layers sampled during Expeditions 350 and 352 and the intention is to closely collaborate with other shipboard scientists of the two expeditions.

IODP Expedition 350 drilled two sites: (1) Site U1436 was drilled in the forearc as a geotechnical hole in preparation for the proposed deep drilling at Site IBM-4. (2) Site U1437 lies about 160 km WSW of Site U1436 in a basin between two Izu reararc seamount chains (Manji and Enpo chains). Coring at Site U1436 recovered ~220 m of sediment - a nearly complete record of Late Pleistocene forearc sedimentation that is strongly influenced by frontal arc explosive volcanism. The sediments (lithostratigraphic Unit I) consist of intercalated tuffaceous mud, mafic ash and scoria lapilli-ash and evolved ash and pumice lapilli-ash (~150 single tephra layers) (Expedition 350 Scientists, 2014). At Site U1437 1806.5 m were recovered in three coherent holes. The sediment inventory is tuffaceous mud and mudstone with intercalated volcaniclastic layers in the uppermost 1300 m (Units I–V), with a gradual change to more volcaniclastic layers (Units VI and VII) (Expedition 350 Scientists, 2014). Shipboard XRF data and preliminary EMP data indicate arc front and reararc sources for the volcaniclastic deposits. In our proposed work we will mainly focus on tephra layers sampled in Unit I (0 to 682 mbsf).

IODP Expedition 352 recovered 1.22 km of igneous basement and 0.46 km of overlying sediment at four sites (Expedition 352 Scientists, 2015). The cored volcanic rocks provide diverse, stratigraphically controlled suites of forearc basalts, related to decompression melting as mantle rose to fill the space created by the initial sinking of the Pacific Plate, and boninite generated slightly later during earliest arc development. The igneous basement is overlain by Late Eocene to Recent sediments. The major lithologies include nannofossil ooze, mud and coarse sand with variable amounts of aeolian contribution, and volcaniclastic material. Three phases of highly explosive volcanism (latest Pliocene to Pleistocene, Late Miocene to earliest Pliocene, Oligocene) were identified, represented by a total of 132 graded, air fall tephra layers, which are likely to correlate between the four drill sites (Expedition 352 Scientists, 2015).

The IBM system is an extraordinarily good place to address fundamental questions regarding the initiation and evolution of subduction zones, such as: (i) how does subduction initiate; (ii) how do ophiolites and continental crust originate; and (iii) how do multiple arc and backarc phases develop and evolve at one subduction zone? Tephra layers in the marine sediment record recovered during the expeditions provide an opportunity to decode some of these mysteries.

It is therefore our particular aim to establish a mostly complete overall tephrostratigraphy that better classifies the long-term origin, style and frequency of larger explosive eruptions from the Izu-Bonin arc. The ~600 Quaternary to Pliocene tephra layers sampled during Expedition 350, and ~150 Quaternary to Oligocene tephra layers recovered during Expedition 352 will enable us to achieve the following objectives:

1. extend the former, more locally restricted, investigations of Izu-Bonin´s geochemical and volcanological evolution based on tephras (e.g., Straub, 1995, 2003; Arculus and Bloomfield, 1992; Arculus et al., 1995) to a widespread temporal and spatial provenance study of the explosive volcanism in that entire region, finally contributing to the knowledge of Izu-Bonin arc evolution. This will be complemented by subsequent correlations between tephras from older DSDP/ODP and our recent IODP sites and will lead, as a first step, to the detailed tephrostratigraphy at the Izu-Bonin arc. With this extensive record, chemical variations over time and along the arc will be elaborated and further interpreted regarding their provenance;
2. study the emplacement and origin of selected marine tephra layers that clearly show emplacement by flow rather than fall processes;
3. study cyclicities that have been observed in marine ash records on a range of time scales, especially at the Ring of Fire. Preliminary results from Expedition 350 and also 352 are promising and indicate probably periodicities in the IBM arc activity. The comparison to other long tephra time series (e.g., CAVA) will additionally give us the possibility to consider global implications.

References:

Arculus, R. J., and Bloomfield, A. L., 1992, Major-element geochemistry of of ashes from Sites 782, 784, and 786 in the Bonin Forearc, in Fryer, P., Pearce, J. A., and Stokking, L. B. e. a., eds., Proceeding of the Ocean Drilling Program Scientific Results, v. 125, p. 277 - 292.

Arculus, R. J., Gill, J. B., Cambray, H., Chen, W., and Stern, R. J., 1995, Geochemical evolution of arc systems in the Western Pacific: the ash and turbidite record recovered by drilling, in Active margins and marginal basins of the Western Pacific, American Geophysical Union, p. 45 - 65.

Expedition 350 Scientists, 2014. Izu-Bonin-Mariana rearc: the missing half of the subduction factory. International Ocean Discovery Program Preliminary Report, 350. http://dx.doi.org/10.14379/iodp.pr.350.2014
Expedition 352 Scientists, 2015. Izu-Bonin-Mariana Fore Arc: Testing subduction initiation and ophiolite models by drilling the outer Izu-Bonin-Mariana fore arc. International Ocean Discovery Program Preliminary Report, 352. http://dx.doi.org/10.14379/iodp.pr.352.2015
Straub, S. M., 1995, Contrasting compositions of Mariana Trough fallout tephra and Mariana island arc volcanics: a fractional crystallisation link: Bulletin of Volcanology, v. 57, p. 403- 421.
Straub, S. M., and Layne, G. D., 2003, The systematics of chlorine, fluorine, and water in Izu arc front volcanic rocks: Implications for volatile recycling in subduction zones: Geochimica Cosmochimica Acta, v. 67, no. 21, p. 4179-4203.

IODP

Galápagos Plinian volcanism- evidence in ODP/IODP Legs offshore Central America

J.C. SCHINDLBECK, S. KUTTEROLF, A. FREUNDT

GEOMAR Helmholtz-Centre for Ocean Research Kiel, 24148 Kiel, Germany

Drill cores recovered during several ODP and IODP Expeditions offshore Central America contain an extensive Early Cenozoic ash layer record. These ash layers have been deposited by plinian eruptions that originated either at the Central American Volcanic Arc (CAVA) or at the Galápagos Hot Spot. While plinian eruptions are well known from the CAVA, volcanism from the Galápagos region is dominantly recorded in effusive and strombolian deposits from subaerial and submarine eruptions although rare large explosive eruptions of evolved trachytic or dacitic compositions did occur in the Pleistocene (e.g., Geist et al., 1994).

We have established a tephrostratigraphy from recent through Miocene times from the unique archive of ODP/IODP sites offhore Central America in which we identify tephra source regions by geochemical compositions of the glass shards. Thus we found numerous CAVA-derived tephra layers characterized by typical arc signatures (e.g., Nb-Ta troughs, LILE enrichments), but more surprisingly also an extensive record of tephra layers mostly of Miocene age featuring ocean island geochemical compositions (e.g., low La/Nb and Ba/La ratios, high Nb/Rb ratios). At this geographical setting the only plausible source for these layers is the Galápagos archipelago. Such Miocene ash layers occur in the cores of ODP Sites 1039, 1241, and 1242. At IODP Site U1381, on the Cocos Ridge offshore Costa Rica, 67 primary Miocene (~8 Ma to ~16.5 Ma) fallout ash layers have been recovered. Inferred transport distances of at least 50 to 450 km from their vents imply Plinian eruptions, although two-thirds of the ash beds formed from basaltic magmas and only one-third from rhyolitic magmas that are typically associated with plinian eruptions. Our age model for Site U1381 based on sediment accumulation rates, $^{40}Ar/^{39}Ar$ dating and biostratigraphic ages, reveals a distinct increase in eruption frequency at around 14 Ma. We interpret this as an increase in magma production rates due to changes in interactions between Galápagos plume and spreading ridge.

References:
Geist, D., Howard, K. A., Jellinek, A. M., and Rayder, S., 1994, The volcanic history of Volcan Alcedo, Galapagos Archipelago: A case study of rhyolitic oceanic volcanism: Bull Volcanol, v. 56, p. 243-260.

IODP

Persistence of atelostomate sea urchins (Spatangoida and Holasteroida; irregular echinoids) in the deep sea, or repeated migration events into the deep-sea?

N. SCHLÜTER[1,2], F. WIESE[1], M. REICH[3,4]

1 Georg-August University of Göttingen, Geoscience Centre, Dept. of Geobiology, Goldschmidtstr. 3, 37077 Göttingen, Germany
2 Geoscience Museum Göttingen, Goldschmidtstr. 1-5, 37077 Göttingen, Germany
3 SNSB – Bavarian State Collection for Palaeontology and Geology, Richard-Wagner-Str. 10, 80333 München, Germany
4 Ludwig-Maximilians University München, Department of Earth and Environmental Sciences, Division of Palaeontology and Geobiology, Richard-Wagner-Str. 10, 80333 München, Germany

Holasteroid and spatangoid echinoids, the only extent atelostomate irregular echinoids, evolved around 145 Myr ago (estimated c. at 145 Myr by Smith & Stockley 2005, Kroh & Smith 2010) and became an important component of the Cretaceous shelf benthos (Kier 1974; Smith 1984). While holasteroid echinoids vanished on the shelf during the early Palaeogene (Smith & Stockley 2005) and are today restricted to the deep-sea only, spatangoids are still present in both habitats, shelf and deep-sea. The history and origin of deep-sea representatives is still unsettled, e.g. the earliest known records of a deep-sea spatangoid so far is from the Santonian, Upper Cretaceous (Smith 2013). The origin of deep sea atelostomates was inferred so far from combined analyses of morphologies and molecular clock studies, and it was inferred that spatangoid deep-sea faunas are not older than 75 Myr (Stockley et al. 2005; Smith & Stockley 2005).

It is suggested, that in earth history at least three phases of independent migration into the deep sea occurred without any phylogenetic connection between these deep sea groups (late Jurassic: disasteroids, late Cretaceous: holasteroids and spatangoids, and in recent times of either latter 2 groups; Smith 2013, Fig. 1), which was supported by the idea that the deep-sea fauna was repeatedly eradicated by mass extinctions, or events which influenced the diversity on the shelf (Oceanic Anoxic Events). However, entire tests are often rare especially in deep-marine settings, hence it is not surprising that this hypothesys was inferred from scattered and rare records from bathyal settings on land. Truly deep-water sediments are particularly rare on land and frequently tectonically overprinted, which leads to the fact that distinct minute, for systematic approaches important, structures in echinoderm fossils are diagenetic altered in a way which precludes morphological analyses.

A more valuable source of data can be given by washing residues of deep sea sediments of IODP/ODP/DSDP material, providing microscopic remains with little diagenetic overprint. In these samples isolated plates and spines of irregular echinoids can be common to very abundant in together with ossicles of other echinoderms such as ophiuroids, crinoids and holothurians. The latter three can generally be identified with great confidence at genus to species level, enabling deep sea palaeobiogeographic research and the reconstruction of

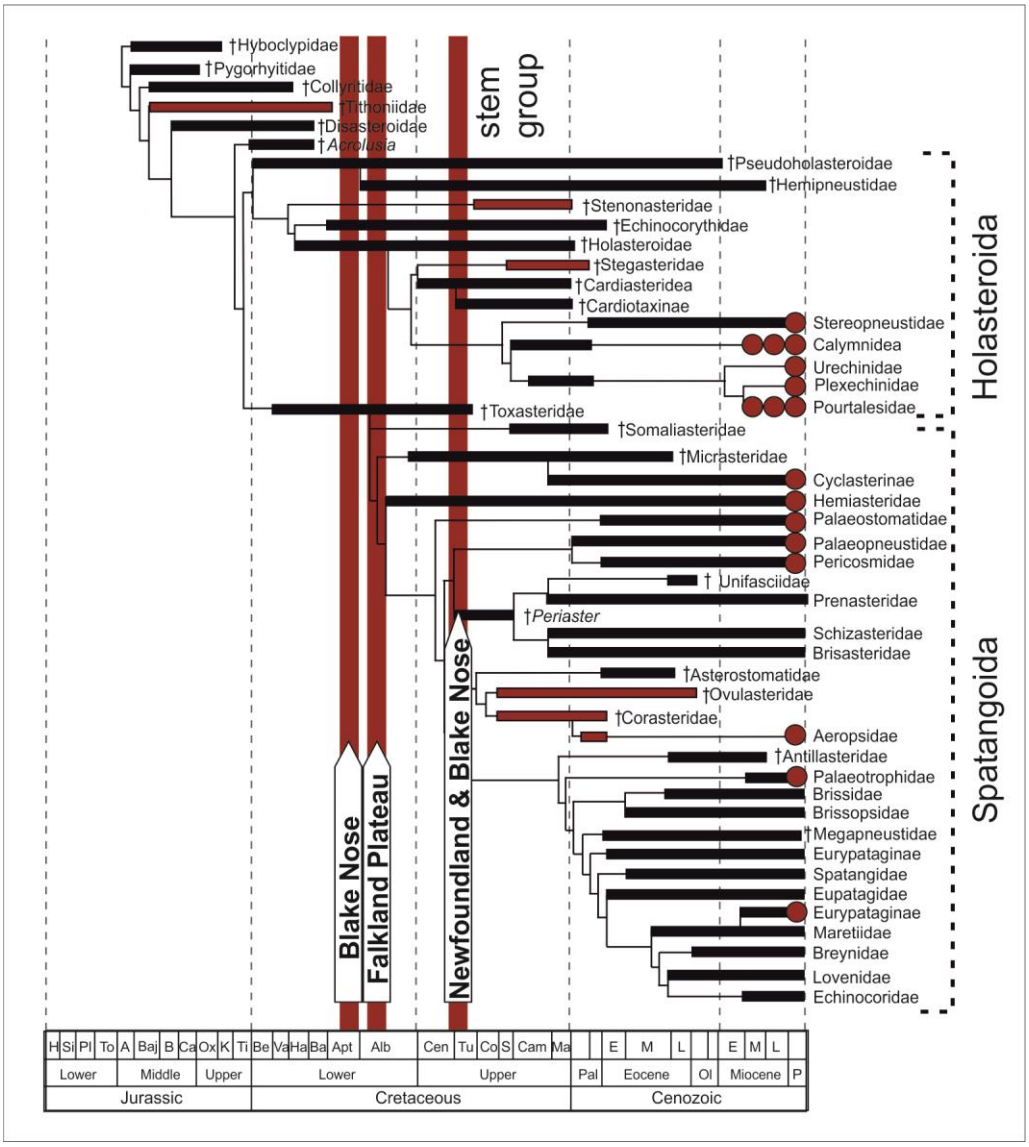

Fig. 1. Phylogeny of atelostomate echinoids calibrated against the fossil record (after Smith 2013, modified). Highlighted (red) deep sea taxa and the stratigraphic position of the atelostomate findings of the Falkland Plateau.

timing of deep sea colonization (Thuy et al. 2012). However, systematic approaches of these atelostomate echinoids rely dominantly on their test architecture, in contrast, there is only little knowledge on the morphology of atelostomate spines. Thus, spines from irregular echinoids has largely been ignored for systematic issues and thus were not useful for any view on the geological history. An actualistic approach of comparing microstructures in spines from holasteroid and spatangoid echinoids resulted in very well definable systematic differences in spines of both groups, which are detectable even in fragments.

Comparing spine microstructures from extant holasteroid and spatangoid echinoids resulted in well definable systematic differences in spines ultrastructure between the both groups, which are detectable even in fragments. Internal morphological features (perforation of the internal cylinder) are therefore crucial to distinguish between holasteroid and spatangoid spines (Fig. 2).

By these results we can report the occurrence of both atelostomate echinoid groups in DSDP samples of early/middle Albian age (Site 327, Falkland Plateau), in DSDP samples of Upper Cenomanian - lowermost Turonian Age (OAE 2 interval, Site 1050C, Blake Nose escarpment and Site 1407A, Newfoundland). These records are clearly evident for an earlier colonisation of the deep sea by the Atelostomata (Echinoidea) than previously suggested. Furthermore, our data contradict previous hypothesis about repeated migration events into the deep sea by atelostomate echinoids. More likely is an autochthonous evolution and accordingly a continuous

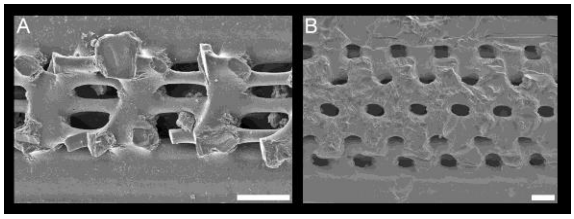

Fig. 2. Morphological systematic important characters (perforation of the cylinder) of atelostomate spines (inner view). **A**: an assumable holasteroid spine with horizontal arrangement of pores; **B**: an assumable spatangoid spine with helicoidal arrangement. Both from the early/middle Albian of the Falkland Plateau, Site 327. Scale bars equal 20 µm.

persistence of atelostomate sea urchins in bathyal habitats, as concluded by a progressively shortening of the gaps in between previous records of deep-marine atelostomate echinoids (Fig. 1).

Our data are in well accordance with the results of Thuy et al. (2012), who showed that the origin of some modern deep sea echinoderm fauna dates back at least to the Lower Cretaceous (Aptian, c. 120 Myr). Our and the data of Thuy et al. (2012) also suggest that the invasion of the Atelostomata is detached from the increase of oceanic surface water productivity in the Upper Cretaceous, which was suggested to trigger immigration of the holasteroid and spatangoids into the deep sea (Smith & Stockley 2005).

Further, our results bear the large potential to trace back the origin of deep sea Atelostomata in time, and a careful re-assessment of the IODP/ODP/DSDP material might be the key to map the atelostomate sea urchins deep time from the inferred moment of its origin to its dispersion into the depth.

References:

Kier, P.M. 1974. Evolutionary trends and their functional significance in the post-Paleozoic echinoids. Journal of Paleontology 48: 1–95.

Kroh, A. & Smith, A.B. 2010. The phylogeny and classification of post-Palaeozoic echinoids. Journal of Systematic Palaeontology 8 (2): 147–212.

Stockley, B., Smith, A.B., Littlewood, T., Lessios, H.A., MacKenzie-Dodds, J.A. 2005. Phylogenetic relationships of spatangoid sea urchins (Echinoidea), taxon sampling density and congruence between morphological and molecular estimates. Zoologica Scripta 34: 447–468.

Smith, A.B. 1984. Echinoid Palaeobiology. Allen & Unwin, London.

Smith, A.B. 2013. Geological history of bathyal echinoid faunas, with a new genus from the late Cretaceous of Italy. Geological Magazine 150 (1): 177–182.

Smith, A.B. & Stockley, B. 2005. The geological history of deep sea colonization by echinoids: the roles of surface productivity and deep-water ventilation. Proceedings of the Royal Society of London B 272: 865–869.

Thuy, B., Gale, A.S., Kroh, A., Kucera, M., Numberger-Thuy, L.D., Reich, M. & Stöhr, S. 2012. Ancient Origin of the Modern Deep-Sea Fauna. PLoS ONE 7(10): e46913. doi:10.1371/journal.pone.0046913.

IODP

The Bengal Fan stratigraphy as a function of tectonic and climate – Analysis of seismic data from the Bay of Bengal and a first comparison to IODP Expedition 354 results

T. SCHWENK[1], V. SPIEß[1], C. FRANCE-LANORD[2] AND IOPD EXP. 354 SCIENTIFIC PARTY

1 Marine Technology / Environmental Research, Department of Geoscience, University of Bremen, Klagenfurter Str., D-28359 Bremen, Germany

2 Centre de Recherches Pétrographiques et Géochimiques, CNRS Université de Lorraine, BP 20, 54501 Vandoeuvre les Nancy, France

The Bengal Fan covers the floor of the entire Bay of Bengal from the continental margins of India and Bangladesh to the sediment-filled Sunda Trench off Myanmar and the Andaman Islands, and along the west side of the Ninetyeast Ridge. The deposition and progradation of the Bengal Fan started in the Eocene after the collision of India with Asia resulting in the build-up of the Himalaya and the formation of a large proto-Bay of Bengal. Continued convergence of the Indian and Australian plates with the Southeast Asian plate reduced the size of the bay and focused the source of turbidites finally into the present Bengal Basin, Bangladesh shelf, and the shelf canyon "Swatch of no Ground". Today, the Bengal Fan is mainly fed by the sediment load of the Ganges and Brahmaputra rivers, which drain the Himalayas at its southern and northern slope, respectively, and deliver their load to the delta in the Bengal Basin, to the Bengal Shelf and to the deep sea fan.

Since roughly 80% of the material eroded from the Himalaya has been deposited in the Bay of Bengal, the Bengal Fan is the most complete recorder to study interactions among the growth of the Himalaya and Tibet, the development of the Asian monsoon, and processes affecting the carbon cycle and global climate. Because sedimentation in the Bengal Fan responds to both, climate and tectonic processes, its terrigenous sediment records the past evolution of both the Himalaya and regional climate. The histories of the Himalaya/Tibetan system and the Asian monsoon require sampling different periods of time with different levels of precision. Therefore IODP Expedition 354 will be carried out in February/March 2015 to drill a transect of sites in the Bay of Bengal. In particular, Expedition 354 will drill six holes in the fan at 8°N which includes 1) one deep site to ~1500 m to reach pre-fan deposits (MBF-3A), b) two sites to ~900 m (MBF-1A and -2A) to recover sediment at least as old as 10-12 million years to study the Neogene fan evolution and the impact of the monsoonal system on sediment supply and flux, and 3) three sites to ~300 m to recover a complete terrigenous record of the Himalayan flux over the last 1-2 million years.

The Bengal Fan was the target of 4 expeditions with RV Sonne in 1994 (SO93), 1997 (SO125/SO126) and 2006 (SO188), all carried out in cooperation between the University of Bremen and the BGR, Hannover. Multichannel-seismic pre-site survey data were collected on cruises SO125 and SO188. The seismic data around 8° N has been interpreted with respect to the presence of channel levee systems and seismic stratigraphy. Several major reflectors and unconformities were traced across the drilling transect revealing increased average sedimentation rates as a function of distance from the basement ridges at 85°E and 90°E. Generally, sedimentation rates were highest in the Pleistocene, lowest in the Pliocene and moderate in the late Miocene. At latest Miocene, the transition from early sheet-like turbidite deposition to the onset of channel-levee systems occurred at 8°N. Since most surface channels reach this part the fan, it is believed that this marks the start of the development of channel-levee systems on the Bengal Fan generally. The onset of channel-levee systems might have two reasons: The initial creation of a canyon as point source or changes in the grain size of the delivered sediments transported by turbidity currents to the fan. The SO125 seismic data revealed two internal regional unconformities. Using the dating of DSDP Site 218, they were dated to have Pleistocene and Pliocene age, respectively. These unconformities are interpreted to be equivalent to unconformities found in the central Indian Ocean, which are related to deformation events of the ocean lithosphere there. Additionally, several faults were identified in the seismic data at 8°N, especially above the western flank of the Ninetyeast Ridge. These faults terminate within Pleistocene sediments, which also suggest tectonic events at least until Pleistocene times.

The target of the here introduced new DFG-funded project "The Bengal Fan stratigraphy as a function of tectonic and climate – Correlation of IODP Expedition 354 results and available seismic data from the Bay of Bengal" is to correlate results from IODP Expedition 354 and the available seismic data net in the Bay of Bengal to establish a new stratigraphy for the Bengal Fan with respect to the regional tectonic and climatic evolution. The existing stratigraphy bases a) on poor age constraints from the just spot-cored DSDP Site 218 and b) only on seismic data gathered during Cruise SO125 around 8°N. By overcoming the poor age constraints from DSDP Site 218, new insights should be gathered about the architecture of the fan in terms of the onset of channel-levee systems and ages as well as lifetimes of individual systems, and about the extent and timing of tectonic events. The results should also give a more regional overview by integrating all pre-site survey seismic data collected during Cruise SO188. All targeted objectives will finally contribute to understand the processes controlling source-2-sink systems in general.

As first step, reprocessing of the SO125 seismic data is carried out. These data were formerly processed for the original drilling proposal in the year 2001, and due to the availability of software and hardware during that time, the processing is not state-of-the art anymore (i.e. large bin sizes, no static corrections, no sophisticated noise reduction). Reprocessing these lines provide a significant improvement of horizontal and vertical resolution as well as signal to noise ration and penetration. On the poster we will show the new processed seimic data including a refinded regional seismo-stratigraphic analysis. First data from the IODP 354 expediton, especially biostratigraphic dating, shall be preliminary linked to the seismic data for an tentative stratigraphic interpretation.

IODP

Pre-site survey for IODP Expedition 363 (West Pacific Warm Pool) – Results from Cruise SO-228 (May 2013)

T. SCHWENK, M. MOHTADI, F. GERNHARDT, F. BERGMANN, S. WENAU

MARUM – Center for Marine Environmental Sciences and Faculty of Geosciences, University of Bremen, Germany

A pre-site survey was carried out during RV Sonne Cruise 228 (EISPAC) in May 2013 to support the IODP proposal 799-Full ("Paleoceanographic records of the Western Pacific Warm Pool variability", by Rosenthal et al.) This proposal received very strong, positive reviews, yet the lack of seismic data was criticized. Therefore the Cruise SO-228 was extended by 4 days for doing such pre-site surveys. The target of this proposal, the Indo-Pacific Warm Pool, is the largest reservoir of warm surface water on earth, the major source of heat to the atmosphere, and a location of deep atmospheric convection and heavy rainfall. Small variations in the sea surface temperature (SST) of the Western Pacific Warm Pool (WPWP) influence the location and strength of convection in the rising limb of the Hadley and Walker circulations, perturbing planetary scale atmospheric circulation, atmospheric heating, and tropical hydrology. Studies of climate variability in the WPWP have relied primarily on the single low sedimentation-rate ODP site 806B from the Ontong Java Plateau, which serves as the warm end-member used to monitor broad scale zonal and merdional gradients throughout the Neogene. Higher-resolution sites are available from marginal seas in the western equatorial Pacific, but they are strongly impacted by local processes. Thus there is a gap in the spatial and temporal coverage of the WPWP that prevents from assessing climate change in this region on various time scales. Over the past decade new coring efforts have demonstrated the possibility of obtaining records from key locations in the WPWP with comparable resolution to records from the high latitude oceans, cave deposits and ice cores. While substantial progress in understanding WPWP climate variability has been made by studying long piston cores, there are still fundamental questions that cannot be addressed without drilling new sites.

During Cruise SO-228 high-resolution multichannel seismic data, sediment echosounder PARASOUND data and swathsounder Kongsberg EM120 data were gathered around two proposed drill sites, one (WP-09A) is located in the Davao Bay off Mindanao, Philippines, the other (WP-05A) is located north of Papua New Guinea in front of the Sepik and Ramu river estuary. Site WP-09A (Davao Bay) was proposed to recover a high-resolution record of the East Asian Monsoon. Since the location is protected from bottom currents and fed by terrigenous material from the Davao River, the Davao Bay provides one of the best areas to retrieve expanded sedimentary sequences for western Pacific paleoceanographic and paleoclimatic studies. Site WP-05A was proposed to recover a high-resolution paleoceanographic record of climate variability in the heart of the WPWP for the last 2 Myr, specifically of the precipitation over Papua New Guinea.

The seismic survey in the Davao Bay revealed that the sedimentation is mainly dominated by mass transport deposits. However, in the northern part of the study area a promising location characterized by parallel, continuous reflectors for Site WP09-A was detected. The seismic survey of the working area around Site WP-05A shows also several slope failures, which resulted in only thin sedimentation cover on top of the basement. Finally, in the north-east part of the study area, undisturbed sediment packages of up to 200 meters thickness could be identified as promising location for site WP-05A.

In the meantime, proposal 779-full passed all relevant IODP panels and is scheduled as IODP Expedition 363 for October/November 2016. Especially the EPSP accepted the proposed locations and target drilling depths for sites WP09-A and WP05-A based on the seismic data collected during SO-228. Finally, IODP Exp. 363 is dedicated to drill 9 sites, additionally 3 alternate sites are suggested. WP-09A is now defined as a priority site, whereas WP-05A is designated as alternate site.

ICDP

A combined surface and borehole seismic survey at the COSC-1 borehole

H. SIMON[1], F. KRAUSS[2], P. HEDIN[3], S. BUSKE[1], R. GIESE[2], C. JUHLIN[3]

1 Institute of Geophysics and Geoinformatics, TU Bergakademie Freiberg
2 Scientific Drilling, Helmholtz Centre Potsdam GFZ German Research Centre for Geosciences
3 Department of Earth Sciences, Uppsala University

The ICDP project COSC (Collisional Orogeny in the Scandinavian Caledonides) focuses on the mid Paleozoic Caledonide Orogen in Scandinavia in order to better understand orogenic processes, from the past and in recent active mountain belts (Gee et al. 2010). The Scandinavian Caledonides provide a well preserved example of a Paleozoic continent-continent collision. Surface geology in combination with geophysical data provide control of the geometry of the Caledonian structure, including the allochthon and the underlying autochthon, as well as the shallow W-dipping décollement surface that separates the two and consist of a thin skin of Cambrian black shales. The structure of the basement underneath the décollement is highly reflective and apparently dominated by mafic sheets intruded into either late Paleoproterozoic granites or Mesoproterozoic volcanics and sandstones. The COSC project will examine the structure and physical conditions of these units, in particular the Caledonian nappes ("hot" allochthon) and the underlying basement. In addition to that, the borehole will provide unique information about the present temperature gradient in the Caledonides, the porosity and permeability of the rock formations, and the petrophysical properties of the rocks at depth.

Existing regional seismic and magnetotelluric data have imaged the geometry of the upper crust (Juhojuntti et al. 2001, Korja et al. 2008), and pre-site seismic reflection surveys were performed in 2010 and 2011 to better define the exact drill site locations (Hedin et al. 2012). The project presented here is dedicated to complement these surface seismic measurements by drillhole-based investigations to better resolve and define the small-scale structures.

During spring/summer 2014 the COSC-1 borehole was drilled to approx. 2.5 km depth near the town of Åre (western Jämtland/Sweden) with nearly 100 % of core recovery and cores in best quality. After the drilling was finished, a major seismic survey was conducted in and around the COSC-1 borehole which comprised both seismic reflection and transmission experiments. Besides a high resolution zero-offset VSP (Vertical Seismic Profiling) experiment also a multi-azimuthal walkaway VSP survey took place. For the latter the source points were distributed along three profile lines centered radially around the borehole (see Fig. 1). For the central part up to 2.5 km away from the borehole, a hydraulic hammer source (Vibsist) was used, which hits the ground for about 20 s with an linear increasing hit rate. For the far offset shots up to 5 km, explosive sources were used. The wavefield of both source types was recorded in the borehole using an array of 15 three-component receivers with a geophone spacing of 10 m. This array was deployed at 7 different depth levels during the survey. At the same time the wavefield was also recorded at the surface by 180 standalone three-component receivers placed along each of the three up to 10 km long lines, as well as with a 3D array of single-component receivers in the central part of the

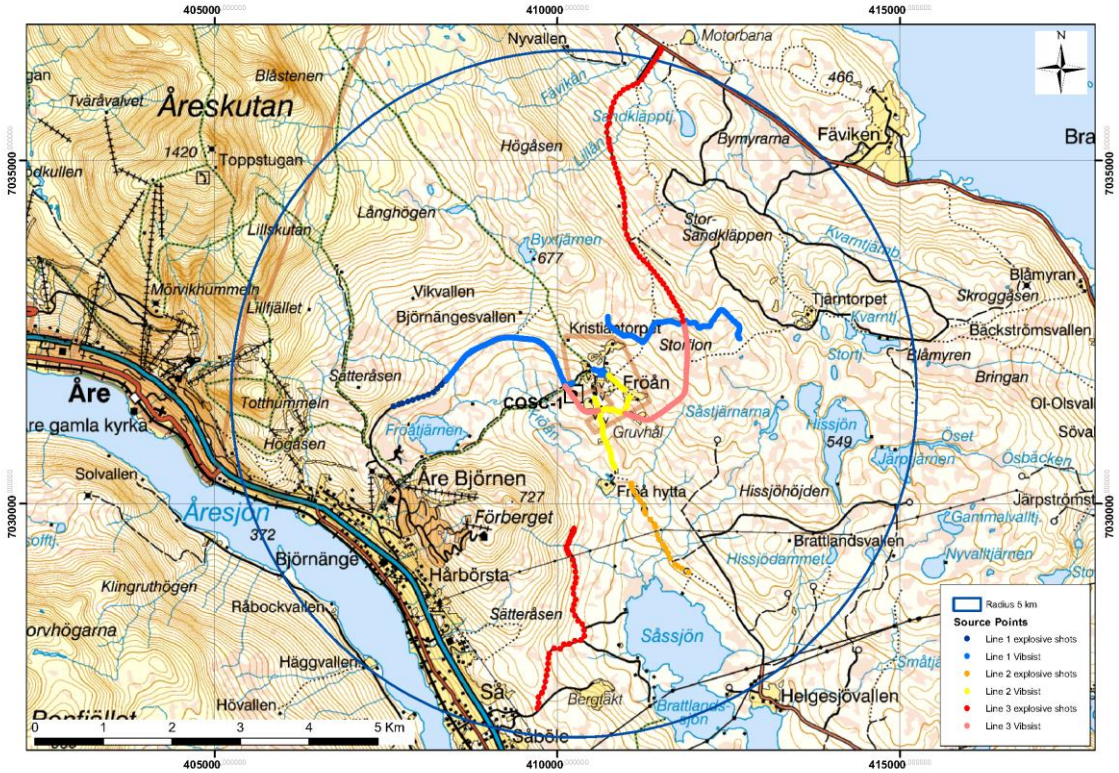

Fig. 1. Distribution of the source points along three profile lines for the multi-azimuthal walkaway VSP (Vertical Seismic Profiling) survey.

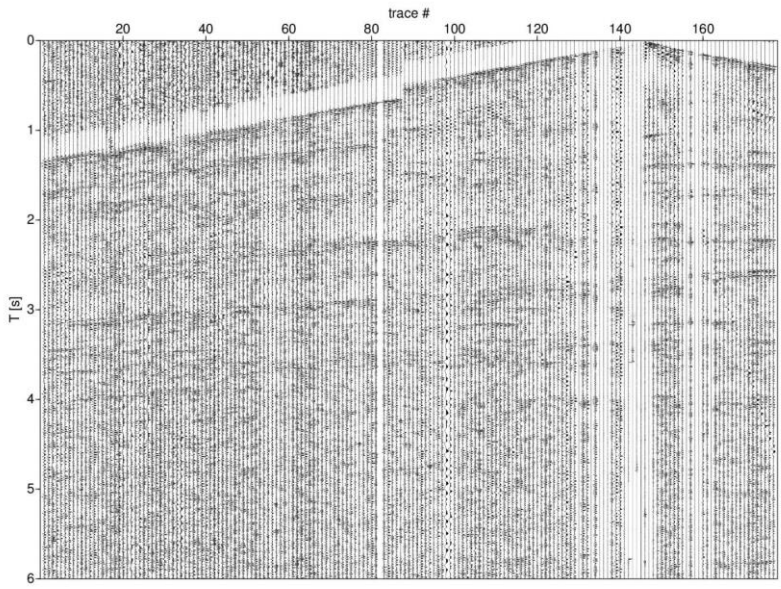

Fig. 2. Exemplary shotgather for one explosive shot from line 2 showing clear and strong reflections up to six seconds two-way-traveltime.

survey area around the borehole.

Here we present first preliminary processing results from the multi-azimuthal walkaway VSP survey and the data that were recorded along the three surface lines. The data quality is generally very good and the shot gathers show many clear and strong reflections up to six seconds two-way-traveltime. One exemplary shotgather for an explosive shot is shown in Fig. 2.

In a first step the data set was used to derive a detailed velocity model around the borehole by inversion of first arrival traveltimes, which is essential for the application of any further imaging approaches. This velocity model was compared to the available logging informations from the COSC-1 borehole and with velocity models derived from older existing high resolution reflection seismic profiles.

The further data processing will employ advanced seismic imaging techniques in order to image and characterize the small scale structures around the COSC-1 borehole including the analysis of anisotropic effects caused by aligned fractures and faults and their relation to the stress regime.

The results of our investigations will be high-resolution images of the fine-scale structures (including lithological boundaries, steeply dipping fault segments, fracture sets, etc.) around the borehole. This information is vital not only for a reliable spatial extrapolation of the structural and petrophysical properties observed in the borehole, but also for a thorough understanding of the tectonic and geodynamic setting, including but not limited to, the past and present stress regime.

References:

Gee, D. G., Juhlin, C., Pascal, C., & Robinson, P. (2010). Collisional Orogeny in the Scandinavian Caledonides (COSC). GFF, 132(1), 29–44.

Hedin, P., Juhlin, C., & Gee, D. G. (2012). Seismic imaging of the Scandinavian Caledonides to define ICDP drilling sites. Tectonophysics, 554-557(0), 30–41.

Juhojuntti, N., Juhlin, C., & Dyrelius, D. (2001). Crustal reflectivity underneath the Central Scandinavian Caledonides. Tectonophysics, 334(3-4), 191–210.

Korja, T., Smirnov, M., Pedersen, L. B., & Gharibi, M. (2008). Structure of the Central Scandinavian Caledonides and the underlying Precambrian basement, new constraints from magnetotellurics. Geophysical Journal International, 175(1), 55–69.

IODP

Earth and Life Processes Discovered from Subseafloor Environment – A Decade of Science Achieved by the Integrated Ocean Drilling Program (IODP)

R. STEIN[1], D. BLACKMAN[2], F. INAGAKI[3], H.-C. LARSEN[4]

1 Alfred-Wegener-Institut Hemholtz-Zentrum für Polar- und Meeresforschung, 27568 Bremerhaven, Germany
2 Scripps Institution of Oceanography, University of California San Diego, La Jolla, CA, USA
3 Kochi Institute for Core Sample Research, Japan Agency for Marine-Earth Science & Technology, Nankoku, Kochi, Japan
4 Lyngfeldts Tvaervej 11, 3300 Frederiksvaerk, Denmark

The Integrated Ocean Drilling Program (IODP: 2003-2013) continued efforts begun in 1968 by the Deep Sea Drilling Project (DSDP: 1968-1983) and, subsequently, the Ocean Drilling Program (ODP: 1983-2003). Crucial records were obtained of past and present processes and interactions within and between the biosphere, cryosphere, atmosphere, hydrosphere and geosphere. The DSDP-ODP exploratory phase resulted in the confirmation of the unifying theory of Plate Tectonics, shortly followed by the development of new fields such as paleoceanography, astronomical geochronology, structure and geodynamics of the ocean crust, geo-resources in oceanic hydrothermal systems, marine gas-hydrate reservoirs, geomicrobiology, and others. Research in IODP through encompassed a wide range of fundamental and applied issues that affect society,

such as global change, biodiversity, the origin of life, natural hazards associated with earthquake processes, and the internal structure and dynamics of our planet. With a multiple-platform approach including the riser-drill ship *Chikyu*, the non-riser drill ship *Joides Resolution* and mission-specific platforms, IODP focused on three broad scientific themes documented in the Initial Science Plan, (1) Deep Biosphere and the Subseafloor Ocean, (2) Environmental Change, Processes and Effects, and (3) Solid Earth Cycles and Geodynamics.

A new book - the „*IODP Book*" – has been published by Elsevier two months ago. This is the first comprehensive compilation of synthesis papers presenting key results of cutting-edge research carried out within the Integrated Ocean Drilling Program during the past decade (IODP: 2003-2013). The different papers are written by international experts in their fields of research. The full scope of IODP achievements covering many of Earths major systems are covered in the results reported.

The *IODP Book* is divided into five parts. Chapter 1 summarises the major highlights obtained during the decade of ocean science research within the IODP. The following Chapters 2 to 4, the „heart of the book", present in more detail the main IODP results devoted to the three main IODP themes *Deep Biosphere and the Subseafloor Ocean*, *Environmental Change, Processes and Effects*, and *Solid Earth Cycles and Geodynamics*. In Chapter 5, an appendix, background information about each expedition are briefly presented in one-page summaries.

In this poster, content, outline, highlights etc. of the *IODP Book* are presented. Further information about the book is available at: http://www.sciencedirect.com/science/bookseries/15725480

References:
Stein, R., Blackman, D. Inagaki, F., and Larsen, H.-C. (Eds.), Earth and Life Processes Discovered from Subseafloor Environment - A Decade of Science Achieved by the Integrated Ocean Drilling Program (IODP), Series Developments in Marine Geology, Vol. 7, Elsevier Amsterdam/New York, 807 pp.

ICDP

Resurgence and collapse processes at the Campi Flegrei caldera (Italy): Results from a seismic reflection Pre-Site Survey for combined IODP/ICDP drilling campaigns

L. STEINMANN[1], V. SPIESS[1], M. SACCHI[2]

1 Department of Geosciences, University of Bremen, Klagenfurter Strasse, D-28359 Bremen, Germany
2 Institute for Coastal Marine Environment (IAMC), Italian Research Council (CNR), Calata P.ta di Massa, Porto di Napoli, 80133 - Napoli, Italy

Large collapse calderas are associated with exceptionally explosive volcanic eruptions, which are capable of triggering a global catastrophe second only to that from a giant meteorite impact. Therefore, active calderas have attracted significant attention in both scientific communities and governmental institutions worldwide. However, the mechanisms for unrest and eruptions at calderas are still largely unknown and, as demonstrated by ample volcanological research in the last decades, they may be very different from those characterizing the more commonly studied stratovolcanoes or shield volcanoes.

One prime example of a large collapse caldera can be found in southern Italy, more precisely in the northern Bay of Naples within the Campi Flegrei Volcanic Area. The Campi Flegrei caldera covers an area of approximately 200 km² defined by a quasi-circular depression, half onland, half offshore. It is still under debate whether the

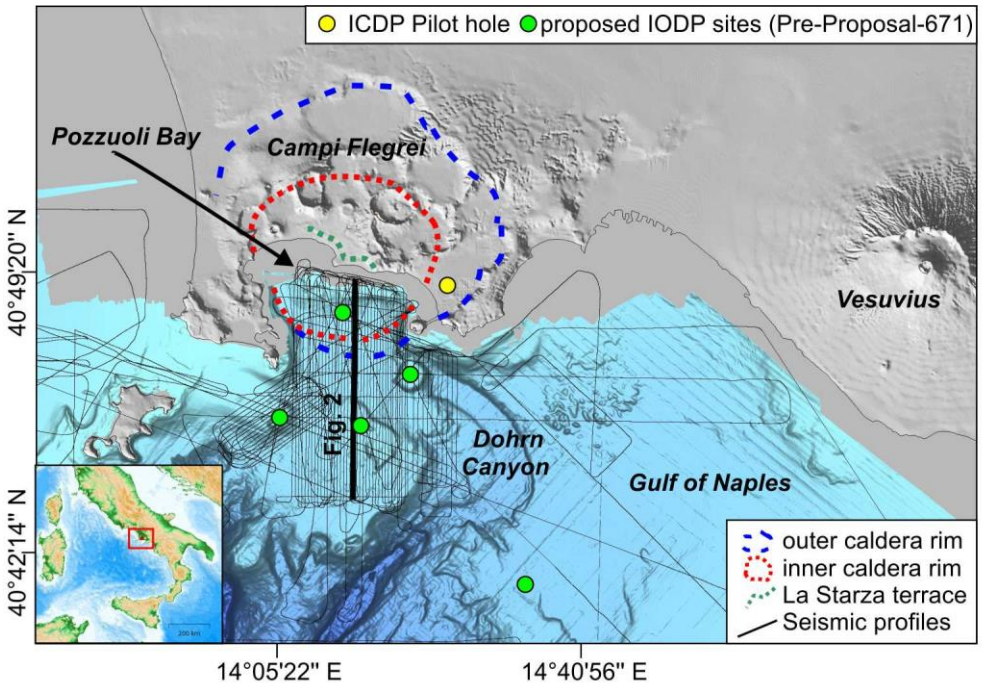

Fig. 1. Overview map of the Gulf of Pozzuoli and the acquired multi-channel high-resolution seismic profiles. The offshore caldera rim is indicated as found in this study while the onshore location was adapted from Acocella (2008):

caldera formation was related to only one ignimbritic eruption namely the Neapolitan Yellow Tuff eruption at 15 ka (e.g. De Vivo et al., 2001; Milia and Torrente, 2007) or if it is a nested-caldera system related to the NYT and the Campanian Ignimbrite eruption at 39 ka (e.g. Orsi et al., 1996; Rosi et al., 1983).

The Campi Flegrei caldera has been the world's most active caldera for the last 40 years, a time period that has been characterized by episodes of unrest involving significant ground deformation (uplift/subsidence) and seismicity, which have nevertheless not yet led to an eruption. Besides these short term ground deformation phases (e.g. 1982-1984, uplift rate of 100 cm/yr) (De Natale et al., 2006), long-term ground deformation with rates of several tens of meters within a few thousand years was also observed. Consequently, the central part of the caldera rose and the La Starza marine terrace emerged ~5,000 years ago (Di Vito et al., 1999). The reason for uplift (magmatic vs. hydrothermal) is still under debate (De Natale et al., 1991; De Vivo and Lima, 2006; Lima et al., 2009). Despite ample research, the submerged part of the Campi Flegrei caldera (e.g. caldera rim, fault-ring) still remains to a large extent unknown. However, understanding the mechanisms for unrest and eruptions is of paramount importance, as a future eruption of the Campi Flegrei caldera would expose more than 500,000 people to the risk of pyroclastic flows.

This study is based on a (semi-3D) grid of high-resolution multi-channel seismic profiles acquired during a joint Italian-German cruise on the R/V URANIA in the Bay of Naples and the Gulf of Pozzuoli in 2008. During this cruise a 50-m-long, 48 channel shallow-water seismic streamer was deployed in combination with a Mini GI-Gun (0.1 L) producing high frequencies of up to 1000 Hz in order to achieve maximum seismic resolution (vertical resolution < 2m) of the uppermost subsurface (<300 m). In total, 146 high-frequency seismic lines were acquired of which 50 are part of a N-S trending grid crossing over the offshore sector of the Campi Flegrei caldera in the Gulf of Pozzuoli. The advantage of the here presented multi-channel data is that they provide a superb signal-to-noise ratio. As part of the multi-channel seismic data processing, the effect of multiples can substantially be reduced, which allows for an imaging of the deeper subsurface structures. The 3D aspect in combination with the superior data quality distinguishes the ongoing project results from the previously published single-channel, mostly very high-resolution seismic studies (e.g. D'Argenio et al., 2004; Milia and Torrente, 2000; Sacchi et al., 2014).

The primary aim of the survey was to provide a robust site survey database for both, the proposed IODP drilling of the Campi Flegrei caldera (*IODP drilling proposal 671-pre*) and the ongoing Campi Flegrei Deep Drilling Project (CFDDP). The main advantage of such marine investigations is that a complete record of volcanic activity can be studied without the challenges posed on land, by the subsequent destruction or burial of earlier features. Besides, the seismic data have the potential to build a bridge between deep tomographic observations and high-frequency boomer profiles that have already been acquired in this volcanic area. In particular, the shallow water seismic reflection profiles may serve as a basis for the correlation of the recently completed onland ICDP pilot hole and the ongoing ICDP drilling with marine deposits and proposed IODP drill sites in the Bay of Naples in order to develop a large scale picture of the study area.

The overarching scientific goal of this project is to refine the geological and tectonic understanding of the offshore sector of the Campi Flegrei caldera with focus on shallow subsurface features (< 300 m). In detail, the main objectives of the present study are to (1) image the stratigraphic sequences inside and outside of the caldera structure, (2) identify deformation patterns (faults, areas of uplift and subsidence) and determining their origin, and (3) establish a conceptual model of the temporal evolution of both sedimentation and deformation at the Campi Flegrei caldera.

Based on the seismic dataset, major stratigraphic units

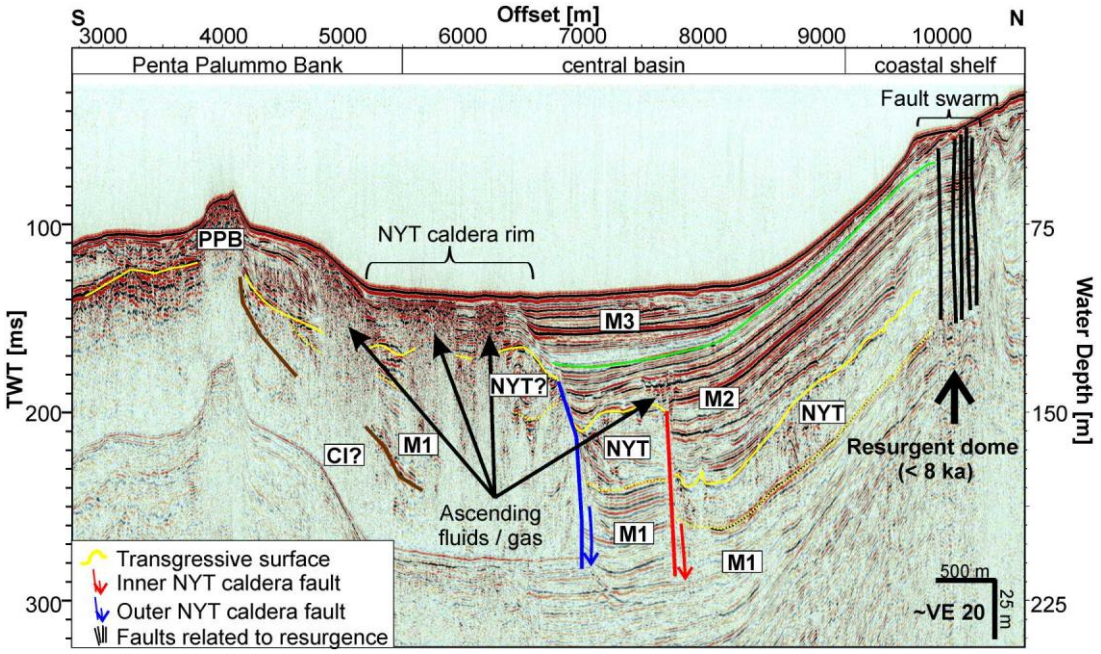

Fig. 2. Multi-channel seismic reflection profile GeoB08-033 (for location see Fig. 1) showing the supposed caldera rim, main seismo-stratigraphic units, uplift-related fault swam and domed layers.

such as the Campanian Ignimbrite (CI) and the Neapolitan Yellow Tuff (NYT) could be traced on regional scales. These ignimbritic deposits are characterized by a chaotic to reflection-free seismic facies. The NYT was deposited during a time period characterized by transgression after the Last Glacial Maximum (LGM). Outside of the caldera depression, the NYT deposit was unaffected by the caldera collapse and, thus, the NYT bottom boundary shows the original elevation (~190 ms TWT; ~140 m) of the lower surface before the collapse (Fig. 2, offset 5000-7000 m). According to Lambeck et al. (2011), the sea-level in the Campi Flegrei area at the time of the NYT emplacement was ~93 m below the present sea-level. Therefore, if it can be assumed that the palaeo-surface before the NYT eruption was at a depth of ~140 m below present day sea-level, it can be concluded that the Gulf of Pozzuoli was already (at least partially) submerged (by ~50 m) before the NYT emplacement and, thus, that the NYT deposited under marine conditions. This hypothesis is further supported by the fact that continuous, well-layered seismic reflections can be observed below the NYT (M1) (Fig. 2), suggesting a marine depositional environment prior the NYT eruption.

The NYT could not be recognized on the outer shelf, which implies that the old volcanic Penta Palummo Bank (>120 ka) acted as barrier for the distribution of the pyroclastic flow deposit. Instead, a progradational and down-stepping reflector stacking pattern (FRST) was identified and interpreted as forced-regression wedge related to a sea-level fall between 120 and 18 ka. The FRST unit is overlain by a thin unit of well-layered, continuous reflector. This unit was interpreted as transgressive sediments that have deposited in the course of rapid sea-level rise after the LGM (<18 ka).

In the Gulf of Pozzuoli, the NYT is vertically displaced along two major normal faults located at offset (=horizontal distance) 7000 m and 7800 m in Fig. 2, respectively. The faults show a circular spatial shape (Fig. 1) and were, thus, interpreted as shallow ring-fault system related to a caldera collapse in the course of the NYT eruption at 15 ka. The inner caldera fault could clearly be identified in the seismic data (indicated in red in Fig. 1 and Fig. 2) while the outer caldera fault (indicated in blue in Fig.1 and Fig. 2) is eroded in parts of the Gulf of Pozzuoli and therefore more difficult to identify on the seismic profiles. This erosion suggests that the Dohrn Canyon has been active after the NYT emplacement and therefore eroded the “caldera rim”. It can be hypothesized that the Dohrn Canyon acted as conduit for the transport of eroded material from coastal areas in the Gulf of Pozzuoli to the deep sea. Since volcanic material such as ignimbrites are often very prone to erosion, a significant amount of sediment was probably transported through the canyon in the past.

On top of the NYT, a package of continuous, well-layered seismic reflections can be observed and was subdivided into two seismic units (M2 and M3) (Fig. 2). These units were interpreted as marine sediments deposited in the course of the ongoing transgression after the NYT emplacement. Seismic Unit M2 shows a uniform thickness suggesting a relatively constant accumulation rate in the entire caldera depression. In contrast, Seismic Unit M3 is characterized by a decrease in thickness and onlap reflector termination in an underlying marine erosional unconformity at offset 8500 m in Fig. 2. This unconformity was interpreted as being related to the onset of the La Starza uplift at ~8 ka. Therefore, it can be concluded that Seismic Unit M2 was deposited in the time span from 15 ka (NYT eruption) to 8 ka. The overlying Seismic Unit M3 was, thus, deposited since the onset of the La Starza uplift at ~8 ka. In the same area where the thickness decrease of Seismic Unit M3 was found, domed layers can be observed (Fig. 2, offset 8500-10500 m). The apex of this dome-like structure is characterized by the occurrence of a swarm of normal faults (Fig.2, offset 10000 m) with maximum vertical displacement of ~10 ms TWT (~8 m). Furthermore, the development of an apical depression as result of extension can be observed. Based on the findings as described above, it can be concluded that the inner part on the caldera depression on the coastal shelf has undergone long-term uplift since the deposition of marine Unit M3 (<8 ka) which is related to a resurgent dome.

Ascending fluids/gases along weak zones (e.g. faults, caldera rim) (Fig. 2) point towards the presence of an underlying hydrothermal system. Therefore, the existence of both, a deep, resurgent magma chamber resulting in the long-term uplift and a shallow hydrothermal system can be hypothesized.

On the poster we present a comprehensive 2D conceptual reconstruction of caldera collapse and resurgence processes in interplay with sea-level changes since the NYT eruption as inferred from the above described results.

References:

Acocella, V., 2008. Activating and reactivating pairs of nested collapses during caldera-forming eruptions: Campi Flegrei (Italy). Geophysical Research Letters 35, L17304.

D’Argenio, A., Pescatore, T., Senatore, M.R., 2004. Sea-level change and volcano-tectonic interplay. The Gulf of Pozzuoli (Campi Flegrei, Eastern Tyrrhenian Sea) during the last 39 ka. Journal of Volcanology and Geothermal Research 133, 105-121.

De Natale, G., Pingue, F., Allard, P., Zollo, A., 1991. Geophysical and geochemical modelling of the 1982–1984 unrest phenomena at Campi Flegrei caldera (southern Italy). Journal of Volcanology and Geothermal Research 48, 199-222.

De Natale, G., Troise, C., Pingue, F., Mastrolorenzo, G., Pappalardo, L., Battaglia, M., Boschi, E., 2006. The Campi Flegrei caldera: Unrest mechanisms and hazards, in: Troise, C., De Natale, G., Kilburn, C.R.J. (Eds.), Mechanisms of Activity and Unrest at Large Calderas. Geological Society, London, pp. 25-45.

De Vivo, B., Lima, A., 2006. Chapter 14 A hydrothermal model for ground movements (bradyseism) at Campi Flegrei, Italy, in: Vivo, B.D. (Ed.), Developments in Volcanology. Elsevier, pp. 289-317.

De Vivo, B., Rolandi, G., Gans, P.B., Calvert, A., Bohrson, W.A., Spera, F.J., Belkin, H.E., 2001. New constraints on the pyroclastic eruptive history of the Campanian volcanic Plain (Italy). Mineralogy and Petrology 73, 47-65.

Di Vito, M.A., Isaia, R., Orsi, G., Southon, J., de Vita, S., D'Antonio, M., Pappalardo, L., Piochi, M., 1999. Volcanism and deformation since 12,000 years at the Campi Flegrei caldera (Italy). Journal of Volcanology and Geothermal Research 91, 221-246.

Lambeck, K., Antonioli, F., Anzidei, M., Ferranti, L., Leoni, G., Scicchitano, G., Silenzi, S., 2011. Sea level change along the Italian coast during the Holocene and projections for the future. Quaternary International 232, 250-257.

Lima, A., De Vivo, B., Spera, F.J., Bodnar, R.J., Milia, A., Nunziata, C., Belkin, H.E., Cannatelli, C., 2009. Thermodynamic model for uplift and deflation episodes (bradyseism) associated with magmatic–hydrothermal activity at the Campi Flegrei (Italy). Earth-Science Reviews 97, 44-58.

Milia, A., 2010. The stratigraphic signature of volcanism off Campi Flegrei (Bay of Naples, Italy). Geological Society of America Special Papers 464, 155-170.

Milia, A., Torrente, M.M., 1999. Tectonics and stratigraphic architecture of a peri-Tyrrhenian half-graben (Bay of Naples, Italy). Tectonophysics 315, 301-318.

Milia, A., Torrente, M.M., 2000. Fold uplift and synkinematic stratal architectures in a region of active transtensional tectonics and volcanism, eastern Tyrrhenian Sea. Geological Society of America Bulletin 112, 1531-1542.

Milia, A., Torrente, M.M., 2007. The influence of paleogeographic setting and crustal subsidence on the architecture of ignimbrites in the Bay of Naples (Italy). Earth and Planetary Science Letters 263, 192-206.
Milia, A., Torrente, M.M., 2011. The possible role of extensional faults in localizing magmatic activity: a crustal model for the Campanian Volcanic Zone (eastern Tyrrhenian Sea, Italy). Journal of the Geological Society 168, 471-484.
Orsi, G., De Vita, S., di Vito, M., 1996. The restless, resurgent Campi Flegrei nested caldera (Italy): constraints on its evolution and configuration. Journal of Volcanology and Geothermal Research 74, 179-214.
Rosi, M., Sbrana, A., Principe, C., 1983. The phlegraean fields: Structural evolution, volcanic history and eruptive mechanisms. Journal of Volcanology and Geothermal Research 17, 273-288.
Sacchi, M., Pepe, F., Corradino, M., Insinga, D.D., Molisso, F., Lubritto, C., 2014. The Neapolitan Yellow Tuff caldera offshore the Campi Flegrei: Stratal architecture and kinematic reconstruction during the last 15 ky. Marine Geology 354, 15-33.

ICDP

Peering into the Cradle of Life: stable isotopic investigation of Paleoarchean sediments from the 3.23 – 3.55 billion years old Barberton Greenstone Belt, South Africa

H. STRAUSS[1], A. MONTINARO[1], A. FUGMANN[1], K. KRIEGER[1], K. SCHIER[1], P. MASON[2], A. GALIC[2]

1 Institut für Geologie und Paläontologie, Westfälische Wilhelms-Universität Münster, Münster, Germany
2 Department of Earth Science, Utrecht University, Utrecht, The Netherlands

Early Earth was considerably different from today: it was characterized by a predominance of oceanic over continental crust (Rollinson, 2007); the oceans were anoxic and characterized by ferruginous conditions (Holland, 2002; Canfield, 2004); the early atmosphere was reducing with abundant carbon dioxide and methane but essentially devoid of free atmospheric oxygen (Holland, 2006; but see Ohmoto et al., 2014 for a different view); life was entirely microbial in nature and is believed to have exclusively inhabited the marine realm (Holland and Turekian, 2004 and references therein).

The 3.55 – 3.23 billion years old Barberton Greenstone Belt in South Africa represents one of the best preserved rock successions from the earliest part of Earth history. The greenstone belt comprises a sequence of volcanic and sedimentary rocks, offering the potential for reconstructing environmental conditions prevailing at the surface of our young planet. Under the auspices of the International Continental Scientific Drilling Program (ICDP), five cores were obtained as part of the project “Peering into the Cradle of Life”, a multinational and multidisciplinary research program. Deciphering the environmental conditions under which life emerged and evolved on Earth represents the central objective of this program.

The stable isotopes of key elements of life, such as carbon, sulfur, or nitrogen, have been used successfully for identifying metabolic pathways and for reconstructing traces of life through time. Abundances of total carbon, total inorganic and organic carbon and total sulfur, and multiple sulfur ($\delta^{34}S$, $\Delta^{33}S$, $\Delta^{36}S$) isotopes of sulfides and sulfates, and organic carbon ($\delta^{13}C_{org}$) and carbonate carbon ($\delta^{13}C_{carb}$) isotopes are investigated in order to constrain sources and processes of biological and abiological cycling of sulfur and carbon in the Paleoarchean. Work centers on the BARB5 drill core that was drilled in the Barite Syncline through the middle part of the Mapepe Formation, Fig Tree Group. The core comprises five different lithologies: (1) laminated carbonaceous siltstone and mostly fine-grained laminated calcareous litharenite, (2) chertarenite and conglomerate, (3) siltstone interbedded with minor litharenite and chert (4) litharenite interbedded with chert and carbonate, and (5) cherty (sub-) litharenite interbedded with mudstone portion (Drabon et al., pers. comm.).

Sulfur: Total sulfur abundances are generally below 3 wt.%. Sulfur isotope results for sedimentary sulfide are highly variable. $\delta^{34}S$ values range between -6.6 and +3.4 ‰ and $\Delta^{33}S$ values between -0.4 and +2.3 ‰. Each lithofacies is characterized by a different sulfur isotopic composition, exhibiting both mass-dependent (i.e. variable $\delta^{34}S$ values) and clearly mass-independent (i.e. non-zero $\Delta^{33}S$ values) sulfur isotopic fractionation. Based on our present understanding the mass-independent sulfur isotopic fractionation unequivocally identifies a photolytic source of sulfur, i.e. UV-induced photochemistry of volcanogenic SO_2 in an anoxic atmosphere (Farquhar et al., 2000; Johnston, 2011; Pavlov and Kasting, 2002). Specifically, the negative $\Delta^{33}S$ values indicate photolytic sulfate as the atmospheric sulfur species, and positive $\Delta^{33}S$ values photolytic elemental sulfur. Both atmospheric sulfur compounds enter the terrestrial marine realm. Subsequent, in part microbial sulfur cycling is indicated by the variable $\delta^{34}S$ values. Predominantly positive $\Delta^{33}S$ values suggest that the (microbial) processing of photolytic elemental sulfur is the key processes in sedimentary sulfur cycling, but clearly negative $\Delta^{33}S$ values indicate that microbial reduction of sulfate played a role as well. Oceanic sulfate and its distinct atmospheric sulfur isotope signature is preserved in sedimentary barite.

Organic Carbon: Total organic carbon contents vary between 0.12 and 3.31 wt.% and display a clear stratigraphic variability with decreasing concentrations up-section. Lithofacies control is not very well expressed, but laminated carbonaceous siltstones exhibit the highest concentrations. Organic carbon isotope valuess ($\delta^{13}C_{org}$) range from -31.8 to -25.6 ‰ and display a steady increase in ^{13}C up-section, independent of lithological changes. Results from the BARB5 core are comparable to other data from Paleoarchean settings and indicate autotrophic carbon fixation as the ultimate process.

Carbonate Carbon: Highly variable carbonate carbon abundances of up to 9.9 wt.% exhibit distinct lithofacies differences. High concentrations characterize the litharenite interbedded with chert. Preliminary carbonate carbon isotope data ($\delta^{13}C_{carb}$) are equally variable between -4.8 and +1.7 ‰.

Summary: Abundances and stable isotopes provide clear evidence for the presence of diverse biological processes within the Paleoarchean anoxic marine realm, archived in sedimentary rocks from the Barberton Greenstone Belt, South Africa. Primary productivity appears to be based on autotrophic carbon fixation, but not necessarily via oxygenic photosynthesis. Mass-dependently fractionated sulfur indicated the microbial processing of

photolytic sulfur compounds, specifically sulfate reduction and elemental sulfur reduction and/or disproportionation.

Acknowledgements: Financial support from the Deutsche Forschungsgemeinschaft (DFG Str 281/36) is gratefully acknowledged.

References:
Canfield, D.E., 2004. The evolution of the Earth surface sulfur reservoir. American Journal of Science. 304, 839-861.
Farquhar, J., Bao, H., Thiemens, M., 2000. Atmospheric Influence of Earth's Earliest Sulphur Cycle. Science 289, 756–758.
Holland H.D., Turekian, K.K., 2004. Treatise on Geochemistry – Volume 8 Biogeochemistry. Elsevier Pergamon.
Holland, H.D., 2006. The oxygenation of atmosphere and ocean. Philosophical transactions of the royar society B 361, 903-915.
Johnston, D.T, 2011. Multiple sulfur isotopes and the evolution of Earth's surface sulfur cycle. Earth-Science Reviews 106, 161-183.
Ohmoto, H., Watanabe, Y., Lasaga, A.C., Naraoka, H., Johnson, I, Brainard, J., Chorney, A., 2014. Oxygen, iron, and sulfur geochemical cycles on early Earth: Paradigms and contradictions. In: G.H. Shaw: Earth's Early Atmosphere and Surface Environment. Geol. Soc. Amer. Spec. Pap. 504, 55-95.
Pavlov, A.A., Kasting, J.F., 2002. Mass-independent fractionation of sulphur isotopes in Archaean sediments: strong evidence for an anoxic Archaean atmosphere. Astrobiology 2, 27-41.
Rollinson, H.R., 2007. Early Earth Systems: A Geochemical Approach. Blackwell Publishing.

ICDP

Chronological, petrological, volcanological, hydrological and paleoclimatological evolution of a 219 m core drilled at Site 2 into Lake Van during the Paleovan ICDP Drilling project, a preliminary synthesis

M. SUMITA, H.-U. SCHMINCKE

GEOMAR Helmholtz-Zentrum für Ozeanforschung Kiel, Wischhofstr. 1-3, 24148 Kiel, Germany

We present a preliminary synthesis of chronological, chemical, mineralogical, volcanological and sedimentological data obtained on ca. 170 of a total of ca. 450-500 tephra layers recovered at Site 2 of the ICDP Paleovan drilling project. We compare these with similar types of data (chemistry, mineralogy, volcanology) from the ca. 570 ka onshore record of Nemrut Volcano adjacent to, and underlying, the west shore of Lake Van.

The main results include: Nemrut explosive activity as recorded in preserved tephras extends from ca. **570 ka to historic** in age onshore and from ca. **580** ka to Holocene in the core. Most individual tephra layers are slightly **peralkaline** trachytes, larger volumes of **rhyolitic** tephras having been erupted at **intervals of 30-40 ka**. Fallout deposits dominate while the larger rhyolite eruptions are generally associated with ignimbrites onshore, thick massive tephra deposits drilled being interpreted as syn-ignimbrite turbidites. We infer stages of caldera collapse to be associated with the large-volume rhyolitic eruptions. Most larger eruptions are compositionaly zoned from evolved to more mafic, magma mingling and mixing being ubiquituous.

Eruptive rates at Nemrut volcano seems to have increased judging from both onshore and core evidence at ca. 200 ka. Tephras from adjacent subalkalic Süphan volcano dominate the felsic tephras in the core prior to about 200 ka but are rarely interlayered with peralkaline tephras in Nemrut volcano. Nemrut volcanic explosive activity appears to have been roughly **periodic** while that of Süphan was more **episodic**, seems to have strongly **waned** during the past 200 ka with **external forcing** (seismic, hydroclastic) having been characteristic forcing mechanisms, the Nemrut system having been open throughout its recorded lifetime.

Basaltic tephras are most common in the lower ca. 100 m of the core and appear to represent dominantly **subaqueous eruption**s. The dominantly **high-Al composition** probably indicates **parent magma to subalkalic Süphan system**. A huge subaqueous to subaerial basaltic eruption at ca. 80 ka is represented onshore by large Incekaya tephra cone and thick widespread fallout onshore and throughout western Lake Van. It forms a major stratigraphic marker in cores of sites 1 and 2 and on land. It is also the **most widespread and voluminous seismic marker bed** and represents one of **largest** – if not the largest – **basaltic explosive eruption globally** with a volume of >1 km^3 (DRE).

We estimate about 30 % of the cored tephra layers to be reworked by various mechanisms. **Wind-transported** tephras appear most common and mostly associated with **dry climate intervals**. They range from nearly pure to mixed tephras containing a large proportion of xenocrysts and nonvolcanic and organic particles. We define thick fallout deposits consisting of fine-grained basal tephra and variously rounded pumice lapilli at the top as **pumice raft deposits** reflecting prolonged abrasion in pumice rafts covering the lake surface. Most significant are **poorly sorted reworked tephra deposits** containg abundant organic debris (plants, shell fragments), many also containing, or being dominated by, gypsum crystals and are interpreted as recording extended periods of low lake levels. Core intervals with abundant reworked tephra layers appear to correlate with **seismically defined low lake level periods**. Such intervals maybe used as independant criteria for recording significant lake level changes. We cannot exclude that they represent distal **tsunami deposits**.

The initial fundamental precise **stratigraphic and temporal correlation** of the upper part of cores from sites 1 and 2, as well as with the onshore tephra record was based on several fallout tephra layers defined by chemical composition, highly concordant $^{40}Ar/^{39}Ar$ ages and nature of the tephra deposit. Tephra layer NF ist the prime example, dated precisely as ca. 30 ka, being rhyolitic in composition and associated with an ignimbrite covering the fallout etc.

There is a tentative correlation of **higher eruption frequency with warm climate** periods both within the cores and on land suggesting magma generation/eruption control via **lithosphere loading**.

References:
Cukur D, Krastel S, Schmincke H-U, Sumita M, Tomonaga, Çağatay N (2014) Drastic lake level changes of Lake Van (eastern Turkey) during the past ca. 600 ka: climatic, volcanic and tectonic control. J Palelimnol 52: 201-214. DOI 10.1007/s10933-014-9788-0
Macdonald R, Sumita M, Schmincke H-U, Baginski B, White JC, Ilnicki SS (2015) Peralkaline felsic magmatism at the Nemrut volcano, Turkey: impact of volcanism on the evolution of Lake Van (Anatolia) IV. Contrib Min Petrol
Schmincke, H. U., Sumita, M. and Cukur, D. and Paleovan Scientific Team (2013) Impact of volcanism of the evolution of Lake Van III: Incekaya - an exceptionally large magnitude (DRE > 1km^3) subaqueous/subaerial explosive basaltic eruption. IODP/ICDP Kolloquium Freiberg.
Schmincke H-U, Sumita M, Paleovan scientific team (2014) Impact of volcanism on the evolution of Lake Van (Anatolia) III: Periodic (Nemrut) vs. episodic (Süphan) eruptions, contrasting eruptive

mechanisms and climate forcing causing a tephra gap between ca. 14 ka and ca. 30 ka. J Volcanol Geotherm Res 285: 195-213. DOI 10.1016/j.jvolgeores.2014.08.015
Stockhecke M, Sturm M, Brunner I, Schmincke H-U, Sumita M, Kwiecien O, Cukur D, Anselmetti FS (2014a) Sedimentary evolution and environmental history of Lake Van (Turkey) over the past 620,000 years. Sedimentology 61: 1830-1861. DOI 10.1111/sed.12118
Sumita M, Schmincke H-U (2013a) Impact of volcanism on the evolution of Lake Van II: Temporal evolution of explosive volcanism of Nemrut Volcano (eastern Anatolia) during the past ca. 0.4 Ma. J Volcanol Geotherm Res 253: 15-34. doi.org/10.1016/j.jvolgeores.2012.12.009
Sumita M, Schmincke H-U (2013b) Erratum to "Impact of volcanism on the evolution of Lake Van II: Temporal evolution of explosive volcanism of Nemrut Volcano (eastern Anatolia) during the past ca. 0.4". J Volcanol Geotherm Res 253: 131-133. Doi: 10.1016/j.jvolgeores.2013.01.008
Sumita M, Schmincke H-U (2013c) Impact of volcanism on the evolution of Lake Van I: Evolution of explosive volcanism of Nemrut Volcano (eastern Anatolia) during the past ca. 0.4 Ma. Bull Volcanol 75: 714-. DOI 10.1007/s00445-013-0714-5

IODP

Constraining the dynamics of fluid flow at the northeastern Pacific continental margin

B.M.A. TEICHERT[1], V. SCHACHT[1], N. GUSSONE[2], C. MÄRZ[3], H. STRAUSS[1]

1 Institut für Geologie und Paläontologie, Westfälische Wilhelms-Universität Münster, Corrensstrasse 24, D-48149 Münster, Germany
2 Institut für Mineralogie, Westfälische Wilhelms-Universität Münster, Corrensstrasse 24, D-48149 Münster, Germany
3 Newcastle University, School of Civil Engineering and Geoscience, Newcastle upon Tyne, NE1 7RU, United Kingdom

During IODP Expedition 341 a cross-margin transect of five sites was drilled on the northeast Pacific continental margin in southern Alaska. Sites U1417 and U1418 are a distal and a proximal record on the Surveyor Fan and provide a sedimentary record reaching back to the late Miocene and early Pleistocene, respectively. The sulfate penetration depth into the sediments is shallowing while the rates of organic matter remineralization and sedimentation increase significantly. First on-board results indicate distinct differences in pore water chemistry between both sites. From distal to proximal, the sulfate penetration depth into the sediments shallows from the distal (U1417) to the proximal (U1418) drill site. At U1418, there is a distinct sulfate-methane transition zone (SMTZ) at about 75 m depth below seafloor, while at U1417 there is a gap between the deepest sulfate penetration and the methanogenic zone. The latter indicates continuous sulfate reduction by organic matter degradation in the upper 200 m due to its typical convex-up curvature (Borowski et al., 1996). In the deeper section, at about 650 m below seafloor, a SMTZ suggests that anaerobic oxidation of methane leads to the depletion of upward diffusing sulfate from probably a deep seawater aquifer that exists at the sediment-seawater contact. In contrast, the more linear sulfate profile at Site U1418 appears to reflect a more focused sulfate consumption driven by an upward methane flux from below at rates substantially higher than those for sulfate reduction of sedimentary organic matter (Borowski et al., 1996). A combination of sulfur and oxygen isotopes of the pore water sulfate supports these first shipboard results.

Within respective convergent continental margin settings, the fluid regimes play a critical role as they impact the geochemical budgets (Torres et al., 2004). Compaction through sediment loading and tectonic compression enhances the fluid flow (Saffer and Bekins, 1999). The faults and fractures that are associated with tectonic deformation act as conduits for upward moving fluids. Processes that alter the overall geochemical fluid composition at depth like e.g. smectite to illite conversion, ash alteration, carbonate dissolution, are critical for understanding the biogeochemical processes acting in shallower parts of the sedimentary succession where the reduction of sulfate dominates (Teichert et al., 2005, 2009; Torres et al., 2004). Strontium isotopes are an ideal tracer for these processes at depth and first results show that different fluid sources at depth can be differentiated.

References:
Borowski, W.S., Paull, C.K., Ussler III, W. (1996) Marine pore-water sulfate profiles indicate in situ methane flux from underlying gas hydrate. Geology 24, 655-658.
Saffer, D.M., Bekins, B.A. (1999) Fluid budgets at convergent plate margins: Implications for the extent and duration of fault zone dilation. Geology 27,1095-1098.
Teichert, B.M.A., Gussone, N., Torres, M.E. (2009) Controls on calcium isotope fractionation in sedimentary porewaters. Earth Planet. Sci. Lett. 279, 373-382.
Teichert, B.M.A., Torres, M.E., Bohrmann, G., Eisenhauer, A. (2005) Fluid sources, fluid pathways and diagenetic reactions across an accretionary prism revealed by Sr and B geochemistry. Earth and Planetary Science Letters 239, 106-121.
Torres, M.E., Teichert, B.M.A., Trehu, A.M., Borowski, W., Tomaru, H. (2004) Relationship of pore water freshening to accretionary processes in the Cascadia margin: Fluid sources and gas hydrate abundance. Geophysical Research Letters, 31(22), 1-4.

IODP

Palagonitization of basalt glass in the flanks of mid-ocean ridges: implications for the bioenergetics of oceanic intracrustal ecosystems

ANDREAS TÜRKE AND WOLFGANG BACH

Fachbereich Geowissenschaften and MARUM, Universität Bremen, Klagenfurter Str. GEO, 28359 Bremen

Background

IODP Expedition 336 had the goal of unraveling the hydrogeological-microbiological-geochemical linkages in the 8 Ma old basement of the western flank of the mid-Atlantic Ridge at 22°45'N, 46°05'W (North Pond). We report results from post-cruise studies of alteration of basalt glass, which is abundant in both basement holes cored during the expedition, and is partially altered to palagonite (a mixture of poorly crstalline phases turning into clay minerals and Fe-oxyhydroxides).

The primary goal of Expedition 336 was examining the extent and nature of intracrustal life in an energy-starved ridge flank underlying an oligotrophic part of the Atlantic. While the energy sources fuelling putative microbial life in basalt are unknown, it has been suggested that steady-state Fe oxidation in ridge flanks can support a microbial biomass production on the order of 10^{11} g C per year (Bach & Edwards, 2003). These authors suggest that most of the Fe oxidation takes place within the first 10 Myrs of ridge flank evolution, and it is uncertain which energy sources chemolithoautotrophs may use in older crust. The drill site

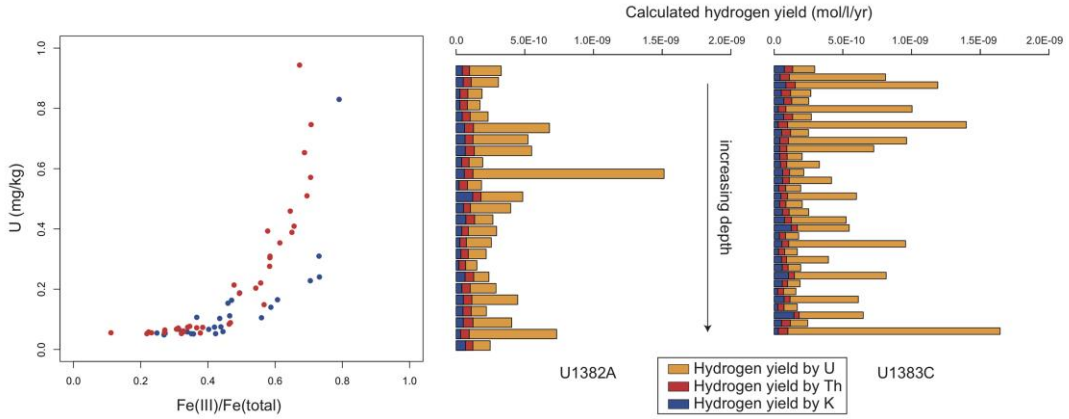

Fig. 1: A) Left: Uptake of U with increasing Fe-oxidation state in whole rock composition. Samples from U1382A in red and U1383C in blue. **B)** Right: Calculated hydrogen yields in mol/cm^3/yr. Bars are structured to indicate individual contribution of U (red), Th (purple) and K (orange).

in the North Pond area is sedimented, but conditions in the basement are still oxic.

Geological setting

The North Pond area is a sediment pond structure of 8 x 15 km in about 4450 m water depth. It is surrended by steep rift mountains rising with elevations of 1 to 2 km. Heat flow meassurements suggest significant fluid flow, below the up to 270 m thick sediment, with seawater circulating from the SW part to the NNE part. North Pond is characterized by low subseafloor fluid temperatures of approximately 2 – 15 °C, high fluid flux (Becker et al., 2001) and, hence, overall high water-to-rock ratios. Sediment thickness decreases from the center towards the edges of the pond, where oxygen profiles indicate that basement fluids are oxygenated (Ziebis et al., 2012). Orcutt et al. (2013) proposed that south-to-north decline in the oxygen concentrations of the basal pore waters is due to microbial respiration of oxygen by microorganisms inhabiting the basaltic aquifer underlying North Pond.

Rationale

The flanks of mid-ocean ridges are the largest reservoir of basalt glass on Earth, and the flow of oxygenated seawater fluxed through these flanks is >10^{16} kg/yr (Wheat et al., 2003). Basalt glass exposed to oxygenated seawater will turn into palagonite along fractures. Hence, a large amount of palagonite forms in this setting. But palagonitization is kinetically sluggish at the prevailing temperatures of < 25 °C, allowing chemolithoautotrophic microbes (i.e., those that fix CO_2 by using inorganic energy sources of energy and electrons) to catalyse oxidation reactions of ferrous iron for catabolic energy gain. Tubular and granular alteration textures, present in basalt glass samples, both from modern and ancient rocks, are interpreted as trace fossils of endolithic microbes, chemically 'drilling' into fresh glass (Thorseth et al., 1995). From these drill cores, we have analyzed fresh glass and adjacent palagonite rinds for major and trace elements by electron microprobe and Laser Ablation Inductively Coupled Plasma Mass Spectrometry, respectively, to determine the geochemical changes involved in palagonitization. We also analyzed whole rock powders to determine the overall crust-seawater exchange in a young ridge flank. Palagonite is an abundant alteration phase in the basaltic ocean crust, along with clay minerals, Fe-oxyhydroxides, and zeolites, and determining geochemical exchange is crucial to understanding bioenergetic landscapes in ridge flanks.

Results

We have analyzed variably altered glassy basalt from both sites where basement was penetrated (U1382 and U1383). Alteration products comprise saponite, celadonite, and zeolites, but palagonite is the most abundant alteration feature at the contacts of lava flow units, where basement permeability is greatest. Representative rock samples where analyzed for major and trace element composition and ferrous/ferric ratios. The iron in palagonite appears to be highly oxidized, containing only little to no ferrous iron. Radioactive elements are enriched in the palagonite relative to the fresh glass, reaching concentrations (U up to 0.62 ppm, Th up to 0.27 ppm and K_2O of up to 3.06 wt%) where radiolytic production of molecular hydrogen (H_2) may be a significant energy source (Blair et al., 2007). We estimated average radiolytic hydrogen yields of 2.26 x 10^{14} mol/yr/cm^3 with uranium as the main hydrogen provider (Figure 1). Where palagonite rinds are thickest, zeolites (mainly phillipsite) froms in the interstital pore space, indicating a slowdown of palagonitization rates.

Discussion

The North Pond Area is a rather young ridge flank (8 Ma) with open fluid circulation beneath a sediment pond. Circulation of seawater is focused in discrete subseafloor aquifers, which likely correspond to contacts of major flow units and breccia (Becker et al., 2001). We have established that the glassy flow margins are most intensely altered (palagonitized and more oxidized) and enriched in U and K. According to wire-line logging formation microscanner data (Edwards et al., 2012), these glassy zones are also most fractured. Due to their fractured nature, these highly altered flow contacts are likely currently permeated by seawater, which would facilitate extant microbial activity. Open circulation of oxygenated seawater has basalt glass with >80% ferrous iron replaced by ferric iron-rich palagonite (whole rock samples feature $Fe(III)/Fe_{tot}$ up to 0.8). In crust less than approximately 10 Myrs old, ferrous iron is still being oxidized and Fe-oxidizing metabolisms is expected to yield highest

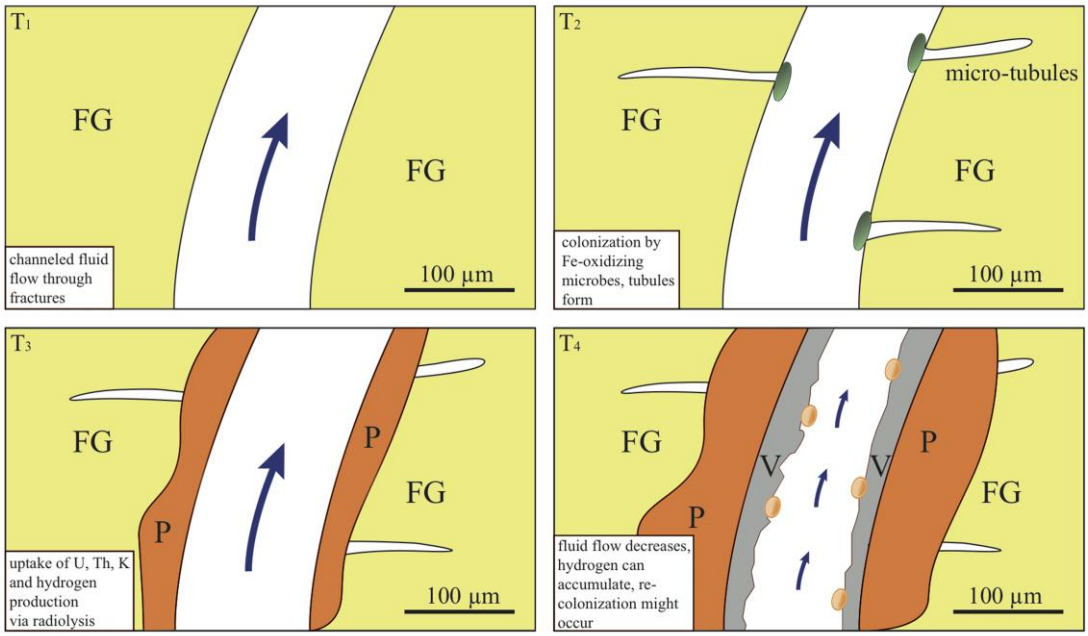

Fig. 2. Conceptual model as hypothesis for a change in bioenergetical conditions in ageing ridge flank systems. **T_1:** Only fresh glass in hyaloclastite samples, with available Fe(II). **T_2:** Microbial colonization (green) and initiation of tubular boring textures. **T_3:** Sluggish palagonitization begins, resulting in uptake of U, Th and K, and increased Fe-oxidation state. Palagonite overgrows tubular textures and Fe(II) is no longer readily available. Microbes might disappear. **T_4:** Minerals (V) precipitate and fill veins, ceasing fluid flow and hydrogen produces by radiolysis could initiate re-colonization (by a different type of microbe?(orange)) and a change in microbial metabolism towards hydrogen consumption.

production of primary biomass in ridge flanks (Bach and Edwards, 2003). Based on our results, we hypothesize that microbial ecosystems in ridge flank habitats undergo a transition in the principal energy carrier fuelling carbon fixation from Fe oxidation in very young crust to H2 consumption in old crust. We argue that thick rinds of palagonite in old crust protect the remaining fresh glass from alteration and thwart the oxidation of ferrous iron in the glass. These palagonite rinds have accumulated enough U and K to release nanomolal quantities of H_2 per year. Unless the H_2 is swept away by rapid fluid flow (i.e. in young flanks), it may easily accumulate to levels high enough to support chemolithoautotrophic life. In older flanks, crustal sealing and sediment accumulation have slowed down seawater circulation and radiolytically produced H_2 greatly increases in significance for catalytic energy supply (Figure 2).

Based on average contents of U, K, and Th, even 1% of the estimated hydrogen yields would be sufficient to have 1 nM H_2(aq) in aquifer seawater, given the flow rates estimated by Langseth et al. (1992). These heat flow studies provide a minimum estimate of water flow and more water flow would dilute the dihydrogen produced. The computed numbers may hence represent maximum estimates of the concentrations of radiolytic H_2 in the aquifers underneath North Pond.

Acknowledgements:

This research used samples and data provided by the Integrated Ocean Drilling Program (IODP). Funding for this research was provided the German Research Foundation DFG (grant BA1605/8). We are grateful to Jörg Erzinger at the GFZ-Potsdam for support with the Fe(II) determinations. We also acknowledge support from Kentaro Nakamura in whole rock analyses.

References:

Bach, W. & Edwards, K. J. (2003). Iron and sulphide oxidation within the basaltic ocean crust: implications for chemolithoautotrophic microbial biomass production. Geochimica et Cosmochimica Acta 67, 3871–3887.

Becker, K., Bartetzko, A. & Davis, E. E. (2001). Leg 174B Synopsis: Revisiting Hole 395A for logging and long-term monitoring of off-axis hydrothermal processes in young oceanic crust. Proceedings of the Ocean Drilling Program, Scientific Results Volume 174B.

Blair, C.C., D'Hondt, S., Spivack, A.J. & Kingsley, R.H. (2007). Radiolytic Hydrogen and Microbial Respiration in Subsurface Sediments. Astrobiology Volume 7, Number 6, 951-970.

Edwards, K.J., Bach, W., Klaus, A., and the Expedition 336 Scientists (2012). Proceedings of IODP, 336: Tokyo (Integrated Ocean Drilling Program Management International, Inc.)

Thorseth, I.H., Torsvik, T. Furnes, H. & Muehlenbachs, K. Microbes play an important role in the alteration of oceanic crust. Chem. Geol. 126, Chem. Geol. 126, 137–146 (1995).

Orcutt, B.N., Wheat, C.G., Hulme, S., Edwards, K.J., Bach, W. (2013). Oxygen consumption in the subseafloor basaltic crust derived from a reactive transport model. Nature communications 4, 2539.

Wheat, C.G., McManus, J., Mottl, M.J. & Giambalvo, E. (2003). Oceanic phosphorus imbalance: the magnitude of the ridge-flank hydrothermal sink. Geophysical Research Letters 30(17).

Ziebis, W., McManus, J., Ferdelman, T., Schmidt-Schierhorn, F., Bach, W., Muratli, J., Edwards, K. J. & Villinger, H. (2012). Interstitial fluid chemistry of sediments underlying the North Atlantic gyre and the influence of subsurface fluid flow. Earth and Planetary Science Letters, 323-324, 79–91.

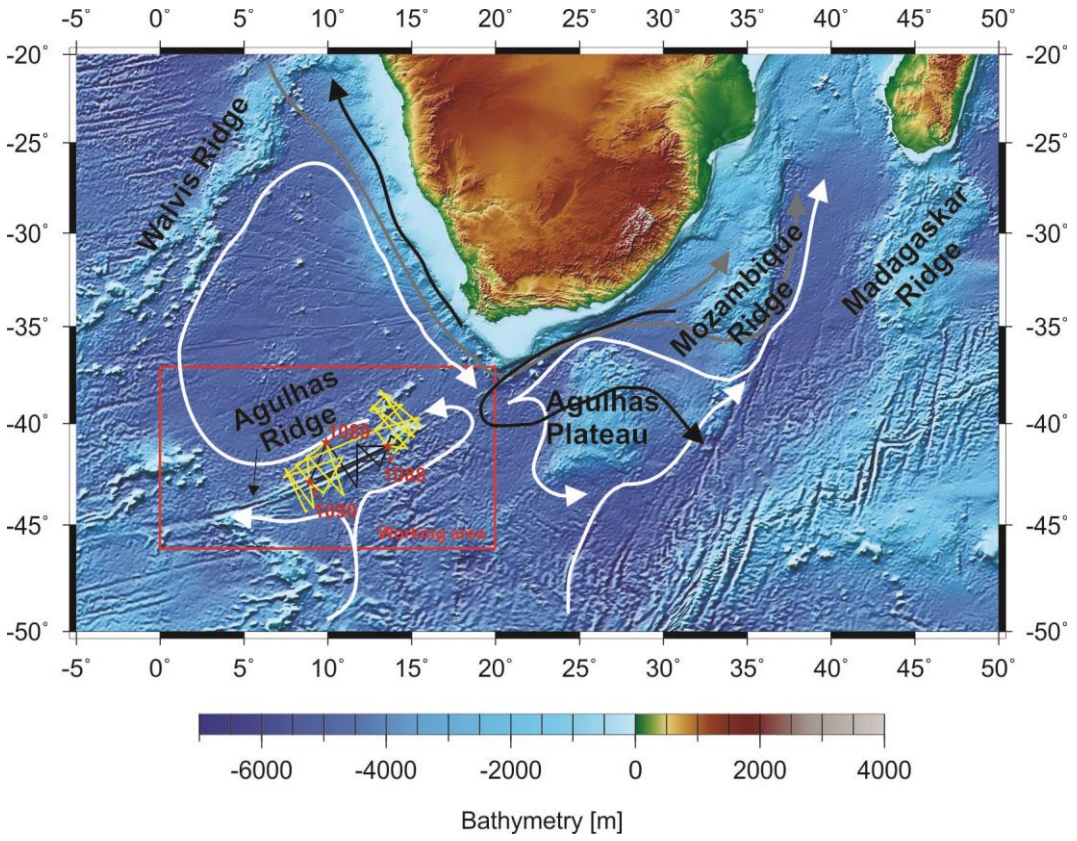

Fig. 1. Bathymetric map with the general circulation scheme of deep-water masses south of Africa (AABW= Antarctic Bottomwater; AAIW= Antarctic Intermediate Water; NADW= North Atlantic Deepwater) and locations of seismic reflection profiles in the area of the Agulhas Ridge (red box).

IODP

A seismic approach to the paleoceanography of the eastern South Atlantic

G. UENZELMANN-NEBEN, J. GRUETZNER

Alfred-Wegener-Institut, Helmholtz-Zentrum für Polar- und Meeresforschung, Bremerhaven, Germany (Jens.Grützner@awi.de)

Geochemical proxies (such as $\delta^{13}C$ or ε_{Nd}) measured on drilled samples helped to decipher variations of water masses related to climate changes in the South Atlantic (e.g. Billups 2002; Scher and Martin, 2008). Information on how these changes in transport influenced the intensity and position of current systems is currently very sparse but can be gained by seismic investigations of contourites (e.g. Gruetzner et al., 2014). With a new proposal, which is based on 5400 km of high-resolution multichannel seismic reflection data acquired during RV Maria S. Merian cruise MSM 19/2 in the Agulhas Ridge area, we aim at a better understanding of both pathways and intensity of the current system in the eastern South Atlantic.

With its high topography the Agulhas Ridge has prevented a direct N-S water mass exchange between the Southern Ocean and the Atlantic and hence has restricted the energy and heat transfer since its formation ~83 Ma. While Antarctic Bottomwater (AABW) and Circumpolar Deepwater (CDW) originating in the Southern Ocean provide the inflow of cold water masses in larger water depths, the Agulhas leakage is the main source of warm and salty waters carried towards the Subpolar North Atlantic (Fig. 1). Sediment drifts have been formed due to this flow pattern since the Oligocene (Wildeboer Schut and Uenzelmann-Neben, 2005). By mapping the drift shapes and distributions we aim to monitor oceanographic variations caused by global climate changes like the onset of the glaciations of East and West Antarctica, the Mid Miocene Climatic Optimum (MMCO), and the glacial/interglacial cycles since the Pliocene. Furthermore the seismic interpretation will help to decipher the influence of tectonic events as the opening of Drake Passage and the closure of the Isthmus of Panama on the position of oceanic fronts and pathways of water masses in the region.

A first interpretation of the seismic lines collected across the northern Agulhas Ridge shows two formation levels of sediment drifts corresponding to the activity depths of AABW/CDW and the Agulhas Rings (Gruetzner and Uenzelmann-Neben, 2014). A correlation with ODP Leg 177 age-depths model and water mass information based on ε_{Nd} values (Scher and Martin, 2008) as well as the seismostratigraphic model of Wildeboer Schut et al. (2002) will allow the development of a chronology for the formation of the sediment drifts. A subsidence analysis in two dimensions along a series of selected profiles will be performed in order to correct for the effects of compaction and determine the volumes and masses of sediment (eroded rock) deposited during each time interval.

References:

Billups, K., 2002. Late Miocene through early Pliocene deep water circulation and climate change viewed from the sub-Antarctic South Atlantic. Palaeogeography, Palaeoclimatology, Palaeoecology 185: 287-307.

Gruetzner, J., Uenzelmann-Neben, G., Franke, D., Arndt, J.E., 2014. Slowdown of Circumpolar Deepwater flow during the Late Neogene:

Evidence from a mudwave field at the Argentine continental slope. Geophysical Research Letters 41: 270-276.
Scher, H.D., Martin, E.E., 2008. Oligocene deep water export from the North Atlantic and the development of the Antarctic Circumpolar Current examined with neodymium isotopes. Paleoceanography 23. PA1205, doi:10.1029/2006PA001400.
Wildeboer Schut, E. and Uenzelmann-Neben, G., 2005. Cenozoic bottom current sedimentation in the Cape Basin, South Atlantic. Geophysical Journal International, 161: 325-333.
Wildeboer Schut, E., Uenzelmann-Neben, G. and Gersonde, R., 2002. Seismic evidence for bottom current activity at the Agulhas Ridge. Global and Planetary Change, 34: 185-198.

ICDP

THE DIATOM FLORA OF LAKE KINNERET (ISRAEL) – PALAEOLIMNOLOGICAL EVIDENCE FOR HOLOCENE CLIMATE CHANGE AND HUMAN IMPACT IN THE SOUTHEASTERN MEDITERRANEAN

H. VOSSEL[1], T. LITT[1], J. M. REED[2]

1 Rheinische Friedrich-Wilhelms-University of Bonn, Steinmann Institute of Geology, Mineralogy & Paleontology, Nussallee 8, 53115 Bonn, Germany, hvossel@uni-bonn.de
2 University of Hull, Department of Geography, Environment and Earth Sciences, Cottingham Road, Hull, HU6 7RX, United Kingdom

The Mediterranean basin is a region of highly complex topography and climatic variability, such that our understanding of the past environmental variability is still limited. Diatoms (single-celled siliceous algae, Bacillariophyceae) are abundant, diverse and sensitive to a wide range of environmental parameters. They are often well preserved in lake sediment records, and have well-recognised potential to generate high-quality paleolimnological data. Diatoms remain one of the least-exploited proxies in Mediterranean palaeoclimate research. Here, we present results of diatom analysis of an 18 m sediment core from Lake Kinneret (Israel) as part of a multi-proxy study of Holocene climate change and human impact in the Levant (http://www.sfb806.uni-koeln.de). Results are compared with other proxy data including pollen, and with output data from regional climate modelling, to strengthen interpretation of environmental change in the southeastern Mediterranean.

The results show remarkable shifts in the diatom flora over the last ca. 8,000 years. Preliminary investigations show that 98% of the diatom taxa can be classified as oligohalobous-indifferent and as alkaliphilous, as is typical of freshwater, alkaline lakes of open hydrology in limestone, karst-dominated catchments.

Changes in the diatom data over time can be interpreted mainly in terms of productivity shifts, with a clear trend from oligotrophic at the base to hypereutrophic in the modern lake. The eutrophication trend accelerates after ca. 3,000 cal. yrs. BP, indicating the influence of increased human activity in the catchment, identified previously by analysis of the vegetational history (Schiebel, 2013).

The analysis of the composition of the diatom flora also provides some evidence for lake-level fluctuations, as a proxy for shifts in moisture availability. Low lake-level stands are characterized by low diatom concentration and increased relative abundance of littoral taxa. High lake-level stands are marked by the clear dominance of planktonic species, such as Cyclotella ocellata PANTOCSEK and Cyclotella paleo-ocellata VOSSEL & VAN DE VIJVER (a newly described centric diatom which may be endemic (Vossel et al., 2015), in phases of high diatom concentration. Such inferred lake-level oscillations correlate well with the output from the climatic models from the Levant region, representing changes in moisture availability (Litt et al., 2012), although the signal is obscured in the last 3,000 years by the effects of anthropogenic eutrophication.

References:

Litt, T.; Ohlwein, C.; Neumann, F. H.; Hense, A. & Stein, M. (2012): Holocene climate variability in the Levant from the Dead Sea pollen record. – Quat. Sci. Rev., 49: 95-105.
Schiebel, V. (2013): Vegetation and climate history of the southern Levant during the last 30,000 years based on palynological investigation. – Unpublished PhD thesis.
Vossel, H.; Reed, J. M.; Houk, V.; Cvetkoska, A. & Van de Vijver, B. (2015): Cyclotella paleo-ocellata, a new centric diatom (Bacillariophyta) from Lake Kinneret (Israel). Fottea, 15 (1), in press.

IODP

Towards a complete and accurate Eocene chronostratigraphic framework

T. WESTERHOLD[1], U. RÖHL[1], T. FREDERICHS[2], S.M. BOHATY[3], J.C. ZACHOS[4]

1 MARUM – Center for Marine Environmental Sciences, University of Bremen, Bremen, Germany
2 Department of Geosciences, University of Bremen, Bremen, Germany
3 Ocean and Earth Science, University of Southampton, National Oceanography Centre, Southampton, SO14 3ZH, UK
4 University of California, Santa Cruz, California, USA

In less than a hundred years from now atmospheric CO_2 concentrations will rise to levels that Earth has not experienced for more than 30 million years. Records from the Eocene and Paleocene greenhouse climate intervals provide an exceptional opportunity to decipher Earth's climate system behavior under those CO_2 concentrations likely to be reached in the near future (Zachos et al. 2008). For the detailed reconstruction of the early Paleogene greenhouse climate system two basic conditions are required: (1) a complete, precise, and highly accurate stratigraphic framework to determine rates of climatic processes and timing of events, and (2) high-resolution stable isotope records for Atlantic, Pacific, and Southern Oceans to correlate paleoceanographic records globally and characterize the overall climate state and its variability.

Efforts to anchor the floating astronomically calibrated Paleogene time scale to the astronomically tuned Neogene time scale (ATNS, Lourens et al. 2004) have been hampered by fundamental problems related to the mid Eocene "cyclostratigraphic gap" (Pälike and Hilgen, 2008; Gradstein et al. 2012). This ~5-myr interval in the middle Eocene lacks detailed cyclostratigraphic records from pelagic drillcores, and existing records from older time intervals are subject to uncertainties and limits of astronomical calculations (Laskar et al. 2004, 2011) and radio-isotopic age constraints (Westerhold et al. 2012). A cyclostratigraphic framework based on the stable long (405-kyr) eccentricity cycle in deep-sea sections has been established for the Paleocene (Lourens et al. 2005, Westerhold et al. 2007, 2008; Atlantic and Pacific), the early to middle Eocene (Lourens et al. 2005, Westerhold & Röhl 2009; Atlantic), late middle Eocene (Pälike et al. 2001, Atlantic), and late middle Eocene to early Oligocene (Röhl et al. 2004, Tasman Sea; Westerhold et al. 2014; Pacific).

Following on from previous studies, a high-resolution stable isotope record and a complete, precise and highly accurate stratigraphic framework for both Atlantic and Pacific Ocean for the entire Paleogene can be achieved by now focusing on missing or incomplete key intervals from ODP Legs 198 (North Pacific) and 208 (South Atlantic). The aim of our ongoing project is to establish for the first time a complete cyclostratigraphic framework based on the identification of the stable long eccentricity cycle for the entire Eocene (~55 to 34 Ma) for both the Atlantic and Pacific oceans at unprecedented resolution. Our project will also substantially contribute to documenting the frequency of hyperthermal events, understanding of their relationship to orbital forcing, and their connection to greenhouse climate.

Here we present the first results from representative sites and selected stratigraphic intervals included in the current study. A crucial step is to establish a complete magnetostratigraphy for the Eocene records from ODP Leg 208 spanning magnetic polarity Chron C18n to C24. We conducted more than two hundred natural remanent magnetization (NRM) analyses allowing a robust magnetostratigraphy spanning the interval from Chron C13n to the top of Chron C23n.2n. Our data validate that the peak-MECO (Middle Eocene Climate Optimum; Bohaty et al. 2009) carbon isotope excursion and the associated dissolution event is directly assigned to the Chron C18n.2n/C18r reversal.

New bulk stable isotope data for Leg 208 sites now span the stratigraphic gap in the middle Eocene and allow the compilation of a complete bulk isotope record for the Eocene at Leg 208 sites. These new carbon isotope records display a pronounced eccentricity related amplitude variation that is prerequisite to further define a cyclostratigraphy based on the stable 405-kyr eccentricity cycle. Preliminary comparison of Atlantic Leg 208 records to Pacific Exp. 320 exhibit similar patterns that could be utilized for detailed correlation across ocean basins.

For Pacific Leg 198 we have generated new high-resolution >38 µm coarse fraction and benthic (*N. truempyi*) stable isotope records. The coarse fraction data show average values around 3 wt% in the interval from Chron C23n to C20r. Pronounced minima in the wt% coarse fraction during this period are typically associated with high peaks in both XRF scanning iron (Fe) and magnetic susceptibility data suggesting the presence of multiple carbonate dissolution events. The benthic isotope data will further test if the dissolution events are associated with stable isotope excursions in the deep sea characteristic for early to middle Eocene hyperthermal events (e.g. Zachos et al. 2005, Lourens et al. 2005, Agnini et al. 2009, Stap et al. 2010, Sexton et al. 2011, Kirtland-Turner et al. 2014). The early Eocene interval at Shatsky Rise reveals relatively high coarse fraction values due to winnowing in Chron C24r as well as a deeper calcite compensation depth (CCD) in Chron C24n in the western equatorial Pacific. Physical property, XRF core scanning and coarse fraction data reveal eccentricity related cycles that will be used to construct a cyclostratigraphic framework for the Pacific from Leg 198 sites.

Another important component of our project is the detailed investigation of the C19r warming event, which is characterized by strong dissolution expressed in a dark, clay-rich layer and a distinct peak in XRF core scanning Fe intensities (Westerhold & Röhl 2013) and a negative carbon isotope excursion (CIE) in bulk sediment at Demerara Rise Site 1260 (Edgar et al. 2007). Our new stable isotope data reveal that this event is present at three additional sites in the North and South Atlantic. The C19r event occurred ~1.0 myr prior to the onset of the MECO (40.5 Ma) and several million years after the Early Eocene Climate Optimum (EECO, 51 Ma) during a period of slightly cooler climate. No significant CCD changes have been observed one million years before and after the event as expressed by regular Fe cyclicity at Site 1260. The duration of the event estimated by orbital calibration is ~40-50 kyr, similar to other transient hyperthermals in the early to middle Eocene. The potential position of the event in the newly investigated sites was initially narrowed by

careful analysis of magnetostratigraphy and XRF scanning data. First results of stable isotope data at Site 702 show a very similar pattern as that observed at Site 1260. Although the magnitude of the bulk $\delta^{13}C$ excursion is comparable, the bulk $\delta^{18}O$ excursion at Site 702 is only a third of that observed at Site 1260 which might be related to diagenetic and/or latitudinal effects. The magnitudes of the CIE and $\delta^{18}O$ excursion are comparable to the H2 event (53.6 Ma) suggesting a similar response of the climate system to carbon cycle perturbations even in relatively cooler climate. For the first time the new records validate the C19r event in the southern South Atlantic and its ocean-wide if not global nature with a ~2°C deep sea warming. However, the effects on biota still need to be investigated.

References:

Agnini, C., P. Macri, J. Backman, H. Brinkhuis, E. Fornaciari, L. Giusberti, V. Luciani, D. Rio, A. Sluijs, and F. Speranza (2009), An early Eocene carbon cycle perturbation at 52.5 Ma in the Southern Alps: Chronology and biotic response, Paleoceanography, doi: 2410.1029/2008pa001649.

Bohaty, S. M., J. C. Zachos, F. Florindo, and M. L. Delaney (2009), Coupled greenhouse warming and deep-sea acidification in the middle Eocene, Paleoceanography, 24(PA2207), doi: 10.1029/2008pa001676.

Edgar, K. M., P. A. Wilson, P. F. Sexton, and Y. Suganuma (2007), No extreme bipolar glaciation during the main Eocene calcite compensation shift, Nature, 448(7156), 908-911, doi: 10.1038/nature06053.

Gradstein, F. M., J. G. Ogg, M. D. Schmitz, and G. M. Ogg (2012), The Geological Timescale 2012, 1176 pp., Elsevier.

Kirtland Turner, S., P. F. Sexton, C. D. Charles, and R. D. Norris (2014), Persistence of carbon release events through the peak of early Eocene global warmth, Nature Geosci, 7(10), doi: 10.1038/ngeo2240.

Laskar, J., M. Gastineau, J. B. Delisle, A. Farrés, and A. Fienga (2011), Strong chaos induced by close encounters with Ceres and Vesta, Astronomy and Astrophysics, 532, L4, doi: 10.1051/0004-6361/201117504.

Laskar, J., P. Robutel, F. Joutel, M. Gastineau, A. Correia, and B. Levrard (2004), A long-term numerical solution for the insolation quantities of the Earth, Astronomy and Astrophysics, 428, 261-285, doi: 10.1051/0004-6361:20041335.

Lourens, L. J., F. J. Hilgen, J. Laskar, N. J. Shackleton, and D. Wilson (2004), The Neogene Period, in A Geological Timescale 2004, edited by F. Gradstein, J. Ogg and A. Smith, pp. 409-440.

Lourens, L. J., A. Sluijs, D. Kroon, J. C. Zachos, E. Thomas, U. Röhl, J. Bowles, and I. Raffi (2005), Astronomical pacing of late Palaeocene to early Eocene global warming events, Nature, 435(7045), 1083-1087, doi: 10.1038/nature03814.

Pälike, H., and F. Hilgen (2008), Rock clock synchronization, Nature Geosci, 1(5), 282-282, doi: 10.1038/ngeo197.

Pälike, H., N. J. Shackleton, and U. Röhl (2001), Astronomical forcing in Late Eocene marine sediments, Earth and Planetary Science Letters, 193, 589-602, doi: 10.1016/S0012-821X(01)00501-5.

Sexton, P. F., R. D. Norris, P. A. Wilson, H. Pälike, T. Westerhold, U. Röhl, C. T. Bolton, and S. Gibbs (2011), Eocene global warming events driven by ventilation of oceanic dissolved organic carbon, Nature, 471(7338), 349-352, doi: 10.1038/nature09826.

Stap, L., L. J. Lourens, E. Thomas, A. Sluijs, S. Bohaty, and J. C. Zachos (2010), High-resolution deep-sea carbon and oxygen isotope records of Eocene Thermal Maximum 2 and H2, Geology, 38(7), 607-610, doi: 10.1130/g30777.1.

Röhl, U., G. Wefer, H. Brinkhuis, C. E. Stickley, M. Fuller, S. A. Schellenberg, and G. L. Williams (2004), Sea level and astronomically induced environmental changes in middle and late sediments from the East Tasman Plateau, in The Cenozoic Southern Ocean: Tectonics, Sedimentation and Climate Change between Australia and Antarctica, edited by N. F. Exon, J. P. Kennett and M. J. Malone, pp. 113-126, Am. Geophys. Union, Geophys. Monogr.

Westerhold, T., and U. Röhl (2009), High resolution cyclostratigraphy of the early Eocene - new insights into the origin of the Cenozoic cooling trend, Clim Past, 5(3), 309-327, doi: 10.5194/cp-5-309-2009.

Westerhold, T., and U. Röhl (2013), Orbital pacing of Eocene climate during the Middle Eocene Climate Optimum and the chron C19r event: Missing link found in the tropical western Atlantic, Geochemistry, Geophysics, Geosystems, 14(11), 4811-4825, doi: 10.1002/ggge.20293.

Westerhold, T., U. Röhl, and J. Laskar (2012), Time scale controversy: Accurate orbital calibration of the early Paleogene, Geochem. Geophys. Geosyst., 13, Q06015, doi: 10.1029/2012gc004096.

Westerhold, T., U. Röhl, H. Pälike, R. Wilkens, P. A. Wilson, and G. Acton (2014), Orbitally tuned timescale and astronomical forcing in the middle Eocene to early Oligocene, Clim. Past, 10(3), 955-973, doi: 10.5194/cp-10-955-2014.

Westerhold, T., U. Röhl, J. Laskar, J. Bowles, I. Raffi, L. J. Lourens, and J. C. Zachos (2007), On the duration of magnetochrons C24r and C25n and the timing of early Eocene global warming events: Implications from the Ocean Drilling Program Leg 208 Walvis Ridge depth transect, Paleoceanography, 22(PA2201), doi:10.1029/2006PA001322.

Westerhold, T., U. Röhl, I. Raffi, E. Fornaciari, S. Monechi, V. Reale, J. Bowles, and H. F. Evans (2008), Astronomical calibration of the Paleocene time, Palaeogeography, Palaeoclimatology, Palaeoecology, 257(4), 377-403, doi: 10.1016/j.palaeo.2007.09.016.

Zachos, J. C., G. R. Dickens, and R. E. Zeebe (2008), An early Cenozoic perspective on greenhouse warming and carbon-cycle dynamics, Nature, 451(7176), 279-283, doi: 10.1038/nature06588.

IODP

Maurice Ewing Bank–Georgia Basin Depth Transect: A Southern Ocean Perspective on Paleogene Climate Evolution (IODP 862-Pre)

T. WESTERHOLD[1], S.M. BOHATY[2], G. UENZELMANN-NEBEN[3] AND 862-PRE PROPONENTS[4]

1 MARUM – Center for Marine Environmental Sciences, University of Bremen, Bremen, Germany

2 Ocean and Earth Science, University of Southampton, National Oceanography Centre, Southampton, UK

3 Alfred-Wegener-Institut, Helmholtz-Zentrum für Polar- und Meeresforschung, Geophysics Section, Bremerhaven, Germany

4 T. Westerhold, S. Bohaty, E. Thomas, H. Scher, V. Spiess, P. Wilson, T. Moore, D. Barbeau, U. Röhl, C. Agnini, F. Florindo, S. Robinson, J. Whiteside, and S. Wise

Twenty-first century atmospheric pCO_2 concentrations will rise to levels that the Earth has not experienced for more than 30 Myr (>500 ppm). Geological records from the Paleogene (66 to 23 million years ago, Ma) provide the means to decipher the operation of the Earth System under high pCO_2 conditions, but tackling this scientifically and societally important problem requires precise integration of climate datasets across latitudes and ocean basins. Currently we lack the continuous high- resolution archives from the southern high latitudes that we need to provide comprehensive information on (sub)polar climate evolution and test competing hypothesized mechanisms of Paleogene climate change, such as the influence of atmospheric pCO_2 change versus the opening of Southern Ocean tectonic gateways.

Here we present the new International Ocean Discovery Program (IODP) pre-proposal 862-Pre (SW Atlantic Paleogene Climate), which is designed to drill a depth transect of Paleogene sites in the subantarctic South Atlantic Ocean on the easternmost tip of the Falkland Plateau (Maurice Ewing Bank and Georgia Basin). In the modern ocean, this is a critical area for deep-water communication between the Pacific and Atlantic oceans across the Drake Passage, with local bathymetry controlling the dispersal and propagation of deep- and bottom-waters throughout the entire Atlantic basin. We propose to drill a composite of Paleogene sections spanning an extensive range of paleo-water depths (~500–4500 m) to determine the timing and variability of deep-water connectivity across the Drake Passage and to test whether the onset of a proto-Antarctic Circumpolar Current (ACC) circulation had a direct impact on high-latitude and global climate evolution. These drillcores will provide crucial insight on the long-standing question of the relative influence of atmospheric pCO_2 drawdown vs. Southern Ocean gateways in driving Paleogene climate evolution.

The target sites are also ideally positioned to assess the relationships between local tectonic subsidence of deep-water barriers, high-latitude climate change, and the onset of bottom-water production in the Weddell Sea and northward propagation into to the deep western Atlantic – a process that, along with ACC circulation, fundamentally altered Cenozoic circulation in the Atlantic. In addition to deep-water circulation history, multi-proxy datasets from expanded hemipelagic sections will shed new light on climate change, biotic shifts, and deep-sea chemistry during the Paleogene, allowing evaluation of: (i) the magnitude of temperature change and response of high-latitude plankton groups across transient 'greenhouse' events, (ii) the initiation of southern high latitude cooling and onset of Antarctic Peninsula glaciation during the middle Eocene - early Oligocene 'greenhouse' to 'icehouse' transition, and (iii) variation in the Calcite Compensation Depth in the South Atlantic and its relation to changes in global carbon cycling.

Following the positive recommendation by the IODP Science Evaluation Panel (SEP) for 862-Pre, a strategy of two companion site survey investigations (SSIs) involving the collection of both multi-channel seismic data and piston cores have been developed for the eastern Falkland Plateau region of the southwest Atlantic Ocean. A German cruise led by Uenzelmann-Neben (AWI, Bremerhaven) and Westerhold (MARUM, Bremen) is proposed to survey the Maurice Ewing Bank extending southward across the Falkland Trough, and a UK-IODP cruise led by Bohaty (Univ. Southampton, UK) is proposed to survey the eastern half of the region across the Georgia Basin and Northeast Georgia Rise. The collaboration between German and UK groups will provide the extensive data coverage needed to survey the entire east–west transect of drillsites to meet the scientific objectives of 862-Pre. This transect is a fundamental requirement to allow reconstruction of deep-water properties across a range of palaeo-water depths and surface-water conditions across several modern frontal boundaries.

IODP

From bycatch to main dish – spines of irregular echinoids as monitors for macrofaunal dynamics in the deep sea during Cenozoic critical intervals? A pilot study.

F. WIESE[1], N. SCHLÜTER[1], M. REICH[2,3], J. ZIRKEL[4], J. HERRLE[4]

1 Georg-August University of Göttingen, Geoscience Centre, Dept. of Geobiology, Goldschmidtstr. 3, 37077 Göttingen, Germany
2 SNSB – Bavarian State Collection for Palaeontology and Geology, Richard-Wagner-Str. 10, 80333 München, Germany
3 Ludwig-Maximilians University München, Department of Earth and Environmental Sciences, Division of Palaeontology and Geobiology, Richard-Wagner-Str. 10, 80333 München, Germany
4 Goethe University Frankfurt, Institute of Geosciences, Dep. of Palaeontology, Altenhoeferallee 1, 60438 Frankfurt am Main, Germany.

The irregular echinoid group Atelostomata (Holasteroida and Spatangoida) flourished and radiated especially during the Cretaceous in shelf seas (Smith 1984, Eble 2000). While the Holasteroida migrated entirely into the deep sea in Cenozoic times (Smith 2004), the Spatangoida occupies both the shelf and the deep sea today. As specialised as deep sea Atelostomata to their environment, is their spine canopy to it various duties (e.g. digging, locomotion, protection, transport of food particles etc.), resulting in highly specialized and very distinct primary spine morphologies. Given its frequency and disparity in DSDP/ODP/IODP deep sea samples, Atelostomata spines bear a so far unexplored potential to decipher deep sea faunal dynamics.

From site U1334C (abyssal tropical Pacific, Leg 320), more than 4000 spine fragments of irregular echinoids were recovered from from 370 samples around mid-Oligocene glaciation Oi-2c (interval ca. 24.2 – 25.6 my). Each sample provided material. Sometimes more than 100 complete spines were recovered from one sample only (13H/5W, 8/10, ca. 20 g sediment processed). Apart from fragments, *quasi* complete spines are abundant, although the base is always lost (Banno 2008: discussion). The spines are excellently preserved, exhibiting sometimes almost pristine structure without any diagenetic syntaxial overgrowths. Based on an assessment of 84 recent Atelostomata (Holasteroida; Spatangoida), we can show that the orientation of pores in the spine (helicoidal: Spatangoida *versus* horizontal: Holasteroida) makes a safe distinction between the two groups possible. A further discrimination is based on i) overall shaft morphology (curved, straight, kinked, thinning towards the tip etc); ii) arrangement and frequency of thorns of the shaft; iii) shape of pores; iv) shape of tips (pointed, spatulate, forked, serrated, spoon-like, leaf-like etc.). The classification follows at first glance parataxonomic procedure as, e.g., in conodonts (Jeppsson 1969) or holothurians (Gilliland 1992) by elaborating unique characters of the spine. At all, it is a bit more difficult, though, because irregular echinoids bear very variable spine morphologies due to its function and position on the test. Some species produce a large number of highly variable spines (e.g. Smith 1980), other develop spines within a narrow morphological range (e.g. *Calymne*; Saucède et al. 2009). Thus, classification of spines must follow a kind of fuzzy systematics, which is

realised by recognition of clusters based on transitional morphologies and overall similarities of spines.

A first analysis shows that throughout the sampled interval, more than 90 % of the spines belong to the Holasteroida. At least two spine assemblages can be recognized, occurring together or separated in the various samples. Assemblage 1 consists exclusively of spatulate to forked and serrated tips of holasteroid spines with almost identical shafts. Assemblage 2 yields leaf-like to spoon-like morphologies with spines thinning markedly at the junction to the tip. Spine morphology and size – pointing at small-sized taxa – suggest a close relation to the recent Calymnidae (*Calymne relicta*; Saucède et al. 2009). Thick (ca. 1 mm diameter) Spatangoida spine fragments are scattered through the samples, suggesting one or more larger species.

The excellent record of atelostomate echinoid spines in DSDP/ODP/IODP cores and the recognition of time-specific spine assemblages bear the immense potential to map the response of a macrofaunal invertebrate group in the deep sea to critical intervals in Cenozoic oceanographic changes for the first time. In particular, the development of the psychrosphere from the middle Eocene on resulted in fundamental faunal turnovers and biogeographic re-organisations among the foraminifera and the ostracods (Benson 1975, Corliss 1997), and this pilot study aims to extract data for the Atelostomata from the Middle Eocene Climate Optimum (MECO) to the late Oligocene warming (time: ca. 20 my): v) Late Oligocene warming; iv) Oi-2c glaciation, mid-Oligocene; iii) Oi-2b glaciation, mid-Oligocene; ii) Upper Eocene temperature decline; i) Middle Eocene climatic optimum (MECO). These intervals cover oceanographic changes from warm bottom water *via* cooling to glaciation and back to warming, reflecting a deep sea bottom water oscillation of ca. 7°C (Zachos et al. 2001). We will consider exclusively data from Leg 320 in order to avoid palaeobiogeographic and water-depth related implications, which can show up when using geographically wide-spread locations with varying water depths.

References:

Banno T. 2008. Ecological and taphonomic significance of spatangoid spines: relationship between mode of occurrence and water temperature. *Paleontological Research* 12:145-157.

Benson R.H. 1975. The origin of the psychrosphere as recorded in changes of deep-sea ostracode assemblages. Lethaia 8: 69–83.

Corliss B.H. 1979. Response of deep-sea benthonic Foraminifera to development of the psychrosphere near the Eocene/Oligocene boundary. *Nature* 282: 63-65.

Eble G.J. 2000. Contrasting evolutionary flexibility in sister groups: disparity and diversity in Mesozoic heart urchins. *Paleobiology* 26 (1): 56-79.

Gilliland P.M. 1992. Holothurians in the Blue Lias of southern Britain. *Palaeontology* 35: 159–210.

Jeppson L. 1969. Notes on Some Upper Silurian Multielement Conodonts. *Geologiska Föreningens i Stockholms Förhandlingar* 91 (1): 12–24.

Saucede T, Mironov AN, Mooi R & David B. 2009. The morphology, ontogeny, and inferred behaviour of the deep-sea echinoid *Calymne relicta* (Holasteroida). *Zoological Journal of the Linnean Society* 155: 630-648.

Smith, AB. 1980. The structure and arrangement of echinoid tubercles. *Philosophical Transactions of the Royal Society, London, Series B* 289: 1–54.

Smith A.B. 1984. Echinoid Palaeobiology. Allen & Unwin, London.

Smith, A.B. 2004. Phylogeny and Systematics of Holasteroid Echinoids and Their Migration Into the Deep-sea. *Palaeontology* 47: 123–150.

Zachos J., Pagani M., Sloan L., Thomas E., Billups K. 2001. Trends, Rhythms, and Aberrations in Global Climate 65 Ma to Present. *Science* 292: DOI: 10.1126/science.1059412.

ICDP

Cotectic compositions of rhyolite as a geobarometer for highly evolved melts of the Yellowstone Snake River Plain

S. WILKE[1], R. ALMEEV[1], E. H. CHRISTIANSEN[2], F. HOLTZ[1]

1 Institute of Mineralogy, Leibniz University of Hannover, Callinstr. 3, 30167 Hannover, Germany

2 Department of Geological Sciences, Brigham Young University, Provo, UT 84602, USA

General aim of the study

The scientific drilling project in the Snake River Plain – Yellowstone (SRPY) volcanic system offers the opportunity of solving a wide amount of questions related to the magmatic processes of that area, such as the chemical and isotopical composition of the recovered basalts and rhyolites, the influence of possible interactions of the magma with the lithosphere, the processes involved in recharge, fractionation and assimilation and the time frame in which these processes take place. As one of the worlds largest Quarternary silicic volcanic centers (Hildreth *et al.*, 1991) the SRPY volcanic system bears an extraordinary opportunity to investigate the interactions of continental lithosphere with a mantle hotspot, currently located beneath the north-western edge of the US-state Wyoming. A row of rhyolite volcanic fields of increasing age ranging from ~0.6 to 2.1 Ma for Yellowstone Plateau volcanic field at the current position to >12.5 Ma for Owyhee-Humboldt volcanic field ~500 km in WSW direction is commonly interpreted as the path of the north american plate above a relatively fix mantle plum (Cathey & Nash, 2004). The most striking feature of the SRPY is however the large volume of bimodal basalt-rhyolite melts, linking the occurrence of more evolved melts to interactions with the lithosphere, usually estimated to take place at depth of ~5 to 15 km. The rather large uncertainty on pressure estimation is related to problems with geobarometry for highly evolved silicic melts as they tend to lack minerals suitable for established geobarometers so far.

Almeev *et al.* (2012) demonstrated that the effect of pressure on the silica content of cotectic rhyolitic melts (in equilibrium with quartz and feldspar) can be utilized as a geobarometer and might be able to fill this gap. The effect of pressure as well as water activity on the composition of the eutectic point is well calibrated in the ternary system quartz (Qz, SiO_2) – albite (Ab, $NaAlSi_3O_8$) – orthoclase (Or, $KAlSi_3O_8$) but few data is available for systems containing normative anorthite (An, $CaAl_2Si_2O_8$) (Tuttle & Bowen, 1958; Luth *et al*., 1964; Holtz *et al.*, 1992; James and Hamilton, 1969). Figure 1 gives an overview of the different effects causing shifts of the eutectic point position. When projected on the Qz-Ab-Or-plane, the presence of An in a melt was found to shift the position of the eutectic point away from the Ab apex (James & Hamilton, 1969) and is therefore limiting the applicability of the haplogranite system Qz-Ab-Or as a geobarometer for natural samples if not taken into account. In addition to this all available data on the position of cotectic curves in granitic systems collected so far were obtained for systems free of additional components such as FeO or TiO_2 that might affect the cotectic compositions. This study explores the effect of An on cotectic curves in rhyolitic systems

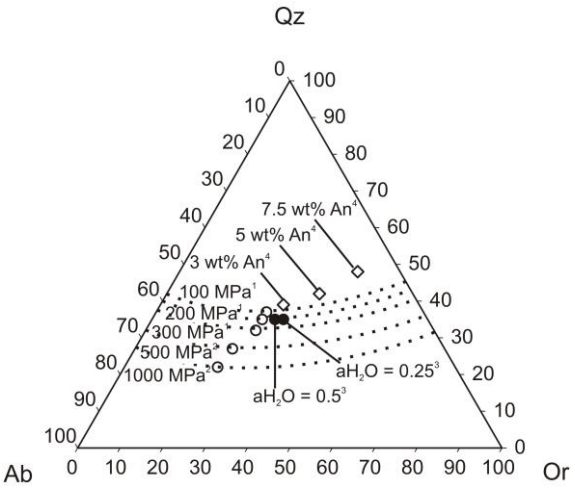

Fig. 1. Effect of pressure (P), water activity (aH_2O) and normative anorthite content (An) on the position of the eutectic point (or cotectic temperature minimum) in the ternary system Qz-Ab-Or. Open symbols represent water-saturated conditions. Round symbols represent An-free conditions. Diamonds refer to experiments conducted at 100 MPa ([4]James & Hamilton, 1969) and black dots to experiments conducted at 200 MPa ([3]Holtz et al., 1992). Open circles represent eutectic points obtained at various P as noted in the diagram ([1]Tuttle & Bowen, 1958; [2]Luth et al., 1964). Dottet lines indicate the positions of the quartz-feldspar cotectic curves at different P for water saturated, An-free conditions. Modified after Wilke *et al.* (in press).

relevant for the SRPY volcanic system and the results are applied as geobarometer for samples from the Kimberly-Drillhole.

Experimental outline

To create a robust dataset for pressure calibration six experimental conditions were chosen to check for the shift of the eutectic point and cotectic curves (when projected onto the ternary system SiO_2 – $NaAlSi_3O_8$ – $KAlSi_3O_8$) as a function of the anorthite content of the melt, water activity and pressure. Our starting compositions host (1) 1.2 wt% H_2O and 3.5 wt% An, (2) 1.2 wt% H_2O and 7 wt% An and (3) 3 wt% H_2O and 3.5 wt% An and the experiments are performed at 200 MPa and 500 MPa pressure. Starting glasses are created from oxide and carbonate powders that are molten two times at 1600°C under 1 atmosphere and afterwards pre-hydrated at 1200°C and 200 MPa in an internally heated pressure vessel (IHPV). These hydrous starting glasses are checked for their chemical composition by electron microprobe and for water content by infrared spectroscopy. The phase relationship experiments are performed in an IHPV at temperatures between 870 °C and 1050 °C. The oxygen fugacity is fixed close to QFM+0 during experiments. Although we apply techniques to enhance the nucleation of phases (e.g. finely ground powdered starting glass), the experimental durations vary between 7 and 13 days depending on the calculated viscosity of the sample melt. This long duration is necessary to achieve near-equilibrium conditions in such highly viscous rhyolitic systems.

Preliminary results from this proposal

22 months after the start of the project a total number of 123 experimental samples were successfully recovered and analyzed. The normative mineral content of the glass phase of each sample was calculated using the CIPW-norm. The eutectic points or cotectic temperature minimum for four of the six experimental conditions are constrained with good precision to be:

(a) Qz42Ab21Or37 for the conditions 3.5 wt% normative An, 3 wt% H_2O and 200 MPa
(b) Qz45Ab15Or40 for the conditions 7 wt% normative An, 1.2 wt% H_2O and 200 MPa
(c) Qz36Ab25Or39 for the conditions 3.5 wt% normative An, 3 wt% H_2O and 500 MPa
(d) Qz38Ab18Or44 for the conditions 7 wt% normative An, 1.2 wt% H_2O and 500 MPa

Under the experimental conditions (a) and (c) where 3.5 wt% normative An is present in the system, quartz, plagioclase and sanidine can crystallize and an eutectic point is observed. Under the experimental conditions (b) and (d) where 7 wt% normative An is present in the system, only quartz and plagioclase can crystallize and no eutectic point but a cotectic T-minimum is observed. This was confirmed in Na_2O-free experiments for experimental setting (b), where anorthite was observed as stable feldspar. Additional experimental and analytical work for the remaining two experimental settings (e) and (f) is under progress. These settings are:

(e) 3.5 wt% normative An, 1.2 wt% H_2O and 200 MPa
(f) 3.5 wt% normative An, 1.2 wt% H_2O and 500 MPa

Implications for SRPY geobarometry

Our results confirm the observation made by James & Hamilton (1969) that normative An will shift the eutectic point of a rhyolitic system away from the Ab apex by enlarging the plagioclase stability field. In an earlier phase of this project Wilke *et al.* (in press) concluded that the effect of An on the position of the eutectic point may be more pronounced than that published by James & Hamilton (1969). However, the systematic dataset obtained for the four conditions (a) – (d) listed above are consistent with the data of James & Hamilton (1969). Thus, at water-saturated conditions as well as at strongly water-undersaturated conditions (this study) a shift of the eutectic point position by 1.31 ± 0.45 wt% Qz per additional wt% normative melt An and -3.51 ± 0.95 wt% Ab per additional wt% normative melt An is observed. We found no evidence that these trends are in any way affected by the presence of FeO and TiO_2. This demonstrates that the effect is similar at pressures of 200 and 500 MPa and that it can be applied for geobarometry for natural rocks. Blundy & Cashman (2001) proposed a correction equation based, although not exclusively, on the results from James & Hamilton (1969), to account for normative An content when calculating the haplogranite Qz-Ab-Or content of natural samples. This equation is widely used in literature to constrain pressure dependent, haplogranite cotectic curves for geobarometry in natural, Ca-bearing samples. It is however important to note that the results given by this equation deviate from the eutectic points determined by James & Hamilton as well as from our eutectic points with increasing normative An. This is less pronounced for the Qz-value that is more crucial for pressure estimation, but given the fact that an increase in pressure of 100 MPa lowers the Qz content of the eutectic point by ≤ 2 wt%, precise knowledge on the effect of An backed up by a broad database is imperative.

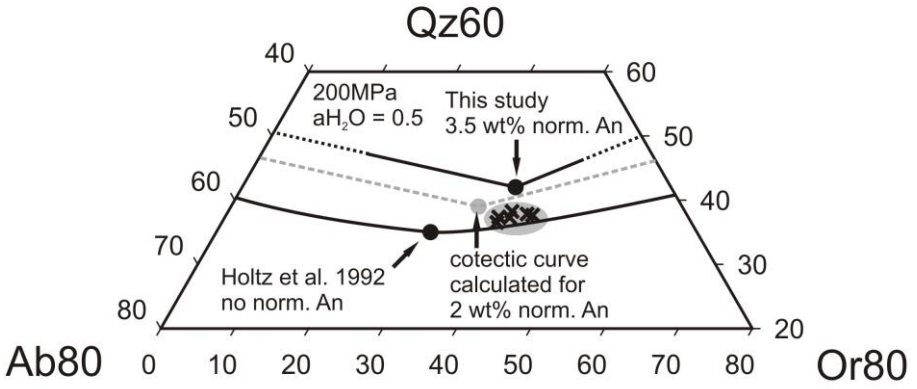

Fig. 2. Ternary plot of natural glasses (crosses) coexisting with quartz and feldspar from the Cougar Point Tuff, SRPY volcanic system (Cathey & Nash, 2004). Two eutectic points and cotectic curves experimentally determined for 200 MPa and $aH_2O = 0.5$ are given as black dots and lines (Holtz et al., 1992, Wilke et al., in press). The grey eutectic point and cotectic curve were interpolated from these two datasets to match the normative An content of the natural glasses of 2 wt%. Figure from Wilke *et al.* (in press)

An example for the application of our results for geobarometry is given in the haplogranite projection on Figure 2, where the eutectic points and cotectic curves for 200 MPa, $aH_2O = 0.5$, with either 0 wt% or 3.5 wt% normative melt An, are plotted together with natural melt compositions. The natural samples used in this example are rhyolitic melts with 2 wt% normative An content coexisting with quartz and at least one feldspar from Cougar Point Tuff, Bruneau-Jarbidge volcanic center, SRPY volcanic system obtained from Cathey & Nash (2004). A third cotectic curve is interpolated to match the 2 wt% An of the natural samples. As the cotectic natural melts plot below the 200 MPa - 2 wt% An cotectic curve, it can be deduced that P for these samples was slightly higher, probably at ~300 MPa.

Further objectives

The analysis and interpretation of the samples from the remaining experimental settings (e) and (f) is a focus of the work scheduled for the next 12 months. These settings are especially close to the natural rhyolites of the SRPY volcanic system and therefore extraordinary valuable when it comes to constraining the pressure for this system. Additional experiments will be conducted to link the experimental settings (a) – (f) to the dataset from James & Hamilton (1969) that was obtained at different pressure and water activity (aH_2O), so that the effect of normative melt An on the position of the eutectic point can better be investigated independently from the other influence parameters.

As the base of experimental data on the effect of An, FeO and TiO_2 is growing, the focus of this study will also shift on to the practical application for geobarometry on rhyolites of the SRPY volcanic system. For this purpose natural samples from the Kimberly-Drillhole that is located in the Twin Falls caldera in southern Idaho are analyzed. The core hosts three large layers of rhyolite only briefly intersected by basaltic lavas and some lacustrine sediments. Melt analyses will be conducted for matrix glass as well as inclusions in feldspar and quartz to determine pre-eruption pressures using the established An-correction for the ternary Qz-Ab-Or system. The derived P values will be compared to the only other approach of pressure determination in highly evolved silicic rocks known to us, the TitaniQ geothermobarometer (Thomas *et al.*, 2010), hopefully providing further insights not only in eruption history but also on the capabilities and limitations of the applied techniques.

References:

Almeev, R. R., Bolte, T., Nash, B.P., Holtz, F., Erdmann, M., Cathey, H.E. (2012),High-temperature, low-H2O Silicic Magmas of the Yellowstone Hotspot: an Experimental Study of Rhyolite from the Bruneau-Jarbridge Eruptive Center, Central Snake River Plain, USA, *J. Petrol.* **53 (9)**, 1837-1866

Blundy, J. & Cashman, K. (2001): Ascent-driven crystallization of dacite magmas at Mount St Helens, 1980-1986. *Contrib. Mineral. Petrol.*, **140**, 631-650

Cathey, H.E., Nash, B.P. (2004): TheCougar Point Tuff: Implications for Thermochemical Zonation and Longevity of High-Temperature, Large-Volume Silicic Magmas of the Miocene Yellowstone Hotspot, *J. Petrol.*, Vol **45**, 27-58

Hildreth, W., Halliday, A.N., Christiansen, R.L. (1991): Isotopic and Chemical Evidence Concerning the Genesis and Contamination of Basaltic and Rhyolitic Magma beneath the Yellowstone Plateau Volcanic Field, *J. Petrol.*, Vol. **32**, 63-138

Holtz, F., Pichavant, M., Barbey, P., Johannes, W., (1992): Effects of H2O on liquidus phase relations in the haplogranite system at 2 and 5 kbar, *Am. Mineral.*, **77**, 1223-1241

James, R.S. & Hamilton, D.L. (1969): Phase Relations in ths System $NaAlSi_3O_8$-$KAlSi_3O_8$-$CaAl_2Si_2O_8$-SiO_2 at 1 Kilobar Water Vapour Pressure, *Contrib. Mineral. Petrol.* **21**, 111-141

Luth, W.C., Jahns, R.H., Tuttle, O.F. (1964): The granite system at pressure of 4 to 10 kilobars, *J. Geophys. Res.*, **69**, 759-773

Thomas, J.B. Watson, E.B., Spear, F.S., Shermella, P.T., Nayak, S.K., Lanzirotti, A. (2010): TitaniQ under pressure: the effect of pressure and temperature on the solubility of Ti in quartz, *Contrib. Mineral. Petrol.*, **160**, 743-759

Tuttle, O.F. & Bowen, N. (1958): Origin of granite in the light of experimental studies in the system $NaAlSi_3O_8$-$KAlSi_3O_8$-SiO_2-H_2O, *Geol. Soc. Am. Mem.*, **74**, 145 pp.

Wilke, S., Klahn, C., Bolte, T., Almeev, R.., Holtz, F. (in press): Experimental investigation of the effect of Ca, Fe and Ti on cotectic compositions of the rhyolitic system, *Eur. J. Min.*, DOI: 10.1127/ejm/2015/0027-2423

IODP

Mid-Ocean Ridge Gabbro-Diorite-Tonalite Plutonic System Recovered from IODP Hole 1256D, Eastern Pacific: Implications for the Nature of Axial Melt Lens beneath Fast-spreading Ridges

C. ZHANG[1], J. KOEPKE[1], M. GODARD[3], L. FRANCE[3]

1 Institut für Mineralogie, Leibniz Universität Hannover, 30167 Hannover, Germany
2 CNRS, Géosciences Montpellier, Université Montpellier 2, 34095 Montpellier, France
3 CRPG-CNRS, Nancy-Université, BP 20, 54501 Nancy, France

The nature of axial melt lens (AML), which has been commonly observed by seismic experiments beneath fast-spreading mid-ocean ridges, is still mysterious concerning its role in the accretion of lower oceanic crust and the evolution and eruption of mid-ocean ridge basalts (MORB). Plutonic rocks including gabbros, diorites and tonalites, which might represent the uppermost part of AML, have been for the time recovered from IODP Hole 1256D at Eastern Pacific. Whole-rock major elements show a wide and continuous compositional range (e.g. Mg# 24~70) and apparent enrichments in Ti and Fe at intermediate MgO (4~6 wt%). Trace elements are characteristic coherent for different lithology groups defined by mineral modes, i.e. gabbro, clinopyroxene-rich diorite, amphibole-rich or Fe-Ti oxide-rich diorite, and quartz-rich tonalite. The gabbros and diorites are consistent to products of magma fractional crystallization, composed of melt and batch cumulate with a varying ratio. The tonalites are likely originated from low-degree partial melting in the sheeted dike overlying the AML rather than extreme fractional crystallization, evidenced by modelled trace elements (especially different in Eu) and liquid mobility. Hydrothermal alteration is pervasive during the cooling of the plutonic system and very strong locally, as evidenced from mineralogy, major and trace elements, which therefore results in difficulties and/or uncertainties for tracing crustal assimilation via mobile elements (e.g. Cl, U and Ce). Combining our data and some key literature data revealing the major elemental compositions of the mantle-derived primitive melt and that eruptible to form lavas and dikes, we propose that the AML probably represent the most evolved magma from deeper connected sills. Residual melts from intermediately differentiated sills might be transported through fractures during rifting and finally erupted. The AML might act as a density and thermal barrier for eruptible melts pooling underneath, but the highly evolved dioritic melts in the AML are not involved in eruption.